DISSERTATION

DEVELOPMENT OF BIOMASS-DERIVED FURANIC MONOMERS FOR BIORENEWABLE POLYESTERS AND POLYURETHANES

Submitted by

Jedediah Forrest Wilson

Department of Chemistry

In partial fulfillment of the requirements

For the Degree of Doctor of Philosophy

Colorado State University

Fort Collins, Colorado

Summer 2019

Doctoral Committee:

Advisor: Eugene Y.-X. Chen

Melissa M. Reynolds
Chris J. Ackerson
Donald W. Radford
Debbie C. Crans

ABSTRACT

DEVELOPMENT OF BIOMASS-DERIVED FURANIC MONOMERS FOR BIORENEWABLE POLYESTERS AND POLYURETHANES

This dissertation describes the development of difuranic diol monomers through the N-heterocyclic carbene (NHC) catalyzed cross-coupling of the biomass-derived platform chemicals, 5-hydroxymethylfurfural (HMF) and furfural (FF), and their subsequent utilization in the synthesis of renewable polyesters and polyurethanes with tunable thermal and mechanical properties through the use of soft and rigid co-monomers. The resulting polymers can undergo reversible cross-linking with bis-maleimide cross-linkers through the thermally reversible Diels-Alder reaction involving both the internal and pendent furan rings. The ability to construct a thermally reversible cross-linked network, coupled with formation of a significant amount (up to 34%) of stable carbonaceous materials when heating the polymers to 700 °C, demonstrates some promising features of this class of new difuranic polymers.

To address the need to enhance the molecular weight of the current furan-based polymers produced by the step-growth polycondensation process, alternative monomer structures have been designed to adopt the chain-growth mechanism. The first such alternative monomer belongs to a class of furan-derived lactones as candidates for ring-opening polymerization (ROP), which have been shown to produce high molecular weight polyesters because they follow the chain-growth mechanism. Two synthetic routes have been explored to produce such lactone monomers, and their polymerization behavior has been subsequently examined. The second such alternative is centered on a multifunctional furan acrylate monomer, methacrylate furan aldehyde (MFA). The studies

tested a hypothesis that auto-tandem or cascading reaction involving the aldehyde functionality in MFA would undergo a benzoin condensation, then the consequent diacrylate would have the appropriate functionality for NHC catalyzed tail-to-tail coupling resulting in a proton transfer polymerization (HTP). It was found that the benzoin condensation was successful but an oxidation occurred at the α-hydroxy of the furoin diacrylate resulting in a highly electrophilic diketone furil diacrylate. Exploration of the coupling mechanism suggests that the enolate acts as a base catalyzing the oxidation. Through careful analysis of the adducts formed when the NHC was reacted with the furil diacrylate showed that the NHC had strong affinity for the diketone moiety thus blocking the HTP pathway. Overall, this work added significantly to our understanding of furans as monomers, NHC catalysis in furan monomer synthesis as well as polymerizations, and enhanced our ability to control thermal and mechanical properties of furan containing polymers.

ACKNOWLEDGEMENTS

Chapter 2. This work was supported by the US Department of Energy, Office of Basic Energy Sciences, grant DE-FG02-10ER16193. This dissertation chapter contains the manuscript of a full paper published in ACS Sustainable Chemistry & Engineering [Wilson, J. F.; Chen, E. Y. -X. ACS Sustainable Chem. Eng. 2016, 4, 4927-4936]

Chapter 3. This work was supported by the US Department of Energy Office of Basic Energy Sciences, grant DE-FG02-10ER16193. This dissertation chapter contains the manuscript of a full paper published in ACS Sustainable Chemistry & Engineering [Wilson, J. F.; Chen, E. Y. -X. ACS Sustainable Chem. Eng. 2019, 7, 7035-7046]

Chapter 3 & 4. This work was supported by the US Department of Energy, Office of Basic Energy Sciences, grant DE-FG02-10ER16193.

DEDICATION

To Carla and Forrest D. Wilson,

Where would I be without you?

To Emily, Forrest J., and Harper Wilson,

Always remember, if you finish it, you win it.

TABLE OF CONTENTS

Appendix C

Appendix D

Chapter 1

Introduction

The purpose of this work is to utilize the abundant biomass-derived furan ring which can be made easily and efficiently from non-food biomass waste produced by industries such as agriculture and forestry. The bio-polymers lignocellulose and cellulose that make up much of this unutilized waste has been efficiently converted to the highly oxygenated platform chemicals 5-hydroxyfurfural (HMF) and furfural (FF). Their convenient functionality provides suitable handles for catalytic conversion to a variety of value-added chemicals, this renders them highly suited for bio-refining platforms. Research into efficient catalytic conversion of furans into monomers with functionality appropriate for polymerization reactions is a key step in the expansion of biorefining technology. Polyesters produced by catalytically up grading HMF into 5-furandicarboxylic acid have been shown to have significantly improved barrier properties when compared to poly(ethylene terephthalate) which is an important material for food packaging. In addition, the furan ring moiety has produced polymers with other interesting properties such as thermally reversable cross-linking through the dynamic covalent bond, resulting from the Diels-Alder reaction between the aforementioned furan and bis-maleimides (Figure 1.1). However, significant challenges remain when these promising platform chemicals are employed in polymerization reactions. The currently employed polymerization techniques that utilize functionalities such dicarboxylic acid require complicated and expensive conditions in order to produce polymers of sufficient molecular weight and lack of coloration. To develop methods to address the remaining problems with furan containing polymers, new monomer functionalities that allows for alternative polymerization pathways need to be developed. The primary aim of this work is to develop

efficient catalytic synthesis for monomers from the platform furan chemicals HMF and FF and evaluate the available polymerization routes and to maximize their material properties.

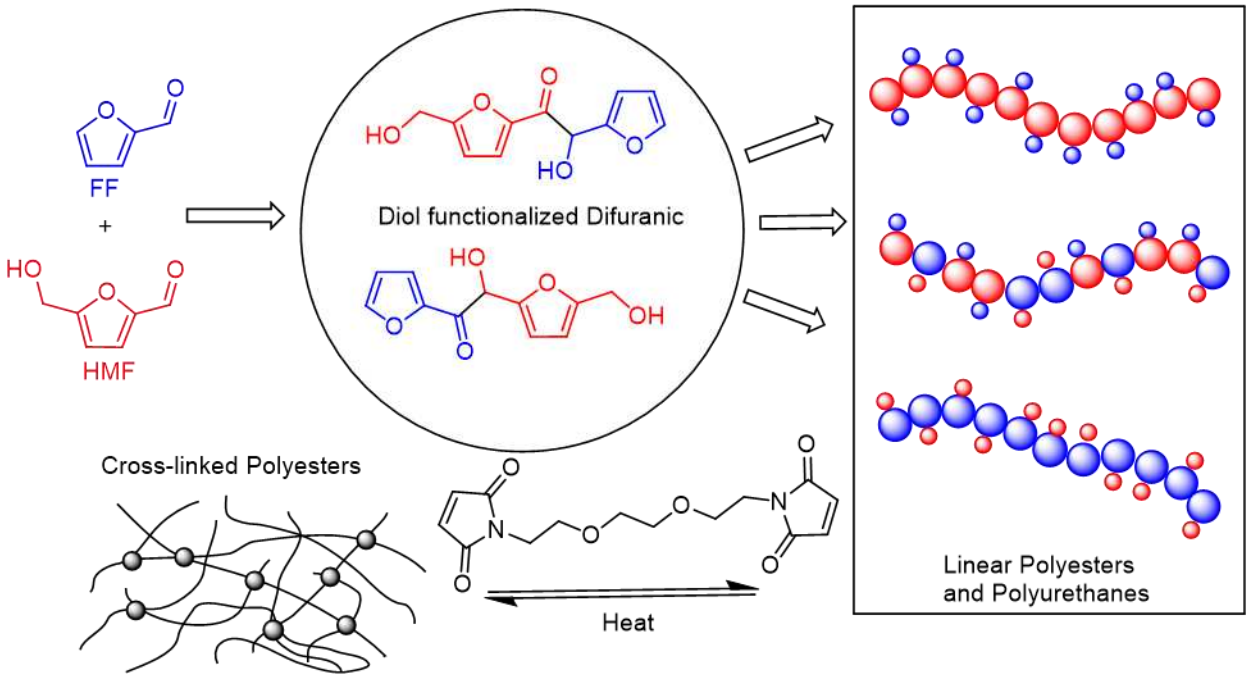

Figure 1.1. Cross coupling of furan platform chemicals HMF and FF to produce diol functionalized monomers utilized for the production of linear polyesters and polyurethanes that undergo thermally reversable cross-linking through Diels-Alder reaction.

The results of these fundamental investigations are discussed in detail in the following chapters:

2) Organocatalytic Cross-coupling of Bio-furanics to Multifunctional Difuranic C_{11} Building Blocks

3) Difuranic Diols for Renewable Polymers with Pendent Furan Rings

4) Biofuran-Based Lactone Monomers and Their Ring-Opening Polymerization Behavior

5) Reactivity and Complexity of a Multifunctional Furan Acrylate Monomer Towards Organocatalysts

6) Conclusion

Chapter 2 reports the successful cross coupling of HMF and FF through the N-heterocyclic carbene (NHC) catalyzed benzoin condensation. Different reaction conditions as well as NHC's with varying steric and electronic environments were screened in an effort to develop a selective process. The limited selectivity achieved resulted in a mixture of the two homo-coupled difuranics as well as the two hetero-coupled isomers. Careful separation of the mixture produced the two difuranic diol's suitable for condensation polymerizations. Conformation of the two isomeric diol structures was obtained through 2D NMR analysis and single crystal x-ray crystallography.

The two diols that resulted from the cross coupling of HMF and FF were then employed in a variety of condensation polymerizations discussed in Chapter 3. By utilizing soft and rigid co-monomers, polymer properties such as glass transition and onset decomposition could be tuned. In addition, mechanical properties like the storage and loss modulus were modified in a controllable fashion. Polymers obtained from the two individual diols had comparable physical properties but it was found that one diol monomer had a steric advantage, resulting in significantly higher molecular weight polymer. Polymers produced from this method still have molecular weights and coloration that limit their applications.

In Chapter 4, an attempt to solve the molecular weight and coloration limitations of the previously discussed materials was made through the development of furan derived lactones. Two strategies were employed, the first one attempted two orthogonal routes to an alcohol-ester functionalized molecule suitable for lactonization. This method resulted in unexpected compounds

not suitable for lactonization, therefore an alternative approach was taken through a Diels-Alder between furfural alcohol and another biomass derived compound, itaconic anhydride. This resulted in a heavily substituted γ-butyrolactone that was unable to polymerize through a ring opening process.

Chapter 5 covers a new kind of difunctional furan monomer that was hypothesized to undergo an auto-tandem NHC catalyzed *cascading* reaction. The monomer has an aldehyde that can undergo a benzoin condensation to produce a furoin diacrylate. The proposed pathway would result in the tail-to-tail coupling of the furoin diacrylate producing a polymeric material through a proton transfer polymerization. The reaction was found to undergo a different pathway resulting in a furil dimethacrylate that contains a strongly electrophilic diketone moiety which reacts with the NHC, inhibiting the proton transfer polymerization route.

The dissertation offered hereinafter was envisaged in a "journal-format" style, in agreement with the Graduate School guidelines at Colorado State University, and it is comprised of four manuscripts, as well as a brief discussion of the impact this work has on the field. Two manuscripts have already been published in peer-reviewed chemistry journals as full-paper articles in ACS Sustainable Chemistry & Engineering. The third and fourth manuscript have been completely prepared and are ready for submission. All the experimental detail, methods, materials characterization, and supporting figures corresponding to each of the individual chapters are consecutively included in Appendixes at the end of this dissertation. This arrangement maintains consistency with the previously published work and also provides a readable format of the research presented in the main chapters.

Chapter 2

Organocatalytic Cross-coupling of Bio-furanics to Multifunctional Difuranic C_{11} Building Blocks

2.1. Synopsis

To synthesize the still missing C_{11} furoins as potential tri-functional difuranic building blocks for biopolymers and biofuels, the route based on the cross-coupling of two bio-furaldehydes, furfural (FF) and 5-hydroxymethylfurfural (HMF), has been investigated using organic *N*-heterocyclic carbene (NHC) catalysts. This NHC-catalyzed coupling reaction in solution gives a statistical mixture of products including homo-coupled C_{10} and C_{12} furoins **1** and **4**, as well as cross-coupled C_{11} furoins **2** and **3**, regardless of the electronics or sterics of the NHC pre-catalyst used, but a slight preference for cross-coupled products (~60% **2** + **3** combined) under neat conditions has been achieved. Cross-coupled products **2** and **3** have been isolated in 48.1% yield and further separated into their pure state in 22.2% and 19.9% yield for **2** and **3**, respectively. The isolated **2** and **3** have been fully characterized by NMR, HRMS, and single crystal X-ray diffraction. A simple metal-free/in-air oxidation reaction converts these two isomeric furoins into the single α-diketone furanil structure **5**, another new C_{11} bio-derived building block.

2.2. Introduction

Annually renewable and abundant nonfood plant biomass, produced via photosynthesis utilizing solar energy and existed in the forms of lignocellulosic materials, holds great promise to provide humanity with a sustainable source of fuels, materials, and chemicals.[1-7] Among which, furaldehydes, particularly furfural (FF) and 5-hydroxylmethylfurfural (HMF) derived from catalytic dehydration of biorefinery pentose and hexose sugars, are considered to be two of the

most important biomass building blocks or platform chemicals.[8-18] Through chemical catalysis, furfurals can be upgraded into drop-in biofuels.[19] However, to produce high-quality liquid fuels requires upgrading of FF and HMF via C–C bond forming, chain-extension reactions,[20-23] as the fuels directly derived from FF and HMF have too high volatility and low energy density to be suitable as fuel additives.[24,25] On the other hand, as such furaldehydes cannot undergo self-aldol condensation due to lack of α-hydrogen, cross-aldol condensation with acetone was then utilized for the chain extension, followed by hydrodeoxygenation processes, to produce C_{9-15} liquid alkane fuels.[24-26]

A unique process that can directly couple two FF and HMF molecules into C_{10} and C_{12} *α*-hydroxy-ketone-linked difuranic compounds (furoins), respectively, is through organocatalysis by *N*-heterocyclic carbene (NHC)-catalyzed umpolung (i.e., polarity inversion) condensation self-coupling of furaldehydes,[27] a process analogous to the benzoin condensation of benzaldehydes.[28-30] In this context, NHC catalysts promote direct coupling of two HMF molecules to form exclusively C_{12} 5,5'-dihydroxymethyl furoin (DHMF).[31,32] Other furaldehydes such as FF and 5-methylfurfural can also be effectively chain-extended using this organocatalytic benzoin condensation method.[32,33] As a C_{12} difuranic building block, DHMF was converted into $C_{10–12}$ linear hydrocarbons,[32] and an integrated catalytic process for conversion and upgrading of biomass feedstocks into DHMF and subsequently into *n*-$C_{12}H_{26}$ alkane fuel was also developed.[34] DHMF, also a triol monomer, was converted to 5,5'-bihydroxymethyl furil (a diol) and 5,5'-bihydroxymethyl hydrofuroin (a tetraol), and these biomass-based polyols were polycondensated with various diisocyanates to produce linear and cross-linked polyurethanes.[35] The umpolung condensation coupling of FF to produce C_{10} furoin is more facile,[31-33,36-40] with the best furoin yield (>99%) achieved most recently by the NHC derived from the acetate substituted thiazolium.[41]

Supported recyclable NHC catalysts have also been recently developed to effectively upgrade FF and HMF into C_{10} and C_{12} furoins.[42,43]

As can be seen from the above literature overview, upgrading of FF and HMF via self-condensation coupling of two FF and HMF molecules into C_{10} and C_{12} furoins with high selectivity and efficiency has been well established.[27] However, organocatalytic cross-coupling between FF and HMF into C_{11} furoins has not been achieved.[44] By possessing three reactive sites (two hydroxyl groups and one nucleophilic carbon at the 5-position of the furan ring) for subsequent functionalization or derivatization, such C_{11} furoins are potentially unique *tri-functional* difuranic building blocks for difuranic polymeric materials (such as polyurethanes, polyesters, and cross-linked materials) and high-energy-density liquid fuels. Accordingly, the central objective of this work was to investigate the catalytic cross-coupling reaction of FF and HMF with the *in-situ* generated organic NHC catalysts as well as isolate and characterize the resulting C_{11} furoins, present in two isomeric structures.

2.3. Results and Discussion

Isolation and characterization of cross-coupled products. In our initial attempts to isolate and characterize the cross-coupled products **2** and **3**, pre-catalyst **A** (Figure 2.1), which can be readily converted into the corresponding stable NHC, 1,3,4-triphenyl-4,5-dihydro-1H-1,2,4-triazol-5-ylidene (TPT), by heating at ≥ 60 °C,[45,46] was selected because of its established high reactivity towards FF and HMF homo-coupling reactions.[31,32,34] For the FF + HMF cross-coupling reaction, it is also highly effective, but not chemoselective, thus producing a statistic mixture of all possible coupling products including both homo-coupled C_{10} (**1**) and C_{12} (**4**) furoins as well as cross-coupled C_{11} furoins **2** and **3** (Figure 2.1). Homo-coupled products **1** and **4** have R_f values

that differ enough to allow for easy separation from cross-coupled products **2** and **3** using routine column chromatography. Thus, a clean fraction containing the combination of the two α-hydroxy-ketone isomers **2** and **3** was obtained. However, separation of these two C_{11} furoin isomers posed a difficult challenge because of their nearly identical polarity and thus nearly identical R_f values under normal benchtop column chromatography conditions. Recrystallization from different solvents or solvent combinations also failed to separate the two isomers. Finally, using automated flash column chromatography (Combi*Flash* R*f*, Teledyne ISCO), coupled with a high performance column (a 220 g RediSep® gold silica column) and ethyl acetate/hexane as the mobile phase, achieved successful separation of the two isomers into their pure state with an isolated yield of 22.2% and 19.9% for **2** and **3**, respectively (see Experimental section for details). The separated isomers were fully characterized by high-resolution mass spectrometry (HRMS), ^{1}H NMR, ^{13}C NMR, 2D NMR, and X-ray diffraction crystallography (for **3**).

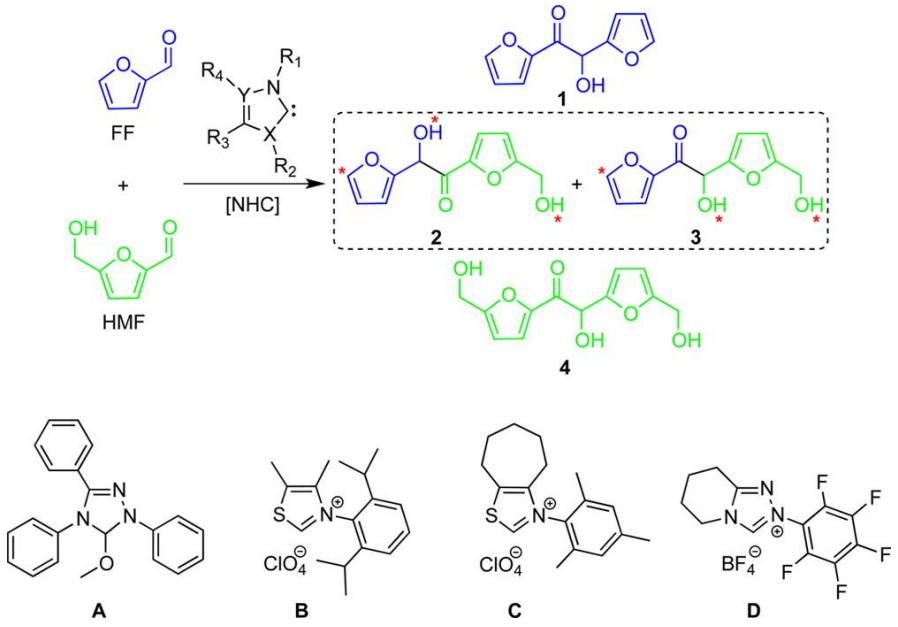

Figure 2.1. NHC-Catalyzed Cross-coupling of FF and HMF, Structures of all possible coupled products, and structures of NHC Pre-catalysts employed in this study.

^{1}H and ^{13}C NMR spectra of the cross-coupled products **2** and **3** were collected in DMSO-d_6 and shown in Figures 2.2 and 2.3, respectively. As anticipated, α-hydroxy-ketone isomers **2** and **3** exhibit many common ^{1}H NMR features, including five sets of downfield proton signals (δ 7.98 – 6.20 ppm) for the HMF (two sets) and FF (three sets) furan rings in the furoin structure (**2**, δ 7.57, 7.47, 6.49, 6.44–6.37 ppm; **3**, δ 7.98, 7.52, 6.68, 6.32, 6.20 ppm), the α-hydroxy-ketone group [**2**, –C(=O)CH$^{5.76}$OH$^{6.09}$; **3**, –C(=O)CH$^{5.75}$OH$^{6.07}$], and the terminal hydroxymethyl group (**2**, –CH$_2$$^{4.44}OH^{5.48}$; **3**, –CH$_2$$^{4.30}OH^{5.17}$). Assignments of their spectral peaks were made possible by additional 2D NMR experiments. For example, multi-bond 2D HMBC NMR experiments were performed on isomer **3**, showing a correlation between proton H_g and carbon C8 but no correlation between proton H_g and carbon C9, which is consistent with the proposed structure of isomer **3**. The structural identification based on these NMR results was later confirmed by the single-crystal X-ray diffraction analysis (*vide infra*). Likewise, multi-bond 2D HMBC NMR of isomer **2** (Figure 4) showed a correlation between proton H_g and carbon C9 but no correlation between proton H_g and carbon C6, consistent with the corresponding isomer structure. Furthermore, 2D HSQC NMR experiments of each isomer showing unique ^{1}H–^{13}C signal correlation between adjacent nuclei (Figures 2.5 and 2.6) proved key to the final assignment of each carbon (Figures 2.2 and 2.3).

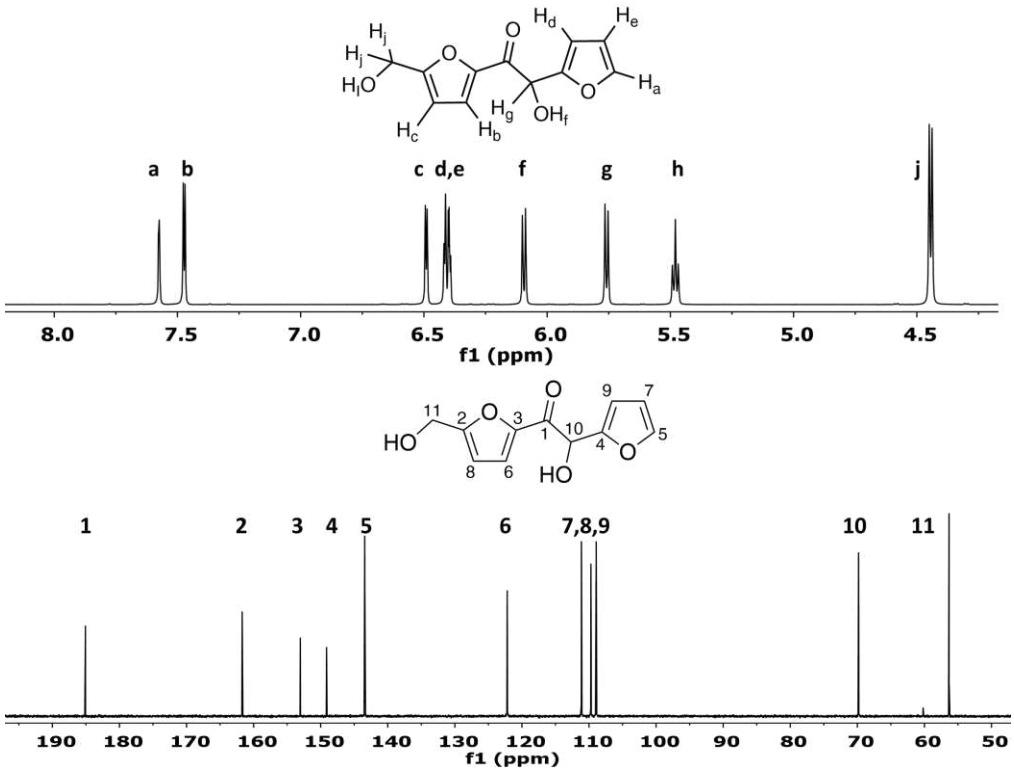

Figure 2.2. ^{1}H NMR (top) and ^{13}C NMR (bottom) of **2** (DMSO-d_6, 25 °C).

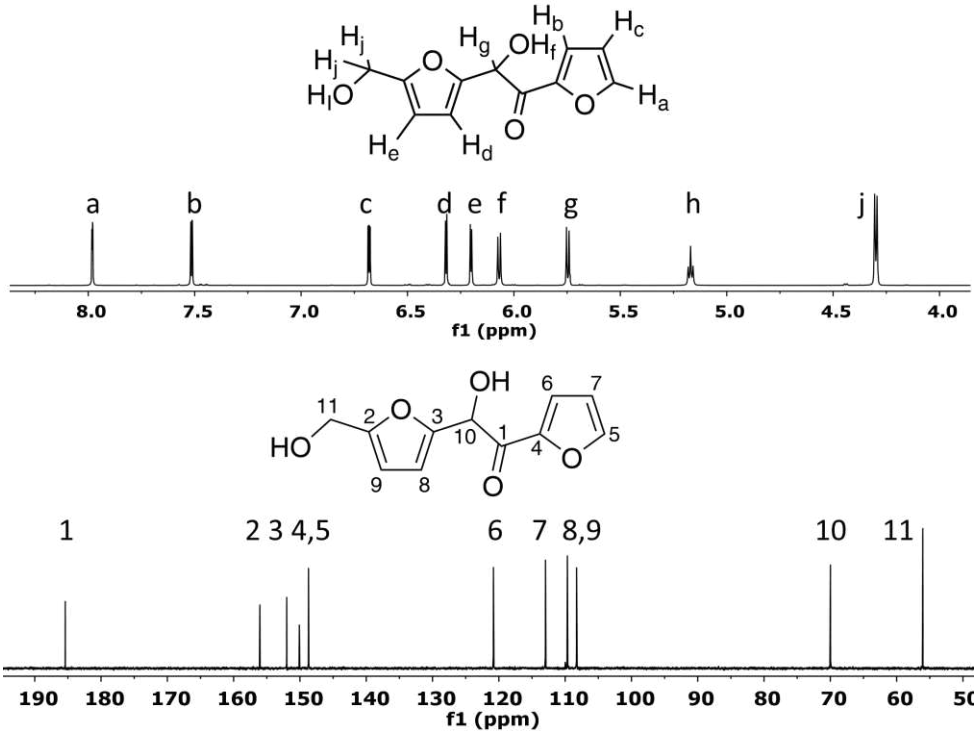

Figure 2.3. ^{1}H NMR (top) and ^{13}C NMR (bottom) of **3** (DMSO-d_6, 25 °C).

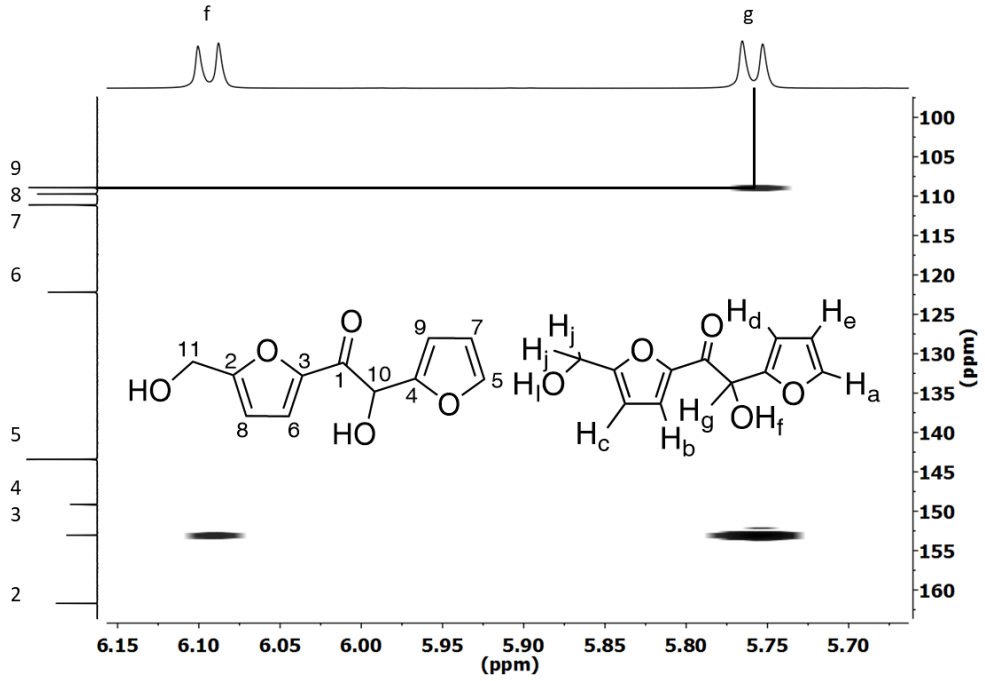

Figure 2.4. HMBC spectrum (DMSO-d_6, 25 °C) of **2** showing multi-bond correlation between H_g and C9 (but not with C6).

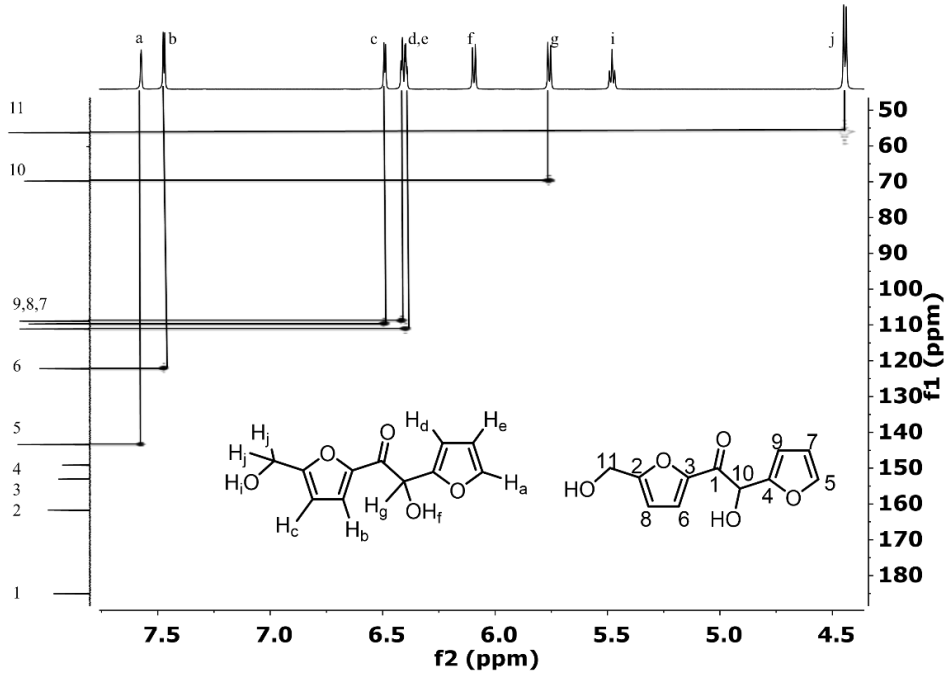

Figure 2.5. HSQC spectrum (DMSO-d_6, 25 °C) of **2** showing ^{1}H–^{13}C signal correlation between adjacent nuclei.

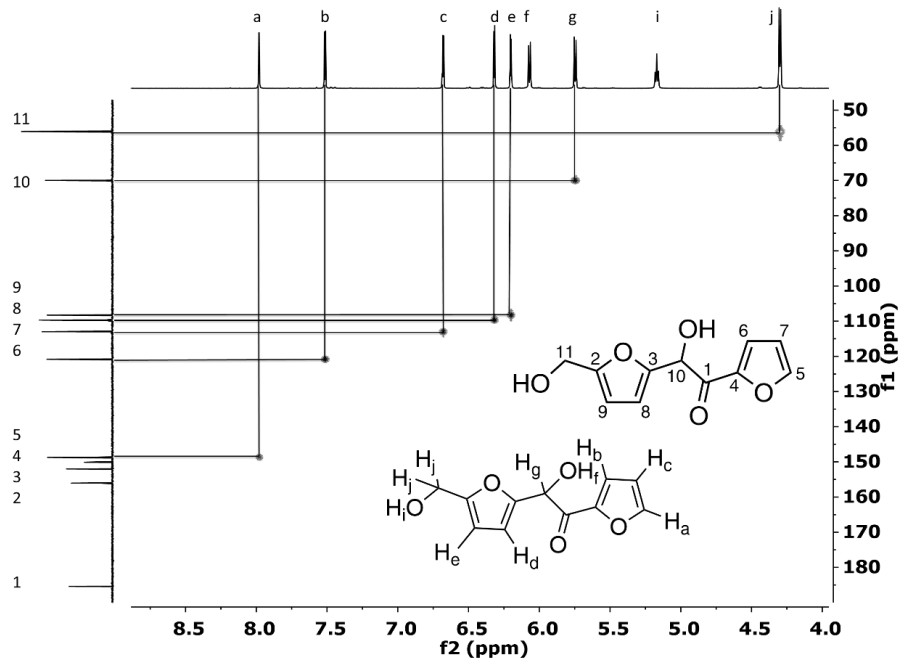

Figure 2.6. HSQC spectrum (DMSO-d_6, 25 °C) of **3** showing ^{1}H–^{13}C signal correlation between adjacent nuclei.

The correct structural assignment of the spectroscopic data was further confirmed by the single-crystal X-ray diffraction analysis of isomer **3** (Figure 2.7). The structural data clearly show a ketone group at C(7) with a bond length of 1.219(3) Å, within the typical range of a C=O bond. The data also reveal two hydroxyl groups: one alpha to the carbonyl, C(6), and a second one on the adjacent furan ring as the CH_2OH group. The bond lengths and angles of the furan rings are typical of an aromatic heterocyclic five-membered ring, with coplanar atoms and substantial sp^2 hybridized bond character. However, the furan ring adjacent to the conjugated ketone group bears a slightly shorter C(9)–C(10) bond (1.386(4) Å) compared to the C(3)-C(4) bond (1.423(3) Å) in the furan ring adjacent to two hydroxymethyl groups.

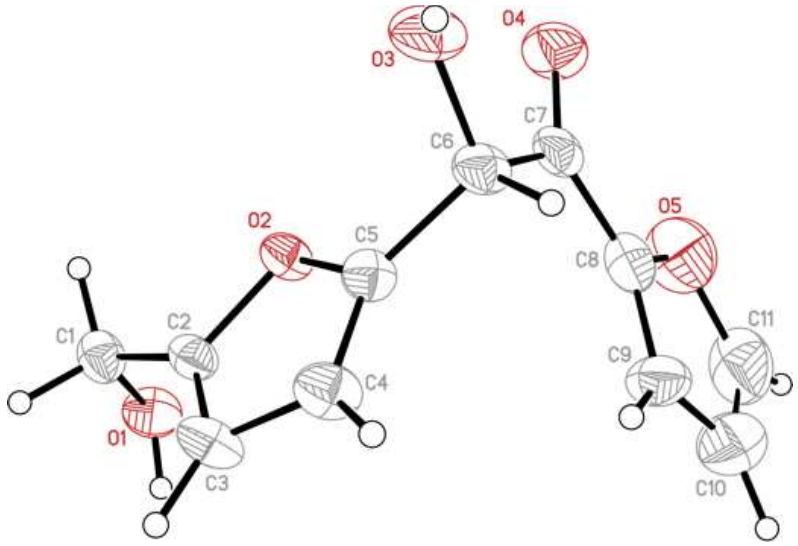

Figure 2.7. X-ray single crystal structure of C_{11} furoin **3** with thermal ellipsoids drawn at the 50% probability.

It is worth emphasizing here that the only structural difference between **2** and **3** is the position of the HMF ring, either adjacent to the ketone group (**2**) or the α-hydroxy group (**3**). Nevertheless, the position of the electron-withdrawing (de-shielding) ketone group brought about the most notable chemical shift differences for the H_a proton of the FF ring (δ 7.57 ppm in **2** vs. δ 7.98 ppm in **3**, where the ketone is adjacent to the FF ring), as well as for H_i and H_j protons of the $–CH_2OH$ group ($–CH_2^{4.44}OH^{5.48}$ in **2**, where the ketone is adjacent to the HMF ring; $–CH_2^{4.30}OH^{5.17}$ in **3**), as depicted in Figure 2.8. Overall, these spectroscopic differences observed in their ^1H and ^{13}C NMR spectra, coupled with 2D NMR methods and X-ray diffraction analysis, enabled us to conclusively identify both cross-coupled isomers, which becomes essential to quantify the formation of the cross-coupled products **2** and **3** vs. the homo-coupled products **1** and **4** in the crude product mixture from the catalyst screening experiments (*vide infra*).

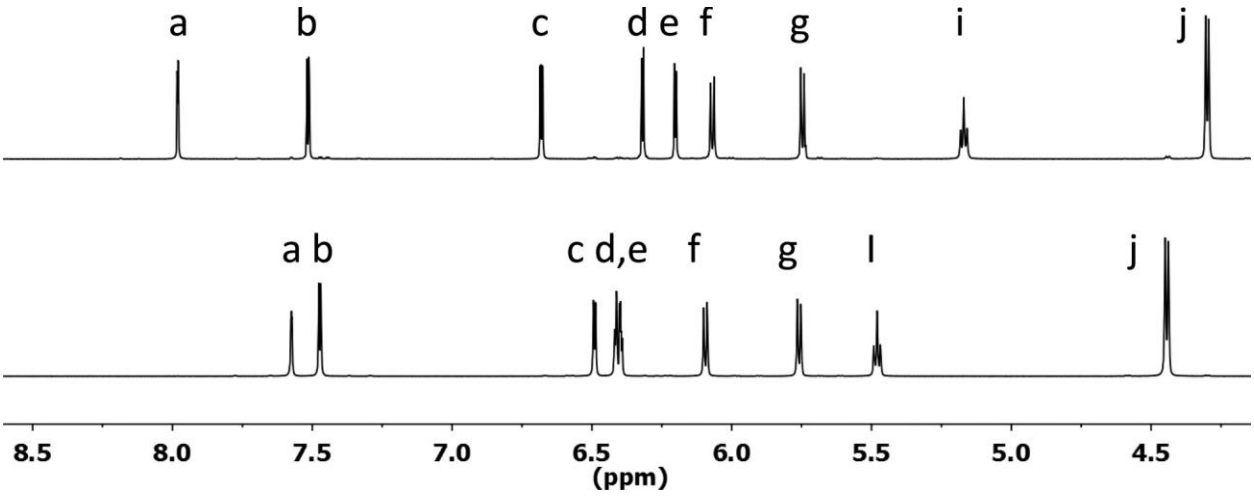

Figure 2.8. Overlay of ^{1}H NMR spectra (DMSO-d_6, 25 °C) of **2** (bottom) and **3** (top).

Chemoselectivity of the cross-coupling reaction. Achieving high chemoselectivity in the benzoin condensation catalyzed by NHCs is rare and limited to the scenarios when certain functional groups are placed at specific positions on the benzaldehyde ring. For example, Glorius and co-workers reported the first example of chemoselectivity achieved for benzoin cross-condensation of benzaldehydes using NHC pre-catalysts **B** and **C**,[47] revealing that if one of the benzaldehydes had a substituent in the *ortho*-position then the cross-coupling selectivity of up to 82% was observed. Gravel and co-workers employed NHC pre-catalyst **D** and achieved high to quantitative selectivity when a benzaldehyde was cross-coupled with 2-phenylacetaldehyde or a linear aldehyde.[48] In fact, the NHC catalyst derived from **D** showed almost negligible activity towards aromatic aldehyde homo-coupling, while the activity toward aliphatic homo-coupling was 90% or better. Likewise, Connon and co-workers found that an analogous *N*-C_6F_5 substituted triazolium NHC precatalyst promotes intermolecular cross-benzoin reactions between 2-substituted benzaldehydes and aliphatic aldehydes with a high level of chemoselectivity (69%).[49] Accordingly, we chose these three pre-catalysts, **B**, **C**, and **D**, together with pre-catalyst **A**, for the current FF + HMF cross-coupling reaction. These four pre-catalysts with ranging electronic and

steric characters, three bases (DBU, DMAP, and Et_3N), and three solvent conditions (THF, EtOH, and neat) were employed for optimization of the cross-coupling reaction targeting better chemoselectivity for the cross-coupled products **2** and/or **3**, the results of which are summarized in Table 2.1. All reactions were carried out in the glovebox under inert atmosphere and quenched with *p*-toluenesulfonic acid (TsOH) to avoid the conversion (oxidation) of the α-hydroxy containing compounds to the α-diketones in air and in the presence of a base such as DBU (*vide infra*).

With the precise identification of the chemical shifts for the α-proton previously obtained, in combination with the aldehyde chemical shifts for FF (9.61 ppm) and HMF (9.54), it was possible to interpret the ^{1}H NMR of the crude products. A representative ^{1}H NMR spectrum of a crude product mixture is shown in Figure 2.9 with the region between 5.66–5.86 ppm enlarged to show that, in many cases, the four α-protons (each appeared as a double) can be distinguished. Occasionally, the α-protons of the two cross-coupled products cannot be discerned, but the two cross-coupled products can always be distinguished from the homo-coupled products. The conversion of the FF and HMF starting materials into the coupled products was determined by the integration of the aldehyde protons compared with the α-hydroxy protons. Some larger (3-g) scale reactions were also performed and quenched with TsOH, showing that the isolated yields of coupled products were in good agreement with the ^{1}H NMR calculated conversions.

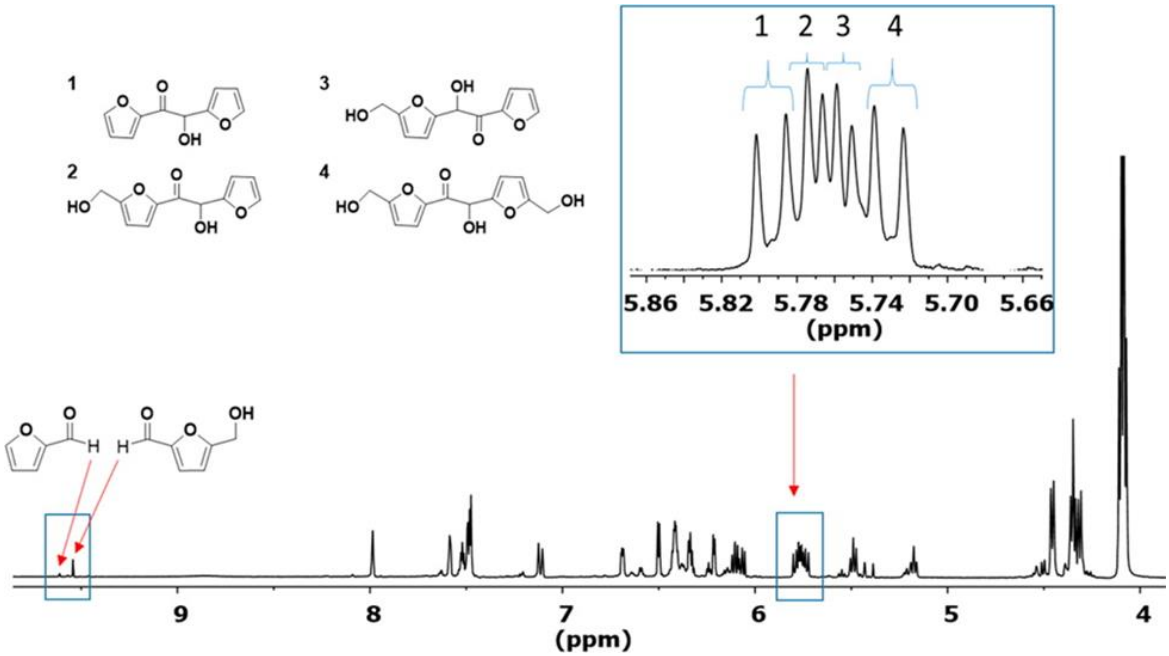

Figure 2.9. A representative 1H NMR (DMSO-d6, 25 °C) of crude coupling reaction products with the region between 5.66–5.86 ppm enlarged.

It can be seen from the table, the total conversion of FF and HMF into the coupled products **1** to **4** for each of the pre-catalysts was high, >90% conversions when the reactions were carried out in a solvent, and even higher when the reactions were carried out under neat conditions. Pre-catalyst **D** substituted with the strongly electron-withdrawing *N*-C_6F_5 group had the best performance of all the pre-catalysts tested, with conversion ranging from 86.8% to 96.5% (runs 36 and 30) in a solvent and from 89.9% to 97.8% (runs 32 and 35) under neat conditions. The lowest conversions were obtained when pre-catalyst **B** was used in a solvent, with conversions between 60.9% and 92.7% (runs 6 and 9), but when neat conditions were utilized conversions increased to 89.7% to 95.2% (runs 11 and 13). Pre-catalyst **A** converted 83.3% to 94.9% (runs 1 and 3) of the aldehydes to coupled products while **C** was able to convert 81.6% to 93.0% (runs 18 and 20) to coupled products with solvent and from 93.0% to 98.6% (runs 22 and 23) without solvent. These results show that the pre-catalysts chosen for these experiments are capable of efficiently coupling

FF and HMF, however these pre-catalysts exhibit no significant chemoselectivity towards the cross-coupled products (*vide infra*).

Table 2.1. FF and HMF cross-coupling reaction optimization results by pre-catalysts A, B, C, and D [a]

Run#	Pre-catalyst	Base	Solvent	Conversion (%) [b] or isolated yield (%) [e]				
				1	**2**	**3**	**4**	Total yield
1			THF	25.1	20.3	16.8	21.1	83.3
2[c,e]			THF	21.7	48.1		22.3	92.1
3	**A**	None	EtOH	27.4	23.3	21.2	23.0	94.9
4			Neat	26.4 ± 0.3	27.6 ± 1.6	19.4 ± 0.8	23.7 ± 1.7	97.1 ± 1.7
5		DBU		35.8 ± 0.5	34.8 ± 1.9		15.0 ± 1.4	85.6 ± 1.5
6		DMAP	THF	30.7	22.6		7.6	60.9
7		Et_3N		31.7	17.4	17.4	11.8	78.3
8		DBU		25.1 ± 0.5	20.0 ± 0.9	19.1 ± 0.5	18.9 ± 1.0	83.1 ± 1.2
9	**B**	DMAP	EtOH	23.2	45.1		23.4	91.7
10		Et_3N		24.4	24.4	24.4	19.5	92.7
11		DBU		23.6 ± 1.5	30.7 ± 1.8	26.1 ± 2.5	9.3 ± 1.9	89.7 ± 1.9
12		DMAP	Neat	24.2 ± 2.3	30.4 ± 0.8	28.5 ± 0.2	10.6 ± 0.3	93.7 ± 0.9
13		Et_3N		23.3 ± 3.8	31.8 ± 0.5	29.0 ± 2.0	10.9 ± 1.4	95.2 ± 0.3
14		DBU		27.4 ± 1.3	23.8 ± 1.7	21.6 ± 0.7	8.1 ± 1.8	80.9 ± 1.2
15		DMAP	THF	29.8 ± 3.2	24.6 ± 2.1	18.8 ± 2.0	19.5 ± 2.0	92.7 ± 0.8
16		Et_3N		29.9 ± 2.4	21.6 ± 2.3	21.8 ± 1.9	18.5 ± 1.9	91.8 ± 0.9
17		DBU		25.4 ± 1.5	21.5 ± 1.2	20.6 ± 0.9	20.7 ± 3.1	88.2 ± 1.3
18		DMAP		55.7	23.5		2.4	81.6
19	**C**	Et_3N	EtOH	32.9 ± 0.9	28.2 ± 0.5	13.8 ± 1.5	12.0 ± 1.3	86.9 ± 0.6
20[c]		Et_3N		13.2 ± 1.1	49.2 ± 0.7		30.6 ± 0.5	93.0 ± 0.3
21[e]		Et_3N		18.6	22.1	19.9	17.8	78.4
22		DBU		25.0 ± 1.5	35.0 ± 1.9	25.0 ± 2.2	8.0 ± 2.0	93.0 ± 0.9
23[c]		DBU	Neat	19.4	27.6	20.3	31.3	98.6
24		DMAP		26.1	35.0	26.0	9.4	96.5
25		Et_3N		24.6 ± 0.9	32.8 ± 0.5	28.1 ± 0.4	9.7 ± 0.4	95.2 ± 1.5
26[c]		DBU		28.2	25.2	20.3	17.5	91.2
27[d]		DBU		53.9	21.1	12.1	7.4	94.5
28[c]		DMAP	THF	23.5	44.0		23.7	91.2
29[c]		Et_3N		20.6	46.3		22.4	89.3
30[d]		Et_3N		54.7±1.2	20.3±1.4	15.5±0.5	6.0±0.6	96.5±0.4
31[c]	**D**	DBU		15.0	23.4	22.1	33.7	94.2
32[c]		DMAP	EtOH	18.3	24.5	21.6	25.5	89.9
33[c]		Et_3N		18.2	26.0	23.7	23.2	91.1
34[c]		DBU		23.4	24.5	23.3	25.4	96.6
35[c]		DMAP	Neat	21.9	35.7	23.5	16.7	97.8
36[c]		Et_3N		20.6	34.7	24.6	6.9	86.8

[a] Conditions: [FF]/[HMF] ratio = 1:1; pre-catalyst loading = 5 mol% (relative to total FF + HMF); solvent = 10 mL; reaction heated at 80 °C for 24 h; all reactions performed under inert, N_2, atmosphere. [b] Determined by ^1H NMR (when standard deviation is reported, the reaction was performed *four times* under identical conditions). [c] [FF]/[HMF] ratio = 1:2. [d] [FF]/[HMF] ratio = 2:1. [e] Isolated yield.

No pre-catalyst, in a solvent and with a [FF]/[HMF] ratio of 1:1, was able to produce more than 48.8% cross-coupled furoins (run 10). When the furaldehyde ratio was changed to 1:2 [FF]/[HMF], a slight increase in conversion to cross-coupled furoins was obtained, observed in runs 20 and 33 where conversions of 49.2% and 49.7% were achieved. However, the conversion to **2** and **3** combined was still below 50%. When the FF ratio was increased to [FF]/[HMF] = 2/1, the transformation to cross-coupled products did not increase (runs 27 and 30). Several of the reactions performed neat afforded conversions to products **2** and **3** combined of around 60% (58.9%, run 12; 60.8%, run 13; 60.9%, run 25; 60.9%, run 35; and 59.3%, run 36), but this level of conversion was obtained with pre-catalysts **B**, **C**, and **D** suggesting that the lack of solvent was chiefly responsible for chemoselectivity not the pre-catalyst. Finally, when a base was employed to activate the NHC pre-catalysts, the selective formation of cross-coupled products was also slightly affected: Et_3N generally afforded a higher amount of cross-coupled products **2** and **3**, while no correlation was observed when using DBU or DMAP as base. In short, the results for each pre-catalyst follow the same general trend of about 40-45% cross-coupling despite which solvent used, but with better values of about 60% under neat conditions regardless of the steric or electronic character of the catalyst. These results led us conclude that any apparent chemoselectivity observed for the current FF + HMF coupling reaction is not a factor of catalyst structural characteristics.

As pre-catalyst **D** gave the overall best performance on the cross-coupling reaction, we examined the product distribution as a function of time using this catalyst system. As shown by Figure 2.10, the cross-coupling of FF and HMF (in a 1:2 ratio) at 60 °C is rapid, achieving 93.5% total conversion to the coupling products in only 9 min. However, there was no noticeable selectivity for the formation of any of the four coupling products, thus giving essentially a

statistical product distribution over the time period monitored. The same reaction carried out at 80 °C enhanced the rate of the coupling reaction but did not improve the selectivity.

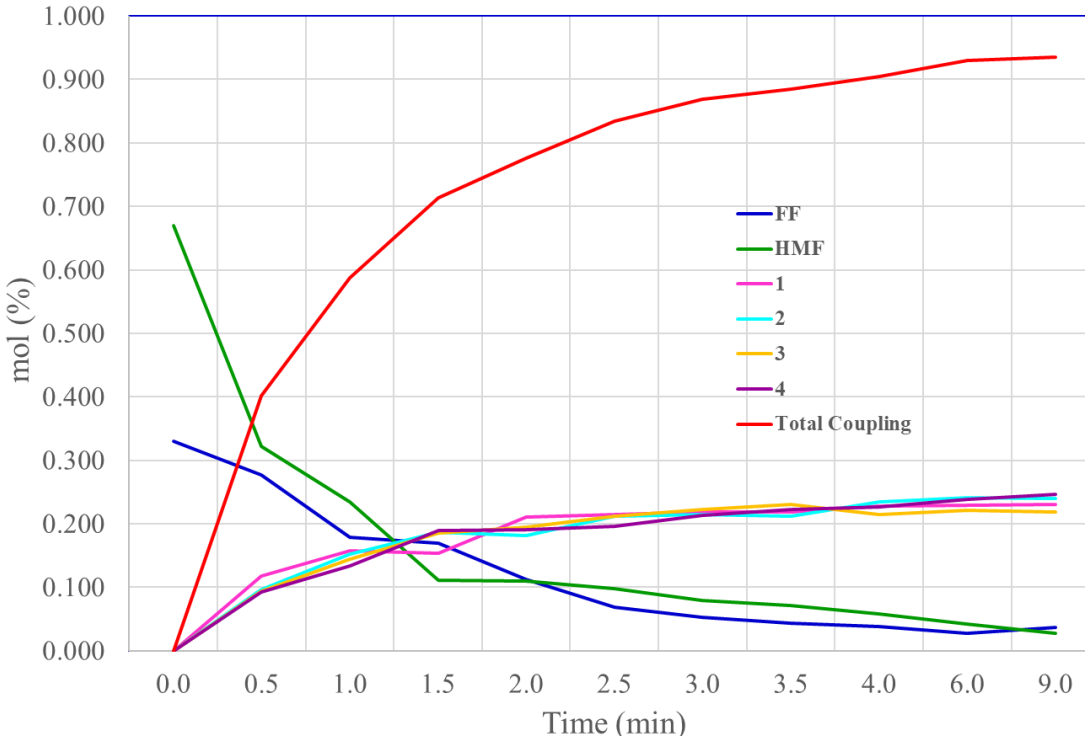

Figure 2.10. Product distribution vs. time for the cross-coupling of FF + HMF (in a 1:2 ratio) by pre-catalyst **D** + Et_3N in EtOH at 60 °C.

Figure 2.11 outlines the proposed mechanism for the NHC-catalyzed coupling of furaldehydes into furoins via the umpolung condensation.[31,32] In this mechanism, nucleophilic attack of a furaldehyde by an NHC generates the carbene-aldehyde tetrahedral zwitterionic intermediate **I**, followed by proton transfer, which affords the hydroxyl enamine, often referred to as the Breslow intermediate (**II**).[32,50-52] This enaminol intermediate functions as an acyl anion equivalent and attacks a second furaldehyde molecule, forming zwitterionic intermediate **III**. Then proton transfer from the Breslow intermediate's alcohol to the oxygen anion, generated by the nucleophilic addition to the second aldehyde, allows the ketone to form and release the carbene catalyst to

complete the catalytic cycle (Figure 2.11). This sequence results in the ketone forming from the oxygen on the first aldehyde attacked. This coupling process is also termed aldehyde umpolung (i.e., polarity inversion) that converts the electrophilic carbonyl carbon to a nucleophilic center as an acyl anion equivalent.[53-61]

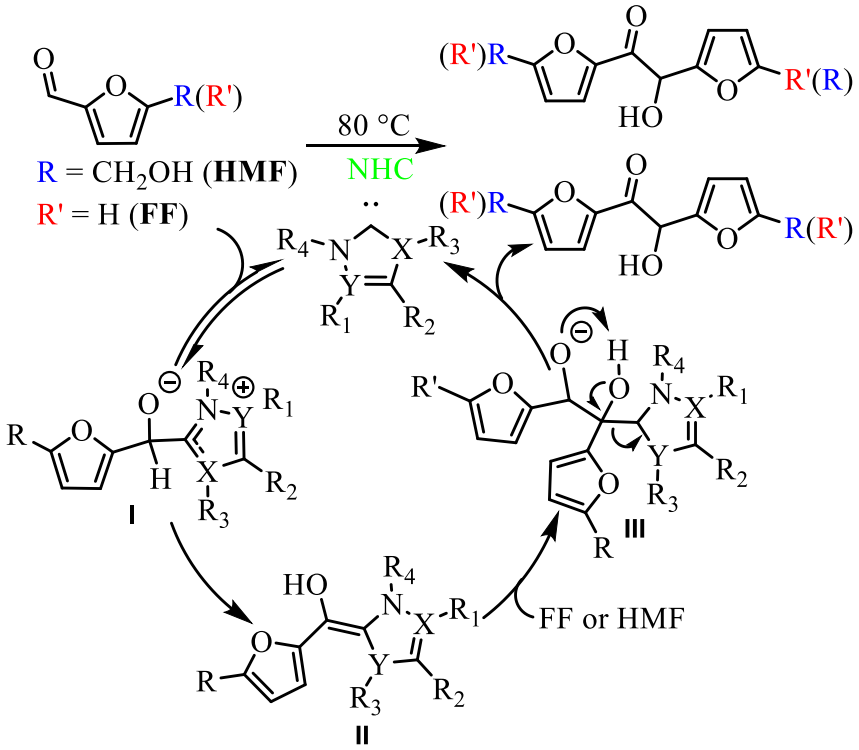

Figure 2.11. Proposed catalytic cycle for the NHC-catalyzed cross-coupling reaction between FF and HMF.

The first step of the overall catalytic cycle is reversible and the differences in the rates of the forward and reverse reaction have been suggested as the cause for the selectivity observed in the coupling of benzaldehydes.[62] When the reverse reaction proceeds slower than the forward reaction, for certain substrates, then the irreversible formation of the Breslow intermediate, from that aldehyde, will be more likely to form. For many of the FF + HMF cross-coupling reactions, slight preference for the formation of **2** over **3** was observed, especially for those reactions performed

under neat conditions where **2** was formed in as much as 10% excess over **3**. The above mechanism allows one to identify which aldehyde is attacked by the carbene first: in the case of product **2,** HMF is the aldehyde initially attacked by the carbene. Hence, the slight preference observed in these experiments may be attributed to a slight decrease in the rate of the reverse reaction allowing more time to form the Breslow intermediate. The stabilization of the acyl anion (Step I, Figure 2.11) in a polar solvent may increase the reverse rate for the adduct formation with HMF thus preventing the preference for HMF carbene formation of the Breslow intermediate.

Selective oxidation of cross-coupled products 2 and 3. We reasoned that α-hydroxy-ketone isomers **2** and **3**, upon selective oxidation under suitable conditions, can be converted into the same compound, α-diketone **5** (Figure 2.12). To this end, we adopted the metal-free oxidation method for converting α-hydroxy-ketones into the corresponding α-diketones by DBU/air.[37] Hence, treatment of the isolated **2** and **3** with DBU (10 mol%) at 70°C open to air led to a total substrate conversion of 86.7% (determined by ^{1}H NMR) and an isolated yield of 75.8% for the pure α-diketone **5**. The NMR spectra of product **5** (Figure 2.13) exhibit most of the same features as the spectra for the furoin precursors, featuring three sets of signals for the FF furan ring (δ 8.23, 7.64, 6.83 ppm), two sets of signals for the HMF furan ring (δ 7.59, 6.65 ppm), and the –CH_2OH group (δ 5.64, 4.55 ppm). Most notably, relative to its furoin precursors, the H_a proton on the FF furan C5 position in **5** is further downfield shifted to 8.26 ppm as a result of additional de-shielding provided by the α-ketones, and the ^{13}C NMR exhibits an additional signal at 178.37 ppm, indicative of the new carbonyl carbon. The 2D gCOSY NMR (Figure 2.14) reveals the correct atom connectivity in the structure.

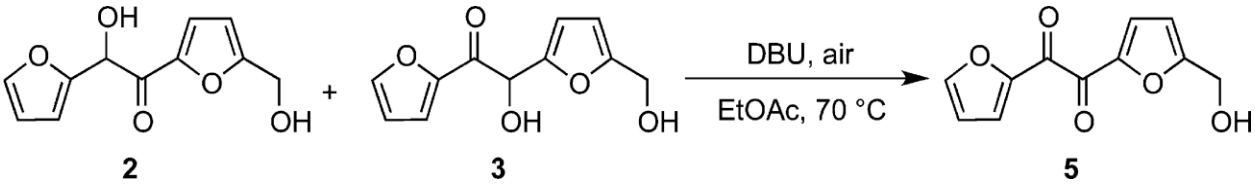

Figure 2.12. Selective oxidation of *α*-hydroxy-ketones **2** and **3** to α-diketone **5**.

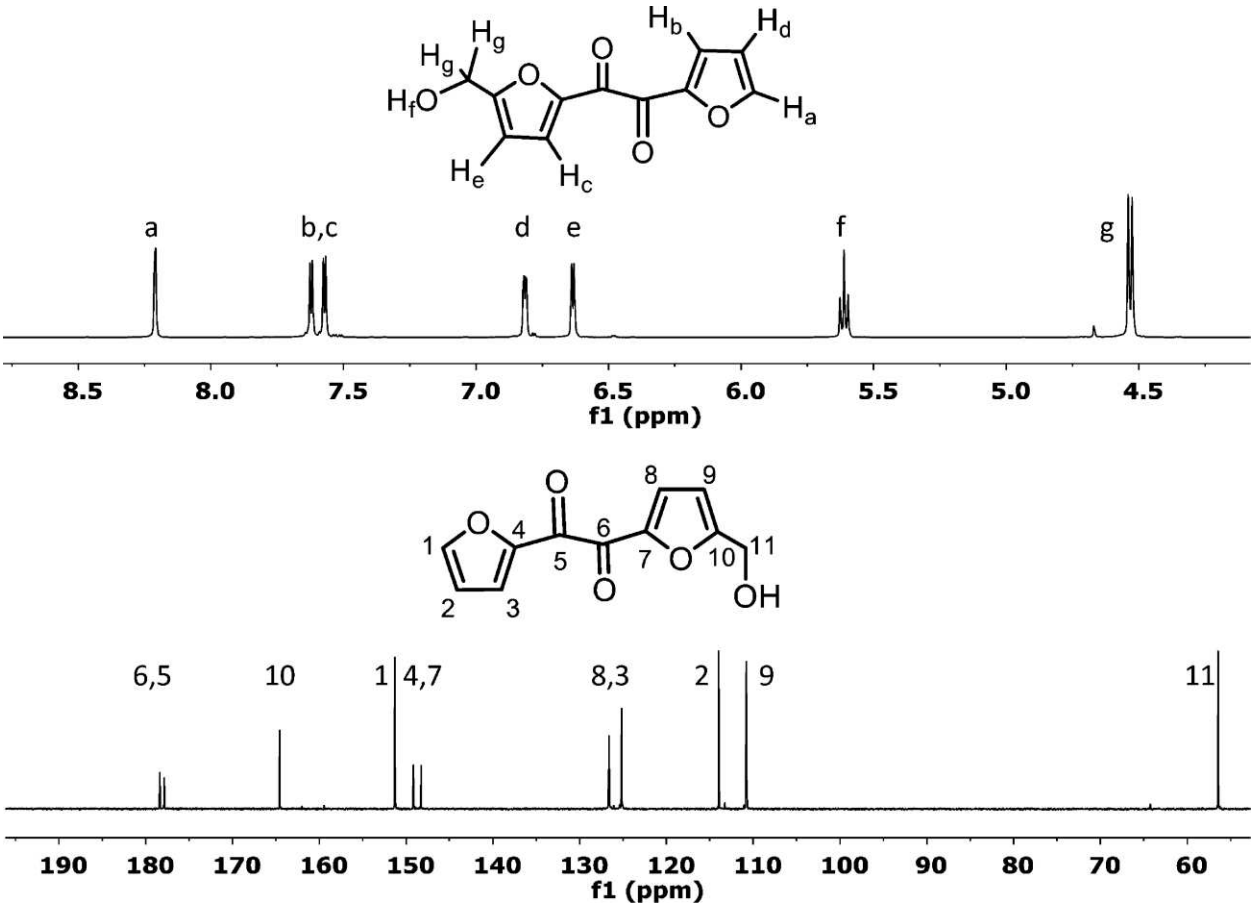

Figure 2.13. ^{1}H NMR (top) and ^{13}C NMR (bottom) of **5** (DMSO-d_6, 25 °C).

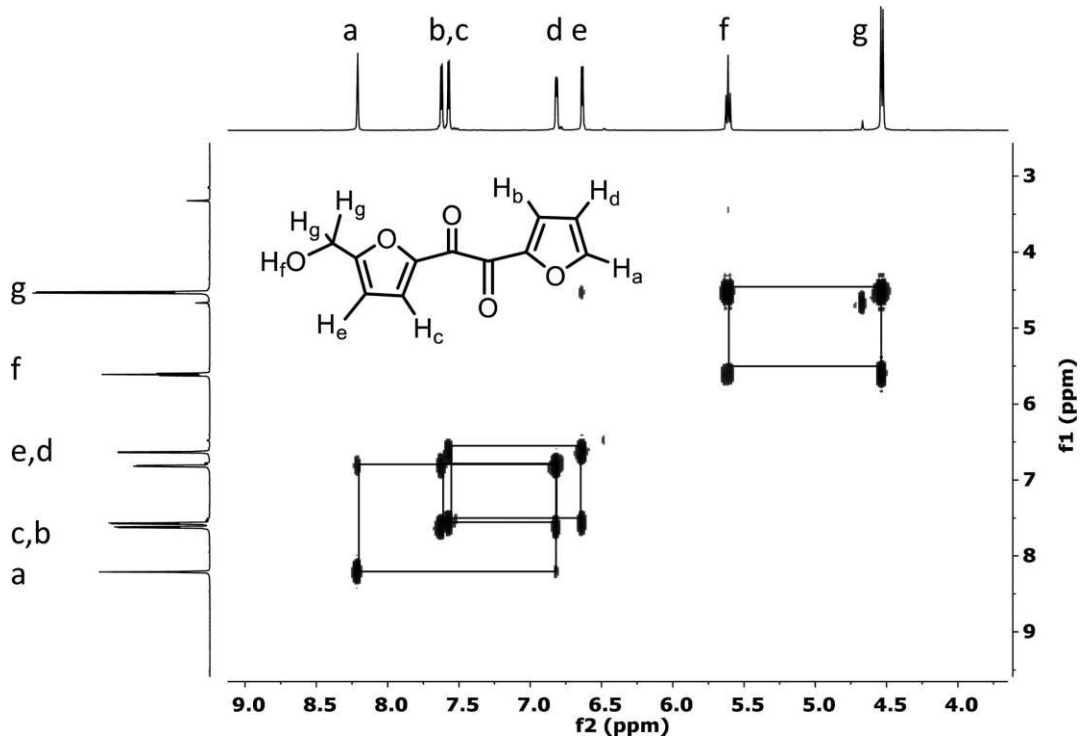

Figure 2.14. gCOSY NMR of **5** (DMSO-d_6, 25 °C).

Performing this reaction in a one-pot fashion using a mixture of coupled products, derived from the direct cross-coupling reaction of FF and HMF, led to a much lower isolated yield of **5** (30%), due to simultaneous oxidation of C_{10} and C_{12} furoins **1** and **4** into their α-diketone derivatives thus complicating the product separation and isolation. Overall, this metal-free, in-air oxidation reaction represents a simple and efficient route to obtain another FF and HMF upgraded product with a new functional handle and the furan rings possessing less electron density.

2.4. CONCLUSION

We have investigated the cross-coupling reaction of bio-furaldehydes FF and HMF in the presence of the *in-situ* generated organic NHC catalysts in detail. The NHC-catalyzed coupling

reaction of FF and HMF in solution results in a statistical mixture of all four possible coupling products including homo-coupled C_{10} and C_{12} furoins **1** and **4**, as well as cross-coupled C_{11} furoins **2** and **3**, regardless of the electronics or sterics of the NHC pre-catalyst used. Slight preference for the cross-coupled products (~60% **2** + **3** combined) under neat conditions was achieved, but the catalyst choice had no noticeable effect, further suggesting that NHC sterics and electronics have no bearing on selectivity for the FF + HMF cross-coupling. Choice of base, solvent, and catalyst can improve the total conversion significantly but not the coupling chemoselectivity.

Isolation and characterization of the cross-coupled products **2** and **3** were successful when high-performance flash column chromatography was utilized. The two cross-coupled products **2** and **3** were obtained in an isolated yield of 48.1%, and further separation of these two was also achieved affording an isolated yield of 22.2% and 19.9% for C_{11} furoin **2** and **3**, respectively. The isolated pure **2** and **3** were fully characterized by ^{1}H NMR, ^{13}C NMR, 2D correlation NMR, HRMS, and single crystal X-ray diffraction (for **3**) to confirm the isomeric structures. Furthermore, a simple selective oxidation reaction under metal-free/in-air oxidation conditions converted the isomeric α-hydroxy-ketones **2** and **3** into the single α-diketone furil structure **5**. Further utilization of the new multifunctional C_{11} furoins **2** and **3** and their α-diketone derivative **5** as bio-derived difuranic building blocks for the synthesis of functional polymers and conversion into biofuels is currently underway. As the conversion of cellulosic biomass such as corn stalk forms a mixture of FF and HMF, the effective cross-coupling system developed by this work should provide insight into the future development of upgrading via both homo- and cross-coupling reactions of such FF and HMF mixture directly, without the need to separate these two furaldehyde's.

References

(1) Caes, B. R.; Teixeira, R. E.; Knapp, K. G.; Raines, R. T. Biomass to furanics: renewable routes to chemicals and fuels. *ACS Sustainable Chem. Eng.* **2015***, 3,* 2591−2605.

(2) Alonso, D. M.; Wettstein, S. G.; Dumesic, J. A. Gamma-valerolactones, a sustainable platform molecule derived from lignocellulosic biomass. *Green Chem.* **2013**, *15*, 85-90.

(3) Gallezot, P. Conversion of biomass to selected chemical products. *Chem. Soc. Rev.* **2012**, *41*, 1538–1558.

(4) Alonso, D. M.; Bond, J. Q.; Dumesic, J. A. Catalytic conversion of biomass to biofuels. *Green Chem.* **2010**, *12*, 1493−1513.

(5) Corma, A.; Iborra, S.; Velty, A. Chemical routes for the transformation of biomass into chemicals. *Chem. Rev.* **2007**, *107*, 2411−2502.

(6) Corma, A.; Huber, G. W. Synergies between bio- and oil refineries for the production of fuels from biomass. *Angew. Chem. Int. Ed.* **2007**, *46*, 7184–7201.

(7) Huber, G. W.; Iborra, S.; Corma, A. Synthesis of transportation fuels from biomass: chemistry, catalysts, and engineering. *Chem. Rev.* **2006**, *106*, 4044−4098.

(8) Wang, T.; Nolte, M. W.; Shanks, B. H. Catalytic dehydration of C6 carbohydrates for the production of hydroxymethylfurfural. *Green Chem.* **2014**, *16*, 548−572.

(9) Saha, B.; Abu-Omar, M. M. Advances in 5-hydroymethylfurfural production from biomass in biphasic solvents. *Green Chem.* **2014**, *16*, 24−38.

(10) Teong, S. P.; Yi, G.; Zhang, Y. Hydroxymethylfurfural production from bioresources; past, present and future. *Green Chem.* **2014**, *16*, 2015−2026.

(11) van Putten, R.-J.; van der Waal, J. C.; de Jong, E.; Rasrendra, C. B.; Heeres, H. J.; de Vries, J. G. Hydroxymethylfurfural, a versatile platform chemical made from renewable resources. *Chem. Rev.* **2013**, *113*, 1499−1597.

(12) Lange, J.-P.; van der Heide, E.; van Buijtenen, J.; Price, R. Furfural–a promising platform for lignocellulosic biofuels. *ChemSusChem* **2012**, *5*, 150−166.

(13) Rosatella, A. A.; Simeonov, S. P.; Frade, R. F. M.; Afonso, C. A. M. Conversion of carbohydrates and lignocellulosic biomass into 5-hydroxymethylfurural using $AlCl_3 \cdot 6H_2O$ catalyst in a biphasic solvent system. *Green Chem.* **2011**, *13*, 754−793.

(14) Zakrzewska, M. E.; Bogel-Łukasik, E.; Bogel-Łukasik, R. Ionic liquid-mediated formation of 5-hydroxymethylfurfural–a promising biomass-derived building block. *Chem. Rev.* **2011**, *111*, 397−417.

(15) Ståhlberg, T.; Fu, W.; Woodley, J. M.; Riisager, A. Synthesis of 5-(hydroymethyl)furfural in ionic liquids: paving the way to renewable chemicals. *ChemSusChem* **2011**, *4*, 451−458.

(16) James, O. O.; Maity, S.; Usman, L. A.; Ajanaku, K. O.; Ajani, O. O.; Siyanbola, T. O.; Sahu, S.; Chaubey, R. Towards the conversion of carbohydrate biomass feedstocks to biofuels via hydroxymethylfurfural. *Energy Environ. Sci.* **2010**, *3*, 1833–1850.

(17) Bozell, J. J.; Petersen G. R. Technology development for the production of biobased products from biorefinery carbohydrates–the US Department of Energy's "Top 10" revisited. *Green Chem.* **2010**, *12*, 539–554.

(18) *Top Value Added Chemicals from Biomass*, Werpy, T.; Petersen, G., Eds. U.S. Department of Energy (DOE) report: DOE/GO-102004-1992, 2004.

(19) Bohre, A.; Dutta, S.; Saha, B.; Abu-Omar, M. M. Upgrading furfurals to drop-in biofuels: an overview. *ACS Sustainable Chem. Eng.* **2015***, 3,* 1263−1277.

(20) Wegenhart, B. L.; Liu, S.; Thom M.; Stanley, D.; Abu-Omar, M. M. Solvent-free methods for making acetals derived from glycerol and furfural and their use as a biodiesel fuel component. *ACS Catal.* **2012**, *2*, 2524–2530.

(21) Balakrishnan, M.; Sacia, E. R.; Bell, A. T. Etherification and reductive etherification of 5-(hydroxymethyl)furans: 5-(alkoxymethyl)furfurals and 2,5-bis(alkoxymethyl)furans as potential bio-diesel candidates. *Green Chem.* **2012**, *14*, 1626–1634.

(22) Corma, A.; de la Torre, O.; Renz, M. Production of high quality diesel from cellulose and hemicellulose by the Sylvan process: catalysis and process variables. *Energy Environ. Sci.* **2012**, *5*, 6328–6344.

(23) Corma, A.; de la Torre, O.; Renz, M.; Villandier, N. Production of high-quality diesel from biomass waste products. *Angew. Chem. Int. Ed.* **2011**, *50*, 2375–2378.

(24) King, A. E.; Brooks, T. J.; Tian, Y.-H.; Batista, E. R.; Sutton, A. D. Understanding ketone hydrodeoxygenation for the production of fuels and feedstocks from biomass. *ACS Catal.* **2015**, 5, 1223–1226.

(25) Sutton, A. D.; Waldie, F. D.; Wu, R.; Schlaf, M.; Silks, L. A. P., III; Gordon, J. C. The hydrodeoxygenation of bioderived furans into alkanes. *Nat. Chem.* **2013,** *5,* 428–432.

(26) Huber, G. W.; Chheda J. N.; Barrett C. J.; Dumesic J. A. Catalytic conversion of biomass to monofunctional hydrocarbons and targeting liquid fuel classes. *Science* **2005**, *308*, 1446–1450.

(27) Liu, D.; Chen, E. Y.-X. Organocatalysis in biorefining for biomass conversion and upgrading. *Green Chem.* **2014**, *16*, 964–981.

(28) Kluger, R.; Tittmann, K. Thiamin diphosphate catalysis: enzymic and nonenzmic covalent intermediates. *Chem. Rev*. **2008**, *108*, 1797–1833.

(29) Breslow, R. On the mechanism of thiamine action. IV.[1] evidence from studies on model systems. *J. Am. Chem. Soc.* **1958**, *80*, 3719–3726.

(30) Breslow, R. rapid deutrium exchange in thiazolium salts. *J. Am. Chem. Soc.* **1957**, *79*, 1762–1763.

(31) Liu, D.; Zhang, Y.; Chen, E. Y.-X. Organocatalytic upgrading of the key biorefining building block by a catalytic ionic liquid and N-heterocyclic carbens. *Green Chem.* **2012**, *14*, 2738–2746.

(32) Liu, D.; Chen, E. Y.-X. Diesel and alkane fuels from biomass by organocatalysis and metal-acid tandem catalysis. *ChemSusChem* **2013**, *6*, 2236–2239.

(33) Wegenhart, B. L.; Yang, L.; Kwan, S. C.; Harris, R.; Kenttaemaa, H. I.; Abu-Omar, M. M. From furfural to fuel: synthesis of furoins by organocatalysis and their hydrodeoxygenation by cascade catalysis. *ChemSusChem* **2014**, *7,* 2742–2747.

(34) Liu, D.; Chen, E. Y. X. Integrated catalytic process for biomass conversion and upgrading to C_{12} furoin and alkane fuel. *ACS Catal.* **2014**, *4,* 1302–1310.

(35) Mou, Z.; Feng, S.; Chen, E. Y.-X. Bio-based difuranic polyol monomers and their derived linear and cross-linked polyurethanes. *Polym. Chem.* **2016**, *7*, 1593−1602.

(36) Kabro, A.; Escudero-Adán, E. C.; Grushin, V. V.; van Leeuwen, P. W. N. M. Biomass conversion to high value chemicals: from furfural to chiral hydrofuroins in two steps. *Org. Lett.* **2012**, *14*, 4014–4017.

(37) Shimakawa, Y.; Morikawa, T.; Sakaguchi, S. Facile route to benzils from aldehydes via NHC-catalyzed benzoin condensation under metal-free conditions. *Tetrahedron Lett.* **2010,** *51,* 1786–1789.

(38) Hashmi, A. S. K.; Wölfle, M.; Teles, J. H.; Frey, W. Bisphenols from furfurals by organocatalysis and gold catalysis. *Synlett.* **2007**, 1747–1752.

(39) Enders, D.; Kallfass, U. An efficient nucleophilic carbene catalyst for the asymmetric benzoin condensation. *Angew. Chem. Int. Ed.* **2002**, *41*, 1743–1745.

(40) Stetter, H.; Raemsch, R. Y.; Kuhlmann, H. Über die präparative nutzung der thiazoliumsalz-katalysierten acyloin- und benzoin-bildung, I. herstellung von einfachen acyloinen und benzoinen. *Synthesis* **1976**, 733–735.

(41) Zang, H.; Chen, E. Y. X. Organocatalytic upgrading of furfural and 5-hydroxymethyl furfural to C_{10} and C_{12} furoins with quantitative yield and atom-efficiency. *Int. J. Mol. Sci.* **2015**, *16,* 7143–7158.

(42) Wang, Lu.; Chen, E. Y.-X. Recyclable supported carbene catalysts for high-yielding self-condensation of furaldehydes into C_{10} and C_{12} furoins. *ACS Catal.* **2015**, *5*, 6907−6917.

(43) Wang, Lu.; Chen, E. Y.-X. An interchangeable homogeneous ⇔ heterogeneous catalyst system for furfural upgrading. *Green Chem.* **2015**, *17*, 5149−5153.

(44) Donnelly, J.; Müller, C. R.; Wiermans, L.; Chuck, C. J.; de María, P. D. Upgrading biogenic furans: blended C10–C12 platform chemicals via lyase-catalyzed carboligations and formation of novel C12 – choline chloride-based deep-eutectic-solvents. *Green Chem.* **2015**, *17*, 2714−2718.

(45) Enders, D.; Breuer, K.; Kallfass, U.; Balensiefer, T. Preparation and application of 1,3,4-triphenyl-4,5-dihydro-1H-1,2,4-triazol-5-ylidene, a stable carbene. Synthesis 2003, 1292–1295.

(46) Enders, D.; Breuer, K.; Raabe, G.; Runsink, J.; Teles, J. H.; Melder, J.-P.; Ebel, K.; Brode, S. Preparation, structure, and reactivity of 1,3,4-triphenyl-4,5-dihydro- 1H-1,2,4-triazol-5-ylidene, a new stable carbene. Angew. Chem. Int. Ed. 1995, 34, 1021–1023.

(47) Piel, I.; Pawelczyk, M. D.; Hirano, K.; Froehlich, R.; Glorius, F. A family of thiazolium salt

derived N-heterocyclic carbenes (NHCs) for organocatalysis: synthesis, investigation and application in cross-benzoin condensation. Eur. J. Org. Chem. 2011, 5475–5484.

(48) Langdon, S. M.; Wilde, M. M. D.; Thai, K.; Gravel, M. Chemoselective N-heterocyclic carbene-catalyzed cross-benzoin reactions: importance of the fused ring in triazolium salts. J. Am. Chem. Soc. 2014, 136, 7539–7542.

(49) O'Toole, S. E.; Rose, C. A.; Gundala, S.; Zeitler, K.; Connon, S. J. Highly chemoselective direct crossed aliphatic−aromatic acyloin condensations with triazolium-derived carbene catalysts. *J. Org. Chem.* **2011**, *76*, 347–357.

(50) Berkessel, A.; Yatham, V. R.; Elfert, S.; Neudörfl, J.-M. Characterization of the key intermediates of carbene-catalyzed umpolung by NMR spectroscopy and X-ray diffraction: Breslow intermediates, homoenolates, and azolium enolates. *Angew. Chem. Int. Ed.* **2013**, *52*, 11158–11162.

(51) Maji, B.; Mayr, H. Structures and ambident reactivities of azolium enolates. *Angew. Chem. Int. Ed.* **2013**, *52*, 11163–11167.

(52) Berkessel, A.; Elfert, S.; Yatham, V. R.; Neudörfl, M.-M.; Schlörer, N. E.; Teles, J. H. Umpolung by N-heterocyclic carbenes: generation and reactivity of the elusive 2,2-diamino enols (Breslow intermediates). *Angew. Chem. Int. Ed.* **2012**, *51*, 12370–12374.

(53) Flanigan, D. M.; Romanov-Michailidis, F.; White, N. A.; Rovis, T. Organocatalytic reactions enabled by N-heterocyclic carbenes. *Chem. Rev.* **2015**, *115*, 9307−9387.

(54) Ryan, S. J.; Candish, L.; Lupton, D. W. Acyl anion free N-heterocyclic carbene organocatalysis. *Chem. Soc. Rev.* **2013**, *42*, 4906−4917.

(55) Grossmann, A.; Enders, D. N-Heterocyclic carbene catalyzed domino reactions. *Angew. Chem. Int. Ed.* **2012**, *51*, 314−325.

(56) Bugaut, X.; Glorius, F. Organocatalytic umpolung: N-heterocyclic carbenes and beyond. *Chem. Soc. Rev.* **2012**, *41*, 3511−3522.

(57) Biju, A. T.; Kuhl, N.; Glorius, F. Extending NHC-catalysis: coupling aldehydes with unconventional reaction partners. *Acc. Chem. Res.* **2011**, *44*, 1182−1195.

(58) Moore, J. L.; Rovis, T. Carbene catalysts. *Top. Curr. Chem.* **2009**, *291*, 77−144.

(59) Marion, N.; Díez-González, S.; Nolan, S. P. N-heterocyclic carbenes as organocatalysts. *Angew. Chem. Int. Ed.* **2007**, *46*, 2988−3000.

(60) Enders, D.; Niemeier, O.; Henseler, A. Organocatalysis by N-heterocyclic carbenes. *Chem. Rev.* **2007**, *107*, 5606−5655.

(61) Bourissou, D.; Guerret, O.; Gabbaï, F. P.; Bertrand, G. Stable carbenes. *Chem. Rev.* **2000**, *100*, 39−91.

(62) Collett, C. J.; Massey, R. S.; Taylor, J. E.; Maguire, O. R.; O'Donoghue, A. C.;Smith, A. D. Rate and equilibrium constants for the addition of N-heterocyclic carbenes benzaldehydes: a remarkable 2-substituent effect. *Angew. Chem. Int. Ed.* **2015**, *54*, 6887–6892.

Chapter 3

Difuranic Diols for Renewable Polymers with Pendent Furan Rings

3.1. Synopsis

Organocatalyzed cross-coupling of biomass platform chemicals furfural and 5-hydroxymethylfurfual has been utilized to prepare a pair of constitutional isomers of difuranic C_{11} diols. Polycondensation of the diols with three diacyl chlorides and polyaddition with two diisocyanates produce linear polyesters and polyurethanes, respectively, with furan rings residing in both the polymer backbone and pendent positions. One monomer isomer has a steric advantage, leading to higher molecular weight polymers. Thermal and mechanical properties of the resulting polymers can be tuned in a broad range by varying the monomer pairs. In addition, a thermally reversible cross-linked network has been realized by applying the Diels-Alder reaction between a bis-maleimide cross-linker and the furan rings located at both the backbone and pendent positions. This property, coupled with formation of a significant amount (up to 34%) of stable carbonaceous materials when heating the difuranic polymers to 700 °C, demonstrates some promising features of this class of new difuranic polymers.

3.2. Introduction

The currently unsustainable utilization of petroleum-based chemical building blocks stimulates intense research to seek renewable sources of industrially important carbon-based compounds.[1,2] As cellulosic material represents the most abundant, naturally occurring carbon-based organic compound on Earth, it provides an abundant and underutilized annually renewable source of

building blocks for fuels, fine chemicals, and monomers for the polymer manufacturing industry.[3] There are numerous examples of efficient routes to furfural (FF) and 5-hydroxyfurfural (HMF) from cellulose that would otherwise be wasted by the agriculture and forestry industries.[4-12] The cationic polymerization of furfuryl alcohol derived from the reduction of FF has produced heavily cross-linked polymers suitable for corrosion resistant coatings as well as materials with significant endurance to heat and acidic conditions,[13] while 2,5-furandicarboxylic acid obtained from the oxidation of HMF has gained significant attention as a possible replacement for petroleum-based terephthalic acid used in the synthesis of the industrially important polyester, poly(ethylene terephthalate) (PET).[14]

The furan equivalent of PET, poly(ethylene furanoate) (PEF) is bio-sourced and exhibits significantly improved gas barrier properties relative to PET, in addition to having attractive mechanical and thermal characteristics.[15-17] Burgess *et al.* suggested that the combination of the increased polarity and angled geometry of the furan ring, which inhibits ring flipping, decreases the ability of penetrants to permeate across polymer membranes of PEF.[15] The effects of pendent groups on gas transport properties of the polymers with rigid backbones were analyzed by Pixton *et. al.*, and they found that the introduction of structural changes that inhibit chain packing, such as bulky pendent groups, can lead to materials with selective permeability appropriate for use as gas separation membranes.[18-19] The increased polarity of the furan ring results in a diene character not present in other polymers with backbones based on rigid aromatic rings.

In organic synthesis, furan-based compounds have been widely used as a diene to react with an appropriate dienophile via the Diels-Alder (DA) reaction.[20-25] In the polymeric materials field the thermally reversible DA cycloaddition between furan rings and maleimides was used to develop polymers with thermal recyclability and self-healing behavior.[26-29] For example, Wudl

and co-workers employed a four-furan-based monomer as a multi-diene and a three-maleimide compound as a multi-dienophile to develop a self-remendable polymeric material under mild conditions.[30] Yoshie and co-workers prepared 2,5-bis(hydroxymethyl)furan-based (co)polyesters and systematically investigated the self-healing ability in the presence of a series of maleimides.[31-32] We recently reported a novel furan-based unsaturated polyester bearing C=C bonds, prepared by the proton-transfer polymerization of furfural dimethacrylate, which showed the unique self-curing ability (without any additional curing agents) to a cross-linked material.[33]

We have been particularly interested in rigid difuranic compounds such as C_{12} 5,5'-dihydroxymethyl furoin (DHMF)[34] and 5,5'-bihydroxymethyl furil,[35-37] conveniently prepared from organocatalyzed self-condensation coupling of HMF and selective oxidation,[34,38] as precursors for diesel and jet fuels and building blocks for polymeric materials such as polyesters and polyurethanes (PUs).[36, 39-40] However, such difuranic polymers synthesized so far have all the furan moieties located on the backbone of the polymer chains, which limited accessibility of the reactive furan rings for post-modifications or curing. In this contribution, we report the synthesis of a series of new linear polyesters and PUs with furan rings residing in both the polymer backbone and pendent positions, using new rigid difuranic C_{11} diol monomers synthesized from the organic *N*-heterocyclic carbene (NHC) catalyzed cross-coupling of FF and HMF.[41] These diols with side-chain furan rings were subsequently utilized to produce unsaturated polyesters and PUs bearing C=C double bonds and exhibiting a wide range of glass transition temperature (T_g) values and storage moduli.

3.3. Results and Discussion

Difuranic Diols from Cross-Coupling of HMF and FF. The two diol-functionalized difuranic C_{11} monomers **A** and **B** were prepared through the NHC-catalyzed umpolung cross-coupling of FF and HMF (Figure 3.1).[41] In our previous work, attempts were made to find a catalyst and reaction conditions that would be selective toward either of the cross-coupled products, but only limited selectivity was obtained.[41] The conditions required for this selectivity also increased complexity of product separation due to the requirement of base to activate the pre-catalyst (in the form of a salt).[42,43] The facile oxidation of the α-hydroxyl to ketone catalyzed by base in the presence atmospheric oxygen [44] rendered that method not desirable for the preparation of C_{11} diol monomers. The current method utilized a stable NHC-MeOH adduct that, upon heating, undergoes MeOH elimination and release of the active NHC catalyst, 1,3,4-triphenyl-4,5-dihydro-1H-1,2,4-triazol-5-ylidene (TPT),[45] for catalysis. This thermal mode of catalyst generation, devoid of base treatment, inhibits the formation of the α-diketone bi-product.

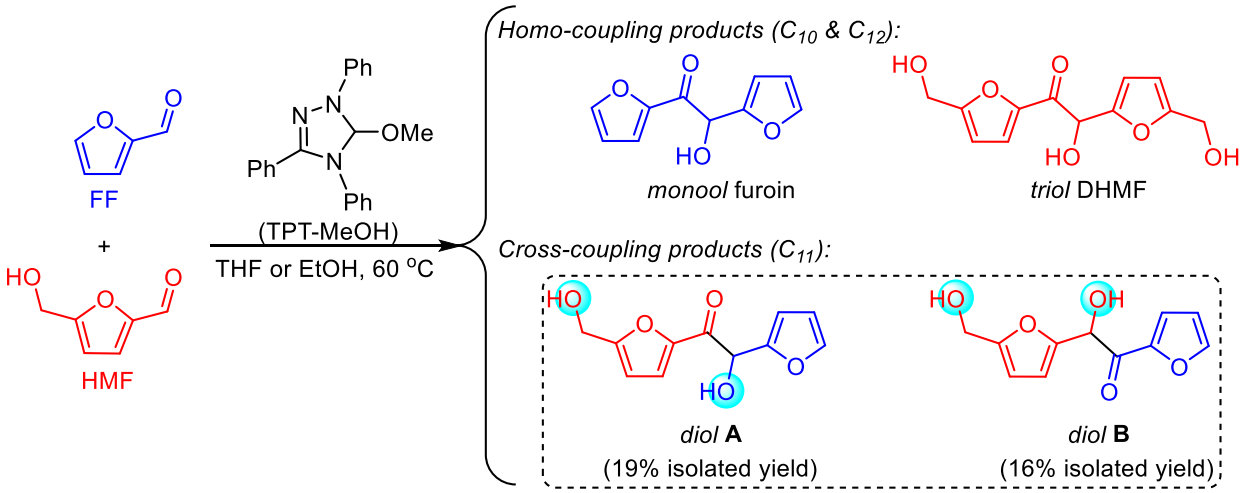

Figure 3.1. Synthetic route to difuranic diol monomers A and B.

The resulting mixture of the difuranic alcohols with carbon counts from C_{10} through C_{12} had the expected distribution with approximately equal portions of each compound (Table 3.1). It has been shown that such furoins can undergo hydrodeoxygenation resulting in linear and branched alkanes with lengths corresponding to the original carbon count,[37, 40, 46-50] and the triol DHMF has been used in the synthesis of several polyesters and PUs.[35-36] The cross-coupling pathway generates C_{11} monomers **A** and **B** with the unique diol structure, which can be separated cleanly from the homo-coupling products C_{10} furoin and C_{12} DHMF using automated flash chromatography. Conversion to cross-coupled C_{11} diols was 43%, based on ^{1}H NMR analysis; however, after the successful separation into monomers **A** and **B,** isolated yield for **A** and **B** were 19% and 16%, respectively (see the Supporting Information for details). Monomers **A** and **B** carry the furan ring moiety in both the main chain as well as in the pendent position, thus presenting an opportunity for constructing unique condensation polymers bearing pendent reactive furan rings.

Polyesters Derived from Difuranic Diols A and B. Initial attempts to synthesize polyesters included deprotonation of the diol with sodium hydride followed by addition of a diacyl chloride, which resulted in only negligible polymer formation. Analysis of the reaction products showed that the majority of the diol was either not deprotonated or oxidized to the corresponding α-diketone. The α-diketone also formed when the diols were heated to melting temperatures, even under inert atmosphere, thus unsuitable for direct polycondensation with a diacid at high temperatures. Next, the Steglich esterification between the diol and a dicarboxylic acid using 4-dimethylaminopyridine as the catalyst was attempted; no polyester was detected when the final products were analyzed. Polycondensation of diols with diacyl chlorides in the presence of base has been shown to be an effective route for the synthesis of many types of polyesters including

furan-based polyesters,[51-53] hence, this route was explored and found to be effective for the current diols as well (Figure 3.2).

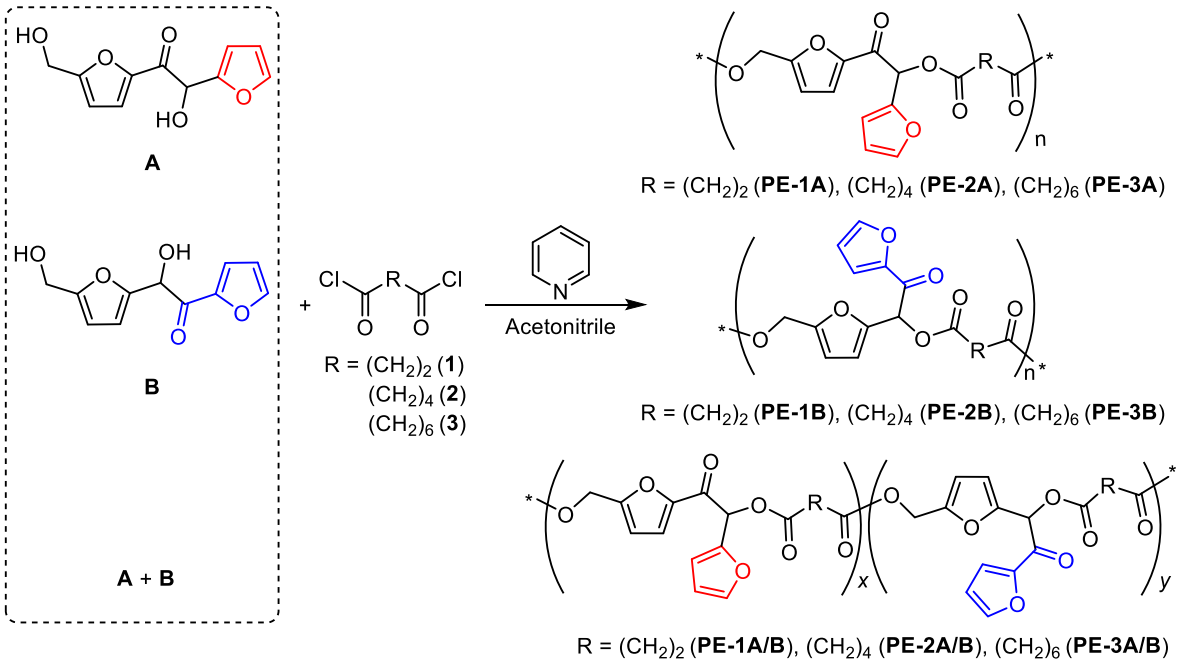

Figure 3.2. Synthesis of linear polyesters with furan pendent groups.

Conditions such as reaction time, temperature, solvent, and base were varied in an effort to maximize yield and number-average molecular weight (M_n) of the resulting polyesters. Our previous work with DHMF polycondensation found that a mixture of tetrahydrofuran (THF) and dichloromethane (DCM) was most effective.[35-36] Starting from this point, a series of polycondensation reactions of difuranic diol **A** or **B**, or **A** + **B** together (denoted as **A/B**) with diacyl chlorides, including succinyl chloride (**1**), adipoyl chloride (**2**), and suberoyl chloride (**3**), were performed in THF and DCM with pyridine (Py) as the base. When THF was used for the reaction with monomer **A** or **B**, precipitation of oligomers limited the polyester yield and M_n, while the reactions performed in DCM with Py afforded a black material An earlier report showed that similar polycondensation performed with triethylamine (Et_3N) resulted in polyester with

significantly less coloring.[35] However, for the present system, substituting Py with Et_3N in DCM induced the formation of the α-diketone by-product, destroying the second alcohol required for the polymerization. When the reaction was performed with Py, no α-diketone byproduct was formed; however, the resulting materials were dark-colored making them unsuitable for applications requiring optical clarity. Thus, Py was subsequently used as the base choice due to its high selectivity for polycondensation, and further experiments were performed to determine the optimal solvent system for these reactions in terms of monomer and polymer solubility as well as the resulting polyester yield and M_n. After evaluating solvents such as THF, DCM, 1,2-dichloroethane, chloroform, acetonitrile (ACN), and trifluoroethanol, ACN was identified as the best medium for the current polycondensation reactions. Next, reaction temperature was optimized to be 45 °C by striking a balance between the rate of the reaction and the bi-product formation. With the above identified optimized conditions, the full series of the reactions outlined in Figure 3.2 were performed, the results of which were summarized in Table 3.1.

Table 3.1. Polycondensation of Diacyl Chlorides with Difuranic Diol A, B, or A + B [a]

Run #	Sample	Diacyl chloride	Diol	Yield [b] (%)	M_n[c] (kg/mol)	$Đ$[c] (M_w/M_n)	T_g [d] (°C)	T_d [e] (°C)	Residue[e] (%)
1	**PE-1A**	**1**	**A**	80	7.67	1.8	65.9	205	27.3
2	**PE-1B**	**1**	**B**	86	6.32	1.5	67.5	202	31.2
3	**PE-1A/B**	**1**	**A+B**	84	5.41	1.6	61.9	200	30.5
4	**PE-2A**	**2**	**A**	84	20.8	2.3	46.2	215	30.4
5	**PE-2B**	**2**	**B**	80	9.18	1.9	46.4	229	30.0
6	**PE-2A/B**	**2**	**A+B**	87	12.0	2.2	45.7	212	28.2
7	**PE-3A**	**3**	**A**	78	20.6	2.1	26.5	243	19.3
8	**PE-3B**	**3**	**B**	73	9.65	1.8	26.6	238	27.8
9	**PE-3A/B**	**3**	**A+B**	73	8.98	2.0	18.0	250	29.6

[a] Conditions: diol (1 equiv.), diacyl chloride (1 equiv.), pyridine (3 equiv.), temperature = 45 °C, time = 72 h. [b] Isolated yield via precipitation into excess methanol. [c] Determined by GPC in DMF with 0.05 M LiBr. [c] Glass-transition temperature (T_g) determined by DSC. [d] Obtained from TGA (% stable carbonaceous residue at 700 °C).

Characterization of Polyesters. The resulting polyester materials have been characterized by 1D and 2D NMR for chain structure, gel permeation chromatography (GPC) coupled with a multi-angle light scattering detector for absolute molecular weight (M_w and M_n) and dispersity ($Đ$), as well as thermal gravimetric analysis (TGA) and differential scanning calorimetry (DSC) for thermal properties (thermal stability and transitions).

As can be seen from Figure 3.3 that compares the ^{1}H NMR spectrum of monomer **B** with the spectra of its corresponding polyester materials, **PE-1B**, **PE-2B**, and **PE-3B** in DMSO-d_6, the signal corresponding to the side-chain furan proton (a) remained the most deshielded and relatively unchanged at 8.03 ppm, regardless of whether it was on the starting monomer or on any of the corresponding polyesters (Figure 3.3). This observation is consistent with this furan ring not being located at the main-chain backbone but in the pendent position. When looking at the proton signals for the series of polyesters derived from monomer **B**, it was also readily apparent that the proton signals for the difuranic portion did not change noticeably as the length of the methylene (CH_2) bridge between the esters increased. Through the use of gCOSY NMR experiments (Figure 3.4) and the lack of shift for proton (a) in monomer **B** (*vide supra*) after polycondensation, each furan ring proton can be readily assigned for all resulting polyesters (Figure 3.3). This same technique was used to assign the signals for the polyesters resulting from monomer **A**, while assignments of signals for **PE-A/B** products (using the monomer mixture of **A** + **B**) were obtained merely by comparison to the analogous **PE-A** and **PE-B** spectra (Figure S3.8). Looking at other important proton signals, it can be shown that the diol was converted to the polyester by the disappearance of the two hydroxyl proton signals at 5.75 ppm (g) and 5.18 ppm (h), Figure 3.3-1, while the signal at 4.30 ppm (i), corresponding to the protons geminal to the terminal hydroxyl group, down-field

shifted to 5.00 ppm (now labeled as f', f'', and f* in the polyester products, Figure 3.3 to 1-4) when monomer **B** underwent polycondensation with an diacyl chloride.

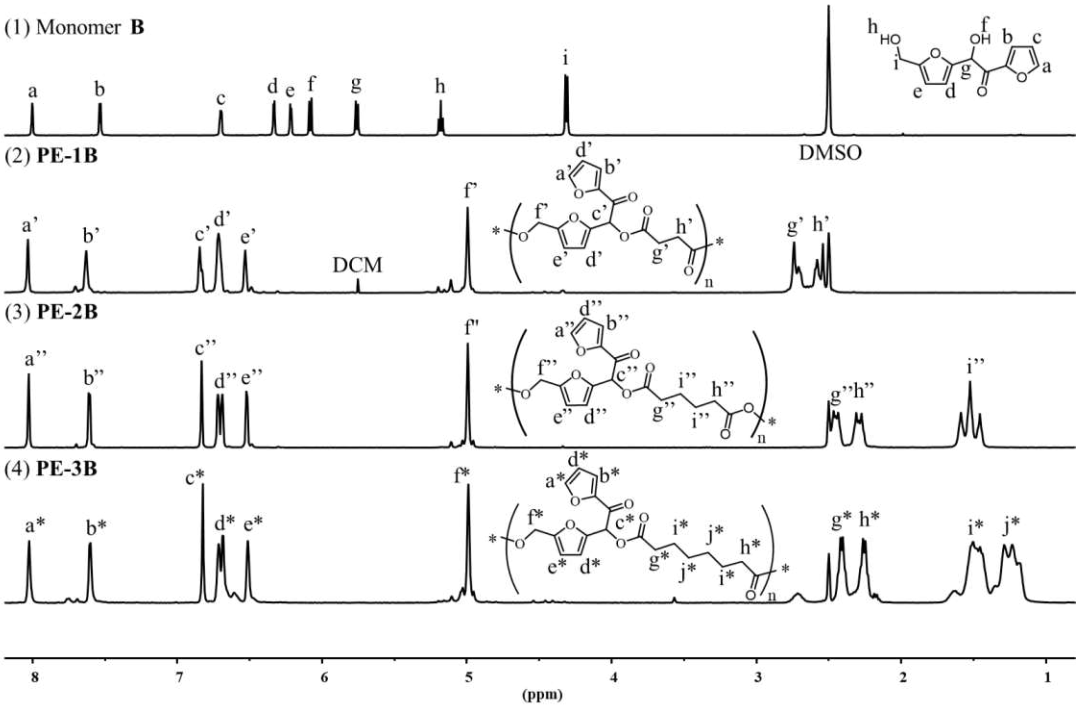

Figure 3.3. Stacked ^{1}H NMR spectra (DMSO-d_6, 25 °C) of monomer **B** (1), **PE-1B** (2), **PE-2B** (3), and **PE-3B** (4).

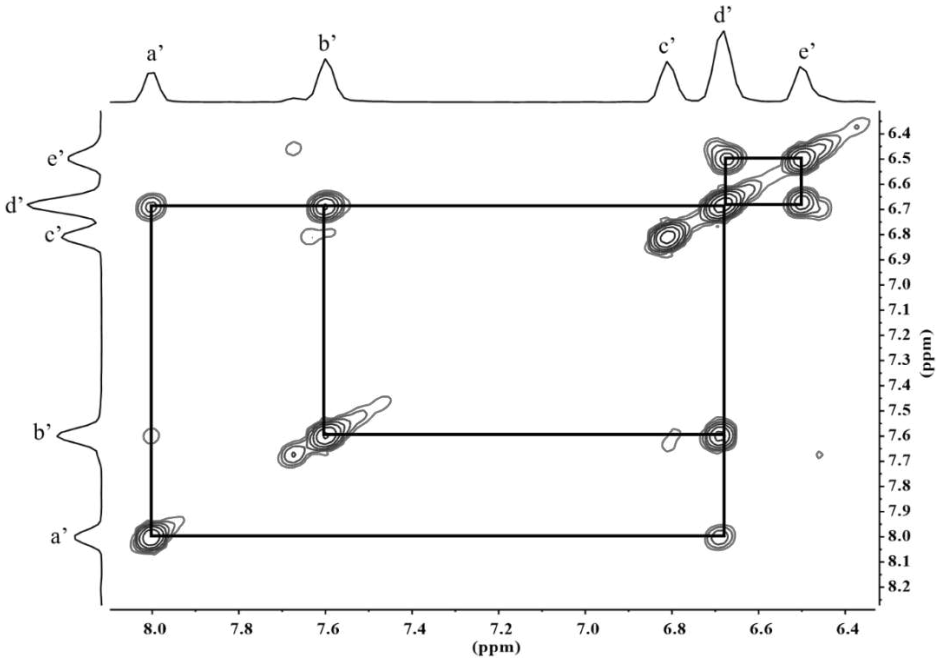

Figure 3.4. gCOSY NMR of **PE-1B** (DMSO-d_6, 25 °C).

The M_n and dispersity ($Đ$) of the resulting polyesters were determined by GPC coupled with a refractive index detector and a Wyatt DAWN HELEOs II multi (18)-angle light scattering detector, performed at 40 °C in DMF with 0.05 M LiBr. The d*n*/d*c* of the polyester was measured to be 0.1038 ± 0.0094 mL/g in DMF, and the final molecular weight results were summarized in Table 3.1. The most interesting observation was that the M_n values of the polyesters made from monomer **A** were considerably higher (by 20~120%) than the polyesters made from monomer **B** with the same diacyl chloride (run 1 vs 2, 4 vs 5, and 7 vs 8, Table 1). In particular, the highest M_n of 20.8 kg/mol for **PE-2A** was the polyester prepared from polycondensation between monomer **A** and adipoyl chloride (**2**), which is >120% higher than the polyester (**PE-2B**) derived from monomer **B** with the same diacyl chloride. This sharp contrast suggests that the structure of monomer **A** has either a steric or electronic advantage for higher reactivity over monomer **B**. The alcohol adjacent to the carbonyl would be slightly less electron rich, but both monomers contain an α-hydroxy. Hence, the similarity in the electronic environment for the internal OH between the two monomers suggests that sterics is more likely the cause of the differing reactivities. The π-π-conjugation between the carbonyl and the adjacent furan ring would render them on the same plane, while the furan ring adjacent to the carbon with the internal alcohol has more freedom in the number of conformations it can take to release the steric pressure during chain growth. For the polyesters made from monomer **A**, the rigid portion is part of the material backbone while the comparatively flexible portion is the pendent furan group, which would allow for easier condensation reactions, while the rigid and flexible arrangement is opposite for the polyesters made from monomer **B**. This key structural difference can explain the sharp molecular weight differences between these two isomeric monomers. Noteworthy also is that when both **A** and **B** were used together as a mixture, the molecular weight of the mixed polyesters (copolymer) was further lowered for the

polycondensation with both succinyl chloride (**1**) and suberoyl chloride (**3**) (run 3 vs 1 or 2, run 9 vs 7 or 8).

The thermal degradation profiles of polyesters reported here were monitored by TGA (Figure 3.5). The onset decomposition temperature (T_d at 5% weight loss) only varied slightly across the diacyl chloride series, with the **PE-1** series only varying by 5 °C (runs 1-3, Table 3.1) while **PE-2** series had a wider range of 17 °C (runs 4-6, Table 3.1, Figure 3.5), and the **PE-3** series showed a medium range of difference of 12 °C (runs 7-9, Table 1) from lowest to highest. In contrast, the difference between **PE-1A/B** and **PE-3A/B** was 50 °C (run 3 vs 9, Table 3.1, Figure 3.5-b). These results showed that increasing the length of the methylene bridge between the ester groups had a more pronounced effect on T_d than the electronic or steric differences between the two isomeric difuranic diol monomers. As would be expected, the polyester with the shortest methylene bridge exhibited the lowest T_d of 200 °C, while the longest methylene linker gave the polyester with the highest T_d up to 250 °C. It is worth noting that these polyesters were not completely decomposed even at 700 °C, with roughly ~30% of highly stable carbonaceous residues remaining for all the runs except 7, which had only 19%. By comparison, less than 5% carbonaceous material remained when TGA analysis was performed on PET-*ran*-PEF with a ratio of 4:1.[54] PEF also showed only a slight amount, less than 10%, of stable residue remaining when analyzed by TGA.[55] Hence, the phenomenon of significant stable carbonaceous materials remaining after TGA analysis up to 700 °C appeared to be unique to the materials made from difuranics, which suggests that there was a degradation pathway present in the polyester from difuranics that is different from that derived from monofuranics such as PEF.

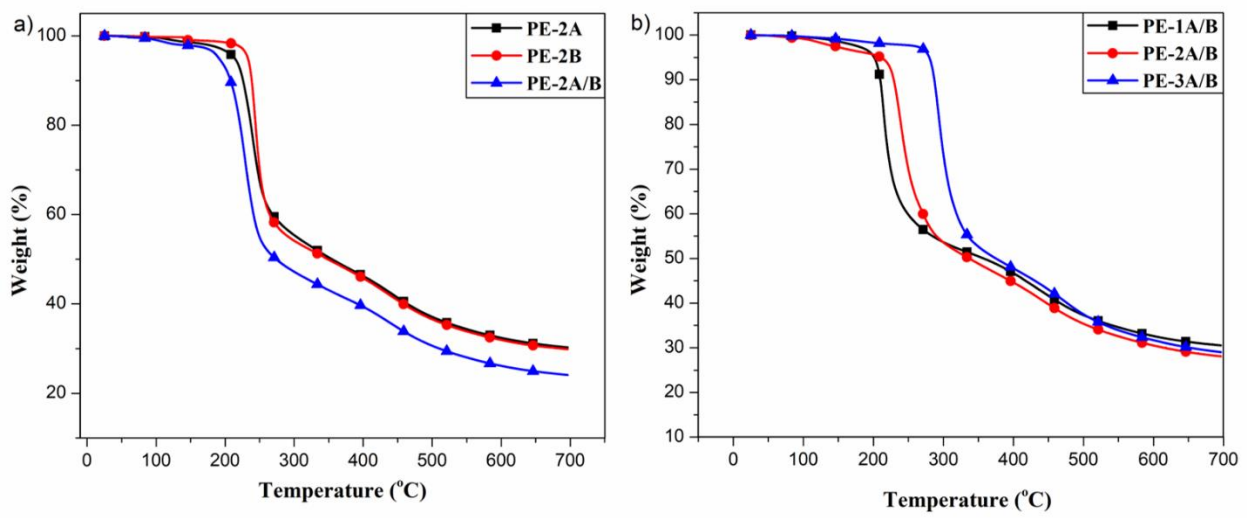

Figure 3.5. TGA traces of **PE-2** series (a) and **PE-A/B** series (b).

The presence of stereo-irregular main-chain chiral centers completely eliminated crystallization thus resulting in amorphous polyester materials. The DSC curves for the polyester series analyzed here clearly showed that the polyester bearing a longer soft segment [-$(CH_2)_6$-], **PE-3A**, has a lower glass transition temperature (T_g) of 26.5 °C (run 7, Table 3.1), compared with the T_g of 65.9 °C for **PE-1A** with a shorter linker [-$(CH_2)_2$-] (run 1, Table 3.1), Figure 3.6-a. The factors that influenced T_g include chain stiffness (or flexibility), molecular symmetry, the presence of a side group (and its size and flexibility), molecular weight, chain branching, cross-linking, and intermolecular forces.[56-57] The two types of pendent groups did not have a significant effect on T_g with differences between polyesters derived from monomers **A** and **B** being less than 3 °C. The polyesters synthesized from a mixture of **A** and **B** had a slight but noticeable trend in T_g, and it exhibited the lowest T_g in each of the diacyl chloride series. While the difference between the polyesters resulted from monomer **A** or **B** is within experimental error, the difference between the **PE-A/B** and either **PE-A** or **PE-B** was noticeable, ranging from 3 to 8 °C. The difference between the two pendent groups appeared to have a minimal effect on T_g, while the methylene bridge chain

length had the most pronounced effect (Figure 3.6-a). The uniformity of thermal characteristics across the diacyl chloride series was more apparent with T_g than with the T_d. The maximum spread of T_d was 17 °C for the **PE-2** series while for that same series the separation for T_g was less than 1 °C for **PE-2** series (runs 4-6 Table 3.1, Figure 3.6-b).

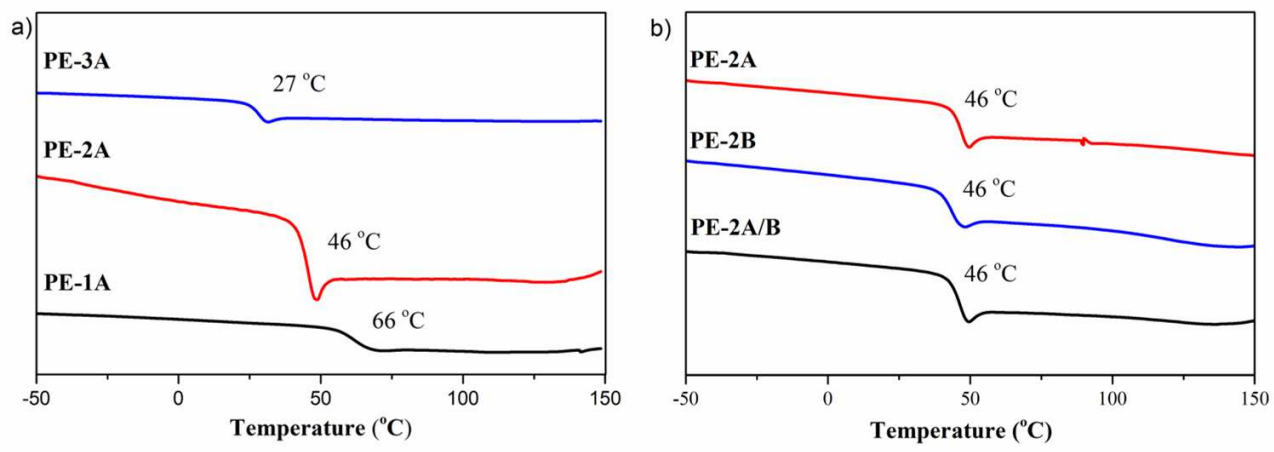

Figure 3.6. DSC curves of **PE-A** (a) and **PE-2** (b) series (second heating scan with a heating rate 5 °C/min).

Polyurethanes Derived from Difuranic Diols A and B. Two diisocynates were chosen based on their differing reactivities for the synthesis of PUs using difuranic diol monomers **A** and **B** (Figure 3.7). Aromatic diisocyanates such as diphenylmethanediisocyanate (MDI) exhibit enhanced reactivity when compared to alkyl diisocyantes such as hexamethylenediisocyanate (HDI).[58] The long $(CH_2)_6$ alkyl chain present in HDI makes the comparison of its derived **PU-4** series to **PE-3** series possible, allowing us to show how the urethane bond changes material propertie when compared to the ester bond. It was hypothosized that the increased reactivty and regidity of MDI should translate into polyurethans with increased M_n and T_g values; however, experiments showed other factors

such as chain flexibilty and material solubility may have greater effects on M_n than the diisocyanate reactivity.

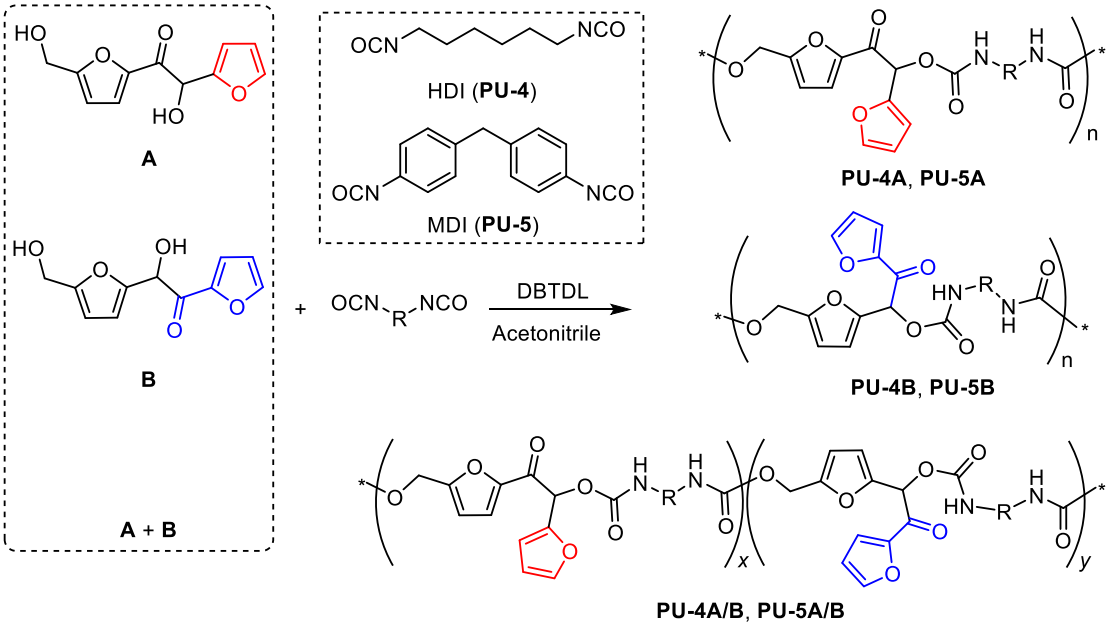

Figure 3.7. Synthesis of linear PUs with furan pendent groups.

Among the many catalysts that have been used to catalyze the synthesis of polyurethanes, the catalyst shown to be most effective for difuranics is dibutyltin dilaurate (DBTDL).[36] Initial attemps with DBTDL as the catalyst for the current polyaddition of difuranic diol **A** or **B** to HDI or MDI in ACN resulted in gel formation, when the product was washed with MeOH and dried, the isolated polyurethane yield was low. The reaction was repeated and monitored by ^{1}H NMR to determine the conversion. It was found that after 24 h all of the primary alcohol had been converted but that a significant amount of the secondery alcohol remained. The reaction was then extended to 48 h, after which ^{1}H NMR (Figure S3.30) clearly revealed the absense of alcohol peaks suggesting that conversion to urethane bonds was complete. The

reactions performed in other solvents such as DMF and THF did not yield better results; thus, ACN was used as the sutiable medium to complete the run series summarized in Table 3.2.

Table 3.2. Polyaddition of Diisocynates with Difuranic Diol A, B or A + B [a]

Run #	Sample	Diisocyanate	Diol	Yield (%)	M_n (kg/mol)	$Đ$ (M_w/M_n)	T_g (°C)	T_d (°C)	Residue (%)
10	**PU-4A**	HDI	**A**	92	23.9	2.0	78	216	20.6
11	**PU-4B**	HDI	**B**	53	8.23	1.7	80	185	24.2
12	**PU-4A/B**	HDI	**A+B**	68	11.5	3.2	93	154	30.2
13	**PU-5A**	MDI	**A**	92	17.6	2.6	87	204	27.2
14	**PU-5B**	MDI	**B**	78	5.25	1.4	100	182	33.8
15	**PU-5A/B**	MDI	**A+B**	91	6.94	1.3	88	191	31.7

[a] Conditions: diol (1.00 mmol), diisocyanate (1.00 mmol), DBTDL (0.03 mmol), temperature = 45 °C, time = 48 h. See footnotes in Table 3.1 for other explanations.

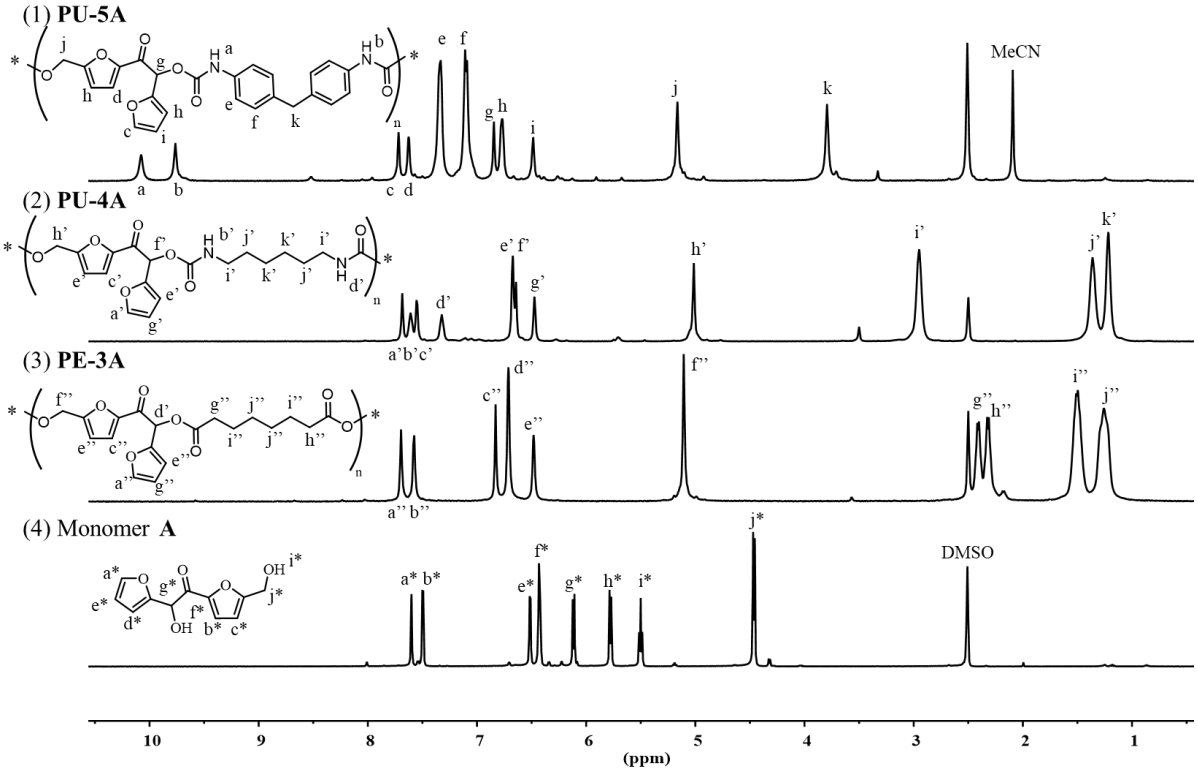

Figure 3.8. Stacked ^{1}H NMR spectra (DMSO-d6, 25 °C) of PU-5A (1), PU-4A (2), PE-3A (3), and monomer A (4) as comparison.

Charecterization of Polyurethanes. As in the case of polyesters, the resulting polyurethane materials have been characterized by 1D and 2D NMR for chain structure, GPC for absolute molecular weight and dispersity, as well as TGA and DSC for thermal stability and transitions. Full ^{1}H NMR spectral assignments of the polyurethanes derived from monomer **A** are depicted in Figure 3.8. When comparing the spectra for polyurethaness to the starting diols and the polyesters synthesized from the same difuranic diol, two trends became readily apparant. The signal at 7.57 ppm belonging to (a*) of monomer **A** shifted slightly down field after polymerization but remained within 0.2 ppm of its original postion: it was shifted to 7.72 ppm and 7.66 ppm for **PU-5A** and **PU-4A**, respectivly, and to 7.73 ppm for the corresponding polyester (**PE-3A**, Figure 3.8-3). This signal belongs to the pendent furan proton furthest from the polymer chain, therfore it is the least shifted before and after the polymerization. The consistency of this signal from the monomer through the polyester and polyurethane polymer series also further supports the reported assignment. Using this proton as an anchor the rest of the ring protons for both the pendent furan ring and the backbone furan ring can be assigned using gCOSY (Figure S3.32). Comparison of the spectra for the **PE-3** and **PU-4** series, which only differ in the addition of the nitrogen, revealed that the N-H peaks were (b') at 7.58 ppm and (d') at 7.29 ppm. Additional evidence for the proper identication of both polyester and polyurethane proton signals can be seen in the comparison of the shifts for (j') and (k') to (i'') and (j''), belonging to the middle eight protons on the alkyl bridge. The assighnment of the N-H peaks for **PU-5** series was aided by comparing the spectra for these materials to the spectra of the previously reported polyurethanes of the similer difuranics made with MDI.[36] The signals for (e) and (f) (Figure 3.8-1) had the charicteristic shift and symmetry for the *para*-substituited phenyl rings. Both

polyesters and polyurethans had a distintive singlet near 5.0 ppm corresponding to the CH_2 adjacent to the acyl or urethane linkage oxygen (i.e., proton (j) in **PU-5A**, (h') in **PU-4A**, (f") in **PE-3A**), which is consistent with literature reports for similer protons.[35-36, 59]

Consistent with the M_n trend observed for the polyesters, the polyurethanes resulted from monomer **A** (runs 10 and 13, Table 3.2) exhibited significantly higher molecular weight: M_n = 23.9 kg/mol for **PU-4A** (run 10, Table 3.2) vs M_n = 8.23 kg/mol for **PU-4B** (run 11, Table 3.2); M_n = 17.6 kg/mol for **PU-5A** (run 13, Table 3.2) vs M_n = 5.25 kg/mol for **PU-5B** (run 14, Table 3.2). Polyurethans (**PU-5**) synthesized from MDI gelled quicker due to poor solubility relative to their HDI counterparts, causing suppressed M_n. As expected, the use of the **A**+**B** monomer mixture afforded the polyurethanes with M_n lying somewhere between the polyurthenane produced by pure **A** and **B** separately (run 12 vs 10 and 11; run 15 vs 13 and 14, Table 3.2).

The TGA traces (Figure 3.6) of the synthesized PUs show a multistep decomposition profile with two primary steps and a minor step between them, which is in line with previously reported furan-based polyurethanes.[36, 60-62] It has also been shown that polyurethanes made from aryl alcohols have reversible urethane linkages at temperatures above 150 °C,[63] and such thermal reversibility of urethane linkages can also explain the multistep degradation observed for the polyurethane materials reported here. The two highest onset decomposition temperatures were observed for the polyurethanes with the highest molecular weight: T_d = 216 °C for **PU-4A** (M_n = 23.9 kg/mol); T_d = 204 °C for **PU-5A** (M_n = 17.6 kg/mol). For the polyester series, the methylene bridge length between the esters had the greatest effect on T_d while for the polyurethane series the M_n appeared to have a greater impact on T_d. As in the case of polyesters discussed above, the

difuranic-based polyurethanes also yielded a significant amount of highly stable carbonaceous residue at 700 °C, ranging from ~21 to 34% (Table 3.2).

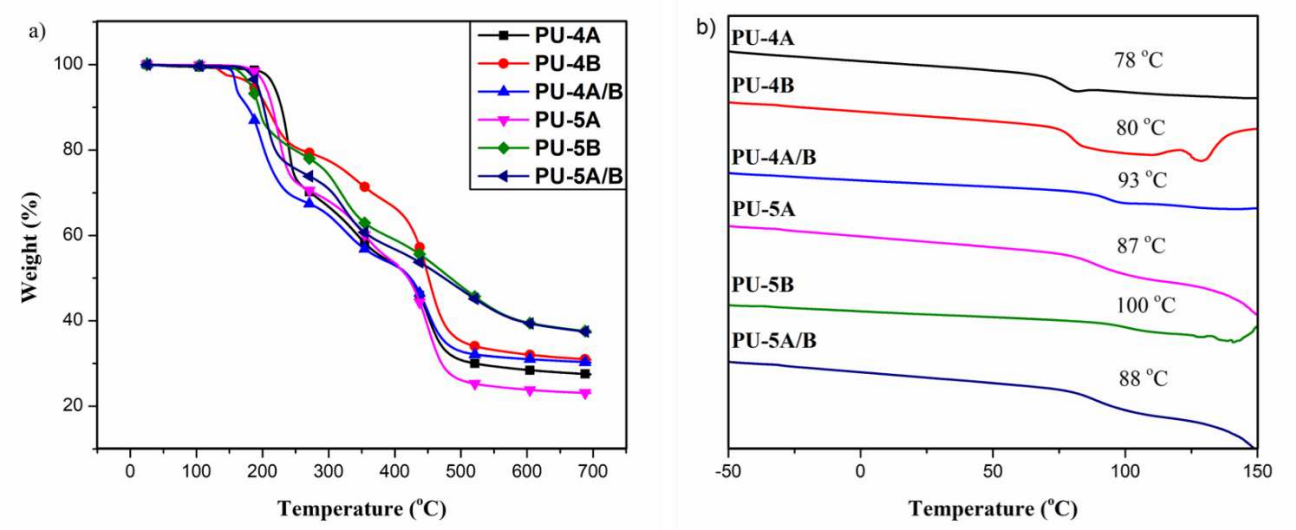

Figure 3.9. TGA (a) and DSC (b, second heating scan at 5 °C/min) analyses of polyurethanes produced from monomers **A** and **B**.

The range of T_g's across the same diisocyanate series was much broader for the PUs than that for the polyesters, with 15 °C separting the highest and lowest T_g's for the **PU-4** (HDI based) materials (runs 10 to 12, Table 3.2, Figure 3.9-b), and 13 °C separating the two extreams for **PU-5** (MDI based) materials (runs 13 to 15, Table 3.2). Intriguingly, there appeared an inverse relationship between the M_n and the T_g of polyurethanes prepared by **A** and **B**: the higher M_n, the lower T_g within the same diisocyanate series. Specifically, the T_g of **PU-4A** (M_n = 23.9 kg/mol) was measured to be 78 °C, while the T_g of **PU-4B** with a much lower M_n of only 8.23 kg/mol was 13 °C higher. The same trend was also observed for the **PU-5** series: T_g = 87 °C for **PU-5A** (M_n = 17.6 kg/mol); T_g = 100 °C for **PU-5B** (M_n = 5.25 kg/mol). While the relative chain stiffness as a result of differing structures in **A** and **B** could be attributed to the observed large T_g differences between polyurethanes from **A** and **B**, this

possible reasoning was refuted by the polyester series described above where there showed no observable T_g differences between polyesters derived from **A** and **B** (*c.f.*, Figure 3.4-b). Hence, the most likely reason for this observed inverse relationship is that hydrogen bonding has a more pronounced effect on oligomers while the longer polymer chains are more effected by weaker intermolecular forces. The polyurethanes synthesized here all exhibited a higher T_g than the polyesters with the lowest polyurethane being 22 °C higher (run 10, Table 3.2) than the polyester with the highest T_g (run 2, Table 3.1). Again, this enhancement is likely the result of hydrogen bonding between the urethane N-H groups in the polyurethane.

Dynamic Mechanical Properties of Polyester and Polyurethane Films. Suitable thin films for dynamic mechanical analysis (DMA) of the selected four polyester and polyurethane materials were prepared by hot press molding, the results of which are summarized in Table 3.3. For the two polyester samples, **PE-2A/B** with a $(CH_2)_4$ linkage and **PE-3A/B** with a $(CH_2)_6$ linkage, the alpha-transition temperature, T_α, given by the maximum value of tan(δ) measured by DMA was about 10 °C higher than the T_g measured by DSC, and the storage modulus (E') of **PE-2A/B** (2.37 GPa), set at a reference temperature of 10 °C, was considerably higher than that of **PE-3A/B** (1.60 GPa). While the polyesters formed from diacyl chloride **2** had a small rubbery plateau region (Figures 3.7, S3.14, and S3.17), increasing the alkyl chain length between the ester groups increased the temperature range of the rubbery plateau (Figure S3.20). Tensile testing gave stress-strain curves for **PE-2A/B** (Figure 3.10) and **PE-3A/B** (Figure S3.21), from which the Young's modulus was calculated to be 63.0 and 0.95 MPa, elongation to break to be 48 and 33%, respectively. In comparison, the polyurethane materials exhibited much higher Young's moduli (934 MPa for **PU-4A/B** and 577 MPa for **PU-5A/B**).

Table 3.3. Summary of Dynamic Mechanical Properties

Sample	M_n (kg/mol)	E' (GPa)	E'' (MPa)	T_α (°C)	Young's Modulus (MPa)
PE-2A/B	11.9	2.37	112	56.0	63.0
PE-3A/B	8.98	1.60	126	28.2	0.95
PU-4A/B	6.60	1.42	112	74.3	934
PU-5A/B	4.40	1.88	121	116	577

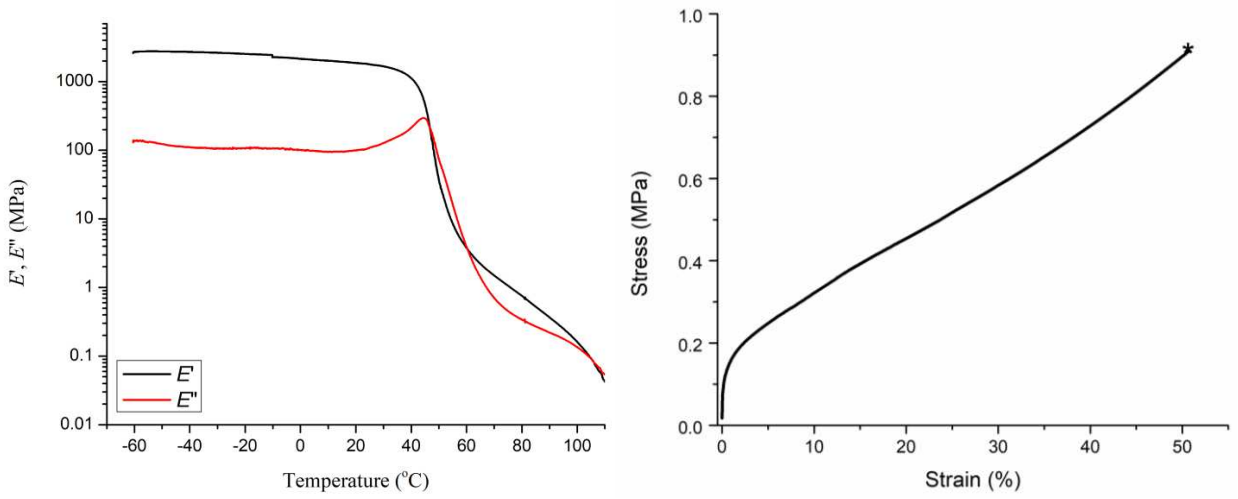

Figure 3.10. DMA and stress-strain curves of **PE-2A/B**.

Thermally Reversible Cross-linking of Polyesters. The presence of reactive C=C bonds in polymers containing furan rings provides convenient functional handles for post functionalization via the thermally reversible DA reaction between a diene (furan ring) and a dienophile (maleimide moiety).[30,64-69] The polymers in the present system have a furan ring located in both the polymer back bone and pendent positions, thus increasing the number and type of furan moieties available for the DA reaction with a bis-maleimide (BM), Figure 3.11. As the polyurethane linkage is known to be reversible above 150 °C and the rDA temperature for solid material is also approximately 150 °C, experiments on DA crosslinking with polyurethanes were not performed because of proximity of the urethan linkage reversibility temperature to rDA temperature.

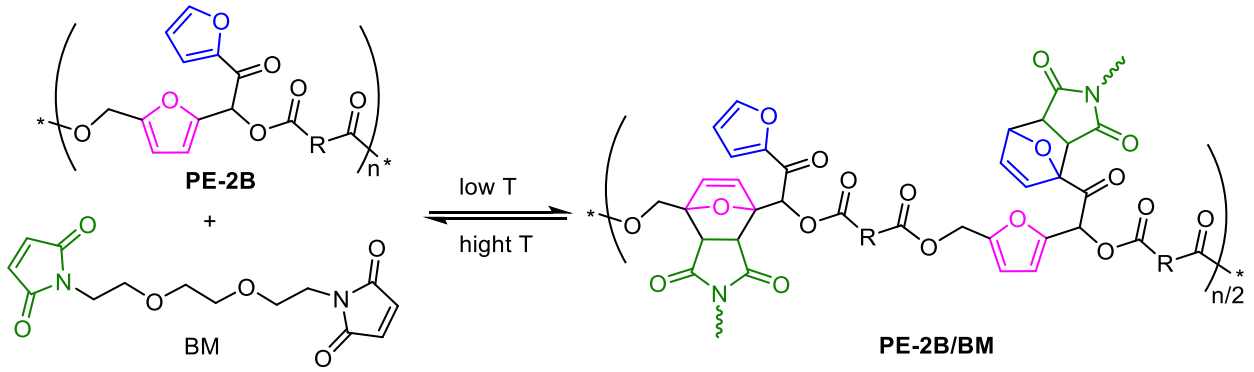

Figure 3.11. Proposed thermally reversible cross-linking of PE with BM.

To test this hypothesis, **PE-2** materials based on adipoyl chloride were reacted with BM (15 mol% relative to the monomer unit) shown in Figure 3.11.[31] It has been shown that the equilibrium concentration of the DA adduct is between 7 and 36% even in the presence of 20-fold excess of furan rings,[70] which suggests that the use of more BM would not result in increased DA adduct formation. In addition, Zeng *et. al.* used nearly the same ratio and found only a small portion of maleimide remained unreacted.[31] The resulting products were completely insoluble in DCM or DMSO, indicating the formation of cross-liked polymer networks;[30-32, 71-72] further confirmation was performed on solid adduct **PE-2A/B/BM** by FTIR (Figure S3.52), showing spectral features consistent with DA adduct formation.[31-32] To monitor the dissolvability of the DA adduct at elevated temperatures, variable-temperature NMR experiments were performed in d_6-DMSO. At 80 °C, the DA adduct sample began to dissolve and was completely dissolved in solution within 1 h. Comparing the spectrum of the dissolved material with the spectra of the polymer and the BM crosslinker showed that the DA adduct was reverted back to the soluble polymer and BM crosslinker (Figure S3.53). Upon cooling the insoluble polymer network reformed, indicating the thermal reversibility of the current system. To test the ability to capture the released linear polymer an experiment was performed where the cross-linked material was heated to above the rDA

initiation temperature in DMF and then quenched while still hot in excess methanol. The precipitate was analyzed, and it was found that the majority of cross-linking had been reversed to reform the linear polyester and the cross-linker had been removed with the precipitation solvent (Figure S3.54). The small amount of the remaining cross-linked material from the BM cross-linker can also be reversed back to the linear polyester by a second precipitation process with a much longer dissolution time period (48 h to five days).

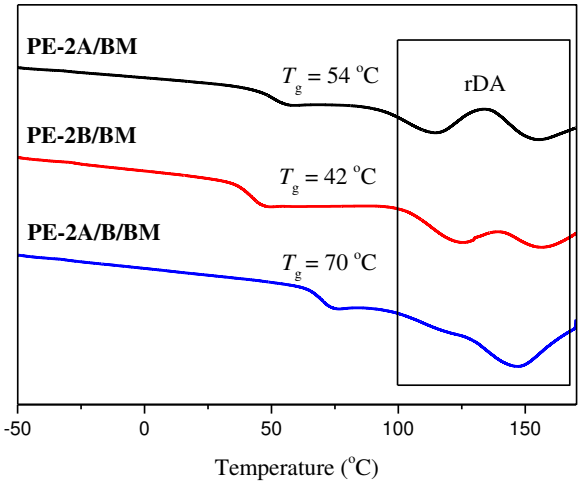

Figure 3.12. DSC heating curves of cross-linked network materials derived from the DA reaction between **PE-2** series and BM.

Another method to show that the thermally reversible DA-rDA process for the cross-linked materials is to monitor the process by DSC.[72-73] This method takes advantage of the endothermicity of the rDA reaction, where the DSC trace typically shows an endothermic transition between 100 °C and 150 °C when the rDA reaction takes place. As can be seen from Figure 3.12, distinctive endothermic transitions upon heating the cross-linked network polymers offer strong evidence that the rDA reaction between the BM cross-linker and the polyester did occur. The DA reaction between furan and maleimide has two possible configurations: endo and exo adducts. The presence

of two endotherms for **PE-2A/BM** and **PE-2B/BM** (Figure 3.12) could be attributed to the different energy requirements for breaking up the two adducts in their respective rDA reaction. An alternative explanation for the observed two endotherms is that the DA adducts derived from the pendent and backbone furan rings have different energy requirements for their respective rDA reaction (a study showed both types of furan rings can react with BM without apparent selectivity, Figure S3.55). On the other hand, **PE-2A/B/BM** appeared to have only one broad endotherm, presumably a result of overlapping of the two endothermic transitions.

3.4. Conclusions

In summary, we have prepared two isomeric difuranic C_{11} diols, **A** with a more electron-rich and flexible pendent furan ring and **B** with a more electron-deficient but rigid pendent furan ring, using organocatalyzed cross-coupling of the biomass platform chemicals FF and HMF, and utilized them to produce polyesters and polyurethanes with furan rings residing in both the polymer backbone and pendent positions. Polycondensation of the difuranic diols and diacyl chlorides led to a series of new linear polyesters, with three different length alkyl bridges between the ester groups acting as soft segments between the rigid difuranics, while polyaddition of the same rigid difuranic diols to diisocyanates afforded a series of PUs with the less reactive and softer HDI connector moiety and the harder but more reactive MDI connector moiety. Although the main objective of this study is to evaluate the properties of materials made from these unique biomass-derived diols, more ideally the synthesis of these materials should avoid using toxic and hazardous acyl chlorides and diisocyantes.[63] Current attempts at using greener methods such as melt polycondensation between the diols and diacids to synthesize polyesters were unsuccessful due to the oxidation side reaction involving the α-hydroxyketone moiety, and the isocyanate-free

synthesis of polyurethanes usually requires to use of diamines, as opposed to diols, as starting materials.[74-75]

Monomer **A** is more reactive in polycondensation reactions and led to polyesters with much higher molecular weight than monomer **B**; however, their thermal and mechanical properties are similar, which, on the other hand, are significantly influenced by the length of the alkyl bridge between the two ester moieties. The polyurethanes produced from monomer **A** continued to have M_n significantly higher than the polyurethanes derived from monomer **B**. The observed intriguing inverse relationship between the M_n and the T_g of polyurethanes prepared by **A** and **B**, the higher M_n, the lower T_g within the same diisocyanate series can be attributed to hydrogen bonding which has a more pronounced effect on lower molecular weight polymers. Such secondary interactions can also account for the polyurethane materials that exhibited much higher Young moduli that the polyesters analyzed by the current study. DMA analysis of polyesters also showed that increasing the alkyl chain length between the ester groups can significantly increase the temperature range of the rubbery plateau.

Several corroborative studies showed cross-linking between the furan-containing polyester and the bis-maleimide cross-linker via the DA reaction and the resulting insoluble cross-linked network polymer can be thermally reversed back to the soluble linear polyester via the rDA reaction at higher temperature. The results also indicated that both the furan ring moieties located at back-bone and pendent positions can participate in this thermally reversible process. These results, together with the observation of a significant amount of stable carbonaceous materials formed (up to 34%) when hearting difuranic polymers to 700 °C (thus a suitable precursor for carbon fibers), highlight two promising features of this class of new polymers having the difuranic moieties and pendent furan rings.

References

(1) Gandini, A.; Lacerda, T. M.; Carvalho, A. J. F.; Trovatti, E., Progress of Polymers from Renewable Resources: Furans, Vegetable Oils, and Polysaccharides. *Chem. Rev.* **2016,** *116*, 1637-1669.

(2) Galbis, J. A.; García-Martín, M. d. G.; de Paz, M. V.; Galbis, E., Synthetic Polymers from Sugar-Based Monomers. *Chem. Rev.* **2016,** *116*, 1600-1636.

(3) Bozell, J. J.; Petersen, G. R., Technology development for the production of biobased products from biorefinery carbohydrates-the US Department of Energy's "Top 10" revisited. *Green Chem.* **2010,** *12*, 539-554.

(4) Liu, D.; Chen, E. Y. -X., Polymeric ionic liquid (PIL)-supported recyclable catalysts for biomass conversion into HMF. *Biomass & Bioenergy* **2013,** *48*, 181-190.

(5) Liu, D.; Chen, E. Y. -X., Organocatalysis in biorefining for biomass conversion and upgrading. *Green Chem.* **2014,** *16*, 964-981.

(6) Caes, B. R.; Teixeira, R. E.; Knapp, K. G.; Raines, R. T., Biomass to Furanics: Renewable Routes to Chemicals and Fuels. *ACS Sustainable Chem. Eng.* **2015,** *3*, 2591-2605.

(7) He, J.; Zhang, Y.; Chen, E. Y.-X., Chromium(0) Nanoparticles as Effective Catalyst for the Conversion of Glucose into 5-Hydroxymethylfurfural. *ChemSusChem* **2013,** *6*, 61-64.

(8) Wang, T.; Nolte, M. W.; Shanks, B. H., Catalytic dehydration of C6 carbohydrates for the production of hydroxymethylfurfural (HMF) as a versatile platform chemical. *Green Chem.* **2014,** *16*, 548-572.

(9) Saha, B.; Abu-Omar, M. M., Advances in 5-hydroxymethylfurfural production from biomass in biphasic solvents. *Green Chem.* **2014,** *16*, 24-38.

(10) Teong, S. P.; Yi, G.; Zhang, Y., Hydroxymethylfurfural production from bioresources: past, present and future. *Green Chem.* **2014,** *16*, 2015-2026.

(11) van Putten, R.-J.; van der Waal, J. C.; de Jong, E.; Rasrendra, C. B.; Heeres, H. J.; de Vries, J. G., Hydroxymethylfurfural, A Versatile Platform Chemical Made from Renewable Resources. *Chem. Rev.* **2013,** *113*, 1499-1597.

(12) Lange, J.-P.; van der Heide, E.; van Buijtenen, J.; Price, R., Furfural—A Promising Platform for Lignocellulosic Biofuels. *ChemSusChem* **2012,** *5*, 150-166.

(13) Choura, M.; Belgacem, N. M.; Gandini, A., Acid-Catalyzed Polycondensation of Furfuryl Alcohol: Mechanisms of Chromophore Formation and Cross-Linking. *Macromolecules* **1996,** *29*, 3839-3850.

(14) Gandini, A.; Silvestre, A. J. D.; Neto, C. P.; Sousa, A. F.; Gomes, M., The furan counterpart of poly(ethylene terephthalate): An alternative material based on renewable resources. *J. Polym. Sci., Part A: Polym. Chem.* **2009,** *47*, 295-298.

(15) Burgess, S. K.; Leisen, J. E.; Kraftschik, B. E.; Mubarak, C. R.; Kriegel, R. M.; Koros, W. J., Chain Mobility, Thermal, and Mechanical Properties of Poly(ethylene furanoate) Compared to Poly(ethylene terephthalate). *Macromolecules* **2014,** *47*, 1383-1391.

(16) Burgess, S. K.; Karvan, O.; Johnson, J. R.; Kriegel, R. M.; Koros, W. J., Oxygen sorption and transport in amorphous poly(ethylene furanoate). *Polymer* **2014,** *55*, 4748-4756.

(17) Burgess, S. K.; Lee, J. S.; Mubarak, C. R.; Kriegel, R. M.; Koros, W. J., Caffeine antiplasticization of amorphous poly(ethylene terephthalate): Effects on gas transport, thermal, and mechanical properties. *Polymer* **2015,** *65*, 34-44.

(18) R., P. M.; R., P. D., Gas transport properties of polyarylates part I: Connector and pendant group effects. *J. Polym. Sci., Part B: Polym. Phys.* **1995,** *33*, 1135-1149.

(19) R., P. M.; R., P. D., Gas transport properties of polyarylates part II: Tetrabromination of the bisphenol. *J. Polym. Sci., Part B: Polym. Phys.* **1995,** *33*, 1353-1364.

(20) Chang, C.-C.; Je Cho, H.; Yu, J.; Gorte, R. J.; Gulbinski, J.; Dauenhauer, P.; Fan, W., Lewis acid zeolites for tandem Diels-Alder cycloaddition and dehydration of biomass-derived dimethylfuran and ethylene to renewable p-xylene. *Green Chem.* **2016,** *18*, 1368-1376.

(21) W., F. R.; Laure, B.; J., P. M.; Dejan-Krešimir, B.; C., H. H.; J., T. C.; D., S. T., Irreversible endo-Selective Diels–Alder Reactions of Substituted Alkoxyfurans: A General Synthesis of endo-Cantharimides. *Chemistry – A European Journal* **2015,** *21*, 6107-6114.

(22) Xue, Y.-P.; Li, W.-D. Z., Formal Total Synthesis of (±)-Estrone via the Furano Diene Approach. *The J. Org. Chem.* **2011,** *76*, 57-64.

(23) Froidevaux, V.; Borne, M.; Laborbe, E.; Auvergne, R.; Gandini, A.; Boutevin, B., Study of the Diels-Alder and retro-Diels-Alder reaction between furan derivatives and maleimide for the creation of new materials. *RSC Adv.* **2015,** *5*, 37742-37754.

(24) Griffith, G. A.; Hillier, I. H.; Moralee, A. C.; Percy, J. M.; Roig, R.; Vincent, M. A., Interplay of Structure and Reactivity in a Most Unusual Furan Diels-Alder Reaction. *J. Am. Chem. Soc.* **2006,** *128*, 13130-13141.

(25) Petronijevic, F.; Timmons, C.; Cuzzupe, A.; Wipf, P., A microwave assisted intramolecular-furan-Diels-Alder approach to 4-substituted indoles. *Chem. Commun.* **2008**, 104-106.

(26) Feng, L.; Yu, Z.; Bian, Y.; Lu, J.; Shi, X.; Chai, C., Self-healing behavior of polyurethanes based on dual actions of thermo-reversible Diels-Alder reaction and thermal movement of molecular chains. *Polymer* **2017,** *124* (Supplement C), 48-59.

(27) Watanabe, M.; Yoshie, N., Synthesis and properties of readily recyclable polymers from bisfuranic terminated poly(ethylene adipate) and multi-maleimide linkers. *Polymer* **2006,** *47*, 4946-4952.

(28) Gandini, A., The furan/maleimide Diels–Alder reaction: A versatile click–unclick tool in macromolecular synthesis. *Prog. Polym. Sci.* **2013,** *38*, 1-29.

(29) Liu, Y.-L.; Chuo, T.-W., Self-healing polymers based on thermally reversible Diels-Alder chemistry. *Polymer Chem.* **2013,** *4*, 2194-2205.

(30) Chen, X.; Dam, M. A.; Ono, K.; Mal, A.; Shen, H.; Nutt, S. R.; Sheran, K.; Wudl, F., A Thermally Re-mendable Cross-Linked Polymeric Material. *Science* **2002,** *295*, 1698-1702.

(31) Zeng, C.; Seino, H.; Ren, J.; Hatanaka, K.; Yoshie, N., Bio-Based Furan Polymers with Self-Healing Ability. *Macromolecules* **2013,** *46*, 1794-1802.

(32) Zeng, C.; Seino, H.; Ren, J.; Hatanaka, K.; Yoshie, N., Self-healing bio-based furan polymers cross-linked with various bis-maleimides. *Polymer* **2013,** *54*, 5351-5357.

(33) Hong, M.; Tang, X.; Falivene, L.; Caporaso, L.; Cavallo, L.; Chen, E. Y. -X., Proton-Transfer Polymerization by N-Heterocyclic Carbenes: Monomer and Catalyst Scopes and Mechanism for Converting Dimethacrylates into Unsaturated Polyesters. *J. Am. Chem. Soc.* **2016,** *138*, 2021-2035.

(34) Liu, D.; Zhang, Y.; Chen, E. Y. -X., Organocatalytic upgrading of the key biorefining building block by a catalytic ionic liquid and N-heterocyclic carbenes. *Green Chem.* **2012,** *14*, 2738-2746.

(35) Mou, Z.; Chen, E. Y. -X., Polyesters and Poly(ester-urethane)s from Biobased Difuranic Polyols. *ACS Sustainable Chem. Eng.* **2016,** *4*, 7118-7129.

(36) Mou, Z.; Feng, S.; Chen, E. Y. -X., Bio-based difuranic polyol monomers and their derived linear and cross-linked polyurethanes. *Polymer Chem.* **2016,** *7*, 1593-1602.

(37) Liu, D.; Chen, E. Y. -X., Integrated Catalytic Process for Biomass Conversion and Upgrading to C-12 Furoin and Alkane Fuel. *Acs Catal.* **2014,** *4*, 1302-1310.

(38) Wang, L.; Chen, E. Y. -X., Recyclable Supported Carbene Catalysts for High-Yielding Self-Condensation of Furaldehydes into C10 and C12 Furoins. *ACS Catal.* **2015,** *5*, 6907-6917.

(39) Zang, H.; Wang, K.; Zhang, M.; Xie, R.; Wang, L.; Chen, E. Y. -X., Catalytic coupling of biomass-derived aldehydes into intermediates for biofuels and materials. *Catal. Sci. Tech.* **2018,** *8*, 1777-1798.

(40) Liu, D.; Chen, E. Y. -X., Diesel and Alkane Fuels From Biomass by Organocatalysis and Metal–Acid Tandem Catalysis. *ChemSusChem* **2013,** *6*, 2236-2239.

(41) Wilson, J.; Chen, E. Y. -X., Organocatalytic Cross-Coupling of Biofuranics to Multifunctional Difuranic C11 Building Blocks. *ACS Sustainable Chem. Eng.* **2016,** *4*, 4927-4936.

(42) Piel, I.; Pawelczyk, M. D.; Hirano, K.; Froehlich, R.; Glorius, F., A Family of Thiazolium Salt Derived N-Heterocyclic Carbenes (NHCs) for Organocatalysis: Synthesis, Investigation and Application in Cross-Benzoin Condensation. *European J. Org. Chem.* **2011**, 5475-5484.

(43) Langdon, S. M.; Wilde, M. M. D.; Thai, K.; Gravel, M., Chemoselective N-Heterocyclic Carbene-Catalyzed Cross-Benzoin Reactions: Importance of the Fused Ring in Triazolium Salts. *J. Am. Chem. Soc.* **2014,** *136*, 7539-7542.

(44) Shimakawa, Y.; Morikawa, T.; Sakaguchi, S., Facile route to benzils from aldehydes via NHC-catalyzed benzoin condensation under metal-free conditions. *Tetrahedron Lett.* **2010**, 1786-1789.

(45) Enders, D.; Breuer, K.; Raabe, G.; Runsink, J.; Teles, J. H.; Melder, J.-P.; Ebel, K.; Brode, S., Preparation, Structure, and Reactivity of 1,3,4-Triphenyl-4,5-dihydro-1H-1,2,4-triazol-5-ylidene, a New Stable Carbene. *Angew. Chem. Int. Ed.* **1995,** *34*, 1021-1023.

(46) Corma, A.; de la Torre, O.; Renz, M., Production of high quality diesel from cellulose and hemicellulose by the Sylvan process: catalysts and process variables. *Energy & Environmental Sci.* **2012,** *5*, 6328-6344.

(47) King, A. E.; Brooks, T. J.; Tian, Y.-H.; Batista, E. R.; Sutton, A. D., Understanding Ketone Hydrodeoxygenation for the Production of Fuels and Feedstocks From Biomass. *ACS Catal.* **2015,** *5*, 1223-1226.

(48) L., W. B.; Linan, Y.; Cheong, K. S.; Remi, H.; I., K. H.; M., A. O. M., From Furfural to Fuel: Synthesis of Furoins by Organocatalysis and their Hydrodeoxygenation by Cascade Catalysis. *ChemSusChem* **2014,** *7*, 2742-2747.

(49) Sutton, A. D.; Waldie, F. D.; Wu, R.; Schlaf, M.; 'Pete' Silks Iii, L. A.; Gordon, J. C., The hydrodeoxygenation of bioderived furans into alkanes. *Nat. Chem.* **2013,** *5*, 428.

(50) Yang, J.; Li, N.; Li, G.; Wang, W.; Wang, A.; Wang, X.; Cong, Y.; Zhang, T., Solvent-Free Synthesis of C10 and C11 Branched Alkanes from Furfural and Methyl Isobutyl Ketone. *ChemSusChem* **2013,** *6*, 1149-1152.

(51) Stille, J. K., Step-growth polymerization. *J. Chem. Ed.* **1981,** *58*, 862.

(52) Gibson, H. W.; Liu, S.; Gong, C.; Ji, Q.; Joseph, E., Studies of the Formation of Poly(ester rotaxane)s from Diacid Chlorides, Diols, and Crown Ethers and Their Properties. *Macromolecules* **1997,** *30*, 3711-3727.

(53) Dutta, S.; Wu, L.; Mascal, M., Production of 5-(chloromethyl)furan-2-carbonyl chloride and furan-2,5-dicarbonyl chloride from biomass-derived 5-(chloromethyl)furfural (CMF). *Green Chem.* **2015,** *17*, 3737-3739.

(54) Sousa, A. F.; Matos, M.; Freire, C. S. R.; Silvestre, A. J. D.; Coelho, J. F. J., New copolyesters derived from terephthalic and 2,5-furandicarboxylic acids: A step forward in the development of biobased polyesters. *Polymer* **2013,** *54*, 513-519.

(55) Jiang, Y.; Woortman, A. J. J.; Alberda van Ekenstein, G. O. R.; Petrović, D. M.; Loos, K., Enzymatic Synthesis of Biobased Polyesters Using 2,5-Bis(hydroxymethyl)furan as the Building Block. *Biomacromolecules* **2014,** *15*, 2482-2493.

(56) Jenekhe, S. A.; Roberts, M. F., Effects of intermolecular forces on the glass transition of polymers. *Macromolecules* **1993,** *26*, 4981-4983.

(57) Cognet-Georjon, E.; Méchin, F.; Pascault, J.-P., New polyurethanes based on 4,4′-diphenylmethane diisocyanate and 1,4:3,6 dianhydrosorbitol, 2. Synthesis and properties of segmented polyurethane elastomers. *Macromol. Chem. Phys.* **1996,** *197*, 3593-3612.

(58) Gilles, T., Chemistry and technology of polyols for polyurethanes. Milhail Ionescu. Rapra Technology, Shrewsbury, UK. *Polym. Intern.* **2007,** *56*, 820-820.

(59) Zhang, Y.; Li, T.; Xie, Z.; Han, J.; Xu, J.; Guo, B., Synthesis and Properties of Biobased Multiblock Polyesters Containing Poly(2,5-furandimethylene succinate) and Poly(butylene succinate) Blocks. *Ind. Eng. Chem. Res.* **2017,** *56*, 3937-3946.

(60) Wang, Z.; Zhang, X.; Zhang, L.; Tan, T.; Fong, H., Nonisocyanate Biobased Poly(ester urethanes) with Tunable Properties Synthesized via an Environment-Friendly Route. *ACS Sustainable Chem. Eng.* **2016,** *4*, 2762-2770.

(61) Boufi, S.; Belgacem, M. N.; Quillerou, J.; Gandini, A., Urethanes and polyurethanes bearing furan moieties. 4. Synthesis, kinetics and characterization of linear polymers. *Macromolecules* **1993,** *26*, 6706-6717.

(62) Boufi, S.; Gandini, A.; Belgacem, M. N., Urethanes and polyurethanes bearing furan moieties: 5. Thermoplastic elastomers based on sequenced structures. *Polymer* **1995,** *36*, 1689-1696.

(63) Delebecq, E.; Pascault, J.-P.; Boutevin, B.; Ganachaud, F., On the Versatility of Urethane/Urea Bonds: Reversibility, Blocked Isocyanate, and Non-isocyanate Polyurethane. *Chemical Reviews* **2013,** *113*, 80-118.

(64) Wang, X.; Chen, S.; Sun, Y.; Zhang, M.; Li, Y.; Li, X.; Wang, H., A furan-bridged D-π-A copolymer with deep HOMO level: synthesis and application in polymer solar cells. *Polymer Chem.* **2011,** *2*, 2872-2877.

(65) Defize, T.; Thomassin, J.-M.; Alexandre, M.; Gilbert, B.; Riva, R.; Jérôme, C., Comprehensive study of the thermo-reversibility of Diels–Alder based PCL polymer networks. *Polymer* **2016,** *84*, 234-242.

(66) Thomas, D.; Raphaël, R.; Jean-Marie, R.; Philippe, D.; Christine, J.; Michaël, A., Thermoreversibly Crosslinked Poly(ε-caprolactone) as Recyclable Shape-Memory Polymer Network. *Macromol. Rapid Commun.* **2011,** *32*, 1264-1269.

(67) Kavitha, A. A.; Singha, N. K., Smart "All Acrylate" ABA Triblock Copolymer Bearing Reactive Functionality via Atom Transfer Radical Polymerization (ATRP): Demonstration of a "Click Reaction" in Thermoreversible Property. *Macromolecules* **2010,** *43*, 3193-3205.

(68) Kavitha, A. A.; Singha, N. K., "Click Chemistry" in Tailor-Made Polymethacrylates Bearing Reactive Furfuryl Functionality: A New Class of Self-Healing Polymeric Material. *ACS Appl. Mater. Interfaces* **2009,** *1*, 1427-1436.

(69) Kuang, X.; Liu, G.; Dong, X.; Wang, D., Triple-shape memory epoxy based on Diels–Alder adduct molecular switch. *Polymer* **2016,** *84*, 1-9.

(70) Pehere, A. D.; Xu, S.; Thompson, S. K.; Hillmyer, M. A.; Hoye, T. R., Diels–Alder Reactions of Furans with Itaconic Anhydride: Overcoming Unfavorable Thermodynamics. *Organic Lett.* **2016,** *18*, 2584-2587.

(71) Zeng, C.; Seino, H.; Ren, J.; Yoshie, N., Polymers with Multishape Memory Controlled by Local Glass Transition Temperature. *ACS Appl. Mater. Interfaces* **2014,** *6*, 2753-2758.

(72) Zhang, Y.; Dai, Z. H.; Han, J. R.; Li, T.; Xu, J.; Guo, B. H., Interplay between crystallization and the Diels-Alder reaction in biobased multiblock copolyesters possessing dynamic covalent bonds. *Polymer Chem.* **2017,** *8*, 4280-4289.

(73) He, J.; Zhang, Y.; Chen, E. Y. -X., Anionic polymerization of biomass-derived furfuryl methacrylate: Controlling polymer tacticity and thermoreversibility. *J. Polym. Sci., Part A: Polym. Chem.* **2013,** *51*, 2793-2803.

(74) Bossion, A.; Aguirresarobe, R. H.; Irusta, L.; Taton, D.; Cramail, H.; Grau, E.; Mecerreyes, D.; Su, C.; Liu, G.; Müller, A. J.; Sardon, H., Unexpected Synthesis of Segmented Poly(hydroxyurea–urethane)s from Dicyclic Carbonates and Diamines by Organocatalysis. *Macromolecules* **2018**, *55,* 5556-5566

(75) Sardon, H.; Pascual, A.; Mecerreyes, D.; Taton, D.; Cramail, H.; Hedrick, J. L., Synthesis of Polyurethanes Using Organocatalysis: A Perspective. *Macromolecules* **2015,** *48*, 3153-3165.

Chapter 4

Biofuran-Based Lactone Monomers and Their Ring-Opening Polymerization Behavior

4.1 Synopsis

Two synthetic strategies were employed to obtain lactones from furans suitable for ring opening polymerization (ROP). The first strategy was to attach appropriate functionality to the 4-postion of the furan ring to generate lactone precursor molecules, including two separate routes that began with the convenient and readily available starting materials furan alcohol and ethyl 3-(furan-2-yl) propionate (EFP). First, an attempt to add a Michael acceptor with acid catalyst onto the 5-position of furfural alcohol was investigated, then an effort was made to add an alkyl alcohol to 5-position of the furan ring in EFP. When it was established that both strategies were unable to produce molecules suitable for lactonization, an alternative method through the generation of a stable Diels-Alder adduct between the two biomass derived compounds furan alcohol and itaconic anhydride was explored. This reaction resulted in a heavily substituted lactone with an additional linear ester, alkene, and ether functionality. Significant effort was made to find appropriate polymerization conditions utilizing both organic and metallic pre-catalysts across a wide temperature range including the low temperatures that were successful for polymerizing substituted and unsubstituted γ-butyrolactones (γ-BL). None of the tested conditions successfully produced ROP products, this is a result of the thermodynamic limitations imposed by the low ceiling temperature of γ-BL ROP, which demands high monomer concentration to polymerize. However, these results do increase our understanding of the thermodynamics of the ROP of substituted γ-BL, as well as add to our understanding of addition reactions to furan rings.

4.2 Introduction

Initially, the interest in polymers from renewable resources was driven by concerns related to the future availability of the fossil fuel feedstocks required for synthesis of common commodity materials.[1-2] However, as the body of research into polymers from renewable feedstocks has grown, it has become clear that these materials have properties that often exceed those of petroleum derived polymers,[1,3-6] including the ability to be chemically recycled, resulting in complete regeneration of monomer.[7-10] One important example is poly(lactide) (PLA) which was first produced as a biodegradable polymer for the medical industry; interestingly, when it was first produced by Dupont the cost per kilogram was nearly $1000.[11-12] However, as research into its production improved it synthesis, and infrastructure for its manufacture was developed, its cost has been reduced enough (~$2/kg) that it has become a polymer regularly used for packaging applications.[11,13] Another example that has seen significant effort towards commercialization due to its enhanced barrier properties and desirable mechanical behavior is the polyester produced from furans such as furan dicarboxylic acid (FDCA) for the synthesis of poly(ethylene furanoate) (PEF).[14] Although PEF has significant promise as a new material, there are still some noteworthy challenges to producing optically clear and high molecular weight materials suitable for commercial applications.[15] Note that neither PLA or PEF are completely and selectively chemically recyclable back to monomers.

One of the reasons PLA has become such an important success story in the field of biomass-based polymers is the development of numerous and economical ROP routes that are capable of producing stereo-regular materials with high number average molecular weight (M_n), as these factors lead to materials with properties suitable for many commercial applications.[16] The bifunctional lactic acid is polymerizable through several condensation methods results in low M_n

oligomers, with the depolymerization of the resulting oligomers producing the dimer lactide.[17] There is an extensive catalog of both organometallic and organic catalyst systems that have been shown to be successful for the ROP of lactide.[18-22] Catalytic ROP easily produces high M_n polyesters because it allows there synthesis through a chain-growth mechanism as opposed to condensation mechanism which requires perfect stoichiometry, monomers of extremely high purity, as well as complicated reaction conditions that allow for the removal of side products generated by the reaction.

One interesting example of a method to produce PEF via ROP is through the depolymerization of PEF samples with M_n < 5 kg/mol to produce a mixture of cyclic dimers, trimers, and tetramers which are then treated with catalytic ROP to produce clear materials with M_n of greater than 30 kg/mol.[15] This was an elegant method with significant improvement over previous examples, however it still produced polymers with limited M_n. An alternative to the depolymerization of furan ester oligomers is to produce furans with an alcohol and ester functionality suitable for lactonization. This would require an alkyl bridge between the alcohol or carboxylic acid to allow the difunctionalized molecule to have sufficient flexibility for the two functionalities to come into proximity and condense into a lactone. An alternative route to a furan-derived lactone was developed by Pehere *et. al.* which is interesting because it utilizes the biomass-derived itaconic anhydride in addition to furfuryl alcohol (FA) resulting in a highly substituted lactone candidate for ROP.

4.3 Results and Discussion

Design and Synthesis of Difunctional Michael Addition Products Suitable for Lactonization.

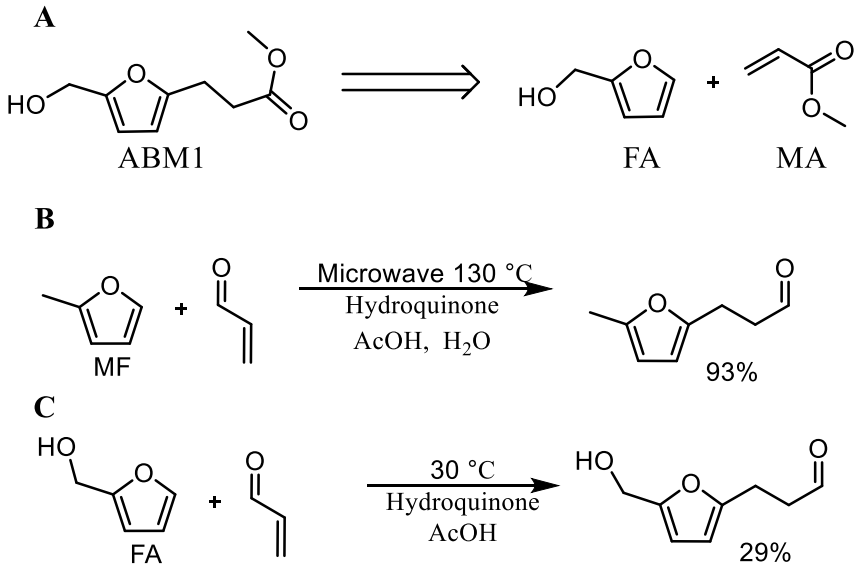

Figure 4.1. (A) Alcohol/ester functionalized furan monomer retrosynthesis from methyl acrylate (MA) and furfuryl alcohol (FA). (B) Michael addition to 2-methylfuran reported by Parson and coworker.[23] (C) Michael addition to furfuryl alcohol reported by Glukhovtsev et.al.[24]

The first step to obtaining an alcohol, ester functionalized furan is to select appropriate synthons. Acrylates, such as methyl methacrylate, have been shown to be a good candidates due to its desirable functionality combined with available sourcing from sugar fermentation.[25] In Figure 4.1, a retrosynthesis based the two biomass derived compounds FA and MA is proposed (**A**), followed by two example synthesis routes based on acid catalyzed Michael additions of acrolein to substituted furans (**B**, **C**).[23-24] Parson's and coworkers utilized 2,5 disubstituted furan as intermediates for the synthesis of highly substituted aromatics.[23] Their procedure for the synthesis of the 2,5 disubstituted furan used Bronsted acid catalyst and microwave heating for the Michael addition of acrolein to MF in high yields (Figure 4.1, **B**). In the second reference from 1963 Glukhovtsev *et. al.* presented a room temperature Bronsted acid catalyzed Michael addition

of acrolein to the alcohol substituted furan, FA, in moderate conditions with a yield of 29%.[24] The synthetic route planned here substitutes MA for acrolein, and uses the same substituted furan, FA, as the reaction shown Figure 4.1 (**C**).

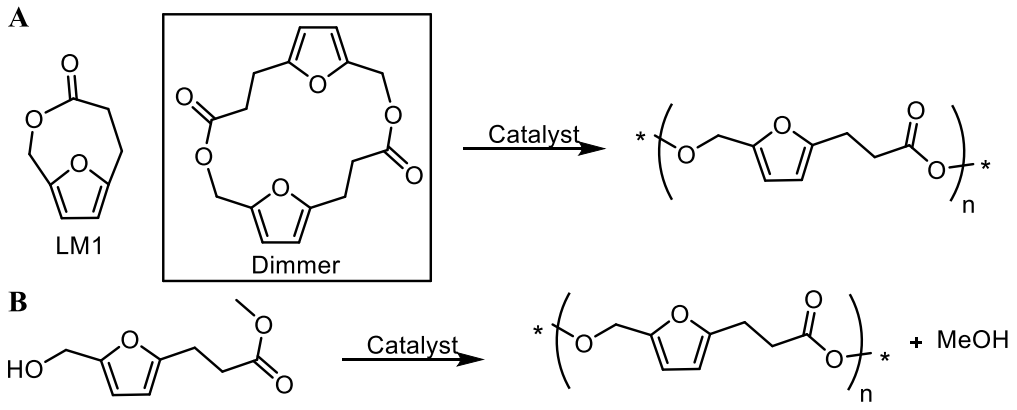

Figure 4.2. (A) Polymerization of lactone version of ABM1 showing the lack of additional products. (B) Polymerization of ABM1 showing additional polymerization product MeOH.

The desired product **ABM1** has a methyl alcohol at the 2-position of the furan ring which is the correct functionality for lactonization, however there are other factors to consider. Furan has aromatic character which causes it to be rigid and planar. The resulting 8-membered lactone was hypothesized to undergo ROP easily, but the structure may be too strained for the ring closing reaction. Dimers or trimers are also suitable ROP candidates (Figure 4.2, **A**),[15] and dimer formation would help to alleviate the obvious strain imparted by the rigid furan ring. However, even if a lactone cannot be realized from **ABM1,** it would make an excellent AB monomer for metal-catalyzed condensation polymerization. There are several advantages to using an AB monomer over using two monomers with the functionality AA and BB when performing condensation polymerizations.[26] Quite possibly the biggest advantage to having AB functionality is that this configuration eliminates the necessity to perform two separate tedious purifications and have very precise measurements of both components. High molecular weight can even be obtained from

monomer with slight impurity if the impurities are not monofunctional or poisonous to any catalyst used for the polymerization. The use of AB monomers also reduces the amount of material eliminated during the condensation polymerization (Figure 4.2, **B**). Based on the two reported Michael addition reactions and **ABM1** potential as a candidate for lactone or AB monomer formation, several reactions were performed with MA, MF and FA to test their feasibility as synthons.

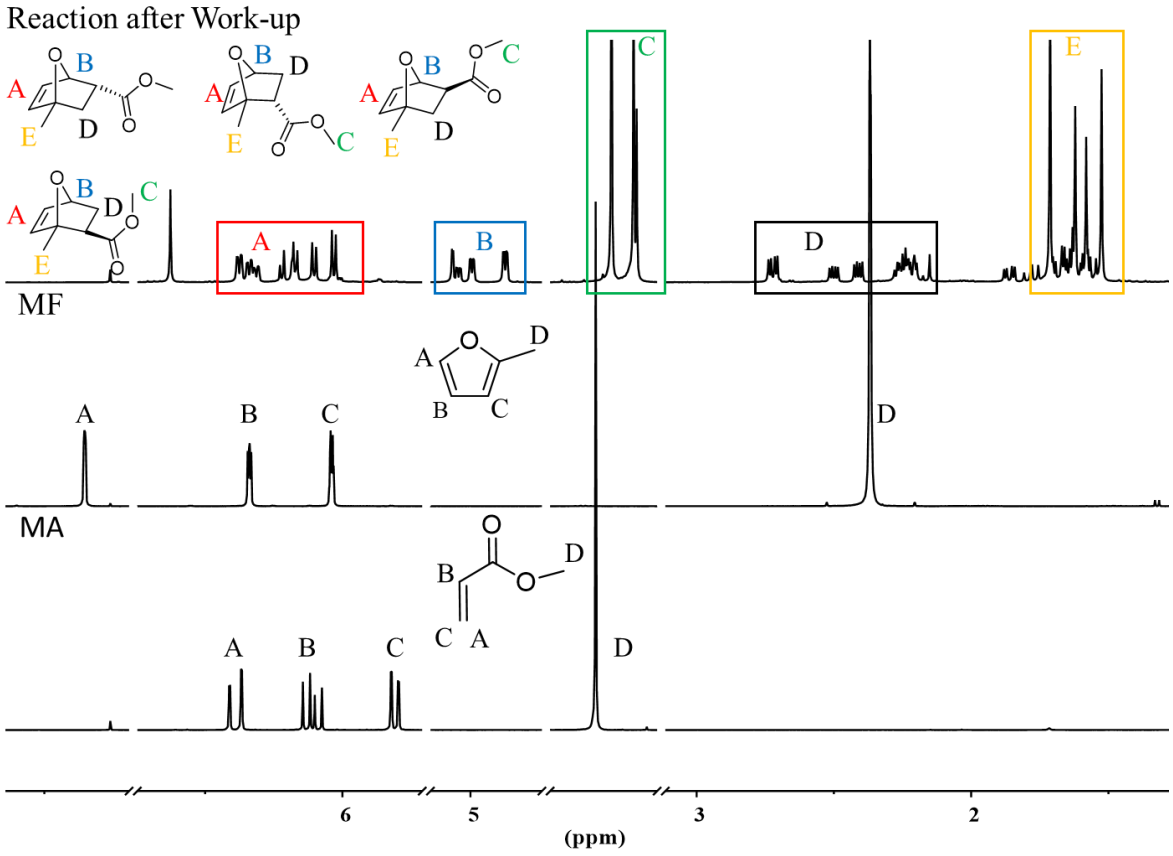

Figure 4.3. Diels-Alder products of acid catalyzed reaction between 2-methylfuran and methyl acrylate in microwave.

Initial reactions performed at 130 °C for 16 h with a 1:1 mixture of AcOH and H_2O produced a transesterification product along with some unidentified side products (S4.1). In an attempt to

eliminate the transesterification, reactions were performed at both 45 °C and 75 °C with FA while holding all other conditions constant. The lower temperature reactions produced only trace amounts of undesired side reaction products with the majority being unreacted FA, suggesting that AcOH and heat were not sufficient to initiate the Michael addition (S4.2). Control reactions performed with MA and the stronger Bronsted acid, sulfuric acid, were performed with similar results. Next, microwave heating conditions were attempted for the coupling reaction using MF and MA in sealed PTFE reactors. The resulting product mixture did not have any unreacted starting material, but was not the desired Michael addition product. However, the splitting pattern matches patterns seen in the literature discussing furan ring Diels-Alder adducts (DA)[27-28], and in work previously performed in by this group (Figure 4.3).[29] The signals around 5.0 ppm are particularly indicative of DA adduct formation, and the roughly equivalent integrations of the signals in the four boxes also suggests the statistical distribution of the four possible DA adducts pictured in Figure 4.3; this is again consistent with similar reactions previously performed by this group.[29] These experiments have shown that temperature, Bronsted acid strength, and microwave radiation are not sufficient to initiate the Michael addition of furan to MA.

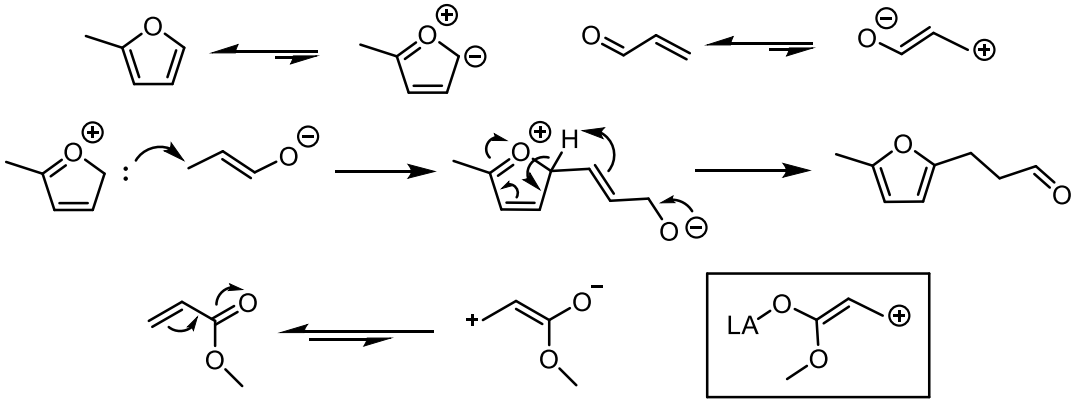

Figure 4.4. Proposed mechanism for the Bronsted acid catalyzed Michael addition of furan to acrolein and increasing MA electrophilicity with a Lewis acid.

Analysis of the proposed mechanism for the reported Michael addition of MF to acrolein showed an important distinction between MA and acrolein:[23] the increased basicity of the oxygen in acrolein helps to increase the zwitterionic resonance character of acrolein (Figure 4.4). The ester carbonyl oxygen for MA is less basic, thus the zwitterionic resonance structure contributes less to its overall reactivity (Figure 4.4). One method to increase the electrophilicity at the β-carbon of the Michael acceptor is to increase the activated state behavior with a Lewis acid (LA). Tris(pentafluorophenyl)borane ($B(C_6F_5)_3$) was selected because of its success in activating α, β-unsaturated carbonyls for polymerization.[30]

A series of small-scale experiments were performed at room temperature over 48 h with both MF and FA resulting in no apparent reaction. Therefore, a small-scale reaction was performed in $CDCl_3$ and monitored closely by ^1H NMR (Figure S4.3). First MA and $B(C_6F_5)_3$ were combined and allowed to react for 15 minutes, then four additions equivalent to the catalyst loading, relative to MA, of FA were made every 20 min over the course of 80 min with no sign of a reaction. This led to the addition of the rest of the FA and the reaction was stirred for 14 h before the next spectrum was collected. Spectra collected at 14 and 72 h showed no sign of successful coupling (Figure S4.3). To eliminate the possible effects of the alcohol, a similar experiment was performed with MF.

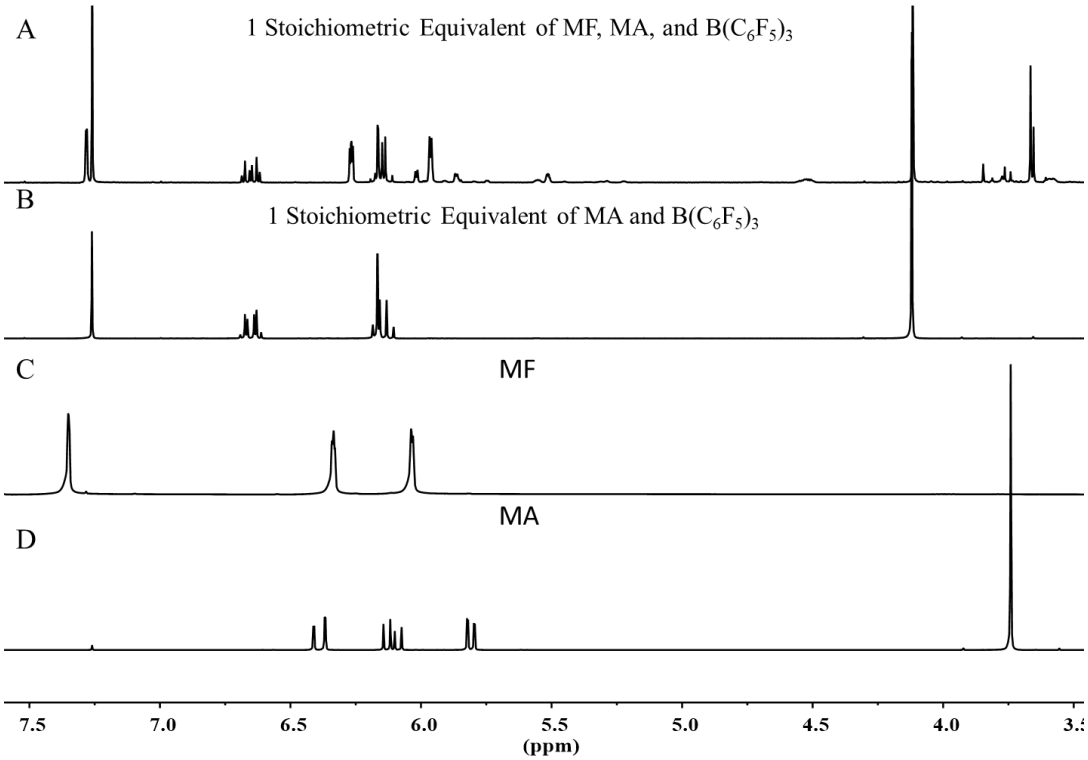

Figure 4.5. ^{1}H NMR scale Lewis acid catalyzed Michael addition of furan to methyl acrylate

One improvement over the previously discussed reaction sequence was to begin with a stoichiometric quantity of MA and $B(C_6F_5)_3$ (Figure 4.5, **B**). When comparing that spectrum to Figure 4.5 (**D**), it becomes obvious that there is a strong interaction between MA and the $B(C_6F_5)_3$ catalyst. When an equivalent of MF is added, the MA/$B(C_6F_5)_3$ adduct does not appear to be affected (Figure 4.5, **A**). With more additions of MA and MF, signals for MA (not catalyst MA adduct) appear while the signals for MF grow showing that the LA activated complex does not have activity towards the furan. At this point it was clear that an alternative method for the synthesis of alcohol-ester furan should be pursued.

Addition of Alcohol Functionality to Furan Ester

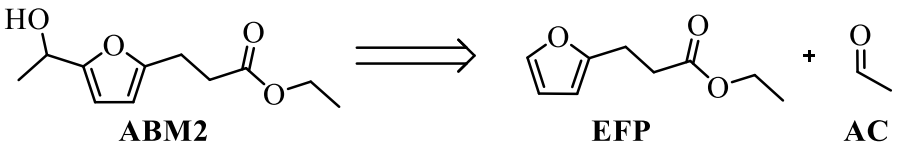

Figure 4.6. Retro synthetic route to alcohol-ester functionalized furan from EFP and AC.

Monomer **ABM2** has several of the advantages that made **ABM1** an attractive target with a proposed route utilizing the commercially available ethyl 3-(furan-2-yl) propionate (EFP) and acetaldehyde (AC). This differs from the first proposed alcohol-ester functionalized furan because the propanoate portion of the molecule is already attached to the furan and the alkyl alcohol is being added (Figure 4.6). The literature example used as the basis for this hypothesis was Wang *et. al's.* work synthesizing a series of geminal dimethyl difuran difunctionalized monomers.[31] This new monomer would require the single addition of one AC to one EFP as opposed to the previous work where two furans were added to one acetone molecule. Initial experiments performed resulted in the spectra shown in Figure 4.8.

The molecule was not immediately identified as the dimer shown in Figure 4.3. Initial attempts to assign the spectrum confirmed that the desired product was not produced. To gain additional evidence for structural identification, an electrospray ionization mass spectrum (ESI-MS) experiment was performed (Figure S4.4). The results showed a product with a chemical formula of $C_{20}H_{30}NO_6$ (380.20 g/mol), corresponding to a formula of $C_{20}H_{26}O_6$ (362.17 g/mol) plus the ammonium ion (NH_4^+), this matches the dimer shown in Figure 4.7. Additional indication of proton assignment was obtained from COSY experiments (S4.5). Once the it was determined that the dimer and not the alcohol was forming, experiments were designed in an effort to eliminate the second addition of EFP to the acetaldehyde (Figure 4.7).

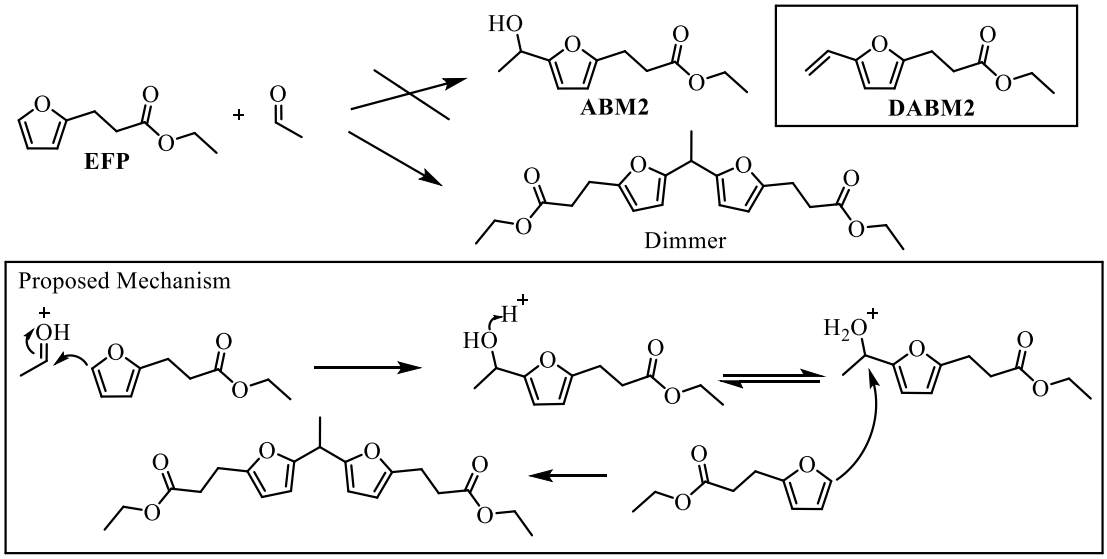

Figure 4.7. Synthesis of AB monomer with additional methyl after alcohol on furan ring along with dimmer actually formed and proposed mechanism for its formation.

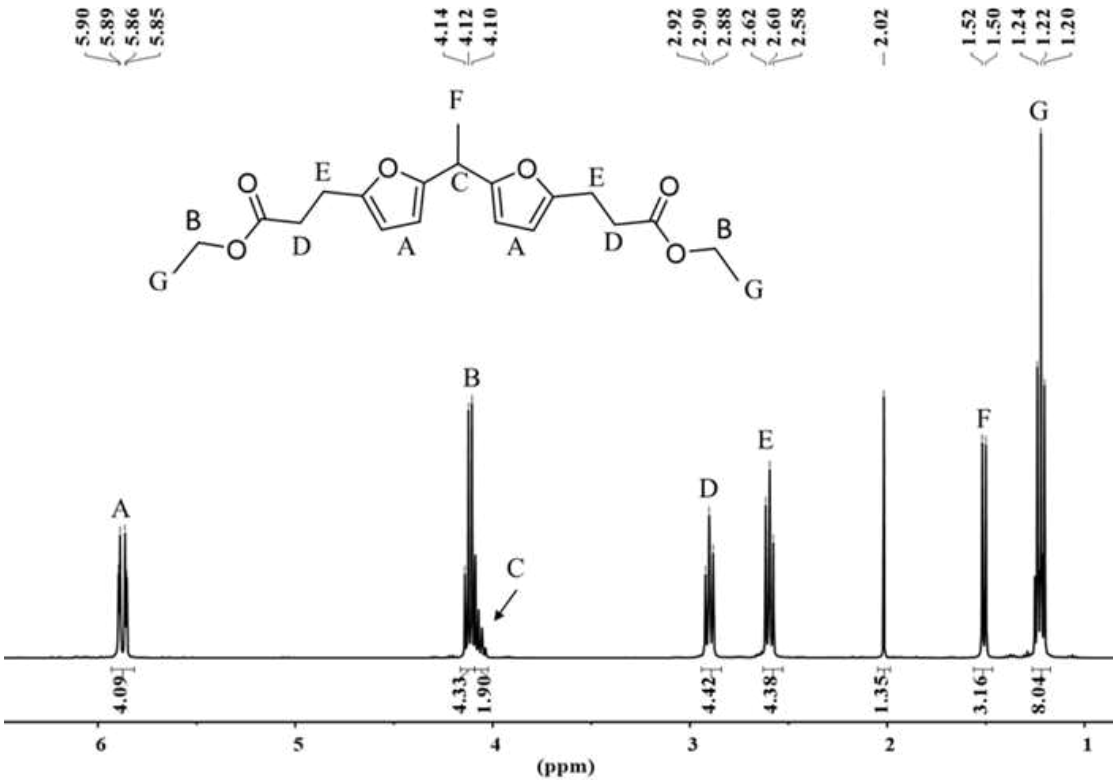

Figure 4.8. Assigned ^{1}H NMR spectrum of product obtained from reaction of AC and EFP.

Analysis of the proposed mechanism was used to develop two strategies in an attempt to eliminate dimmer formation (Figure 4.7). For the initial experiments, a simple 1:1 stoichiometry of acetaldehyde and EFP was used, and an 25% excess of acetaldehyde was utilized for the follow-up experiment. Identification of the products was aided by GC/MS (gas chromatography mass spectra). The GC trace showed one minor product with a mass of 195 g/mol and a major product of 362 g/mol. The signal corresponding to 195 g/mol is close to the mass of **DABM2** (194 g/mol) which is the dehydration product of **ABM2**, however the major product still had a mass matching the dimmer (Figure 4.7). The next attempt utilized an increased ratio of acetaldehyde to EFM (2:1, acetaldehyde to EFP), and while this resulted in increased production of the **DABM2** is substantial however **ABM2** was still present. An experiment with water added was performed to try to shift equilibrium away from the dehydration of **ABM2.** The water did not prevent the dehydration or addition of the second EFP, but it also did not stop the reaction. This evidence that the second addition does not proceed through and S_N1 mechanism because carbocations cannot form in an aqueous solution, but the fact that the desired product still did not form led to developing an alternative route to a furan derived lactone.

Exploring the ROP of a Highly Substituted Butyrolactone derived from FF and Itaconic Anhydride.

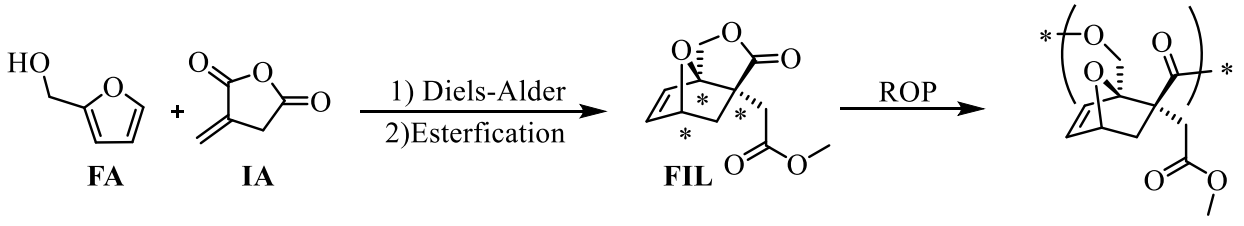

FA **IA** **FIL**

Figure 4.9. Pehere et. al.'s synthesis of highly substituted butyrolactone from FA and IA as a candidate for ROP.

The synthesis for methyl 2-((3aR,6R)-1-oxo-6,7-dihydro-3H-3a,6-epoxyisobenzofuran-7a(1H)-yl)acetate (**FIL**) reported by Pehere and coworkers is simple, high yielding, and utilizes the two biomass derived compound FA and IA (Figure 4.9).[28] The Diels-Alder portion only requires mixing IA and FA together and stirring for 48 hours, the reactants were simply combined in 20 mL scintillation vial then were stirred on an orbital shaker at room temperature for 48 h. The DA product precipitates from the excess FA and can be washed with DCM to produce a surprisingly clean carboxylic acid that can be used directly in the next step (Figure 4.10, top). The stereo-control of the DA reaction, combined with the kinetic preference to form the lactone, result in thermodynamically stable fused ring GBL with 3 defined stereocenters[28]. The second step was an acid catalyzed esterification with MeOH resulting in the methyl ester (Figure 4.10, bottom).

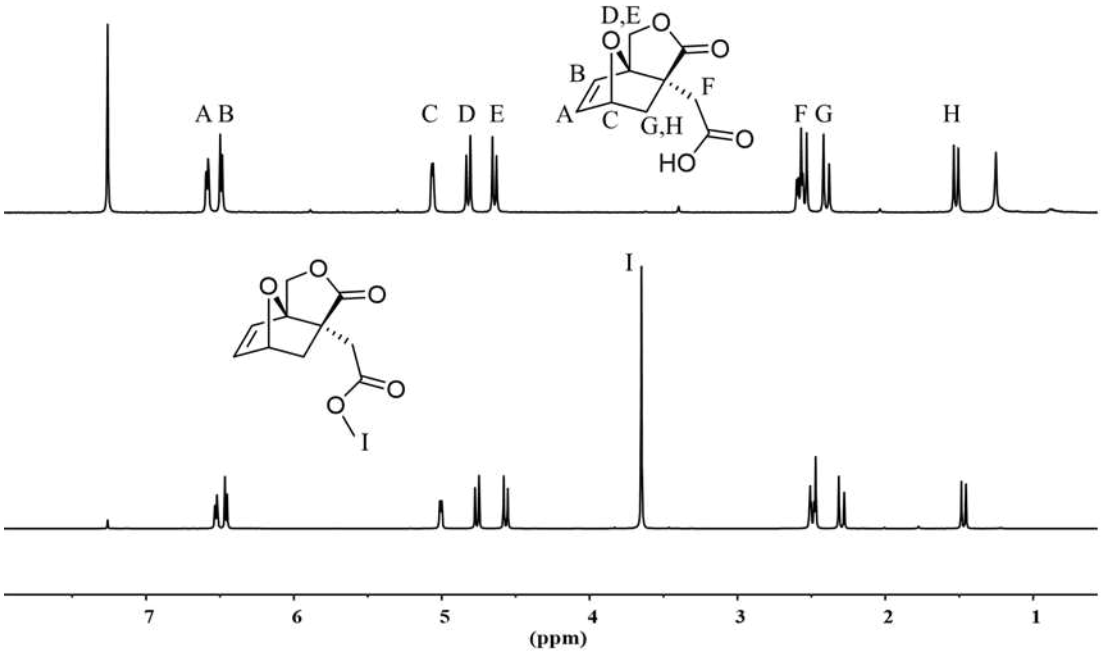

Figure 4.10. Top assigned 1H NMR of 14. Bottom 1H NMR of FIL with ester methyl assigned.

The product from the esterification step is not pure enough to be used directly in ROP reactions. Accordingly, two different purification steps have been developed. The first purification

performed was a manual column, which resulted in a slightly beige powder and a clean ^{1}H NMR. Experiments performed to determine the appropriate solvent for polymerizations showed that **FIL** had low solubility at room temperature but high solubility at 100 °C in toluene, this led to trying a recrystallization after the column. The recrystallized methyl ester produced shiny white cubic crystals with the ^{1}H NMR shown in Figure 4.10, bottom. Attempts to skip column chromatography and purify with just recrystallization had mixed results. With high purity **FIL** available, experiments were conceived to realize the ROP.

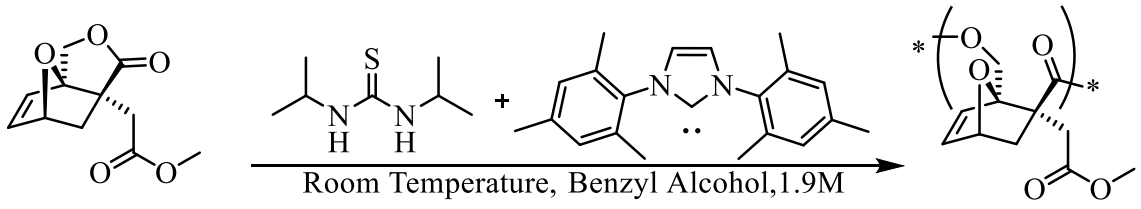

Figure 4.11. Proposed organically catalyzed ROP of FIL**.**

The first polymerization system attempted was the organic thiourea/base combination extensively studied by Waymouth *et al.* as well as others (Figure 4.11).[22, 32-36] The thiourea and carbene system chosen was shown by Cywar *et al.* to have good activity for ROP of a similar trans-fused GBL 4,5-trans-cyclohexyl-fused γ-butrolactone (4,5-T6GBL), and reactions were performed in chloroform, DCM, and toluene.[37] There was some concern about chlorinated solvents with 1,3-dimesityl-1H-imidazol-3-ium-2-ide (IMes) but the issues with solubility limited the alternatives therefore chloroform and DCM were used with awareness of potential issues. The monomer is a crystalline solid with limited solubility in any solvent tested at this point. The maximum concentration achievable in solvents tested was 1.9M at room temperature in chloroform, less at

temperatures of -60 °C. After unsuccessful initial trials, an NMR scale reaction was performed to try to elucidate the cause.

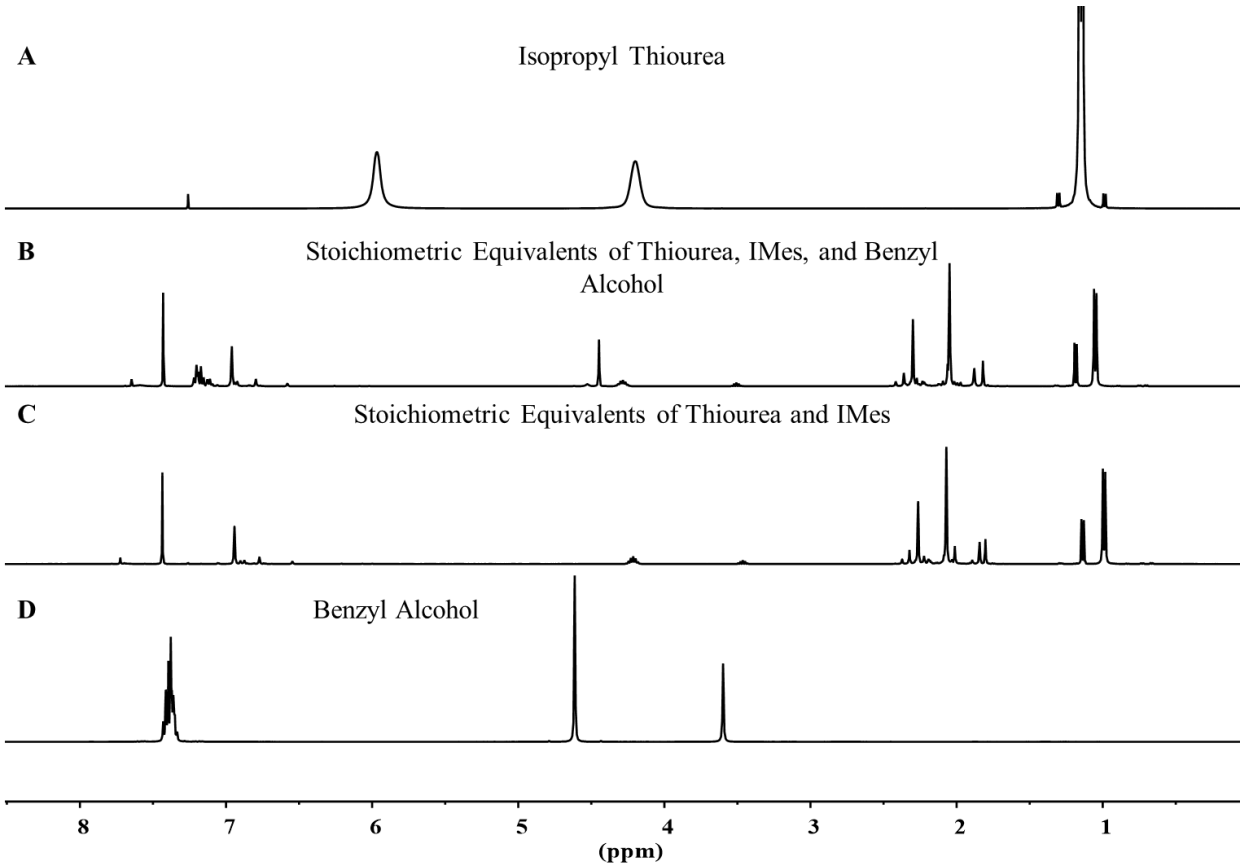

Figure 4.12. ^{1}H NMR scale stoichiometric reaction of isopropyl thiourea, IMes, and benzyl alcohol

When stoichiometric equivalents of IMes were added to 1,3-diisopropylthiourea (thiourea), Figure 4.12 **A** to **C**, an obvious reaction can be seen by the disappearance of the N-H protons at 4.19 and 5.96 ppm (Figure 4.12, **A**) as well as the splitting of the isopropyl signal at 1.14 ppm (Figure 4.12, **A**), separating into two signals with one shifted up-field. In addition, when a stoichiometric equivalent of benzyl alcohol initiator was added, shifts in both the phenyl and benzyl protons can be observed, as well as the disappearance of the signal at 3.6 ppm most likely

the signal for the alcohol proton (Figure 4.12, **B**). The resulting shifts seen as the thiourea, IMes, and benzyl alcohol are combined are consistent with the proposed mechanism confirming that IMes deprotonates the thiourea.[38] Then, the alcohol proton coordinates to the activated nitrogen. If ROP was to commence, then the monomer would also coordinate with the thiourea-alcohol complex.

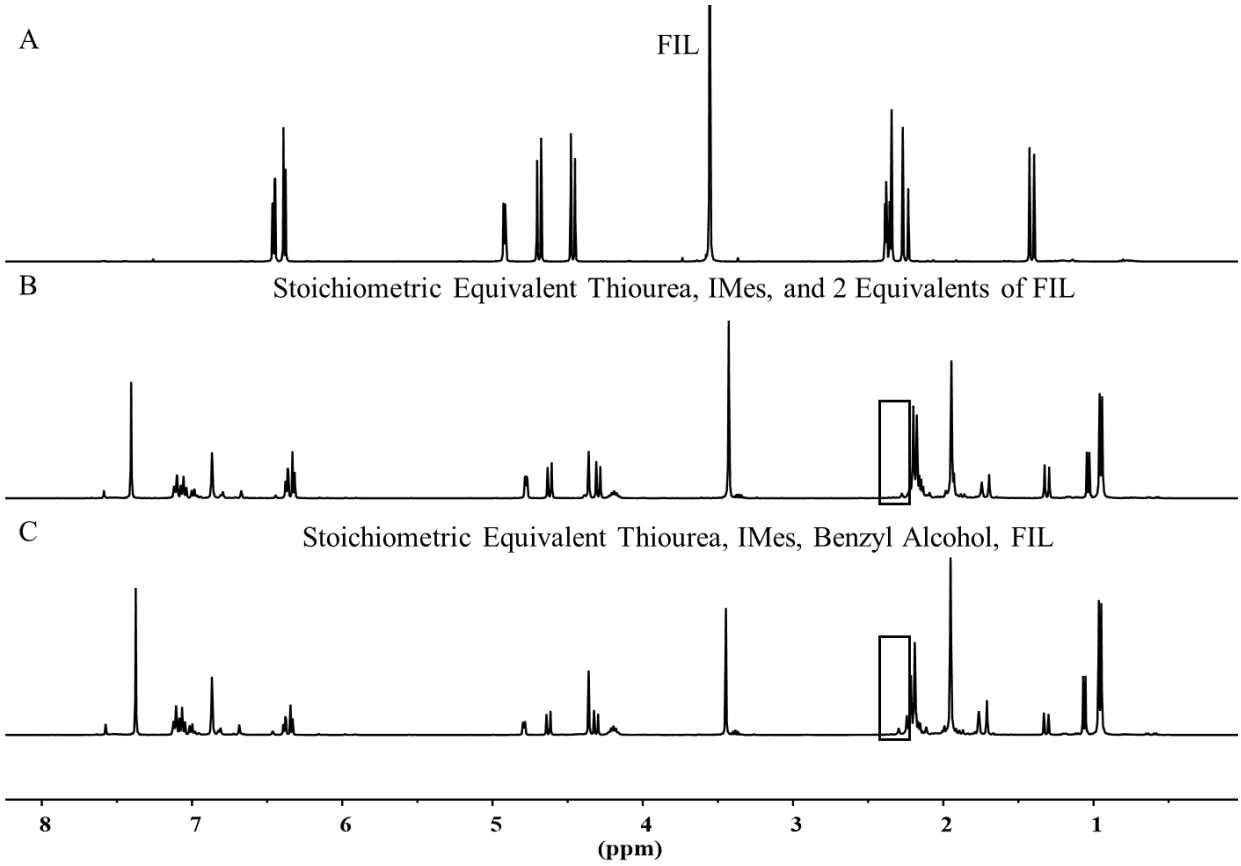

Figure 4.13. ^{1}H NMR scale stoichiometric reaction of isopropyl thiourea, IMes, benzyl alcohol, and FIL

Once it was established that the thiourea was activated by IMes and that the initiator was complexing with the catalyst, two separate stoichiometric additions of monomer were made. The doublets at 4.67 and 4.47 ppm belonging to the methylene attached to the acyl lactone oxygen should shift after polymerization. Figure 4.13 **B** and **C** show that these doublets are unaffected after the addition of one and then the second equivalent of monomer. The signals for thiourea,

IMes, and benzyl alcohol were also unaltered. The only signal that changed were the protons alpha to the ester carbonyl (Figure 4.13, **B** and **C** boxed). This is evidence that the catalyst is interacting with the ester and not the lactone. This is inconsistent with previous work done by Lohmeijer *et. al.* which showed that there was an association constant of nearly zero when thiourea was reacted with linear polyesters and a significantly larger constant, about 40, when thiourea was reacted with cyclic esters (lactones).[39] One possible reaction occurring could be the deprotonation of the alpha carbon, however the fact that this signal is still unaffected upon addition of the second monomer equivalent makes this hypothesis unlikely. The second possible reaction is the complexing of the thiourea with that monomer and transesterification, but again the fact that this signal is not affected by the addition of the second equivalent of monomer suggests that this is not a valid explanation either. Whatever the cause of the shift is, ROP is not occurring. Reactions were subsequently performed at lower temperatures in an attempt to overcome the large negative entropic change of 5-membered ring ROP.[7]

The importance of concentration on the ring ROP of GBL type monomers has been well established by this group[7, 9-10]. So, the first step was to try to find a solvent that allowed a concentration of 5M or more to be obtained. In addition to the solvents tested previously THF and acetonitrile were examined for ability to achieve higher concentrations. The monomers solubility in acetonitrile was comparable to chloroform and DCM however the freezing point was too high to be used in the low temperature reactions. The maximum monomer concentration obtainable in THF was only slightly more than 1.7M. A series of reactions were performed at -60 °C in THF, and deuterated chloroform. Two of the reactions performed in chloroform included a $La[N(SiMe_3)_2]_3$ catalyzed and benzyl alcohol-initiated polymerization (monomer, catalyst, and initiator ratio; 50:1:3) and also an anionic polymerization reaction with potassium methoxide. The

reaction performed in THF was identical to the La complex catalyzed reaction performed in $CDCl_3$. All three reactions were performed at 1.6M, the maximum molarity achievable at this temperature with this monomer in the solvents tested. Reactions were monitored by taking aliquots every four hours from reaction and immediately quenching with benzoic acid, not surprisingly they showed no polymer formation even after 24 hours. The inability of this monomer to undergo ROP is consistent with the hypothesis that high concentration is essential to achieve obtainable ceiling temperatures (T_c).[7, 10, 37]

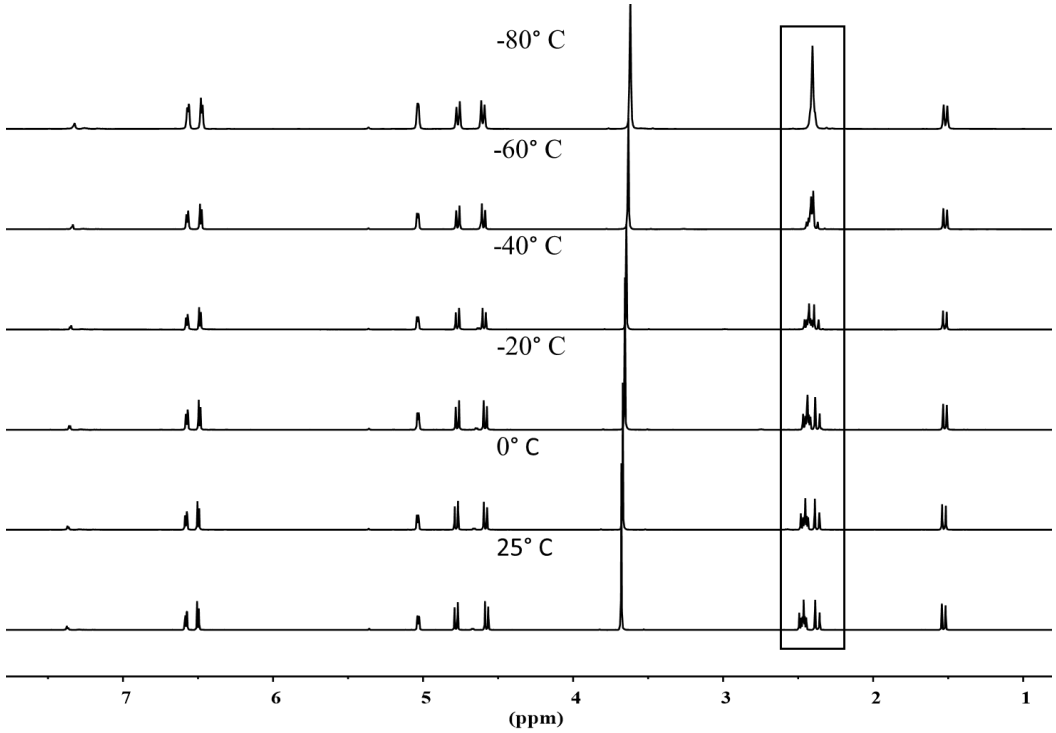

Figure 4.14. VT ^{1}H NMR sequence with FIL, La catalyst, and benzyl alcohol initiator in CD_2Cl_2

Up to this point, several attempts at the selective ring opening polymerization (ROP) of FIL using organic catalyst system, anionic initiator, and $La[N(SiMe_3)_2]_3$ were covered. One important observation derived from the work so far is that solubility of **FIL** in toluene, DCM, and chloroform is a limiting factor. Other solvents such as acetonitrile are unsuitable because of their relatively

high freezing point. The maximum solubility attained at room temperature was 1.9M in chloroform and only 0.7M in THF. Obviously, these results are not promising, however in their work developing a selective technique for the ROP of α-methylene-γ-butyrolactone (MBL) Tang and coworkers developed a variable temperature (VT) ^{1}H NMR experiment to determine T_c,[9] and this experiment was performed with **FIL** to determine if the monomer had an attainable T_c.

For the VT NMR experiments the monomer/catalyst/initiator ratio of 60/1/3 was loaded, into a sealed J-Young tube, inside a N_2 filled glove box, then run in a precooled 500 MHz NMR. The solvent chosen was CD_2Cl_2 based on freezing temperature not monomer solubility, the maximum concentration achievable was 1M. The monomer, pre-catalyst, and initiator ratio were based on the Tang *et. al.* results for the selective ROP of MBL, in this work it was determined that the ratio of initiator to catalyst of 1:3 was important for ROP selectivity.[9] At first glance, there does appear to be a change in the intensity of the singlet just above 5 ppm, but once the integration was checked it was found that it did not change in any of the six experiments shown here (Figure 4.14). There is an obvious change in the signals belonging to the methyl ester around 2.5 ppm (Figure 4.14, box), however as temperature increases, they return to normal suggesting that this change is a result of decreased bond rotation, due to the low temperature, and not catalyst interaction. The previously reported successful ROPs of 5-membered lactones were achieved using high concentration (5M) because T_c is inversely proportional to concentration. The importance of high concentration to T_c, which is very low for γ-BL type monomers due to the large entropic penalty of ROP,[7] can account for the lack of polymer formation for this γ-BL type monomers because of its low solubility. Due to the inability of **FIL** to undergo ROP at low temperatures an experiment was performed with $La[n(SiMe_3)_2]_3$ and no initiator in the melt. The results are shown in S4.6, and it appears that both the lactone and the methyl esters have reacted because of the disappearance of

their signals. However, the product did not have physical characteristics that would suggest that the product was polymer.

4.4 Conclusions

The two methods employed to synthesize alcohol/ester functionalized furans from FA and EFP utilized orthogonal approaches. The first approach was the Michael addition of FA to MA which showed that regardless of conditions or catalyst the β-carbon was not electrophilic enough for the Michael addition, however these experiments did show that under microwave heating conditions MA had sufficient dienophilic behavior to achieve quantitative conversion to DA adduct. In contrast to the Michael addition route, the second method employed added the alcohol functionality to the ester functionalized furan EFP through an acid catalyzed addition of AC. Initial results showed the formation of AC linked EFP dimmers. Use of excess AC led to formation of a mixture of the dimmer and the alkene, ester functionalized furan **DABM2.** Addition of water to the reaction did not eliminate the dehydration however it did show that the reaction was tolerant of water. Both routes to an alcohol/ester functionalized furan produced unexpected products that increased our understanding of furan substitution chemistry.

The previously reported highly substituted GBL type monomer **FIL** was synthesized and then analyzed for potential as a substrate for ROP. An organic catalyst system employing benzyl alcohol initiator, thiourea and IMes that work through a hydrogen-bond activator mechanism were explored. Careful analysis of stoichiometric reactions between the **FIL** and catalyst system show catalyst interaction at the linear ester component and not the lactone. Another catalyst system investigated continued to use benzyl alcohol as the initiator but changed from organic to metallic pre-catalyst. This La complex with initiator was used at temperatures from -80° C to room temperature, and without initiator in the melt at 135 °C. The fact that ROP was not realized helps

to improve our understanding of γ-BL ROP thermodynamics because it offers more evidence of limitations imposed by T_c on monomers with poor solubility. The fact that **FIL** is solid and has poor solubility limited reaction concentrations, likely suppressing T_c to unattainable levels.

References

(1) Gandini, A.; Lacerda, T. M.; Carvalho, A. J. F.; Trovatti, E., Progress of Polymers from Renewable Resources: Furans, Vegetable Oils, and Polysaccharides. *Chem. Rev.* **2016**, 116, 1637-1669.

(2) Chu, S.; Majumdar, A., Opportunities and challenges for a sustainable energy future. *Nature* **2012**, 488, 294-303.

(3) Gandini, A., The furan/maleimide Diels–Alder reaction: A versatile click–unclick tool in macromolecular synthesis. *Prog. Polym. Sci.* **2013**, 38, 1-29.

(4) Gandini, A.; Belgacem, M. N., Furans in polymer chemistry. *Prog. Polym. Sci.* **1997**, 22, 1203-1379.

(5) Moreau, C.; Belgacem, M. N.; Gandini, A., Recent Catalytic Advances in the Chemistry of Substituted Furans from Carbohydrates and in the Ensuing Polymers. *Top. Catal.*, **2004**, 27, 11-30.

(6) Dhers, S.; Vantomme, G.; Avérous, L., A fully bio-based polyimine vitrimer derived from fructose. *Green Chem.* **2019**, 21, 1596-1601.

(7) Hong, M.; Chen, E. Y.-X., Completely recyclable biopolymers with linear and cyclic topologies via ring-opening polymerization of γ-butyrolactone. *Nature Chem.* **2016**, 8, 42-49.

(8) Tang, J.; Chen, E. Y. X., Increasing complexity in organopolymerization of multifunctional γ-butyrolactones. *Eur. Polym. J.* **2017**, 95, 678-692.

(9) Tang, X.; Hong, M.; Falivene, L.; Caporaso, L.; Cavallo, L.; Chen, E. Y.-X., The Quest for Converting Biorenewable Bifunctional α-Methylene-γ-butyrolactone into Degradable and

Recyclable Polyester: Controlling Vinyl-Addition/Ring-Opening/Cross-Linking Pathways. *J. Am. Chem. Soc.* **2016**, 138, 14326-14337.

(10) Zhu, J.-B.; Watson, E. M.; Tang, J.; Chen, E. Y.-X., A synthetic polymer system with repeatable chemical recyclability. *Science* **2018**, 360, 398-403.

(11) Schneiderman, D. K.; Hillmyer, M. A., 50th Anniversary Perspective: There Is a Great Future in Sustainable Polymers. *Macromolecules* **2017**, 50, 3733-3749.

(12) Larson, A. A., A: O'Brian, K. Natureworks: Green Chemistry's Contribution to Biotechnology Innovation, Commercialization, and Strategic Positioning. . https://saylordotorg.github.io/text_sustainability-innovation-and-entrepreneurship/s12-01-natureworks-green-chemistry-s-.html.

(13) Hillmyer, M. A., The promise of plastics from plants. *Science* **2017**, 358, 868-870.

(14) Bomgardner, M. M., Building a Better Plastic Bottle *C & EN* **2017**, 17-19.

(15) Rosenboom, J.-G.; Hohl, D. K.; Fleckenstein, P.; Storti, G.; Morbidelli, M., Bottle-grade polyethylene furanoate from ring-opening polymerisation of cyclic oligomers. *Nature Communications* **2018**, 9, 2701-2708.

(16) Dechy-Cabaret, O.; Martin-Vaca, B.; Bourissou, D., Controlled Ring-Opening Polymerization of Lactide and Glycolide. *Chem. Rev.* **2004**, 104, 6147-6176.

(17) Inkinen, S.; Hakkarainen, M.; Albertsson, A.-C.; Södergård, A., From Lactic Acid to Poly(lactic acid) (PLA): Characterization and Analysis of PLA and Its Precursors. *Biomacromolecules* **2011**, 12, 523-532.

(18) Kricheldorf, H. R.; Berl, M.; Scharnagl, N., Poly(lactones). 9. Polymerization mechanism of metal alkoxide initiated polymerizations of lactide and various lactones. *Macromolecules* **1988**, 21, 286-293.

(19) Degée, P.; Dubois, P.; Jérŏme, R.; Jacobsen, S.; Fritz, H.-G., New catalysis for fast bulk ring-opening polymerization of lactide monomers. *Macromolecular Symposia* **1999**, 144, 289-302.

(20) Gibson, V. C.; Marshall, E. L., 9.1 - Metal Complexes as Catalysts for Polymerization Reactions. In *Comprehensive Coordination Chemistry II*, McCleverty, J. A.; Meyer, T. J., Eds. Pergamon: Oxford, 2003; pp 1-74.

(21) Chisholm, M. H.; Gallucci, J.; Phomphrai, K., Lactide polymerization by well-defined calcium coordination complexes: comparisons with related magnesium and zinc chemistry. *Chem. Comm.* **2003**, 48-49.

(22) Kamber, N. E.; Jeong, W.; Waymouth, R. M.; Pratt, R. C.; Lohmeijer, B. G. G.; Hedrick, J. L., Organocatalytic Ring-Opening Polymerization. *Chem. Rev.* **2007**, 107, 5813-5840.

(23) Parsons, P. J.; Allen, L. A. T.; Jones, D. R.; Padgham, A. C.; Pryke, J. A.; McKenna, J.; O'Reilly, D., Approaches to the Synthesis of Highly Substituted Aromatic and Fused Rings: Metal-Catalysed versus Thermal Cyclisation. *Synthesis* **2018**, 50, 84-101.

(24) Glukhovtsev, V. G.; Zakharova, S. V.; Petrov, A. D., Reaction of furan alcohols and their derivatives with α,β-unsaturated aldehydes and ketones. *Dokl. Akad. Nauk SSSR* **1963**, 570-572.

(25) Bloom, P. D. V., P. Monomers and Polymers from Bioderived Carbon Monomers and Polymers from Bioderived Carbon. 2009/0018300, 2009.

(26) Stille, J. K., Step-growth polymerization. *Journal of Chemical Education* **1981**, 58, 862-866.

(27) Hanlon, A. M.; Martin, I.; Bright, E. R.; Chouinard, J.; Rodriguez, K. J.; Patenotte, G. E.; Berda, E. B., Exploring structural effects in single-chain "folding" mediated by intramolecular thermal Diels–Alder chemistry. *Polymer Chem.* **2017**, 34, 5120-5128.

(28) Pehere, A. D.; Xu, S.; Thompson, S. K.; Hillmyer, M. A.; Hoye, T. R., Diels–Alder Reactions of Furans with Itaconic Anhydride: Overcoming Unfavorable Thermodynamics. *Organic Letters* **2016**, 18, 2584-2587.

(29) Wilson, J. F.; Chen, E. Y. X., Difuranic Diols for Renewable Polymers with Pendent Furan Rings. *ACS Sustainable Chem. Eng.* **2019**, 7, 7035-7046.

(30) McGraw, M.; Chen, E. Y.-X., Catalytic Lewis Pair Polymerization of Renewable Methyl Crotonate to High-Molecular-Weight Polymers. *ACS Catal.* **2018**, 8, 9877-9887.

(31) Wang, L.; Eguchi, Y.; Chen, E. Y.-X., Streamlined Synthesis of Biomonomers for Bioresourced Materials: Bisfuran Diacids, Diols, and Diamines via Common Bisfuran Dibromide Intermediates. *Ind. Eng. Chem. Res.* **2017**, 56, 11380-11387.

(32) Pothupitiya, J. U.; Hewawasam, R. S.; Kiesewetter, M. K., Urea and Thiourea H-Bond Donating Catalysts for Ring-Opening Polymerization: Mechanistic Insights via (Non)linear Free Energy Relationships. *Macromolecules* **2018**, 51, 3203-3211.

(33) Lin, L.; Han, D.; Qin, J.; Wang, S.; Xiao, M.; Sun, L.; Meng, Y., Nonstrained γ-Butyrolactone to High-Molecular-Weight Poly(γ-butyrolactone): Facile Bulk Polymerization Using Economical Ureas/Alkoxides. *Macromolecules* **2018**, 51, 9317-9322.

(34) Dove, A. P.; Pratt, R. C.; Lohmeijer, B. G. G.; Waymouth, R. M.; Hedrick, J. L., Thiourea-Based Bifunctional Organocatalysis: Supramolecular Recognition for Living Polymerization. *J. Am. Chem. Soc.* **2005**, 127, 13798-13799.

(35) Dove, A. P., Organic Catalysis for Ring-Opening Polymerization. *ACS Macro Lett.* **2012**, 1, 1409-1412.

(36) Lin, B.; Waymouth, R. M., Organic Ring-Opening Polymerization Catalysts: Reactivity Control by Balancing Acidity. *Macromolecules* **2018**, 51, 2932-2938.

(37) Cywar, R. M.; Zhu, J.-B.; Chen, E. Y. X., Selective or living organopolymerization of a six-five bicyclic lactone to produce fully recyclable polyesters. *Polymer Chem.* **2019**, 10, 3097-3106.

(38) Zhang, X.; Jones, G. O.; Hedrick, J. L.; Waymouth, R. M., Fast and selective ring-opening polymerizations by alkoxides and thioureas. *Nature Chemistry* **2016**, 8, 1047-1053.

(39) Lohmeijer, B. G. G.; Pratt, R. C.; Leibfarth, F.; Logan, J. W.; Long, D. A.; Dove, A. P.; Nederberg, F.; Choi, J.; Wade, C.; Waymouth, R. M.; Hedrick, J. L., Guanidine and Amidine Organocatalysts for Ring-Opening Polymerization of Cyclic Esters. *Macromolecules* **2006**, 39, 8574-8583.

Chapter 5

Reactivity and Complexity of a Multifunctional Furan Acrylate Monomer Towards Organocatalysts

5.1 Synopsis

The catalytic upgrading of the biomass derived platform chemical 5-hydroxymethylfurfural (HMF) has received significant attention, especially due to its potential as a monomer for polymers with improved barrier and mechanical properties. One method of upgrading the value of HMF is to convert it to multifunctional furan acrylate monomers. NHC (N-heterocyclic carbenes) have been shown to catalyze several reactions involving furans including benzoin condensations of aldehydes and tail-to-tail coupling of furan diacrylates. In this work a monomer with both an aldehyde suitable for benzoin condensation and an acrylate Michael acceptor was developed. The methacrylate furan aldehyde (MFA) was then utilized in a series of TPT (1,2,4-triphenyl-4,5-dihydro-1*H*-1,2,4-triazol-5-ylidene) catalyzed reactions designed to be auto-tandem or *cascading*. The hypothesized *cascading* sequence started with the TPT catalyzed benzoin condensation to produce a furoin moiety followed by the tail-to-tail coupling of Michael acceptors referred to as proton transfer polymerization (HTP). Initial experiments produced an un-identified small molecule, that after isolation was identified as furil dimethacrylate (FDMA). Attempted tail-to-tail coupling reactions were performed on FDMA directly proving that FDMA is inactive towards TPT catalyzed tail-to-tail coupling. Appropriate controls testing the chemoselectivity of TPT with FDMA showed that TPT was preferentially reacting with the diketone carbons and not the β-carbon of the Michael acceptor, inhibiting the HTP pathway. To prevent diketone formation, a series of experiments was performed to determine why the α-hydroxy furoin product of the benzoin condensation was oxidizing to the diketone furil. Analysis of the proposed mechanism for

both the benzoin condensation and the HTP combined with variable temperature (VT) NMR experiments show that the enolate formed when TPT adds to the Michael acceptor acts as a base to catalyze the oxidation of the α-hydroxyl furoin into a diketone furil. The resulting FDMA cannot undergo HTP because TPT preferentially interacts with diketone carbons over the Michael acceptor.

5.2 Introduction

The primary source of functionalized carbon skeletons for chemical industries, as well as the source of thermal energy used for power generation and transportation, are fossil fuels. It is not hard to make the argument that fossil fuel refining is the lynch pin industry that holds our modern way of life together. As alternatives to burning fossil fuels to generate electricity continue to progress, development of biorefining will remain important to generate functionalized carbon skeletons for fine chemical, commodity chemical, and materials industries.[1-11] Ideally biorefining utilizes non-food waste organic materials from agriculture and forestry industries. Lignocellulose makes up a significant portion of these materials and is comprised of important biopolymers such as cellulose, hemicellulose, and lignin.[12 5, 7-10] There is a significant body of work showing that the platform chemicals 5-hydroxymethylfurfural (HMF) and furfural (FF) can be efficiently produced from cellulose and hemicellulose.[2, 7, 12-19] Therefore there is economic and environmental incentive to develop chemistries associated with these molecules.

The aldehyde functionality present in both HMF and FF has been used as a convenient functional handle for a series of upgrading reactions. One reaction that has been extensively studied for furan-aldehyde upgrading is the carbene catalyzed benzoin condensation first reported

by Ukai in 1943,[20] followed by Breslow who added significantly with his mechanistic work related to the enaminol intermediate (Breslow intermediate) in 1958.[21] Our group has used a variety of triazolium, thiazolium, and imidazolium based carbene's to explore both the homo-coupling of HMF as well as the cross coupling of HMF and FF in our work to increase the value of these biorefining platform chemicals.[5-6, 22-23] In the course of this work one carbene catalyst has stood out as having exceptional selectivity in a variety of reactions. The methanol adduct TPT-OMe (5-methoxy-1,3,4-triphenyl-4,5-dihydro-1H-1,2,4-triazole) of the active triazolylidene carbene TPT (1,2,4-triphenyl-4,5-dihydro-1*H*-1,2,4-triazol-5-ylidene) which can be generated in situ with heat or easily converted to the stable active carbene with vacuum and heat.[24] In addition to Benzoin condensations, TPT has catalyzed the tail-to-tail coupling of Michael acceptors.[25-26] This reaction is very sensitive to carbene structure. Similar carbene's produce single addition[27], cyclo-dimerization,[28] cyclo-tetramerization,[29] and vinyl polymerization products.[27, 30] Thus, drastic changes in reactivity can be observed from subtle derivatization of the carbene structure. The ability for TPT to catalyze both a benzoin condensation and a tail-to-tail Michael addition raises the exciting possibility of combining these reactions into one pot auto-tandem processes.

The catalytic upgrading of complex biomass derived chemicals with multiple functionalities through a *cascading* (auto-tandem) reaction sequence (Scheme 1, Pathway A) where the aldehydes would undergo benzoin condensation,[5, 31] followed by the tail-to-tail coupling of the Michael acceptors,[32-35] would produce unique polymers with in interesting selection of functional handles. The alcohol resulting from the benzoin condensation portion of the cascading reaction could facilitate hydrogen bonding, increasing intermolecular forces, and could provide a convenient handle for post functionalization reactions that include esterification's with acyl chlorides and formation of urethan bonds with isocyanates.[22, 36-37] The electron poor alkene resulting from the

tail-to-tail coupling of Michael acceptors that result from the proton transfer polymerization (HTP) process can undergo a thermally reversable Diels-Alder (DA or rDA) to form a polymer with the ability to cross-link reversable without the addition of cross-linking agents.[34, 38-40] The unique combination of a benzoin condensation and HTP joint one pot reaction sequence with the resulting functionality make the *cascading* polymerization an interesting experimental avenue to pursue.

5.3 Results and Discussion

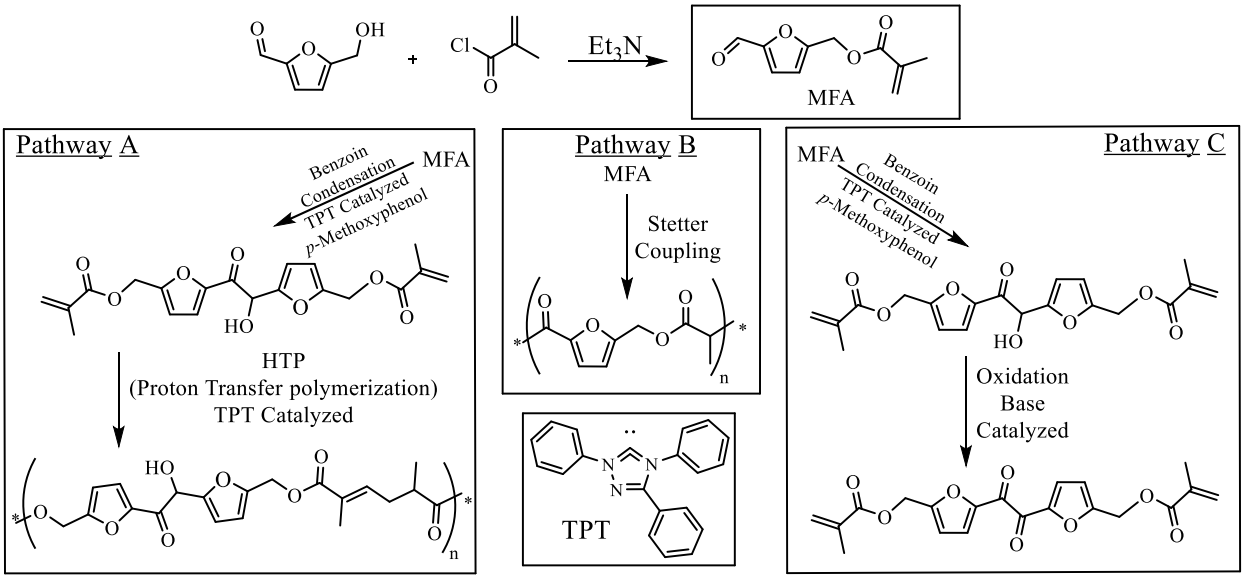

Figure 5.1. Synthesis of HMF acrylate followed by three proposed possible pathways, Pathway A an NHC Catalyzed Cascading Reaction, Pathway B the direct coupling of aldehyde and Michael acceptor functionality, Pathway C benzoin coupling of aldehydes followed by oxidation of furoin into Furil.

Cascading Benzoin condensation and proton transfer polymerization. Designing a monomer with appropriate functionality to undergo both a benzoin condensation and a tail-to-tail coupling of Michael acceptors requires the presence of an aldehyde and a Michael acceptor. Furfuryl methacrylate has been used as substrate for anionic polymerization,[41] while both FF and

HMF have been utilized in a series of reactions that include the addition of acyl chlorides to the HMF alcohol as well as the coupling of aldehydes through benzoin condensation.[5, 31, 36] This experience lead to the development of the methacrylate furanoate aldehyde (MFA) from the addition of HMF to methacryloyl chloride (Figure 5.1). The reaction proceeds with a high yield (88% isolated) producing a viscous amber liquid (^{1}H NMR S5.1).

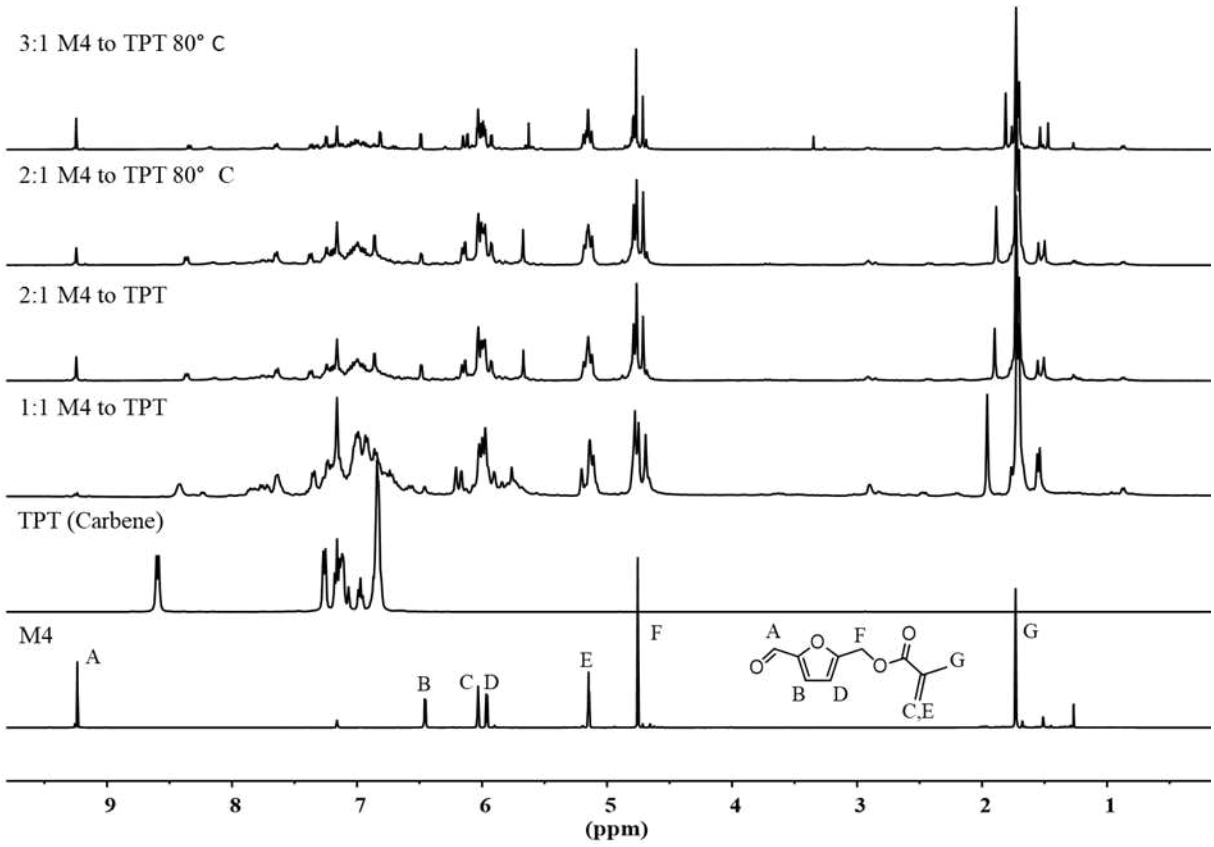

Figure 5.2. ^{1}H NMR spectra in d_6-benzene of stoichiometric TPT MFA reactions

Initial experiments to test MFA's ability to undergo the cascading reaction sequence proposed (Figure 5.1, Pathway A) were performed by adding stoichiometric amounts of MFA to the activated TPT and *p*-methoxyphenol (MP) in d_6-benzene at NMR scale using a J-Young tube and air free conditions (Figure 5.2). Inclusion of the radical inhibitor MP has been proven to prevent vinyl addition polymerization under these conditions.[34-35] Figure 5.2 shows that the first

stoichiometric equivalent of MFA with TPT reacts almost completely at the aldehyde (9.22 ppm, A) at room temperature, however the signals belonging to the β-protons labeled C and E in Figure 5.2 shift slightly but remain, suggesting the benzoin condensation is commencing but the tail-to-tail coupling is not proceeding. The second addition of MFA did not significantly change the spectrum, but it did result in a larger aldehyde peak. The sample was then heated at 80° C, the temperature required for tail-to-tail coupling.[25, 29, 33-35] There was obvious change as additional equivalents were added, new peaks near 6.9 and 7.2 ppm began to appear. A fourth addition as well as 16 h of heating was performed, but not shown, because there was no detectable change. A couple of conclusions can be taken from this experiment: first if heating had resulted in quantitative benzoin condensation aldehyde signals would have completely disappeared, and second, if tail-to-tail coupling had commenced, peaks associated with HTP would appear.

The work previously performed by Miao *et. al.* showed several distinct signals when HTP was sucsefull.[34] The signals indicative of HTP products are produced at about 1.1 ppm (CH_3 β-ester carbonyl), a group of signals between 2-3 ppm (alkyl protons α,β-ester carbonyl), and another distinctive signal near 6.7 ppm (unsaturated proton β-ester carbonyl). These signals are consistent across the entire sequence of substrates tested, which includes, a furan diacrylate ester comparable to the MFA discussed here. Several more NMR scale reactions with varying ratios of MFA to catalyst (always 10:1 catalyst to MP per *Miao et. al's.* previous work[34-35]) were performed. They did show that a reaction was taking place, but they continued to lack the distinctive signals belonging to HTP products. The lack of formation of any of the telling signals, during the NMR scale reaction of MFA and TPT, combined with the presence of both aldehyde and β-proton signals suggested that the *cascading* benzoin HTP system was not going to be facile.

Several reactions were performed at the half gram scale in an attempt to find effective conditions to produce the *cascading* reaction. Reactions were performed with both TPT and TPT-OMe using the air free Schlenk line techniques proven to be successful for previous work with polyesters and polyurethanes.[22] The first couple of reactions were performed with insufficient catalyst to completely convert the aldehyde so catalyst loading was increased from 5% to 10%. There did not appear to be a difference in level of conversion or the resulting product when TPT-OMe was used compared to TPT, however the crude spectra from each reaction still lacked the signals suggestive of successful HTP. A reaction was performed using a fused ring triazolium and DBU system found to be successful for cross coupling of HMF and FF. It did convert the aldehyde completely at 5% NHC loading but the product still lacked the signals that would indicate successful *cascading* reaction. Figure 5.3 shows a typical crude ^{1}H NMR with high conversion, aldehyde peak is almost completely gone, unfortunately the signals associated with HTP are still lacking.

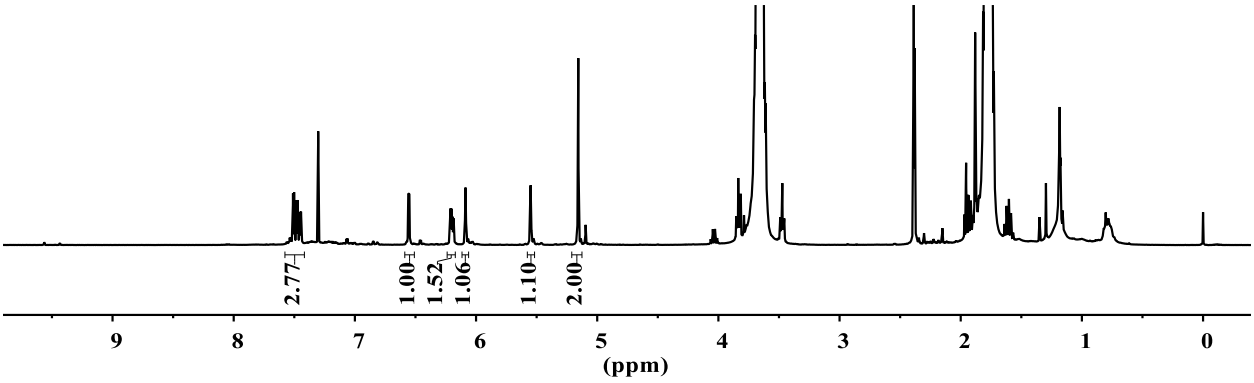

Figure 5.3. ^{1}H NMR spectra in $CDCl_3$ of crude reaction of MFA and TPT

Characterization of product produced by TPT catalyzed coupling of MFA. An alternative to the benzoin condensation between aldehyde followed by the tail-to-tail coupling between the activated alkenes is the direct NHC catalyzed umpolung coupling of aldehydes to

Michael acceptors known as the Stetter reaction (Figure 5.1, Pathway B).[26, 42-44] This reaction produces a 1,4 carbonyl different from the tail-to-tail connectivity of the HTP, however this reaction still results in saturated carbons that would produce signals in the upfield or shielded region. In Figure 5.3 there are some signals that could possibly be attributed to a Stetter product, especially the distinct signals at about 1.1 and 2.4 ppm. The products from these reactions did not precipitate with MeOH, nor did they have any characteristics that suggested that they were polymers. To test if they were oligomers MALDI-TOF was performed on several samples, masses between 200-1000 g/mol were found. However, none could be correlated with the possible Stetter or HTP oligomers of MFA.

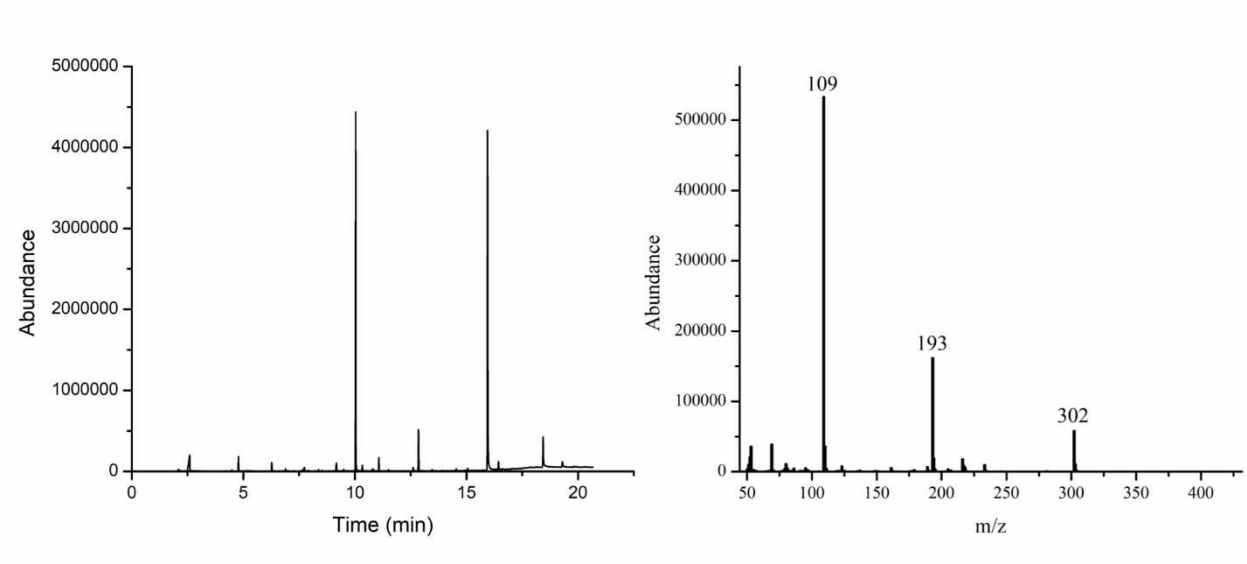

Figure 5.4. GC/MS chromatography trace and mass spectrum for chromatography peak at about 17 min.

With the knowledge that the products were not polymers but small molecules with low molecular weights the materials from several reactions were analyzed by GC/MS in attempt to better understand the number of components and identity of each component of the crude reaction, for several of the reactions there were two distinct signals on the chromatography trace one at 10

min, and another at about to 17 min. The signal at 10 min corresponds to starting material (MFA), and the second signal near 17 min belongs to the mass spectrum shown in Figure 5.4. The parent ion peak has a mass of 302 m/z which did not match any of the hypothesized structures. To isolate the compound producing the mass of 302 m/z the crude reaction was purified with column chromatography. Once an appropriate solvent system was determined a bright yellow compound with a clean ^{1}H NMR was obtained. GC/MS was repeated with the pure compound producing the same results, so a sample was prepared for direct injection TOF-MS analysis which resulted in a value of 404.1345 m/z (S5.2). This corresponds to a compound with a chemical formula of $C_{20}H_{22}NO_{8,}$ when ammonia was subtracted the resulting molecular formula was $C_{20}H_{18}O_{8}$ with a charge to mass ratio of 386.1006 m/z. This mass was 2 m/z less that the benzoin condensation product of MFA (Figure 5.5, **A**), once this data was available, it became obvious that the outcome of the reaction was the oxidized product of the benzoin condensation of MFA. The 302 m/z peak from the GC/MS could also be identified as the fragment in Figure 5.5, (**A**).

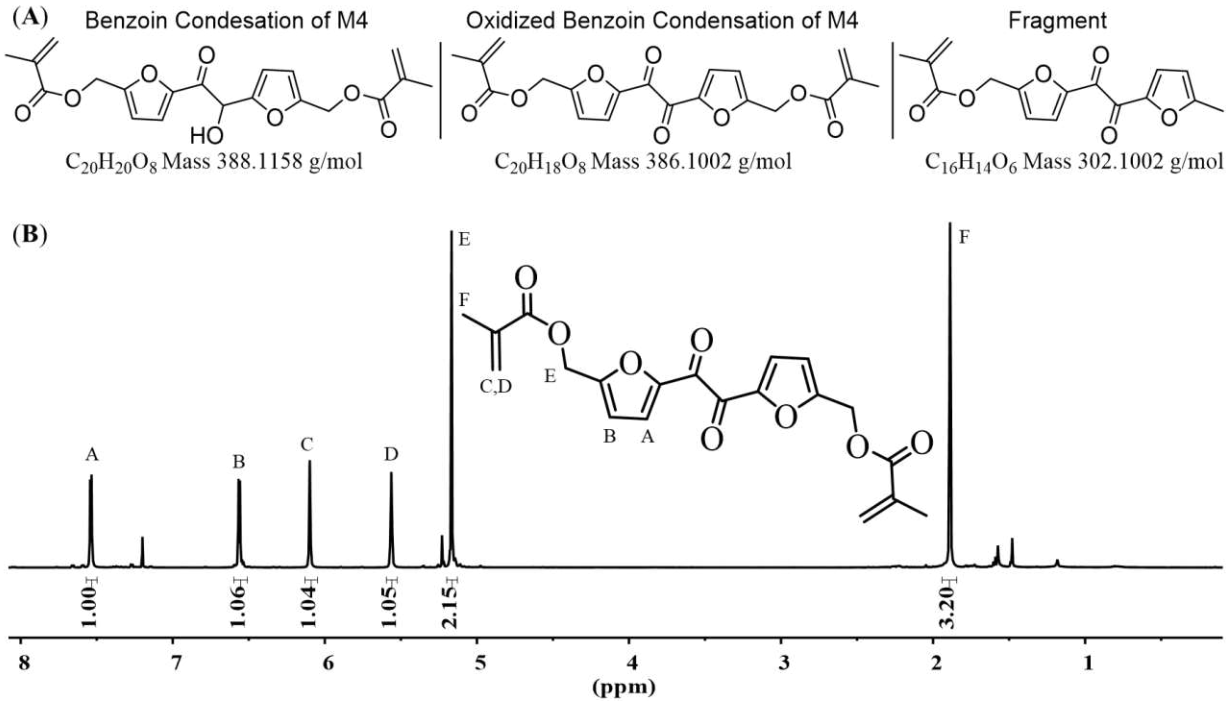

Figure 5.5. (**A**) Hypothesized structures and their masses; (**B**) Assigned ^{1}H NMR spectra in $CDCl_3$ of oxidized benzoin condensation product of MFA.

With the primary product of the reaction identified and isolated (Figure 5.5, **B**), comparison to spectra obtained from crude reactions showed that the furil dimethacrylate (FDMA) and unreacted MFA were the primary products in each experiment performed (S5.3). This led to several control experiments including changing the conditions from the Schlenk line technique to the sealed pressure reactor used for the synthesis of furoin diols. When the furoin diols were coupled by TPT, the use of sealed reactors was effective in preventing oxidation of the α-hydroxy.[31] Unfortunately, the oxidation still proceeded in these reactions. The next control experiment performed was the reaction of the isolated FDMA with TPT to see if this substrate alone would proceed with HTP. The reaction was heated to 80° C and analyzed at 18 h and 36 h. No HTP products were observed, but there was an interesting change in peaks assigned to furan rings (S5.4). This signal shift is evidence that TPT interacts with one of the α-diketones in the furil moiety. The third control experiment performed was the TPT catalyzed tail-to-tail coupling of furan methacrylate, this experiment was performed with the same TPT batch used for all previous experiments. The reaction definitely produced tail-to-tail coupling and contained the expected signals at about 1.1 ppm, the group of signals between 2-3 ppm, and the signal near 6.6 belonging to the alkene proton of HTP (Figure 5.6). Finally, the two carbenes $I^{i}Pr$ (1,3-diisoptopylimidazol-2-ylidene) and $I^{t}Bu$

(1,3-di-tert-butylimidazol-2-ylidene) were tested. The reaction of MFA and I^{t}Bu had low conversion to FDMA (S5.5), while the reaction of MFA and I^{i}Pr showed no activity at all (S5.6).

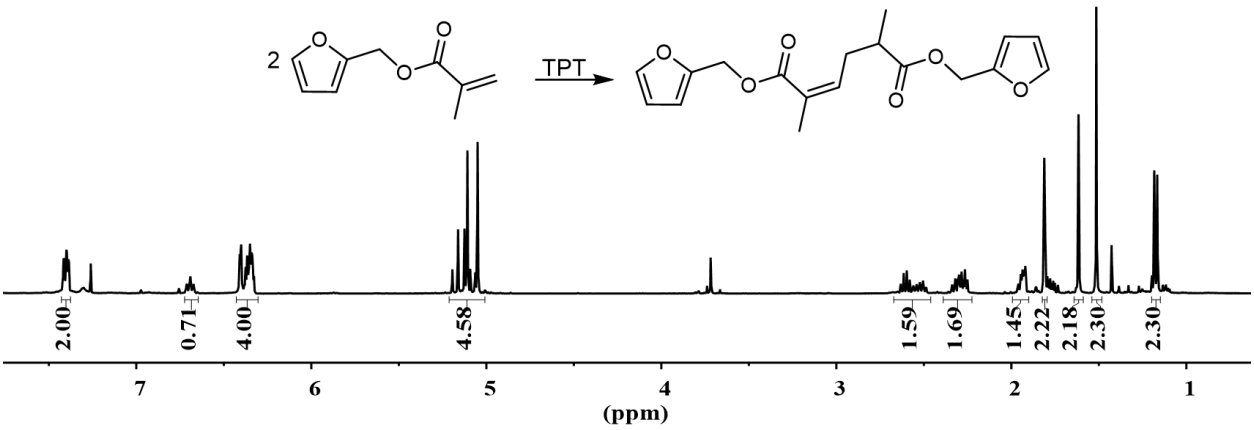

Figure 5.6. ^{1}H NMR spectra of tail-to-tail coupled dimmer of furan methacrylate catalyzed by TPT

The small amount of FDMA isolated from the initial attempts at developing the cascading reaction was completely used for the characterization and the one control reaction with TPT. To gain a better understanding of the interaction between TPT and FDMA, NMR scale stoichiometric reaction needed to be conducted. Instead of producing more FDMA through coupling of MFA it was determined that it could be relatively easily synthesized directly through the benzoin condensation of HMF with TPT followed by the selective oxidation of the α-hydroxy with MnO_4 (S5.7). Once the furil diol was obtained, the terminal hydroxyls were added to methacryloyl chloride resulting in the same FDMA produced by the failed cascading reaction (S5.7). This material was then used for control reactions as well as NMR scale experiments with TPT to determine why the tail-to-tail coupling was not proceeding.

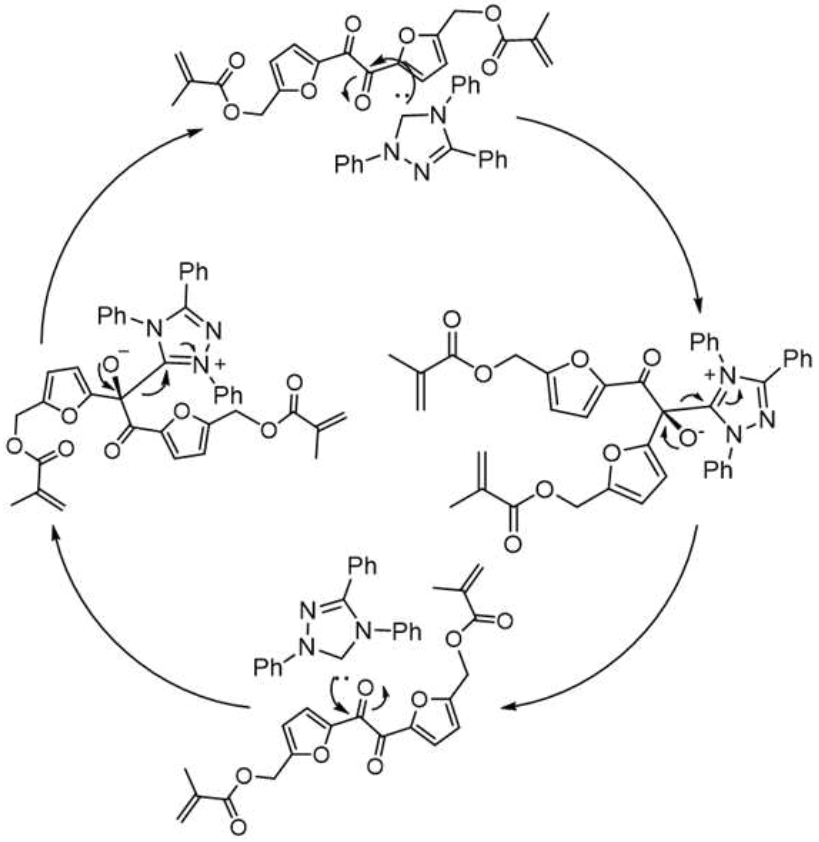

Figure 5.7. Proposed unproductive reaction sequence with furil (diketone) and TPT catalyst.

Catalyst interaction with FDMA. The first control reaction performed with the intentionally synthesized FDMA was the TPT catalyzed attempt at HTP with a temperature of 110° C. A similar reaction was performed with FDMA isolated from previous attempts at cascading reactions with a temperature of 80° C, both reactions did not produce the desired HTP products. In fact, both attempted reactions did not change the starting material in any way. The second reaction run at a higher temperature is evidence that it's not a simple matter of this substrate having a slightly higher activation energy for HTP than the previously examined substrates. When a close comparison to successful tail-to-tail coupling of Michael acceptors was made one functionality of FDMA stood out,[25, 28, 32-35, 45] FDMA has a strongly electrophilic diketone moiety.

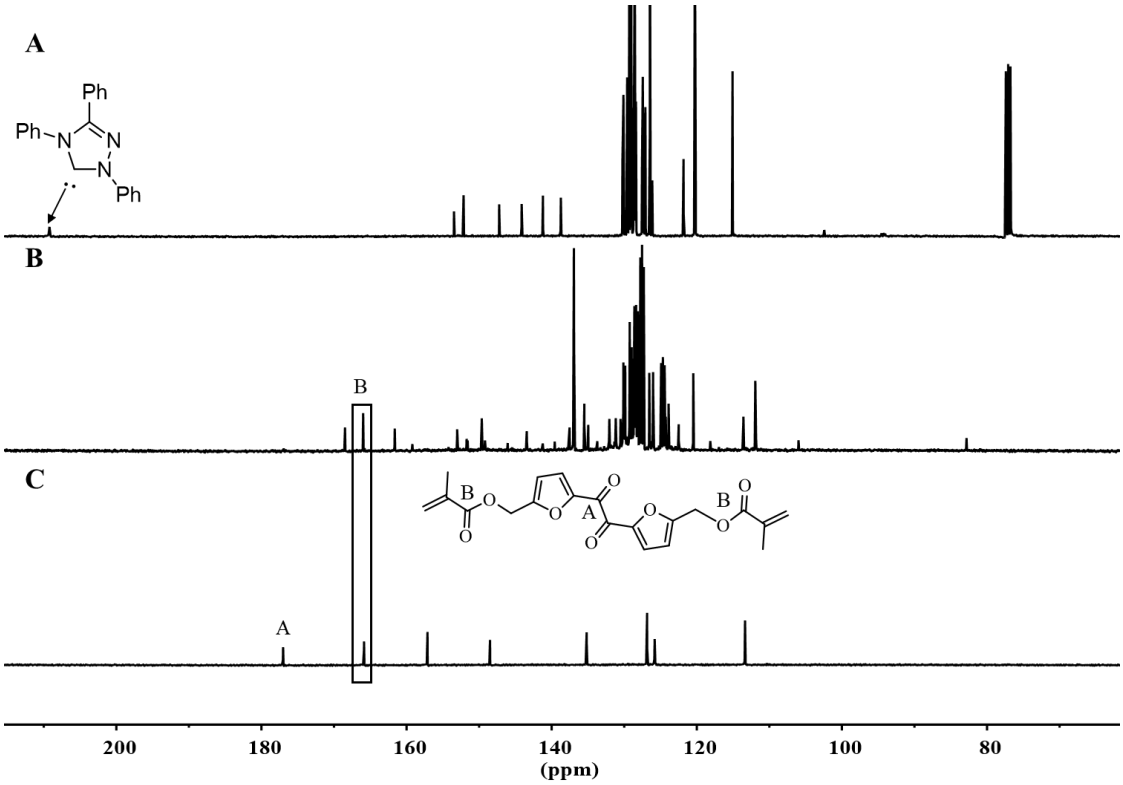

Figure 5.8. (**A**) ^{13}C NMR spectrum of TPT in DMSO-d_6, (**B**) 1:1 stoichiometric equivalent of FDMA and TPT, (**C**) FDMA with carbonyl's labelled.

Of course, the product from each of the reported successful HTPs has carbonyl functionalities however each of these are esters or amides.[25, 28-29, 32-35, 45] In one of original reports of the carbene catalyzed umpolung coupling of Michael acceptors Glorius et. al. found that the highly electrophilic α, β-unsaturated aldehydes underwent irreversible binding with the catalyst (TPT).[32] A ketone would not be able to undergo irreversible binding, but could still form a zwitterionic intermediate. Regeneration of the ketone would free the carbene to attack the neighboring ketone or any other ketone (Figure 5.7). The diketone moiety is definitely more electrophilic than the β-carbon of a Michael acceptor. A simple experiment that could help understand the chemoselectivity of the TPT is to add stoichiometric equivalents of TPT and FDMA at NMR scale to see which carbon or carbons on the substrate are interacting with the carbene.

The ^{13}C NMR was performed on a stoichiometric quantity of FDMA and TPT in DMSO-d_6 to determine which carbon was reacting with the carbene. Figure 5.8 **A** shows the ^{13}C spectra of TPT, the signal at 209 ppm is characteristic of the free carbene.[24, 35, 42, 46] The disappearance of this signal when one equivalent of FDMA is added is evidence that the carbene had completely reacted with the substrate (Figure 5.8, **B**). When comparing the spectra for FDMA (Figure 5.8, **C**) with the spectra for the 1:1 stoichiometric equivalent it is obvious that the signal at 177 ppm belonging to the two α-diketone carbons had disappeared, on figure 5.8 **C** a signal at 168 ppm appears that could be the upfield shifted ketone carbons. The Michael acceptor carbonyl carbons at 166 ppm for FDMA (Figure5. 8, **C**) are present in the spectra for the stoichiometric equivalents (Figure 5.8, **B**) suggesting no reaction is taking place at the Michael acceptor. An additional indication of lack of reaction at the Michael accepter β-carbon would be the un-altered presence of the corresponding carbon signal, HMBC NMR was used to assign the ^{13}C spectra and it was determined that the Michael acceptor β-carbon had a shift of 127 ppm (S5.9), this means the signal is overlapping with the signals for TPT FDMA. The three pieces of evidence, disappearance of carbene signal, disappearance of α-diketone signal, and apparent retention of Michael accepter carbonyl signal lead to the conclusion that the carbene is reacting with α-diketone moiety and not the β-carbon of the Michael acceptor.

Determining cause of α-hydroxy oxidation. One important question remains: what is driving the oxidation of the α-hydroxy? Significant work with the benzoin condensation of furan aldehydes has progressed without forming the diketone furil, this suggests that there is a step in the HTP mechanism that is causing the oxidation. The proposed mechanism for the Benzoin condensation is shown in scheme 3 **A**.[5, 21, 29, 31] This can be compared to the proposed mechanism for tail-to-tail coupling shown in scheme 3 **B**.[25, 28-29, 33-35, 45] In the proposed mechanism for the Benzoin coupling

of furan aldehydes there are 3 summary steps: nucleophilic attack of a furan aldehyde by TPT to generate the zwitterionic intermediate (**A**I), after which a H-transfer generates the enaminol often referred to as the Breslow intermediate (**A**II). This intermediate has actually reversed the polarity of the aldehyde carbon, and is why this coupling is referred to as umpolung. The Breslow intermediate (**A**II) effectively acts like an acyl anion and attacks another aldehyde, resulting in a second zwitterionic intermediate (**A**III). The H-transfer (1,4-H shift) regenerates the carbene catalyst completing the cycle and constructing a α-hydroxy ketone.

The umpolung tail-to-tail coupling of Michael acceptors catalyzed by TPT proceeds through a proposed mechanism similar to that of Benzoin condensation but with one important difference that may explain the oxidation of the α-hydroxy (Figure 5.9, **B)**. The 5 elementary steps of the reaction include: Michael addition of TPT to monomer generating an enolate (**BI**), H-transfer to produce the enamine (deoxy-Breslow intermediate) resulting in a nucleophilic β-carbon (**BII**), enamine addition to Michael acceptor (**BIII**), then H-transfer and release of the active carbene completing the cycle (Figure 5.9, **B**). Both proposed mechanisms contain H-transfer steps and oxygen anions, but the proposed mechanism for HTP includes enolates not present in the Benzoin condensation.

(**A**) Proposed Benzoin Condensation Mechanism

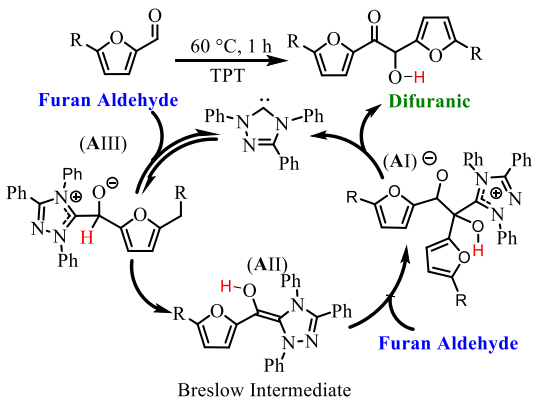

(**B**) Proposed HTP Mechanism

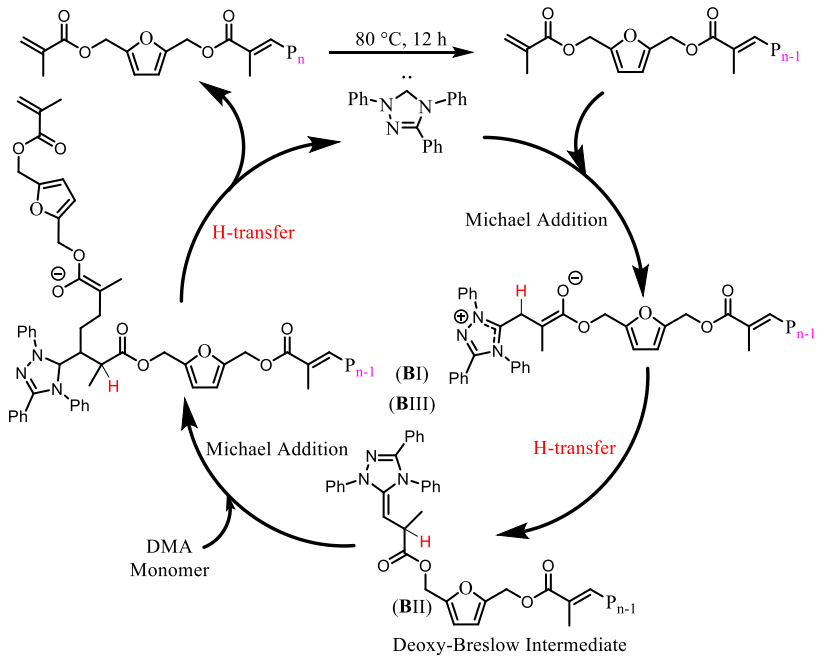

(**C**) Proposed Oxidation Mechanism

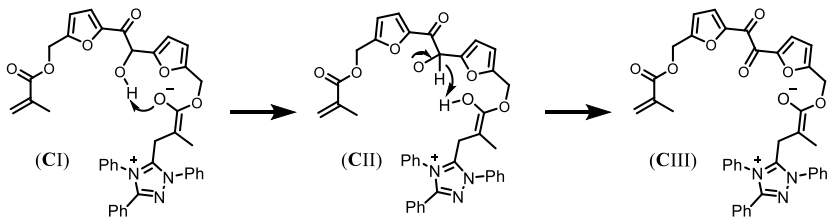

Figure 5.9. (A) Proposed mechanism for the Benzoin condensation of furan aldehydes,[5, 21,31] (B) Proposed mechanism for HTP polymerization through tail-to-tail coupling of Michael acceptors,[34-35] (C) Proposed oxidation furoin mechanism.

The base catalyzed oxidation of benzoin products to benzil was reported by Shimakawa *et. al.*, they found that using air free conditions with *in situ* carbene generation from NHC salt with base, inhibits oxidation while running the same reaction open to air results in benzil (diketone) formation.[47] Our group has utilized this selectivity, as well as different carbene generation strategies, to exclusively form furoins (α-hydroxy ketones). The inability to prevent oxidation in the proposed *cascading* reactions even in the strictest air free conditions and with carbene that was pre-generated (no base present) suggests that the mechanism for HTP must have an intermediate acting as the required base. In Figure 5.9 **C,** a mechanism is proposed that uses the enolate anion to deprotonate the α-hydroxy triggering its oxidation to furil (α-diketone); essentially it is proposed that the enolate acts as the base. To test this hypothesis a series of variable temperature (VT) experiments were performed on MFA with TPT catalyst in DMSO-d_6.

In Miao *et. al's.* work, a careful ^{1}H NMR analysis of stoichiometric equivalents of TPT and dimethacrylate (DMA) was conducted.[35] In addition the deoxy-Breslow intermediate was isolated and characterized.[25, 32] As it turns out, generation of the deoxy-Breslow intermediate is relatively fast while the subsequent nucleophilic addition to the Michael acceptor was slow making its detection possible.[25, 32] In these previous examples it was possible to observe the deoxy-Breslow intermediate with NMR. If MFA was forming a deoxy-Breslow intermediate during the VT ^{1}H NMR experiments, it should be detectable. So, the fact that during these experiments there was no sign of deoxy-Breslow intermediate formation (S5.10) is indicative of the proposed oxidation mechanism (Figure 5.9, **C**). According to the mechanistic study performed by Suzuki and coworkers the generation of the enolate is rapid.[25] In the scenario where there is a successful Benzoin condensation the intramolecular transfer of TPT to the Michael acceptor would be

kinetically favored resulting in the enolate which could undergo the proposed oxidation in Figure 9 **C** resulting in FDMA, then the carbene would intramolecularly transfer to the highly electrophilic diketone and proceed through the unproductive pathway (Figure 5.7).

5.4 Conclusions

The monomer MFA was developed with both an aldehyde and Michael acceptor functionality so it could undergo an auto-tandem or *cascading* reaction. The first step of the proposed *cascading* reaction of MFA was assumed to be the TPT catalyzed benzoin condensation of the aldehyde functional groups to produce the diacrylate furoin, followed by the tail-to-tail coupling of the Michael acceptors catalyzed by TPT. Initial experiments showed an undetermined reaction was proceeding, the products of this reaction were isolated and characterized by GC/MS, ESI-MS and NMR. It was shown that the reaction does not proceed through the alternative pathway where NHC catalyzes the direct umpolung addition of aldehyde to Michael acceptor (Figure 1, Pathway 2) but was found to be producing the FDMA (Figure 1 2, Pathway C). Significant work was done in an attempt to prevent the oxidation of the α-hydroxy into a ketone. Once it was determined that the oxidation was inherent to the process a series of experiments were performed to understand the reaction mechanism.

The primary product of the TPT catalyzed coupling of MFA, FDMA was synthesized using a three-step process and tested for its ability to undergo HTP these experiments found it to be inactive. In an attempt to understand the catalysts behavior with FDMA both a ^{1}H and ^{13}C NMR were taken of a 1:1 stoichiometric mixture of FDMA and TPT, the carbene signal at 209 ppm combined with the disappearance of the diketone signal at 177 ppm show that the TPT is reacting

at the ketone and not the β-carbon of the Michael acceptor. This evidence shows that the formation of FDMA prevents the second step of the *cascading* reaction. Analysis of the proposed mechanisms for the Benzoin condensation and HTP show that HTP has an enolate intermediate that is not present during Benzoin condensations. The oxidation of furoin α-hydroxy has been shown to be catalyzed by base, the enolate intermediate can act as the required base to produce the furil diketone. This work has established that the proposed cascading reaction where TPT catalyzes the Benzoin condensation between aldehydes followed by the tail-to-tail coupling of Michael acceptors is blocked by the formation of a highly electrophilic diketone which intercepts the carbene catalyst preventing the HTP step.

References

(1) Wegenhart, B. L.; Liu, S.; Thom, M.; Stanley, D.; Abu-Omar, M. M., Solvent-Free Methods for Making Acetals Derived from Glycerol and Furfural and Their Use as a Biodiesel Fuel Component. *ACS Catal.* **2012**, 2, 2524-2530.

(2) Yang, J.; Li, N.; Li, G.; Wang, W.; Wang, A.; Wang, X.; Cong, Y.; Zhang, T., Solvent-Free Synthesis of C10 and C11 Branched Alkanes from Furfural and Methyl Isobutyl Ketone. *ChemSusChem* **2013**, 6, 1149-1152.

(3) Dalvand, K.; Rubin, J.; Gunukula, S.; Clayton Wheeler, M.; Hunt, G., Economics of biofuels: Market potential of furfural and its derivatives. *Biomass Bioenergy* **2018**, 115, 56-63.

(4) Zang, H.; Wang, K.; Zhang, M.; Xie, R.; Wang, L.; Chen, E. Y. X., Catalytic coupling of biomass-derived aldehydes into intermediates for biofuels and materials. *Catalysis Science & Technology* **2018**, 7, 1777-1798.

(5) Liu, D.; Zhang, Y.; Chen, E. Y.-X., Organocatalytic upgrading of the key biorefining building block by a catalytic ionic liquid and N-heterocyclic carbenes. *Green Chem.* **2012**, 10, 2738-2746.

(6) Liu, D.; Chen, E. Y.-X., Polymeric ionic liquid (PIL)-supported recyclable catalysts for biomass conversion into HMF. *Biomass & Bioenergy* **2013**, 48, 181-190.

(7) Alonso, D. M.; Bond, J. Q.; Dumesic, J. A., Catalytic conversion of biomass to biofuels. *Green Chem.* **2010**, 9, 1493-1513.

(8) Liu, D.; Chen, E. Y.-X., Organocatalysis in biorefining for biomass conversion and upgrading. *Green Chem.* **2014**, 3, 964-981.

(9) Bozell, J. J.; Petersen, G. R., Technology development for the production of biobased products from biorefinery carbohydrates-the US Department of Energy's "Top 10" revisited. *Green Chem.* **2010**, 12, 539-554.

(10) James, O. O.; Maity, S.; Usman, L. A.; Ajanaku, K. O.; Ajani, O. O.; Siyanbola, T. O.; Sahu, S.; Chaubey, R., Towards the conversion of carbohydrate biomass feedstocks to biofuels via hydroxylmethylfurfural. *Energy & Environmental Science* **2010**, 12, 1833-1850.

(11) Esposito, D.; Antonietti, M., Redefining biorefinery: the search for unconventional building blocks for materials. *Chemical Society Reviews* **2015**, 16, 5821-5835.

(12) Rosatella, A. A.; Simeonov, S. P.; Frade, R. F. M.; Afonso, C. A. M., 5-Hydroxymethylfurfural (HMF) as a building block platform: Biological properties, synthesis and synthetic applications. *Green Chem.* **2011**, 4, 754-793.

(13) Körner, P.; Jung, D.; Kruse, A., The effect of different Brønsted acids on the hydrothermal conversion of fructose to HMF. *Green Chem.* **2018**, 10, 2231-2241.

(14) Yang, Y.; Hu, C.-w.; Abu-Omar, M. M., Conversion of carbohydrates and lignocellulosic biomass into 5-hydroxymethylfurfural using AlCl3·6H2O catalyst in a biphasic solvent system. *Green Chem.* **2012**, 2, 509-513.

(15) Lange, J.-P.; van der Heide, E.; van Buijtenen, J.; Price, R., Furfural—A Promising Platform for Lignocellulosic Biofuels. *ChemSusChem* **2012**, 5, 150-166.

(16) Teong, S. P.; Yi, G.; Zhang, Y., Hydroxymethylfurfural production from bioresources: past, present and future. *Green Chem.* **2014**, 4, 2015-2026.

(17) Corma, A.; de la Torre, O.; Renz, M., Production of high quality diesel from cellulose and hemicellulose by the Sylvan process: catalysts and process variables. *Energy & Environmental Science* **2012**, 4, 6328-6344.

(18) Corma, A.; de la Torre, O.; Renz, M.; Villandier, N., Production of High-Quality Diesel from Biomass Waste Products. *Angew. Chem. Int. Ed.* **2011**, 50, 2375-2378.

(19) Jia, S.; He, X.; Ma, J.; Wang, K.; Xu, Z.; Zhang, Z. C., Efficient synthesis of 5-hydroxymethylfurfural from mannose with a reusable MCM-41-supported tin catalyst. *Catalysis Science & Technology* **2018**, 21, 5526-5534.

(20) Ukai, T. T., R.; Dokawa, S. , *J. Pharm. Soc. Jpn.* **1943**, 296.

(21) Breslow, R., On the Mechanism of Thiamine Action. IV.1 Evidence from Studies on Model Systems. *J. Am. Chem. Soc.* **1958**, 80, 3719-3726.

(22) Wilson, J. F.; Chen, E. Y. X., Difuranic Diols for Renewable Polymers with Pendent Furan Rings. *ACS Sustainable Chem. Eng.* **2019**, 7, 7035-7046.

(23) Liu, D.; Chen, E. Y.-X., Integrated Catalytic Process for Biomass Conversion and Upgrading to C-12 Furoin and Alkane Fuel. *ACS Catal.* **2014**, 4, 1302-1310.

(24) Enders, D.; Breuer, K.; Raabe, G.; Runsink, J.; Teles, J. H.; Melder, J.-P.; Ebel, K.; Brode, S., Preparation, Structure, and Reactivity of 1,3,4-Triphenyl-4,5-dihydro-1H-1,2,4-triazol-5-ylidene, a New Stable Carbene. *Angew. Chem. Int. Ed.* **1995**, 34, 1021-1023.

(25) Matsuoka, S.-i.; Ota, Y.; Washio, A.; Katada, A.; Ichioka, K.; Takagi, K.; Suzuki, M., Organocatalytic Tail-to-Tail Dimerization of Olefin: Umpolung of Methyl Methacrylate Mediated by N-Heterocyclic Carbene. *Org. Lett.* **2011**, 13, 3722-3725.

(26) Jousseaume, T.; Wurz, N. E.; Glorius, F., Highly Enantioselective Synthesis of α-Amino Acid Derivatives by an NHC-Catalyzed Intermolecular Stetter Reaction. *Angew. Chem. Int. Ed.* **2011**, 50, 1410-1414.

(27) Zhang, Y.; Chen, E. Y.-X., Conjugate-Addition Organopolymerization: Rapid Production of Acrylic Bioplastics by N-Heterocyclic Carbenes. *Angew. Chem. Int. Ed.* **2012**, 51, 2465-2469.

(28) Nzahou Ottou, W.; Bourichon, D.; Vignolle, J.; Wirotius, A.-L.; Robert, F.; Landais, Y.; Sotiropoulos, J.-M.; Miqueu, K.; Taton, D., Cyclodimerization versus Polymerization of Methyl Methacrylate Induced by N-Heterocyclic Carbenes: A Combined Experimental and Theoretical Study. *Chem.: Eur. J.* **2014**, 20, 3989-3997.

(29) Kato, T.; Ota, Y.; Matsuoka, S.-i.; Takagi, K.; Suzuki, M., Experimental Mechanistic Studies of the Tail-to-Tail Dimerization of Methyl Methacrylate Catalyzed by N-Heterocyclic Carbene. *J. Org. Chem.* **2013**, 78, 8739-8747.

(30) Zhang, Y.; Schmitt, M.; Falivene, L.; Caporaso, L.; Cavallo, L.; Chen, E. Y.-X., Organocatalytic Conjugate-Addition Polymerization of Linear and Cyclic Acrylic Monomers by N-Heterocyclic Carbenes: Mechanisms of Chain Initiation, Propagation, and Termination. *J. Am. Chem. Soc.* **2013**, 135, 17925-17941.

(31) Wilson, J.; Chen, E. Y.-X., Organocatalytic Cross-Coupling of Biofuranics to Multifunctional Difuranic C11 Building Blocks. *ACS Sustainable Chem. Eng.* **2016**, 4, 4927-4936.

(32) Biju, A. T.; Padmanaban, M.; Wurz, N. E.; Glorius, F., N-Heterocyclic Carbene Catalyzed Umpolung of Michael Acceptors for Intermolecular Reactions. *Angew. Chem. Int. Ed.* **2011**, 50, 8412-8415.

(33) Matsuoka, S.-i.; Awano, N.; Nakazawa, M.; Suzuki, M., Tail-to-tail dimerization and Rauhut-Currier reaction of disubstituted Michael acceptors catalyzed by N-heterocyclic carbene. *Tetrahedron Lett.* **2016**, 50, 5707-5711.

(34) Hong, M.; Chen, E. Y.-X., Proton-Transfer Polymerization (HTP): Converting Methacrylates to Polyesters by an N-Heterocyclic Carbene. *Angew. Chem. Int. Ed.* **2014**, 53, 11900-11906.

(35) Hong, M.; Tang, X.; Falivene, L.; Caporaso, L.; Cavallo, L.; Chen, E. Y.-X., Proton-Transfer Polymerization by N-Heterocyclic Carbenes: Monomer and Catalyst Scopes and Mechanism for Converting Dimethacrylates into Unsaturated Polyesters. *J. Am. Chem. Soc.* **2016**, 138, 2021-2035.

(36) Mou, Z.; Chen, E. Y.-X., Polyesters and Poly(ester-urethane)s from Biobased Difuranic Polyols. *ACS Sustainable Chem. Eng.* **2016**, 4, 7118-7129.

(37) Mou, Z.; Feng, S.; Chen, E. Y.-X., Bio-based difuranic polyol monomers and their derived linear and cross-linked polyurethanes. *Polymer Chem.* **2016**, 8, 1593-1602.

(38) Thomas, D.; Raphaël, R.; Jean-Michel, T.; Christine, J.; Michaël, A., Thermo-Reversible Reactions for the Preparation of Smart Materials: Recyclable Covalently-Crosslinked Shape Memory Polymers. *Macromol. Symp.* **2011**, 309, 154-161.

(39) Turkenburg, D. H.; Fischer, H. R., Diels-Alder based, thermo-reversible cross-linked epoxies for use in self-healing composites. *Polymer* **2015**, 29, 187-194.

(40) Zhang, Y.; Dai, Z. H.; Han, J. R.; Li, T.; Xu, J.; Guo, B. H., Interplay between crystallization and the Diels-Alder reaction in biobased multiblock copolyesters possessing dynamic covalent bonds. *Polymer Chem.* **2017**, 79, 4280-4289.

(41) He, J.; Zhang, Y.; Chen, E. Y.-X., Anionic polymerization of biomass-derived furfuryl methacrylate: Controlling polymer tacticity and thermoreversibility. *Journal of Polymer Science Part A: Polymer Chemistry* **2013**, 51, 2793-2803.

(42) Enders, D.; Han, J.; Henseler, A., Asymmetric intermolecular Stetter reactions catalyzed by a novel triazolium derived N-heterocyclic carbene. *Chem. Comm.* **2008**, 34, 3989-3991.

(43) de Alaniz, J. R.; Rovis, T., The Catalytic Asymmetric Intramolecular Stetter Reaction. *Synlett* **2009**, 131, 1189-1207.

(44) Flanigan, D. M.; Romanov-Michailidis, F.; White, N. A.; Rovis, T., Organocatalytic Reactions Enabled by N-Heterocyclic Carbenes. *Chem. Rev.* **2015**, 115, 9307-9387.

(45) Fukumoto, A.; Arimoto, M.; Matsuoka, S.-i.; Suzuki, M., Polycondensation of methacrylates: auto-tandem organocatalysis using N-heterocyclic carbenes. *Polymer Chem.* **2018**, 43, 5295-5302.

(46) Enders, D.; Breuer, K.; Kallfass, U.; Balensiefer, T., Preparation and Application of 1,3,4-Triphenyl-4,5-dihydro-1H-1,2,4-triazol-5-ylidene, A Stable Carbene. *Synthesis* **2003**, 339, 1292-1295.

(47) Shimakawa, Y.; Morikawa, T.; Sakaguchi, S., Facile route to benzils from aldehydes via NHC-catalyzed benzoin condensation under metal-free conditions. *Tet. Lett.* **2010**, 51, 1786-17

Chapter 6

Conclusion

6.1 Conclusion

The impressive barrier properties of poly(ethylene furanoate) suggests that other furan based polymers have attractive features that need to be explored.[1-5] The carbene catalyzed benzoin condensation of the two biomass derived platform chemicals 5-hydroxymethylfurural (HMF) and furfural (FF) results in highly functionalized furoin compounds.[6-9] This is a desirable reaction for the up-grading FF and HMF, through the course of biorefining, because efficient paths for the chain extension of furan's will be essential if biorefining is going to develop to the point where it can compete with petroleum refining to produce the myriad of commodity and fine chemicals we rely on. Organocatalysis is considered a sustainable alternative to organometallic systems, the organic catalysts used in this work carbenes also have a substantial structural library available with many varying steric and electronic environments that have been utilized to obtain stereo and chemo-selectivity.

The carbene hetero-coupling of HMF and FF has two possible isomers of the diol furoin, in addition to the monol along with the triol homo-coupled furoin products. In an attempt to develop a catalytic system with some selectivity towards hetero-coupling four catalysts were chosen based on their steric and electronic environments. Two electron rich thiazolium carbene pre-catalysts one with a sterically demanding environment and one with a sterically open environment were chosen based on their previous success with cross coupling of ortho substituted aryl aldehydes and unsubstituted aryl aldehydes.[10] For electron deficient catalysts triazoliums were chosen with both sterically demanding[11] as well as sterically open environments.[12-14] Conditions such as solvent and

base were varied in an attempt to identify a set of requirements that could lead to selectivity. The most selective catalyst system employed produced 60% diol with solvent free conditions and the pre-catalyst 3-mesityl-5,6,7,8-tetrahydro-4H-cyclohepta[d] thiazole-3-ium perchlorate with the base 1,8-diazabicyclo[5.4.0]undec-7-ene (DBU). The presence of base caused the formation of furil, to prevent this side reaction the pre-catalyst 5-methoxy-1,3,4-triphenyl-4,5-dihydro-1H-1,2,4-triazoline (TPT-OMe), which uses heat instead of base to generate carbene in situ, was used for the production of diols for polymerization reactions.

Commodity polymers are important products of petroleum refining, the full realization of biorefing will require the development of polymers with superior properties utilizing biorefing feed stocks. Furans and the carbene catalyzed coupling, or chain extension, of HMF and FF produce a mixture of $C_{10} - C_{12}$ difuranic furoins.[6-7, 15-16] This mixture can be utilized to produce transportation fuels through the process of hydrodeoxygenation, [9, 15, 17-21] the triol furoin can be used as a feedstock for the production of a variety polyurethanes and polyesters.[22-23] The ability for one reaction to produce several components suitable as feedstocks for polymerization, fine chemical production, as well as for transportation fuel manufacture make this type of catalytic up-grading particularly attractive.

The two diol functionalized furoins have been employed to produce polyesters and polyurethanes with the unique feature of two types of furan ring pendent groups as well as furan rings in polymer backbone.[24] One monomer has a steric advantage that allows polymers made from it to achieve number average molecular weights (M_n) in excess of 20 kg/mol while polymers made from the other are limited to 9 kg/mol. Thermal properties such as glass transition (T_g) and unset decomposition temperature (T_d) were controlled through the use of rigid and soft comonomers. Unsurprisingly, the trend is that the softer the comonomer, for example long alkyl

chains, the lower the T_g combined an increase in T_d. The type of furan ring pendent group (i.e. which difuranic monomer) does not affect thermal properties. The glassier polyurethanes had higher tensile modulus, while polyesters with longer alkyl chains between ester functionalities had more elastic behavior. The highest T_g's obtained from polyesters were 66° C which made them slightly less glassy than poly(ethylene terephthalate) (PET) with a glass transition of 75° C.[1] However, all the polyurethanes have T_g's in excess of 85° C which is the T_g of poly(ethylene furanoate) which has been shown to have selected barrier properties 19 times greater than that of PET. The potential for improved barrier properties is promising but limitations in M_n as well as the coloration of resulting materials requires the development of alternative furan-based monomers and polymerization techniques.

One method utilized for the production of high M_n poly(lactide) is to convert the lactic acid monomer into a cyclic ester generating substrates suitable for catalyzed ring opening polymerization (ROP).[25-30] Two synthetic pathways were analyzed in an attempt to produce a furan ring containing monomer with alcohol and ester functionality suitable for use as a AB type monomer or for conversion to cyclic esters. The first route evaluated attempted the acid catalyzed addition of the Michael acceptor methyl methacrylate to furfuryl alcohol (FA), this resulted in transesterification or generation of Diels-Alder (DA) adducts. The second approach attempted the addition of enol to ethyl 3-(furan-2-yl) propionate (EFP) ideally resulting in addition of alcohol, however the final product was the vinyl substituted EFP. With these routes depleted an alternative based on formation of a highly substituted lactone was found.

The DA reaction between FA and another biomass derived compound itaconic anhydride (IA) results in highly substituted fused ring γ-butyrolactone (GBL) with an ether, alkene, and a linear ester functionality. The lactone did have trans stereo chemistry observed for the 4,5-*trans*-cyclo-

hexyl-fused GBL (4,5-T6GBL) and 3,4-*trans*-cyclo-hexyl-fused GBL (3,4-T6GBL) suggesting that room temperature ROP would be possible (Figure 6.1). To test this theory the organic catalyst system shown in the box in Figure 6.1 was utilized based on its previous success with ROP of 4,5-T6GBL.[31] This system was unable to realize ROP so an inorganic lanthanum (La) systems was unsuccessfully attempted at both low temperatures (-80° C through 0° C) as well as in the melt, these systems have been effective for the ROP of both strained 5-membered lactones monomers (3,4-T6GBL) as well as unstrained 5-membered lactones (γ-butyrolactone and α-methylene-γ-butyrolactone).[32-34] The inability of any of the tested catalysts systems to recognize ROP may be attributed to their poor solubility resulting in low reaction concentration, in several of the reported systems high reaction concentrations were essential to their success.[31-33]

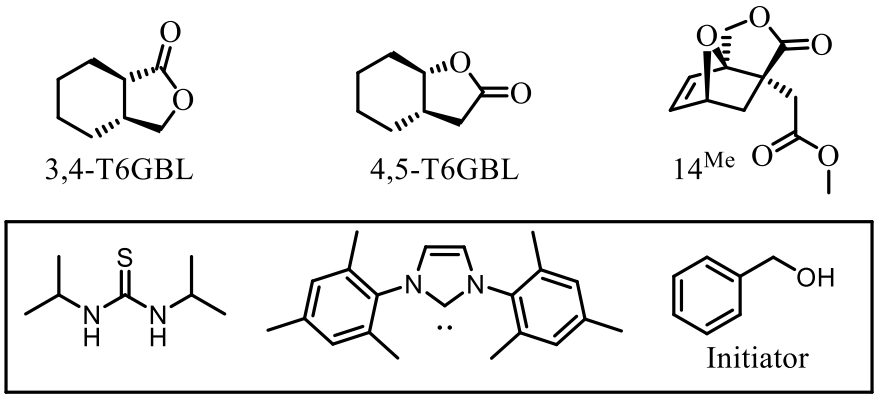

Figure 6.1. Top: structures of 3,4-T6GBL, 4,5-T6GBL, and the highly substituted 14^{Me}, Bottom: organic catalyst system used for attempted room temperature ROP.

The inability to obtain a furan containing lactone or cyclic ester highlighted the difficulty in finding effective strategies for obtaining high molecular weight polymers with furan ring containing moieties, after exploring the available options a new hypothesis was formulated based on previous success with TPT-OMe catalyzed reactions for both up-grading as well as polymerization. The hypothesized system required a difunctional monomer with both a Michael

acceptor and an aldehyde functionality, the developed monomer (Figure 6.2, A) was produced by the simple addition of HMF to methyl methacryloyl chloride in the presence of amine base. The proposed pathway started with the aldehyde undergoing a benzoin condensation resulting in a furoin with a dimethylacrylate functionality suitable for NHC catalyzed tail-to-tail coupling of Michael acceptors.[35-40] Similar processes have been termed auto-tandem catalysis because the same catalyst is responsible for both the benzoin condensation and tail-to-tail coupling of Michael acceptors.[40]

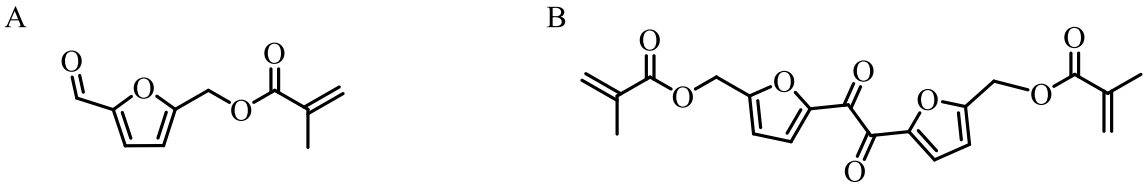

Figure 6.2. A methacrylate furan aldehyde (MFA), B dimethacrylate furil.

Experiments were performed in an attempt to realize the auto-tandem catalysis or cascading reaction of the difunctional monomer with activated TPT using a variety of conditions, however analysis of the resulting products showed that TPT successfully catalyzed the benzoin condensation but that the tail-to-tail coupling reaction was not proceeding as expected. The product of the reaction is the di-ketone furoin shown in Figure 6.2, B. The oxidation of the α-hydroxy of furoin into the second ketone of furil is facile, preventing this oxidation was always a concern with the early work coupling of HMF and cross coupling of FF with HMF. Careful choice of NHC catalyst combined with strict air free conditions was sufficient to prevent oxidation in those scenarios. In the auto-tandem catalysis scenario there are enolates present that act as base causing the oxidation, which in turn results in diketone that complexed with the TPT blocking the tail-to-tail coupling pathway.

This work significantly increased our understanding of the cross-benzoin reaction between HMF and FF by successfully generating the isomeric cross-coupling products as well as fully characterizing them. They were then utilized to make a series of polyesters and polyurethanes showing that one of the two isomers had a steric advantage allowing a significantly higher degree of polymerization to be obtained, however the thermal and mechanical properties of the polymers appear to be identical regardless of isomer choice. The resulting polymers still had limited molecular weight and undesirable coloration. In an attempt to produce high molecular weight materials with better coloration properties unsuccessful attempts at the synthesis of furan containing lactones and cyclic esters were made, then a highly substituted GBL was produced through a Dials-Alder reaction between FA and IT which failed to undergo ROP. This work improved our understanding of both furan chemistry as well as limitations of the ROP of highly substituted GBL. These experiments lead to a proposed auto-tandem catalysis reaction sequence between a difunctional furan monomer (Figure 6.2, A) with TPT that resulted in the furil dimethacrylate shown in (Figure 6.2, B).

References

(1) Burgess, S. K.; Leisen, J. E.; Kraftschik, B. E.; Mubarak, C. R.; Kriegel, R. M.; Koros, W. J., Chain Mobility, Thermal, and Mechanical Properties of Poly(ethylene furanoate) Compared to Poly(ethylene terephthalate). *Macromolecules* **2014,** 47, 1383-1391.

(2) Burgess, S. K.; Karvan, O.; Johnson, J. R.; Kriegel, R. M.; Koros, W. J., Oxygen sorption and transport in amorphous poly(ethylene furanoate). *Polymer* **2014,** 55, 4748-4756.

(3) Burgess, S. K.; Lee, J. S.; Mubarak, C. R.; Kriegel, R. M.; Koros, W. J., Caffeine antiplasticization of amorphous poly(ethylene terephthalate): Effects on gas transport, thermal, and mechanical properties. *Polymer* **2015,** 65, 34-44.

(4) Burgess, S. K.; Kriegel, R. M.; Koros, W. J., Carbon Dioxide Sorption and Transport in Amorphous Poly(ethylene furanoate). *Macromolecules* **2015,** 48, 2184-2193.

(5) Burgess, S. K.; Wenz, G. B.; Kriegel, R. M.; Koros, W. J., Penetrant transport in semicrystalline poly(ethylene furanoate). *Polymer* **2016,** 98, 305-310.

(6) Liu, D.; Zhang, Y.; Chen, E. Y.-X., Organocatalytic upgrading of the key biorefining building block by a catalytic ionic liquid and N-heterocyclic carbenes. *Green Chem.* **2012,** 14, 2738-2746.

(7) Liu, D.; Chen, E. Y.-X., Polymeric ionic liquid (PIL)-supported recyclable catalysts for biomass conversion into HMF. *Biomass & Bioenergy* **2013,** 48, 181-190.

(8) Liu, D.; Chen, E. Y.-X., Organocatalysis in biorefining for biomass conversion and upgrading. *Green Chem.* **2014,** 16, 964-981.

(9) Liu, D.; Chen, E. Y.-X., Integrated Catalytic Process for Biomass Conversion and Upgrading to C-12 Furoin and Alkane Fuel. *ACS Catal.* **2014,** 4, 1302-1310.

(10) Piel, I.; Pawelczyk, M. D.; Hirano, K.; Froehlich, R.; Glorius, F., A Family of Thiazolium Salt Derived N-Heterocyclic Carbenes (NHCs) for Organocatalysis: Synthesis, Investigation and Application in Cross-Benzoin Condensation. *European Journal of Organic Chemistry* **2011,** 5475-5484.

(11) Langdon, S. M.; Wilde, M. M. D.; Thai, K.; Gravel, M., Chemoselective N-Heterocyclic Carbene-Catalyzed Cross-Benzoin Reactions: Importance of the Fused Ring in Triazolium Salts. *J. Am. Chem. Soc.* **2014,** 136, 7539-7542.

(12) Enders, D.; Breuer, K.; Raabe, G.; Runsink, J.; Teles, J. H.; Melder, J.-P.; Ebel, K.; Brode, S., Preparation, Structure, and Reactivity of 1,3,4-Triphenyl-4,5-dihydro-1H-1,2,4-triazol-5-ylidene, a New Stable Carbene. *Angew. Chem. Int. Ed.* **1995,** 34, 1021-1023.

(13) Enders, D.; Kallfass, U., An Efficient Nucleophilic Carbene Catalyst for the Asymmetric Benzoin Condensation. *Angew. Chem. Int. Ed.* **2002,** 41, 1743-1745.

(14) Enders, D.; Han, J.; Henseler, A., Asymmetric intermolecular Stetter reactions catalyzed by a novel triazolium derived N-heterocyclic carbene. *Chem. Comm.* **2008,** 3989-3991.

(15) Liu, D.; Chen, E. Y.-X., Diesel and Alkane Fuels From Biomass by Organocatalysis and Metal–Acid Tandem Catalysis. *ChemSusChem* **2013,** 6, 2236-2239.

(16) Wilson, J.; Chen, E. Y.-X., Organocatalytic Cross-Coupling of Biofuranics to Multifunctional Difuranic C11 Building Blocks. *ACS Sustainable Chem. Eng.* **2016,** 4, 4927-4936.

(17) Corma, A.; de la Torre, O.; Renz, M.; Villandier, N., Production of High-Quality Diesel from Biomass Waste Products. *Angew. Chem. Int. Ed.* **2011,** 50, 2375-2378.

(18) King, A. E.; Brooks, T. J.; Tian, Y.-H.; Batista, E. R.; Sutton, A. D., Understanding Ketone Hydrodeoxygenation for the Production of Fuels and Feedstocks From Biomass. *ACS Catal.* **2015,** 5, 1223-1226.

(19) L., W. B.; Linan, Y.; Cheong, K. S.; Remi, H.; I., K. H.; M., A. O. M., From Furfural to Fuel: Synthesis of Furoins by Organocatalysis and their Hydrodeoxygenation by Cascade Catalysis. *ChemSusChem* **2014,** 7, 2742-2747.

(20) Sutton, A. D.; Waldie, F. D.; Wu, R.; Schlaf, M.; 'Pete' Silks Iii, L. A.; Gordon, J. C., The hydrodeoxygenation of bioderived furans into alkanes. *Nature Chemistry* **2013,** 5, 428.

(21) Yang, J.; Li, N.; Li, G.; Wang, W.; Wang, A.; Wang, X.; Cong, Y.; Zhang, T., Solvent-Free Synthesis of C10 and C11 Branched Alkanes from Furfural and Methyl Isobutyl Ketone. *ChemSusChem* **2013,** 6, 1149-1152.

(22) Mou, Z.; Feng, S.; Chen, E. Y.-X., Bio-based difuranic polyol monomers and their derived linear and cross-linked polyurethanes. *Polymer Chem.* **2016,** 7, 1593-1602.

(23) Mou, Z.; Chen, E. Y.-X., Polyesters and Poly(ester-urethane)s from Biobased Difuranic Polyols. *ACS Sustainable Chem. Eng.* **2016,** 4, 7118-7129.

(24) Wilson, J. F.; Chen, E. Y. X., Difuranic Diols for Renewable Polymers with Pendent Furan Rings. *ACS Sustainable Chem. Eng.* **2019**.

(25) Degée, P.; Dubois, P.; Jérŏme, R.; Jacobsen, S.; Fritz, H.-G., New catalysis for fast bulk ring-opening polymerization of lactide monomers. *Macromolecular Symposia* **1999,** 144, 289-302.

(26) Chisholm, M. H.; Gallucci, J.; Phomphrai, K., Lactide polymerization by well-defined calcium coordination complexes: comparisons with related magnesium and zinc chemistry. *Chem. Comm.* **2003,** 48-49.

(27) Dechy-Cabaret, O.; Martin-Vaca, B.; Bourissou, D., Controlled Ring-Opening Polymerization of Lactide and Glycolide. *Chem. Rev.* **2004,** 104, 6147-6176.

(28) Kamber, N. E.; Jeong, W.; Waymouth, R. M.; Pratt, R. C.; Lohmeijer, B. G. G.; Hedrick, J. L., Organocatalytic Ring-Opening Polymerization. *Chem. Rev.* **2007,** 107, 5813-5840.

(29) Williams, C. K., Synthesis of functionalized biodegradable polyesters. *Chemical Society Reviews* **2007,** 36, 1573-1580.

(30) Dove, A. P., Organic Catalysis for Ring-Opening Polymerization. *ACS Macro Lett.* **2012,** 1, 1409-1412.

(31) Cywar, R. M.; Zhu, J.-B.; Chen, E. Y. X., Selective or living organopolymerization of a six-five bicyclic lactone to produce fully recyclable polyesters. *Polymer Chem.* **2019**.

(32) Tang, X.; Hong, M.; Falivene, L.; Caporaso, L.; Cavallo, L.; Chen, E. Y.-X., The Quest for Converting Biorenewable Bifunctional α-Methylene-γ-butyrolactone into Degradable and Recyclable Polyester: Controlling Vinyl-Addition/Ring-Opening/Cross-Linking Pathways. *J. Am. Chem. Soc.* **2016,** 138, 14326-14337.

(33) Hong, M.; Chen, E. Y.-X., Towards Truly Sustainable Polymers: A Metal-Free Recyclable Polyester from Biorenewable Non-Strained γ-Butyrolactone. *Angew. Chem. Int. Ed.* **2016,** 55, 4188-4193.

(34) Zhu, J.-B.; Chen, E. Y.-X., Catalyst-Sidearm-Induced Stereoselectivity Switching in Polymerization of a Racemic Lactone for Stereocomplexed Crystalline Polymer with a Circular Life Cycle. *Angew. Chem. Int. Ed.* **2019,** 58, 1178-1182.

(35) Hong, M.; Tang, X.; Falivene, L.; Caporaso, L.; Cavallo, L.; Chen, E. Y.-X., Proton-Transfer Polymerization by N-Heterocyclic Carbenes: Monomer and Catalyst Scopes and Mechanism for Converting Dimethacrylates into Unsaturated Polyesters. *J. Am. Chem. Soc.* **2016,** 138, 2021-2035.

(36) Hong, M.; Chen, E. Y.-X., Proton-Transfer Polymerization (HTP): Converting Methacrylates to Polyesters by an N-Heterocyclic Carbene. *Angew. Chem. Int. Ed.* **2014,** 53, 11900-11906.

(37) Matsuoka, S.-i.; Ota, Y.; Washio, A.; Katada, A.; Ichioka, K.; Takagi, K.; Suzuki, M., Organocatalytic Tail-to-Tail Dimerization of Olefin: Umpolung of Methyl Methacrylate Mediated by N-Heterocyclic Carbene. *Organic Letters* **2011,** 13, 3722-3725.

(38) Kato, T.; Ota, Y.; Matsuoka, S.-i.; Takagi, K.; Suzuki, M., Experimental Mechanistic Studies of the Tail-to-Tail Dimerization of Methyl Methacrylate Catalyzed by N-Heterocyclic Carbene. *J. Org. Chem.* **2013,** 78, 8739-8747.

(39) Matsuoka, S.-i.; Awano, N.; Nakazawa, M.; Suzuki, M., Tail-to-tail dimerization and Rauhut-Currier reaction of disubstituted Michael acceptors catalyzed by N-heterocyclic carbene. *Tetrahedron Lett.* **2016,** 57, 5707-5711.

(40) Fukumoto, A.; Arimoto, M.; Matsuoka, S.-i.; Suzuki, M., Polycondensation of methacrylates: auto-tandem organocatalysis using N-heterocyclic carbenes. *Polymer Chem.* **2018,** 9, 5295-5302.

Appendix A

Experimental Details and Supporting Information for Chapter 1:

A.1. Materials, Reagents, and Methods. All oxygen- and moisture-sensitive manipulations were carried out in a nitrogen-filled glovebox or under nitrogen atmosphere using standard Schlenk techniques. HPLC-grade organic solvents were sparged extensively with nitrogen during filling of the solvent reservoir and then dried by passage through activated alumina (for Et_2O and CH_2Cl_2) followed by passage through Q-5-supported copper catalyst (for toluene and hexanes) stainless steel columns. Tetrahydrofuran (THF) was refluxed over metallic sodium/potassium alloy with benzophenone and distilled under nitrogen atmosphere before use. Acetonitrile and *n*-pentane were distilled over calcium hydride. Furfural (Alfa Aesar) was vacuum-distilled over calcium hydride prior to use. Triethylamine (Et_3N, Alfa Aesar) and 1,8-diazabicyclo[5.4.0]undec-7-ene (DBU, Aldrich) were dried with activated molecular sieves. 5-Hydroxymethylfurfural (HMF, Acros Organics), 4-dimethylaminopyridine (DMAP, Matrix Scientific), 3-bromo-2-butanone (Alfa Aesar), carbon disulfide (Fisher Scientific), sodium perchlorate monohydrate (Alfa Aesar), *p*-toluenesulfonic acid monohydrate (Alfa Aesar), *N*-bromosuccinimide (Alfa Aesar), 2,6-diisopropyl-aniline (Alfa Aesar) 2,4,6-trimethylaniline (Alfa Aesar), phenylhydrazine (Alpha Aesar), aniline (Alfa Aesar), sodium hydroxide (Fisher Scientific), dimethyl sulfoxide (Fisher Scientific), thionyl chloride (Fluke), absolute ethanol (Pharmco-Aaper), and hydrochloric acid (EMD) were purchased from the respective commercial vendors as indicated and used as received. Pre-catalysts 5-methoxy-1,3,4-triphenyl-4,5-dihydro-1*H*-1,2,4-triazoline (**A**),[1,2] 3-(2,6-diisopropylphenly)-4,5-dimethylthiazol-3-ium perchlorate (**B**),[3]and 3-mesityl-5,6,7,8-tetrahydro-4*H*-cyclohepta[*d*] thiazole-3-ium perchlorate (**C**),[3] and 2-(perfluorophenyl)-5,6,7,8-tetrahydro-

[1,2,4]triazolo[4,3-a] pyridine-2-ium tetrafluoroborate (**D**)4 were prepared according to literature procedures.

^{1}H and ^{13}C NMR spectra were recorded on a Varian 400 MHz or a 500 Bruker MHz spectrometer. High-resolution mass spectrometry (HRMS) data were collected on an Agilent 6220 Accurate time-of-flight LC/MS spectrometer with a C_{12} column. Flash chromatography was performed on a Teledyne Isco CombiFlashR_f® system with 24 g, 40 g, 80 g, and 220 g standard and high-performance silica columns.

Synthesis of 2-(furan-2-yl)-2-hydroxy-1-(5-(hydroxymethyl)furan-2-yl)ethan-1-one (2) and 1-(furan-2-yl)-2-hydroxy-2-(5-(hydroxymethyl)furan-2-yl)ethan-1-one (3) and their separation. Pre-catalyst **A** (300 mg, 91 μmol) was combined with FF (750 μl, 6.9 mmol) and HMF (1.0 mL, 13 mmol) in 15 mL THF in a glass pressure vessel under N_2 in a glovebox. The vessel was then sealed and heated in an oil bath at 80 °C for 24 h with stirring. After heating was complete, the crude material was loaded onto 10 g silica gel. Flash chromatography was performed with an 80 g gold silica column. The solvent ratio started at 8 minutes of 20% EtOAc and 80% hexanes. The EtOAc rose to 55% over 12 minutes and then held at 55% for 8 minutes. After completion of hold time, the fraction of EtOAc rose to 100% over 7 minutes and then held at 100% for 10 minutes. This procedure was adequate to separate the two cross-coupling products (C_{11} furoins) from HMF and homo-coupling products (C_{10} furoin **1** and C_{12} furoin **4**), but an additional column was needed to isolate the two cross-coupling products. The second separation performed on the combined cross-coupling product (**2** and **3**) fraction was performed with a 40 g gold silica column with the two cross-coupling products achieving separation when the EtOAC and hexane were at 1:1 ratio, affording pure **2** and **3**.

In an example preparative scale reaction, pre-catalyst **B** (500 mg, 1.34 mmol), FF (1.11 mL, 13.4 mmol), HMF (3.40 g, 26.9 mmol), and Et_3N (350 μL) were combined with 120 mL of anhydrous EtOH in a 150 mL glass pressure vessel under N_2 atmosphere in a glovebox. The sealed pressure vessel was then removed from the glovebox and heated in an oil bath at 80 °C for 24 h with magnetic stirring. Upon completion of the heating, the glass pressure vessel was brought back to the glovebox and the reaction was quenched with TsOH (767 mg, 4.0 mmol). The quenched mixture was then prepared for flash chromatography by loading the material on 25 g silica gel. Flash chromatography was performed using a 220 g RediSep® gold silica column and EtOAc : hexanes. The isolated yield was 22.2% and 19.9% for C_{11} furoin **2** and **3**, respectively.

In another procedure used for the isolation of C_{11} furoins as a mixture, pre-catalyst **A** (440 mg, 1.34 mmol), FF (1.11 mL, 13.4 mmol) and HMF (3.40 g, 26.9 mmol) were combined with 120 mL of anhydrous EtOH in a 150 mL glass pressure vessel under N_2 atmosphere in a glovebox. The sealed pressure vessel was then heated in an oil bath at 80 °C for 24 h with magnetic stirring. The reaction was then prepared for flash chromatography by loading the material on 25 g silica gel. Flash chromatography was performed using a 220 g RediSep® gold silica column and EtOAt/Hexanes. The isolated yield of **2** and **3** combined was 2.53 g (48.1 %).

^{1}H NMR (500 MHz, DMSO-d_6) for C_{11} furoin **2**: δ 7.57 (dd, J = 1.8, 0.9 Hz, 1H, furan ring H), 7.47 (d, J = 3.6 Hz, 1H, furan ring H), 6.49 (d, J = 3.5 Hz, 1H, furan ring H), 6.44 – 6.37 (m, 2H, furan ring H), 6.09 (d, J = 6.3 Hz, 1H, CHO*H*), 5.76 (d, J = 6.2 Hz, 1H, C*H*OH), 5.48 (t, J = 5.9 Hz, 1H, CH_2O*H*), 4.44 (d, J = 5.8 Hz, 2H, CH_2OH). ^{13}C NMR (126 MHz, DMSO-d_6): δ 185.07 (C1), 161.71 (C2), 153.04 (C3), 149.13 (C4), 143.43 (C5), 122.19 (C6), 111.13 (C7), 109.72 (C8), 108.93 (C9), 69.81 (C10), 56.32 (C11). HRMS calculated for $C_{11}H_{14}O_5N^+$ $[M + NH_4]^+$: m/z = 240.0867; found: 240.0868.

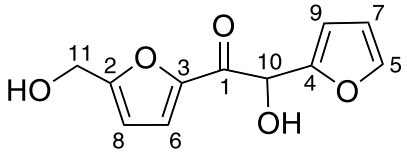

^{1}H NMR (500 MHz, DMSO-d_6) for C_{11} furoin **3**: δ 7.98 (dd, J = 1.7, 0.7 Hz, 1H, furan ring H), 7.52 (dd, J = 3.7, 0.7 Hz, 1H, furan ring H), 6.68 (dd, J = 3.6, 1.7 Hz, 1H, furan ring H), 6.32 (d, J = 3.2 Hz, 1H, furan ring H), 6.20 (d, J = 3.2 Hz, 1H, furan ring H), 6.07 (d, J = 6.2 Hz, 1H, CHO*H*), 5.75 (d, J = 6.1 Hz, 1H, C*H*OH), 5.17 (t, J = 5.7 Hz, 1H, CH_2O*H*), 4.30 (d, J = 5.5 Hz, 2H, C*H*$_2$OH). ^{13}C NMR (126 MHz, DMSO-d_6): δ 185.40 (C1), 156.05 (C2), 152.00 (C3), 150.10 (C4), 148.71 (C5), 120.82 (C6), 112.97 (C7), 109.66 (C8), 108.27 (C9), 69.99 (C10), 56.06 (C11). HRMS calculated for $C_{11}H_{14}O_5N^+$ $[M + NH_4]^+$: m/z = 240.0867; found: 240.0866.

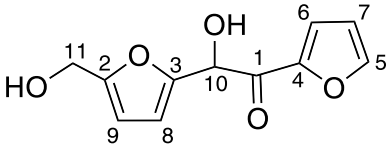

Pre-catalyst screening for the cross-coupling reaction. HMF (0.168 g, 1.34 mmol) and FF (111 µL, 1.34 mmol) were combined along with a pre-catalyst (134 µmol) and a base in 20 mL vial in a glovebox. The base to pre-catalyst ratios were used as follows: [DBU]/[pre-catalyst] = 1:1, [DMAP]/[pre-catalyst] = 1:1.5, and [Et_3N]/[pre-catalyst] = 1:2. The reaction mixture was heated while stirring at 80 °C for 24 h in glovebox. After heating was complete an aliquot was taken from the crude mixture and ^{1}H-NMR was taken in DMSO-d_6 to determine the product distribution (i.e., molar fractions of furoins **1**, **2**, **3**, and **4**).

Product distribution verse time experiments. Furaldehydes (FF, 110 µL, 1.35 mmol; HMF 340 mg, 2.70 mmol) were combined in a Schlenk flask in an argon-filled glove box. An oil bath was heated to the appropriate temperature (60° C or 80° C), the charged Schlenk flask was placed in the oil bath, and then Et_3N and precatalyst **D** (75 mg, 200 µmol) dissolved in EtOH were added to start the reaction. Aliquots (0.10 mL) were taken at the indicated times with a 1.0 mL syringe and added to a 1.5 mL vial with a septum cap. The vial was charged with 0.7 mL NMR solvent solution, which was prepared by combining ~ 8 mg *p*-toluenesulfonic acid with 17 mL DMSO-d_6.

Once all aliquots were taken then NMR samples were prepared from the small vials for determining the product distribution by NMR.

Synthesis of 1-(furan-2-yl)-2-(5-(hydroxymethyl)furan-2-yl)ethane-1,2-dione (5). DBU (20.0 µL, 135 µmol), **2** (75.0 mg, 338 µmol), and **3** (75.0 mg, 338 µmol) were refluxed for 8 h at 70 °C open to atmosphere. The resulting mixture was purified with flash chromatography to produce 0.114 g (75.8%) of the pure **5**.

^{1}H NMR (400 MHz, DMSO-d_6) for **5**: δ 8.23 (d, J = 1.9 Hz, 1H, furan ring H), 7.64 (dd, J = 3.7, 2.2 Hz, 1H, furan ring H), 7.59 (dd, J = 3.6, 2.1 Hz, 1H, furan ring H), 6.83 (dt, J = 3.6, 1.8 Hz, 1H, furan ring H), 6.65 (t, J = 2.9 Hz, 1H, furan ring H), 5.64 (td, J = 6.1, 2.1 Hz, 1H, $CH_2O\mathit{H}$), 4.55 (dd, J = 6.0, 2.1 Hz, 2H, $C\mathit{H}_2OH$). ^{13}C NMR (101 MHz, DMSO-d_6): δ 178.37, 177.87, 164.56, 151.34, 149.14, 148.26, 126.63, 125.17, 113.98, 110.79, 56.45. HRMS calculated for $C_{11}H_{12}O_5Na^+$ $[M + Na]^+$: m/z = 243.0264; found: 243.0266.

Single-crystal X-ray analysis of C$_{11}$ furoin 3. Single crystals of colorless needles suitable for X-ray diffraction were grown from a saturated solution of **3** in ethyl acetate and diffusion of hexanes into the saturated EtOAc at room temperature over a period of one week. X-ray diffraction intensities were collected on a Bruker SMART APEX CCD Diffractometer using MoKa (0.71073 Å) radiation at 120 K. The structures were solved by direct methods and refined using the Bruker SHELXTL program library by full-matrix least squares on F^2 for all reflections.[5] All non-hydrogen atoms were refined with anisotropic displacement parameters, whereas hydrogen atoms were included in the structure factor calculations at idealized positions.

References

(1) Enders, D.; Breuer, K.; Kallfass, U.; Balensiefer, T. Preparation and application of 1,3,4-triphenyl-4,5-dihydro-1H-1,2,4-triazol-5-ylidene, a stable carbene. *Synthesis* **2003**, 1292–1295.

(2) Enders, D.; Breuer, K.; Raabe, G.; Runsink, J.; Teles, J. H.; Melder, J.-P.; Ebel, K.; Brode, S. Preparation, structure, and reactivity of 1,3,4-triphenyl-4,5-dihydro- 1H-1,2,4-triazol-5-ylidene, a new stable carbene. *Angew. Chem. Int. Ed.* **1995**, *34*, 1021–1023.

(3) Piel, I.; Pawelczyk, M. D.; Hirano, K.; Froehlich, R.; Glorius, F. A family of thiazolium salt derived N-heterocyclic carbenes (NHCs) for organocatalysis: synthesis, investigation and application in cross-benzoin condensation. *Eur. J. Org. Chem.* **2011**, 5475–5484.

(4) Langdon, S. M.; Wilde, M. M. D.; Thai, K.; Gravel, M. Chemoselective N-heterocyclic carbene-catalyzed cross-benzoin reactions: importance of the fused ring in triazolium salts. *J. Am. Chem. Soc.* **2014**, *136*, 7539–7542.

(5) *SHELXTL*, Version 6.12; Bruker Analytical X-ray Solutions: Madison, WI, 2001.

Appendix B

Experimental Details and Supporting Information for Chapter 3

B.1. Materials, Reagents, and Methods

Materials. All the synthesis and manipulations of air and moisture sensitive materials were carried out in oven dried Schlenk-type glassware on a high-vacuum line or in a dry inert gas (N_2 or Ar) filled glovebox. Hexamethylenediisocyanate (HDI), 2,4-toluenediisocyanate (TDI), diphenylmethanediisocyanate (MDI), and dibutyltindilaurate (DBTDL) were purchased from Sigma-Aldrich and used as received. Succinyl chloride (1), adipoyl chloride (2), and suberoyl chloride (3) were purchased from Alfa Aesar; liquid diacyl chlorides (1, 2, and 3) were freshly distilled before use. 5-Hydroxymethylfurfural (HMF) was purchased from Ark Pharm and used as received, while furfural (FF) was purchased from TCI America and dried with CaH_2 for 24 h and then vacuum distilled. HPLC-grade dichloromethane (DCM) and *N,N*-dimethyl formamide (DMF) were sparged extensively with nitrogen during filling of the solvent reservoir and then dried by passage through activated alumina stainless steel columns. Tetrahydrofuran (THF) was dried by distillation over sodium with benzophenone as indicator under a nitrogen atmosphere. Anhydrous acetonitrile 99.8% was purchased from Sigma-Aldrich was used as received. Deuterated dimethyl sulfoxide (DMSO-d_6) was degassed and stored in a glovebox over activated Davison 4 Å molecular sieves.

Methods. NMR spectra were recorded on a Varian Inova spectrometer (400 MHz for ^{1}H NMR and 100 MHz for ^{13}C NMR). Chemical shifts for ^{1}H and ^{13}C NMR spectra were referenced in ppm relative to tetramethylsilane with the solvent residual resonances as the internal standard (DMSO-d_6: δ 2.50 ppm for ^{1}H NMR and 39.52 ppm for ^{13}C NMR; $CDCl_3$: δ 7.26 ppm for ^{1}H NMR and

77.16 ppm for ^{13}C NMR). High-resolution mass spectrometry (HRMS) data were collected on an Agilent 6220 Accurate time-of-flight LC/MS spectrometer. Fourier transform infrared (FTIR) spectroscopy was performed on a Thermoscientific (Nicolet iS50) FT-IR spectrometer equipped with a diamond attenuated total reflectance (ATR) at room temperature in the range of 550–4000 cm^{-1}. Determination of dn/dc and polymer number-average molecular weight (M_n) and dispersity ($Đ = M_w/M_n$) were measured by gel permeation chromatography (GPC) analyses carried out at 40 ºC and a flow rate of 0.5 mL/min, with 0.05M LiBr in DMF as the eluent on an Agilent HPLC system equipped with one guard column and two PLgel 5 μm mixed-C gel permeation columns and coupled with a Wyatt DAWN HELEOs II multi (18)-angle light scattering detector. Data analysis was performed with Wyatt ASTRA 7.1.2 molecular weight characterization software. Thermal properties of the polymers were measured on a TA Q50 thermal gravimetric analyzer (TGA), and a TA Q20 differential scanning calorimetry (DSC) analyzer under dry nitrogen flow of 40 mL/min. For TGA analysis, polymer samples were heated from ambient temperature to 700 ºC at a heating rate of 10 ºC/min under a nitrogen atmosphere. For DSC analysis, polymer samples were first heated from room temperature to 100-120 ºC at 10 ºC/min, equilibrated at this temperature, then cooled to –50 ºC at 5 ºC/min, allowed to equilibrate, and reheated to 150-200 ºC at 5 ºC/min. The glass transition temperature (T_g) was obtained from the second heating cycle. For mechanical analysis, a TAQ800 DMA instrument was utilized in multi-frequency strain mode with a Tension-film clamp. Thin films suitable for mechanical analysis were prepared by compression molding using a Carver Bench Top Laboratory Press (Model 4386) equipped with a two-column hydraulic unit (Carver, Model 3912, maximum force 24000 psi). Materials were combined with 3~5% by weight butylated hydroxytoluene and loaded between non-stick Teflon paper sheets into a steel tile mold with inset dimensions 50 mm by 50 mm with a depth of 1 mm (Carver, Model

818701D) and compressed between two 6" by 6" electrically heated platens (EHP) at clamp force 5000 psi and temperature between 20-40 °C above the T_g for that particular material. Then the 50 mm square was cut to a width of either 13 mm or 5.3 mm with a length of 40 mm (DMA specimens were either 5.3 mm or 13 mm wide, 40 mm long, and 1 mm thick). The analysis was performed with an oscillating strain of 0.15% at a frequency of 1 Hz with a temperature ramp from -50.0 °C to 190.0 °C at a rate of 3 °C a minute. Stress-strain measurements were made on the same instrument in DMA strain rate mode with a displacement ramp set for 200 µm a minute with a constant temperature of 30 °C.

Modified Synthesis of 2-(furan-2-yl)-2-hydroxy-1-(5-(hydroxymethyl)furan-2-yl)ethan-1-one (Diol Monomer A) and 1-(furan-2-yl)-2-hydroxy-2-(5-(hydroxymethyl)furan-2-yl)ethan-1-one (Diol Monomer B). HMF (7.40 g, 0.06 mol), FF (6.0 mL, 0.07 mol) and TPT-OMe (0.384 g, 1.20 mmol) were disolved in 300 mL of THF (EtOH) then sealed in a glass pressure vessel in an argon or nitrogen filled glove box. The reaction vessel was then removed from the glove box and heated at 60°C, with magnetic stirring (400 ppm), for 20 h. The seal was removed and the contents were immediatly loaded onto silica gel for automated flash chromotography. Upon completion of the chromotography, the fractions corrasponding to diol monomers A and B were combined and the solvent was removed by rotory evaporation under vacumm. The recovered diol was dissolved 40 mL ethyl acetate and then precipitated with 100 mL of heaxanes. The solid was seperated with vacuum filtration, and heated to 50°C under vacumm for 8 h. Conversion by ^{1}H-NMR was 43%, and isolated yield for A was 2.77 g (19%) and for B was 2.33 g (16%).

Synthesis of PEs. A general procedure for the synthesis of PEs was described as follows. A 50 mL, 2-neck flask and condenser dried in oven overnight were sealed with septums and cooled under a flow of dry N_2 for 2 h. Diol (1 equiv.) and pyridine (3 equiv) were combined with 15 mL

solvent in a glovebox and loaded into a 25 mL a syringe, then diacid chloride (1 equiv) and 3 mL solvent were loaded into a separate syringe. Reactants were removed from the glovebox and the syringe containing diol was added to the magnetically stirring (400 rpm) reaction vessel under dry nitrogen. Then the diacid was then slowly added over the course of 20 min, upon completion of reactant addition the heating was started (45 °C) and continued for 72 h. After heating, the reaction was cooled and a samle of the crude reaction was prepared for ^{1}H-NMR analaysis. Then the reaction mixture was slowly added to a magnetically stirred 100 mL of MeOH and then allowed to settle overnight. Solid was removed with filtration, rinsed with additional MeOH, and dried for 24 h under vacuum at 60 °C.

PE-1A by monomer A (1.09 g, 4.9 mmol), succinyl chloride (4.9 mmol, 530 µL), isolated yield (1.19 g, 80%). ^{1}H NMR (400 MHz, DMSO-d_6) δ 7.70 (s, 1H), 7.63 – 7.54 (m, 1H), 6.88 – 6.81 (m, 1H), 6.72 (d, J = 4.2 Hz, 2H), 6.56 – 6.46 (m, 1H), 5.11 (s, 2H), 2.73 (d, J = 8.2 Hz, 2H), 2.64 (d, J = 9.7 Hz, 2H). ^{13}C NMR (101 MHz, DMSO-d_6) δ 179.16, 171.60, 155.55, 149.12, 146.64, 145.38, 122.09, 113.16, 112.89, 111.66, 70.79, 58.12, 28.70, 28.53.

PE-1B by monomer B (1.06 g, 4.8 mmol), succinyl chloride (4.8 mmol, 525 µL), isolated yield (1.25 g, 86%). ^{1}H NMR (400 MHz, DMSO-d_6) δ 8.03 (s, 1H), 7.63 (d, J = 3.4 Hz, 1H), 6.88 – 6.80 (m, 1H), 6.75 – 6.66 (m, 2H), 6.56 – 6.46 (m, 1H), 4.99 (s, 2H), 2.72 (d, J = 12.5 Hz, 2H), 2.69 – 2.52 (m, 2H). ^{13}C NMR (101 MHz, DMSO-d_6) δ 179.04, 171.42, 151.51, 149.29, 147.29, 121.37, 113.80, 113.29, 112.53, 70.78, 58.16, 28.74.

PE-1A/B by monomer A and B mixture (1.99 g, 9.0 mmol), succinyl chloride (9.0 mmol, 988 µL), isolated yield (1.20 g, 84%). ^{1}H NMR (400 MHz, DMSO-d_6) δ 8.03 (s, 1H), 7.70 (s, 1H), 7.63 (s, 1H), 6.84 (d, J = 7.2 Hz, 2H), 6.53 (s, 1H), 6.49 (s, 1H), 5.11 (s, 2H), 4.99 (s, 2H), 2.72 (d, J = 14.7 Hz, 4H), 2.58 (s, 1H). ^{13}C NMR (101 MHz, DMSO-d_6) δ 179.14, 179.04, 179.02,

179.00, 178.97, 178.95, 178.92, 178.90, 178.86, 171.65, 171.62, 171.60, 171.57, 171.44, 171.38, 171.32, 155.70, 155.58, 155.55, 151.51, 149.50, 149.48, 149.30, 149.22, 149.11, 149.02, 148.93, 147.40, 147.33, 147.29, 147.25, 147.23, 147.18, 146.60, 145.48, 145.40, 145.38, 145.35, 145.26, 145.17, 121.42, 113.96, 113.94, 113.89, 113.87, 113.84, 113.82, 113.80, 113.76, 113.71, 113.65, 113.47, 113.43, 112.97, 112.89, 112.83, 112.80, 112.77, 111.81, 111.66, 70.80, 70.77, 28.67, 28.64, 28.61, 28.59

PE-2A by monomer A (2.00 g, 9.0 mmol), adipoyl chloride (9.0 mmol, 1.31 mL), isolated yield (2.65 g, 83%). ^{1}H NMR (400 MHz, DMSO-d_6) δ 7.70 (s, 1H), 7.58 (s, 1H), 6.84 (s, 1H), 6.72 (s, 2H), 6.48 (s, 1H), 5.11 (s, 2H), 2.45 (d, J = 7.0 Hz, 3H), 2.36 (d, J = 7.7 Hz, 3H) ^{1}H NMR (400 MHz, DMSO-d_6) δ 7.70 (s, 1H), 7.58 (s, 1H), 6.84 (s, 1H), 6.72 (s, 2H), 6.48 (s, 1H), 5.11 (s, 2H), 2.45 (d, J = 7.0 Hz, 3H), 2.36 (d, J = 7.7 Hz, 3H), 1.55 (t, J = 15.3 Hz, 7H). ^{13}C NMR (101 MHz, DMSO-d_6) δ 179.37, 172.60, 172.44, 155.71, 149.16, 146.77, 145.32, 121.96, 113.06, 112.79, 111.64, 70.57, 57.76, 33.14, 24.07.

PE-2B by monomer B (1.97 g, 8.9 mmol), adipoyl chloride (1.289 mL, 8.9 mmol), isolated yield (4.56 g, 79%). ^{1}H NMR (400 MHz, DMSO-d_6) δ 8.03 (s, 1H), 7.61 (d, J = 3.4 Hz, 1H), 6.83 (s, 1H), 6.70 (d, J = 13.4 Hz, 2H), 6.52 (s, 1H), 4.99 (s, 2H), 2.45 (d, J = 12.9 Hz, 3H), 2.29 (d, J = 14.5 Hz, 3H), 1.52 (t, J = 26.1 Hz, 5H). ^{13}C NMR (101 MHz, DMSO-d_6) δ 179.26, 172.64, 172.39, 151.71, 149.38, 147.37, 121.20, 113.68, 113.23, 112.36, 70.62, 57.75, 33.20, 24.06.

PE-2A/B by monomer A (1.75 g, 7.9 mmol) and monomer B (1.58 g, 7.1 mmol), adipoyl chloride (2.176 mL, 14.9 mmol), isolated yield (2.69 g, 87%). ^{1}H NMR (400 MHz, DMSO-d_6) δ 8.03 (s, 1H), 7.70 (s, 1H), 7.59 (d, J = 10.3 Hz, 1H), 6.83 (s, 2H), 6.70 (d, J = 11.7 Hz, 4H), 6.52 (s, 1H), 6.48 (s, 1H), 5.11 (s, 2H), 4.99 (s, 2H), 2.48 – 2.39 (m, 7H), 2.39 – 2.25 (m, 3H), 1.56 (d, J = 26.1 Hz, 7H). ^{13}C NMR (101 MHz, DMSO-d_6) δ 179.37, 179.26, 172.64, 172.39, 155.71,

151.71, 149.38, 149.16, 147.37, 146.77, 145.32, 144.74, 143.78, 127.05, 121.96, 121.20, 113.69, 113.68, 112.79, 112.40, 111.63, 70.62, 57.76, 33.22, 32.92, 24.04.

PE-3A by monomer A (0.268 g, 1.2 mmol), suberoyl chloride (218 µL, 1.2 mmol), isolated yield (0.174 g, 77%). ^{1}H NMR (400 MHz, DMSO-d_6) δ 7.73 (s, 1H), 7.61 (d, J = 3.6 Hz, 1H), 6.86 (d, J = 1.8 Hz, 1H), 6.74 (d, J = 3.4 Hz, 2H), 6.51 (d, J = 2.7 Hz, 1H), 5.13 (s, 2H), 2.43 (d, J = 6.8 Hz, 2H), 2.34 (q, J = 7.2 Hz, 2H), 1.62 – 1.44 (m, 6H), 1.28 (t, J = 15.9 Hz, 6H). ^{13}C NMR (101 MHz, DMSO-d_6) δ 179.39, 172.76, 155.73, 149.18, 146.81, 145.28, 121.92, 113.03, 112.72, 111.59, 70.52, 57.68, 33.45, 28.28, 24.52.

PE-3B by monomer B (0.268 g, 1.2 mmol), suberoyl chloride (218 µL, 1.2 mmol), isolated yield (0.174 g, 73%). ^{1}H NMR (400 MHz, DMSO-d_6) δ 8.02 (s, 1H), 7.60 (s, 1H), 6.82 (s, 1H), 6.70 (d, J = 13.1 Hz, 2H), 6.51 (s, 1H), 4.99 (s, 2H), 2.41 (d, J = 6.6 Hz, 3H), 2.26 (d, J = 7.0 Hz, 3H), 1.48 (d, J = 19.2 Hz, 1H), 1.25 (d, J = 18.7 Hz, 2H). ^{13}C NMR (101 MHz, DMSO-d_6) δ 179.27, 172.79, 151.75, 149.40, 147.39, 121.14, 113.63, 113.23, 112.36, 70.57, 57.68, 33.53, 33.22, 28.29, 24.55.

PE-3A/B by monomer A (0.599 g, 2.7 mmol) and monomer B (0.433 g, 2.0 mmol), suberoyl chloride (837 µL, 4.7 mmol), isolated yield (1.29 g, 73%). ^{1}H NMR (400 MHz, DMSO-d_6) δ 8.03 (s, 1H), 7.70 (s, 1H), 7.59 (d, J = 10.3 Hz, 1H), 6.83 (s, 2H), 6.70 (d, J = 11.7 Hz, 4H), 6.52 (s, 1H), 6.48 (s, 1H), 5.11 (s, 2H), 4.99 (s, 2H), 2.48 – 2.39 (m, 7H), 2.39 – 2.25 (m, 3H), 1.56 (d, J = 26.1 Hz, 7H). ^{13}C NMR (101 MHz, DMSO-d_6) δ 179.37, 179.26, 172.64, 172.39, 155.71, 151.71, 149.38, 149.16, 147.37, 146.77, 145.32, 144.74, 143.78, 127.05, 121.96, 121.20, 113.69, 113.68, 112.79, 112.40, 111.63, 70.62, 57.76, 33.22, 32.92, 24.04.

Sythesis of PUs. A typical procedure is described as follows: Diol A and/or B and 1 equivalent of a diisocyanate were dissolved in 20 mL ACN under N_2 and drawn into a 25 mL syringe, while a second

syringe with DBTDL (0.03 equiv) and ACN was prepared. The two syringes were removed from glove box and loaded into a 2-neck round bottom flask fitted with a condensor and septums under N_2 using standard schlink procedures (glassware was dried overnight in oven and assembled with a positive flow of N_2, and cooled for several h before reaction). The reaction mixture was placed in a temperature-controlled oil bath with magnetic stirring (45 °C, 350 rpm) for 48 h then slowly added to 100 mL of stirring methanol. Quenched material was allowed to settle for 16 h then the resulting material was filtered, rinsed witrh additional MeOH then residual solvant was removed by heating to 70 °C for 24 h under vacuum.

PU-4A by monomer A (2.14 g, 9.6 mmol), HDI (1.55 mL, 9.6 mmol), isolated yield (3.48 g, 92%). ^{1}H NMR (400 MHz, DMSO-d_6) δ 7.66 (s, 1H), 7.57 (d, J = 6.0 Hz, 1H), 7.52 (d, J = 3.6 Hz, 1H), 7.30 (d, J = 5.7 Hz, 1H), 6.72 – 6.58 (m, 3H), 6.45 (s, 1H), 4.99 (s, 2H), 3.05 – 2.83 (m, 5H), 1.54 – 1.26 (m, 5H), 1.19 (s, 5H). ^{13}C NMR (101 MHz, DMSO-d_6) δ 180.76, 156.38, 155.78, 155.31, 149.29, 147.52, 144.96, 121.62, 112.58, 112.33, 111.52, 70.21, 57.66, 29.67, 26.26.

PU-4B by monomer B (2.23 g, 10.0 mmol), HDI (1.610 mL, 10.0 mmol), isolated yield (2.04 g, 53%) ^{1}H NMR (400 MHz, DMSO-d_6) δ 8.02 (s, 1H), 7.70 – 7.55 (m, 2H), 7.24 (s, 1H), 6.78 – 6.70 (m, 1H), 6.65 (s, 2H), 6.55 – 6.43 (m, 1H), 4.89 (s, 2H), 2.94 (s, 6H), 1.53 – 1.29 (m, 6H), 1.21 (s, 6H). ^{13}C NMR (101 MHz, DMSO-d_6) δ 180.68, 155.94, 155.25, 152.33, 149.62, 149.09, 147.86, 120.82, 113.30, 113.18, 111.94, 70.21, 57.57, 29.62, 26.25.

PU-4A/B by monomer A (1.67 g, 7.5 mmol) and monomer B (1.58 g, 7.1 mmol), HDI (2.311 mL, 14.6 mmol), isolated yield (3.88 g, 68%). ^{1}H NMR (400 MHz, DMSO-d_6) δ 8.00 (s, 1H), 7.66 (s, 1H), 7.58 (d, J = 3.2 Hz, 2H), 7.52 (s, 1H), 7.30 (s, 1H), 6.70 (s, 1H), 6.63 (dd, J = 10.0, 3.9 Hz, 6H), 6.45 (d, J = 3.2 Hz, 2H), 4.99 (s, 2H), 4.87 (s, 2H), 2.91 (q, J = 6.4 Hz, 12H), 1.33 (q, J = 7.1 Hz, 12H), 1.20 (d, J = 8.3 Hz, 12H). ^{13}C NMR (101 MHz, DMSO-d_6) δ 180.76, 156.38,

155.95, 155.78, 155.26, 152.34, 149.62, 149.29, 149.09, 147.86, 147.52, 121.62, 120.82, 113.31, 113.18, 112.54, 112.33, 111.93, 111.54, 70.21, 70.19, 57.66, 29.61, 26.25.

PU-5A by monomer A (1.37 g, 6.1 mmol), MDI (1.54, 6.1 mmol), isolated yield (0.17 g, 92%). ^{1}H NMR (400 MHz, DMSO-d_6) δ 10.08 (s, 1H), 9.73 (d, *J* = 28.5 Hz, 1H), 7.67 (d, *J* = 36.9 Hz, 2H), 7.34 (d, *J* = 7.7 Hz, 4H), 7.10 (d, *J* = 8.1 Hz, 5H), 6.86 (d, *J* = 7.3 Hz, 1H), 6.78 (d, *J* = 6.1 Hz, 2H), 6.49 (s, 1H), 5.17 (s, 2H), 3.79 (s, 2H). ^{13}C NMR (101 MHz, DMSO-d_6) δ 180.32, 155.99, 153.11, 152.64, 149.34, 147.00, 145.24, 136.93, 136.17, 129.39, 118.85, 113.12, 112.87, 111.66, 70.44, 58.03.

PU-5B by monomer B (2.39 g, 10.7 mmol), MDI (2.69, 10.7 mmol), isolated yield (3.97 g, 78%). ^{1}H NMR (400 MHz, DMSO-d_6) δ 7.70 (s, 1H), 7.62 – 7.57 (m, 1H), 6.89 – 6.82 (m, 1H), 6.72 (d, *J* = 4.2 Hz, 2H), 6.51 – 6.46 (m, 1H), 5.11 (s, 2H), 2.73 (d, *J* = 8.2 Hz, 2H), 2.64 (d, *J* = 9.7 Hz, 2H). ^{13}C NMR (101 MHz, DMSO-d_6) δ 180.18, 153.28, 152.58, 152.06, 149.52, 147.67, 137.21, 136.94, 129.49, 121.19, 118.70, 113.89, 113.31, 112.56, 70.43, 57.93, 31.11.

PU-5A/B by monomer A (1.16 g, 5.3 mmol) and monomer B (0.874 g, 3.9 mmol), MDI (2.29, 9.2 mmol), isolated yield (3.12 g, 91%). ^{1}H NMR (400 MHz, DMSO-d_6) δ 10.08 (d, *J* = 8.9 Hz, 1H), 9.72 (d, *J* = 28.7 Hz, 1H), 8.05 (s, 0H), 7.72 (s, 1H), 7.67 (d, *J* = 3.6 Hz, 0H), 7.62 (d, *J* = 3.6 Hz, 1H), 7.34 (d, *J* = 7.9 Hz, 5H), 7.10 (d, *J* = 8.2 Hz, 5H), 6.85 (d, *J* = 7.4 Hz, 1H), 6.79 – 6.72 (m, 2H), 6.59 (d, *J* = 3.2 Hz, 1H), 6.49 (d, *J* = 2.8 Hz, 1H), 5.17 (d, *J* = 2.4 Hz, 1H), 5.12 – 4.96 (m, 1H), 3.79 (s, 2H). ^{13}C NMR (101 MHz, DMSO-d_6) δ 180.31, 155.98, 153.28, 152.63, 152.06, 149.34, 147.67, 147.00, 136.94, 136.92, 136.33, 129.39, 129.33, 118.83, 118.72, 118.63, 112.89, 70.42, 67.45, 25.56.

Cross-linking of PE-2 Series with Bismaleimide. The cross-linker 1,1'-((ethane-1,2-diylbis(oxy))bis(ethane-2,1-diyl))bis(1H-pyrrole-2,5-dione) (BM) was synthesized using

literature procedures.[1] PE and BM (15 mol % to difuranic monomer unit) was dissolved in 10 mL DCM and mixed on an orbital shaker at 200 rpm for 20 min. The solution was then poured into a PTFE mold and solvent was allowed to evaporate for 16 h at room temperature, after that it was dried an additional 24 h at 50 °C under vacuum. The resulting material was directly used for analysis.

B.2.

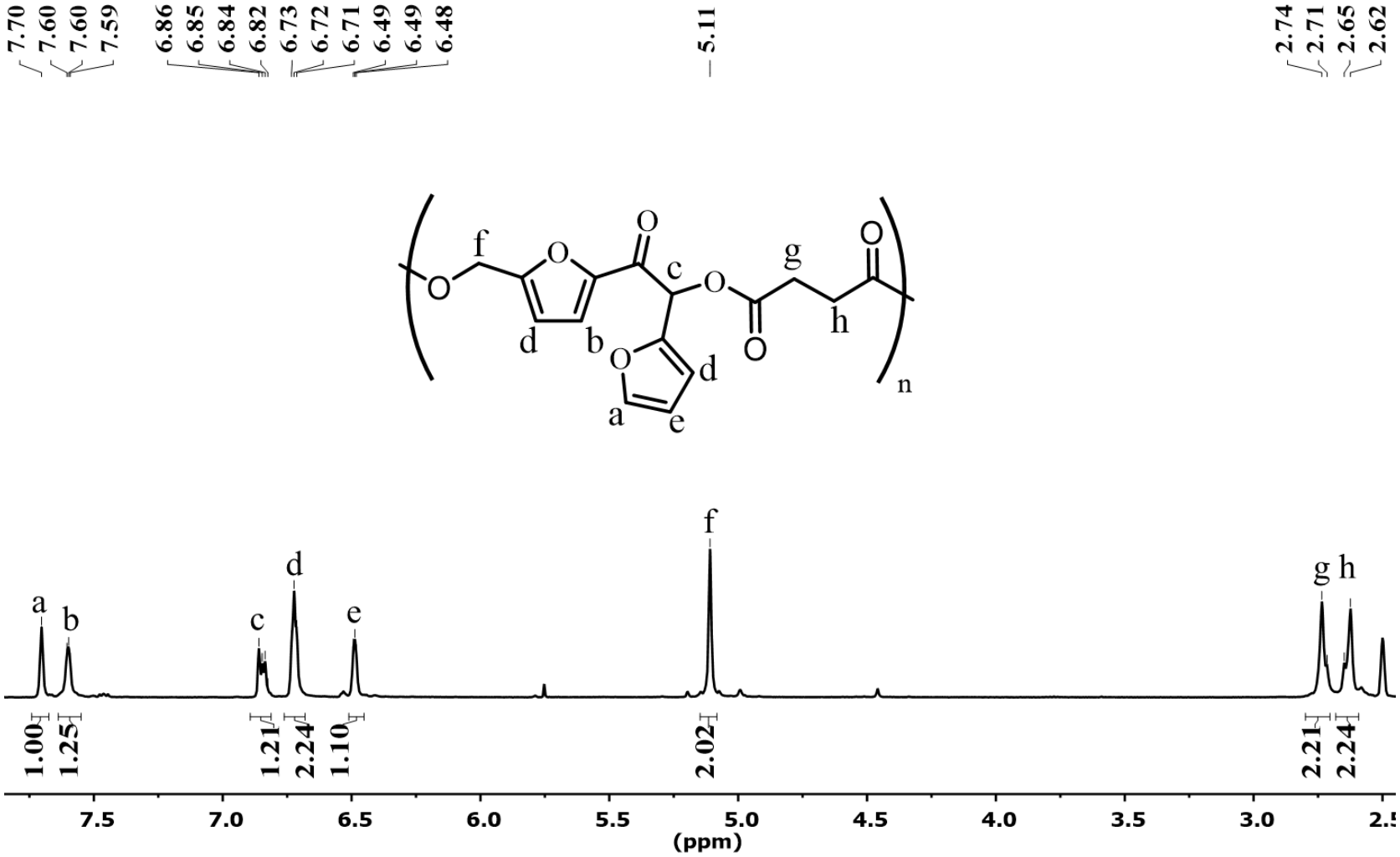

Figure S3.1. ^{1}H NMR (DMSO-d_6) of **PE-1A**.

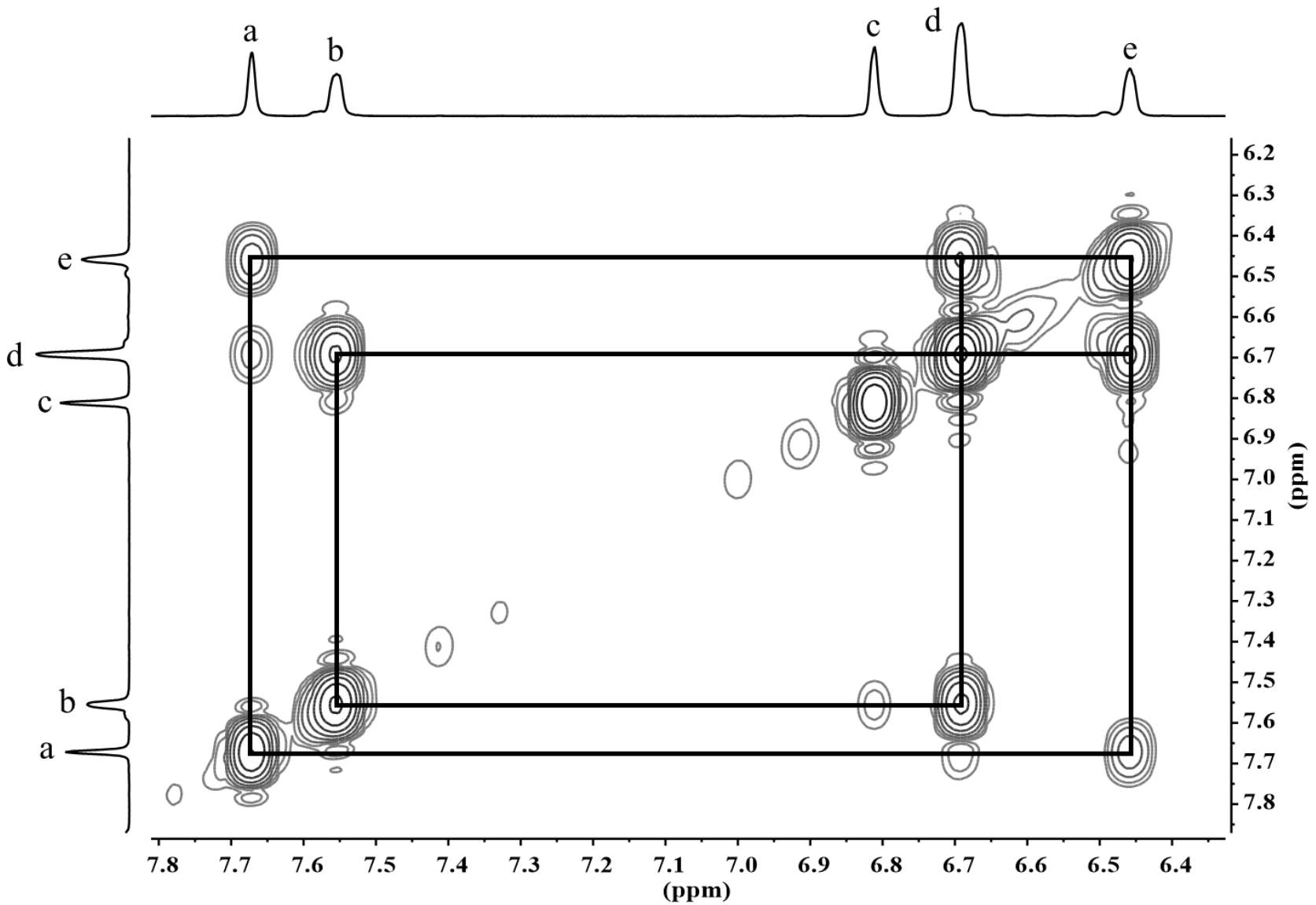

Figure S3.2. gCOSY (DMSO-d_6) (Identifies ring proton) of **PE-1A**.

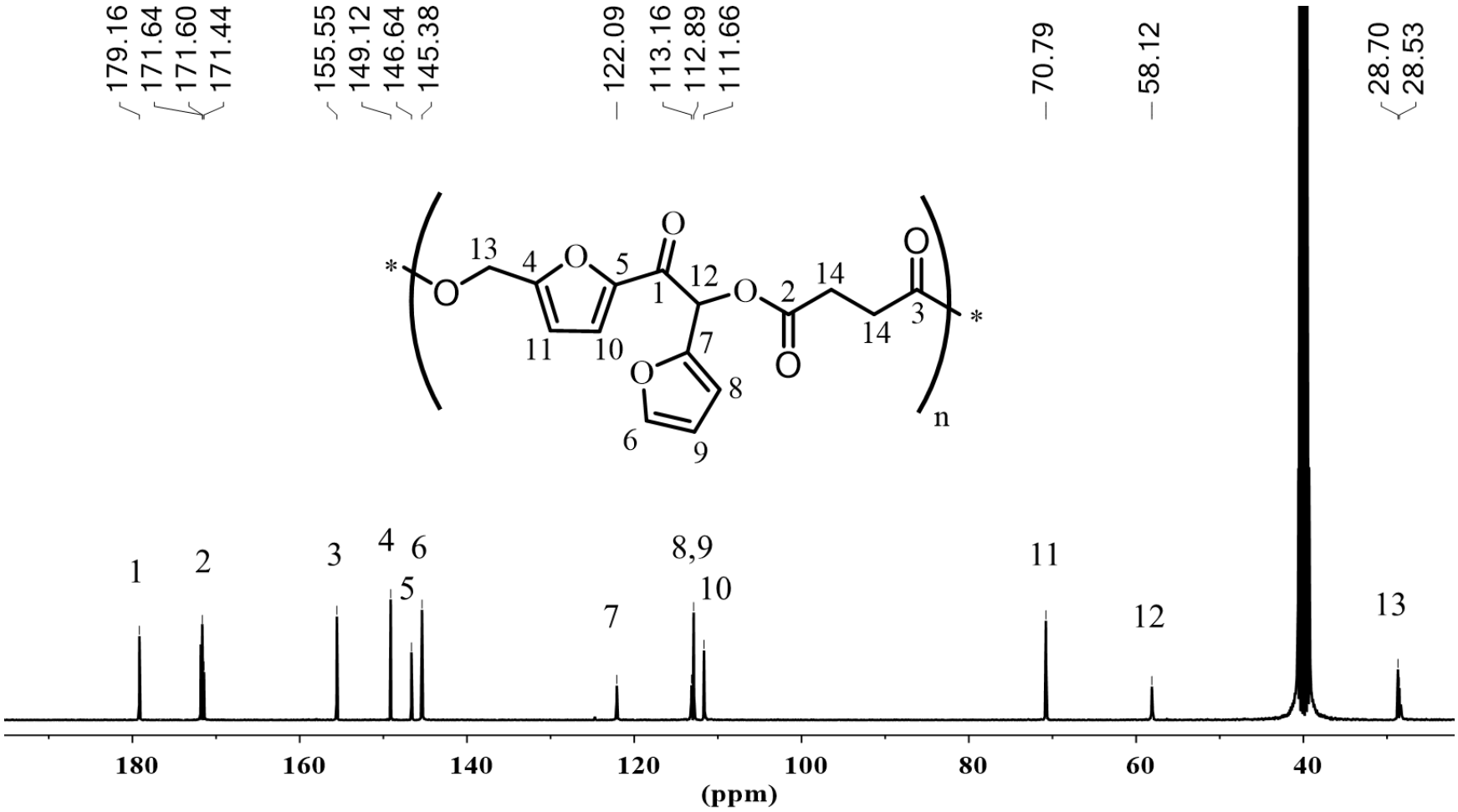

Figure S3.3. ^{13}C NMR (DMSO-d_6) of **PE-1A**.

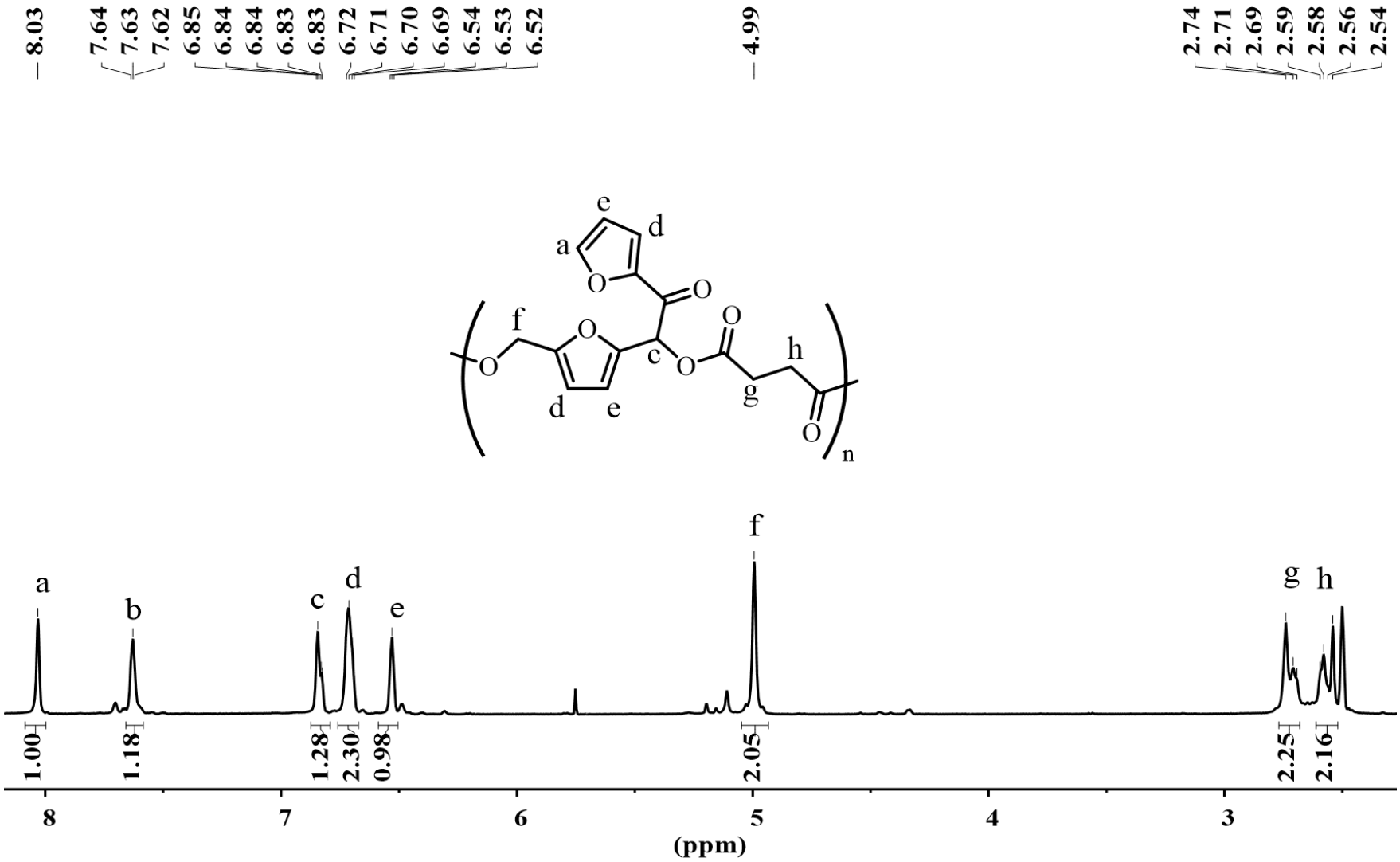

Figure S3.4. ^{1}H NMR (DMSO-d_6) of **PE-1B**.

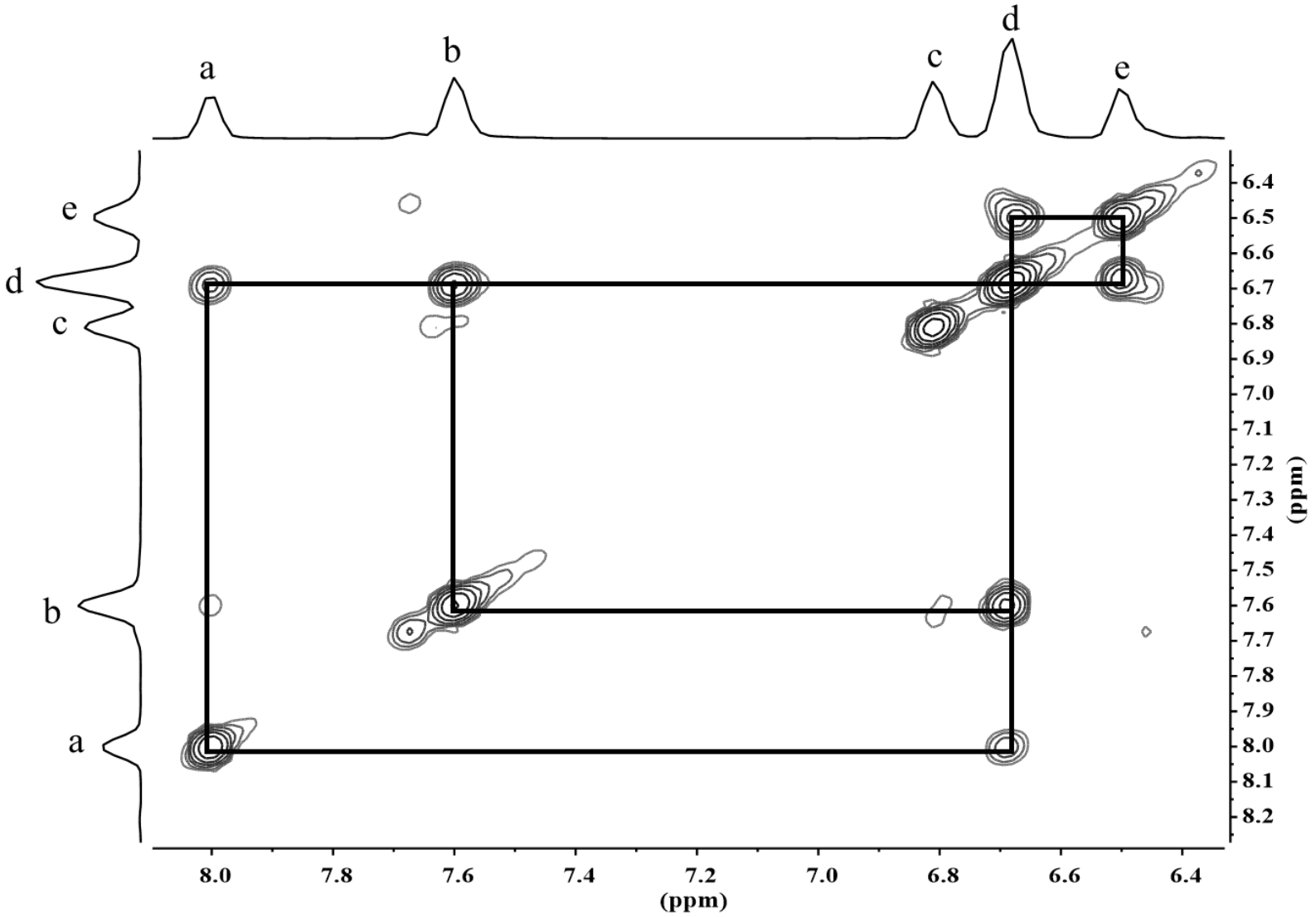

Figure S3.5. gCosy (DMSO-d_6) of **PE_1B**.

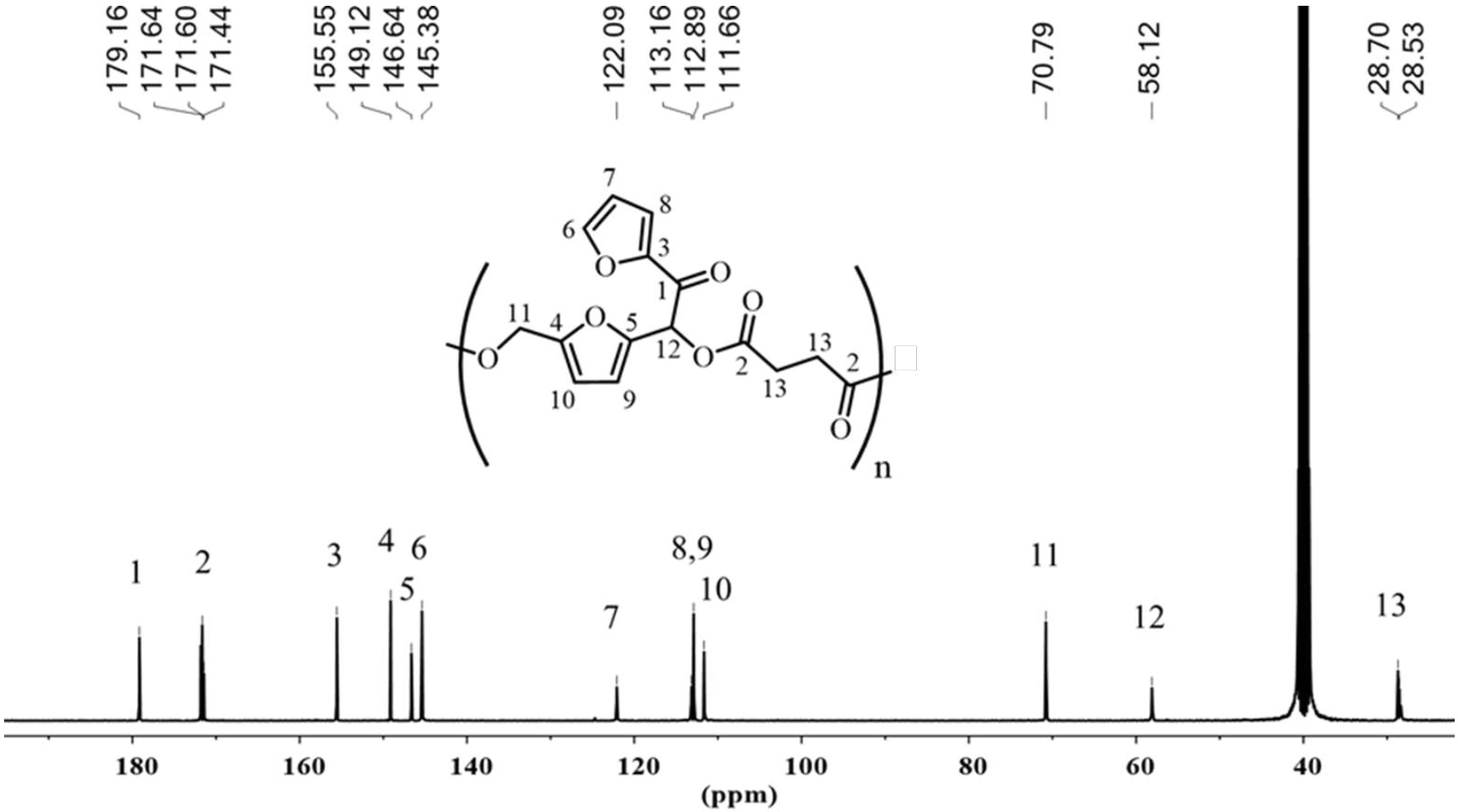

Figure S3.6. ^{13}C NMR (DMSO-d_6) of **PE-1B**.

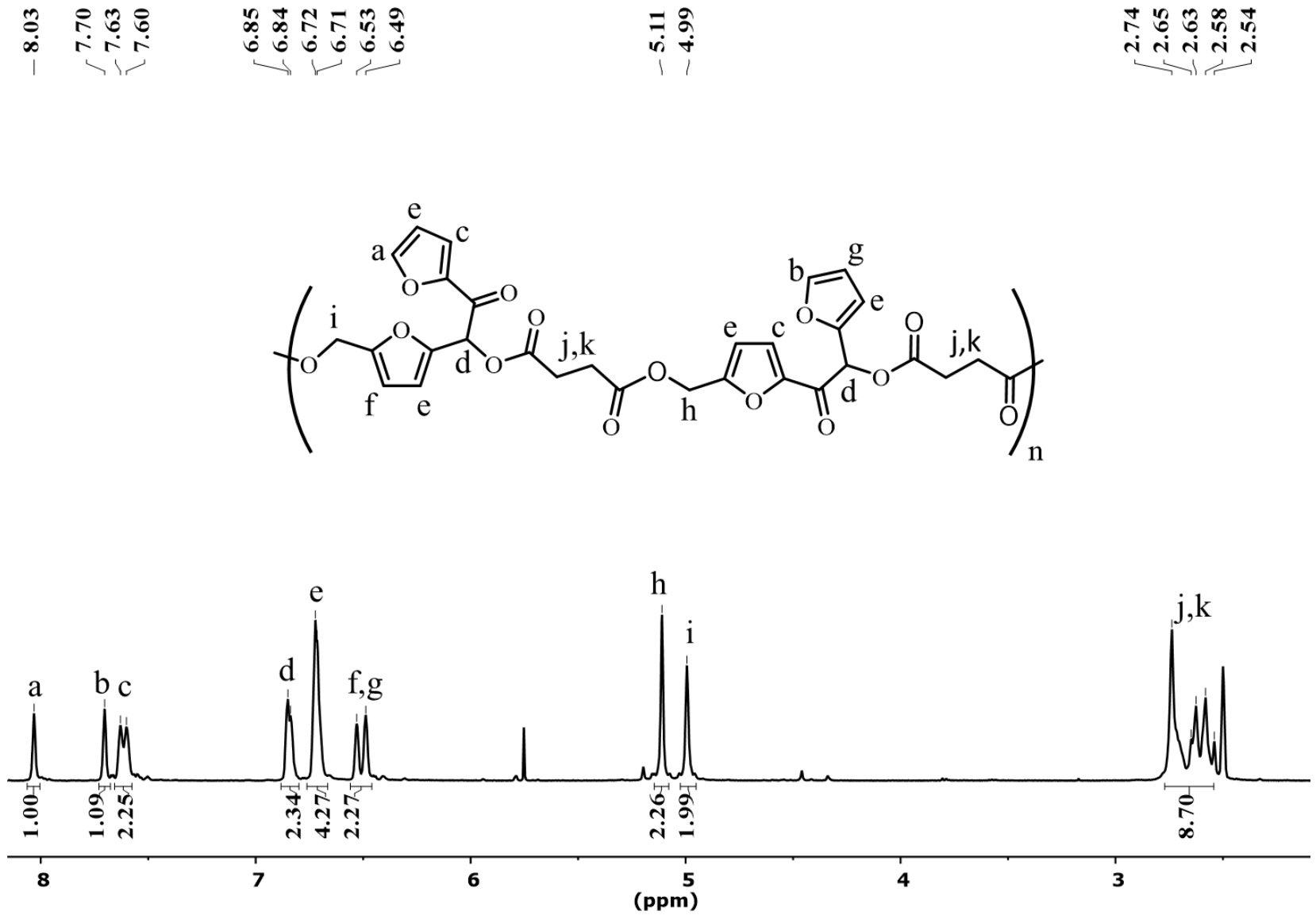

Figure S3.7. ^{1}H NMR (DMSO-d_6) of **PE-1A/B**.

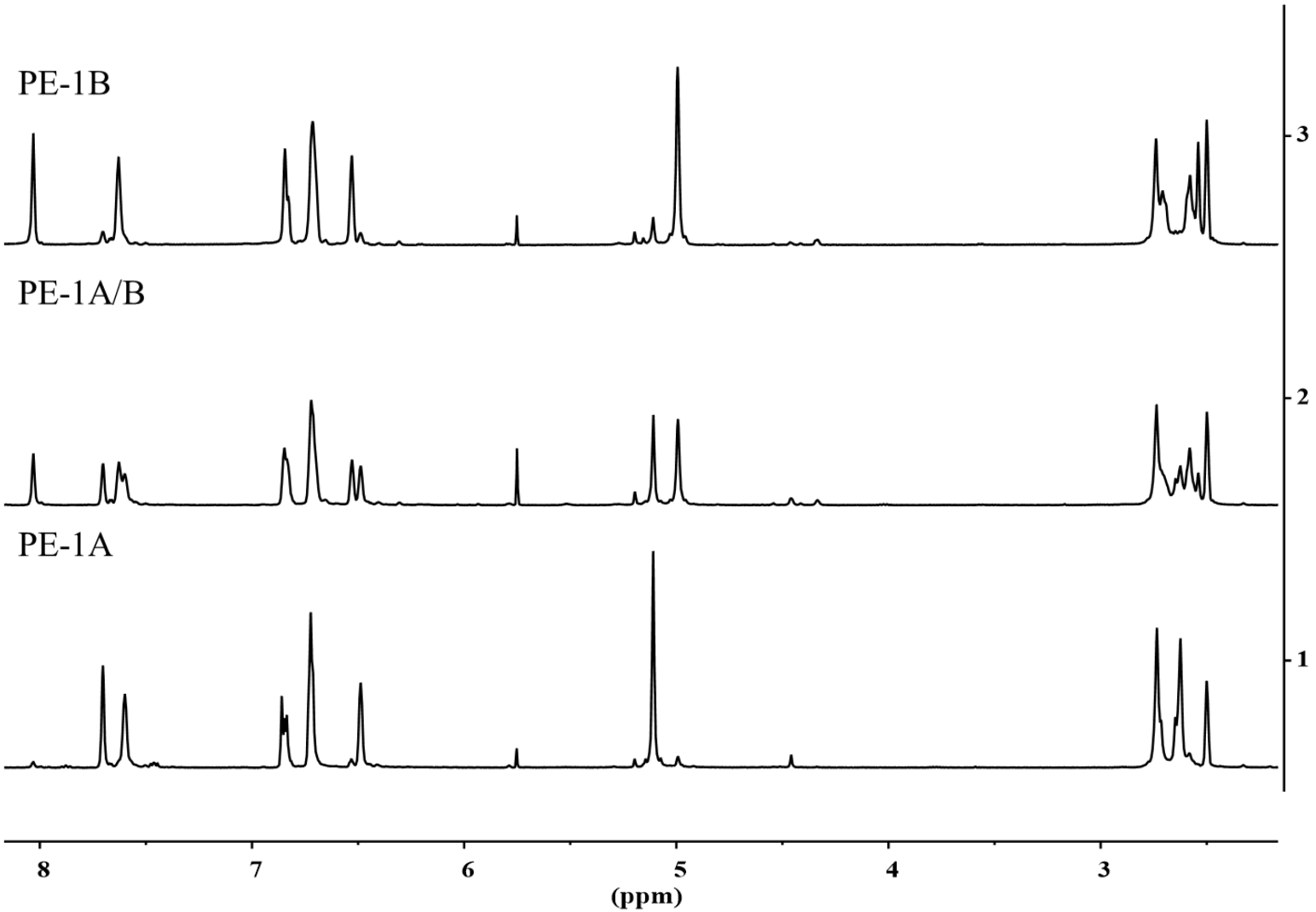

Figure S3.8. Stacked **PE-1** ^{1}H NMR series (DMSO-d_6) (Shows that the proton signals for **PE-1A/B** match the polymer made from **a** and **b**).

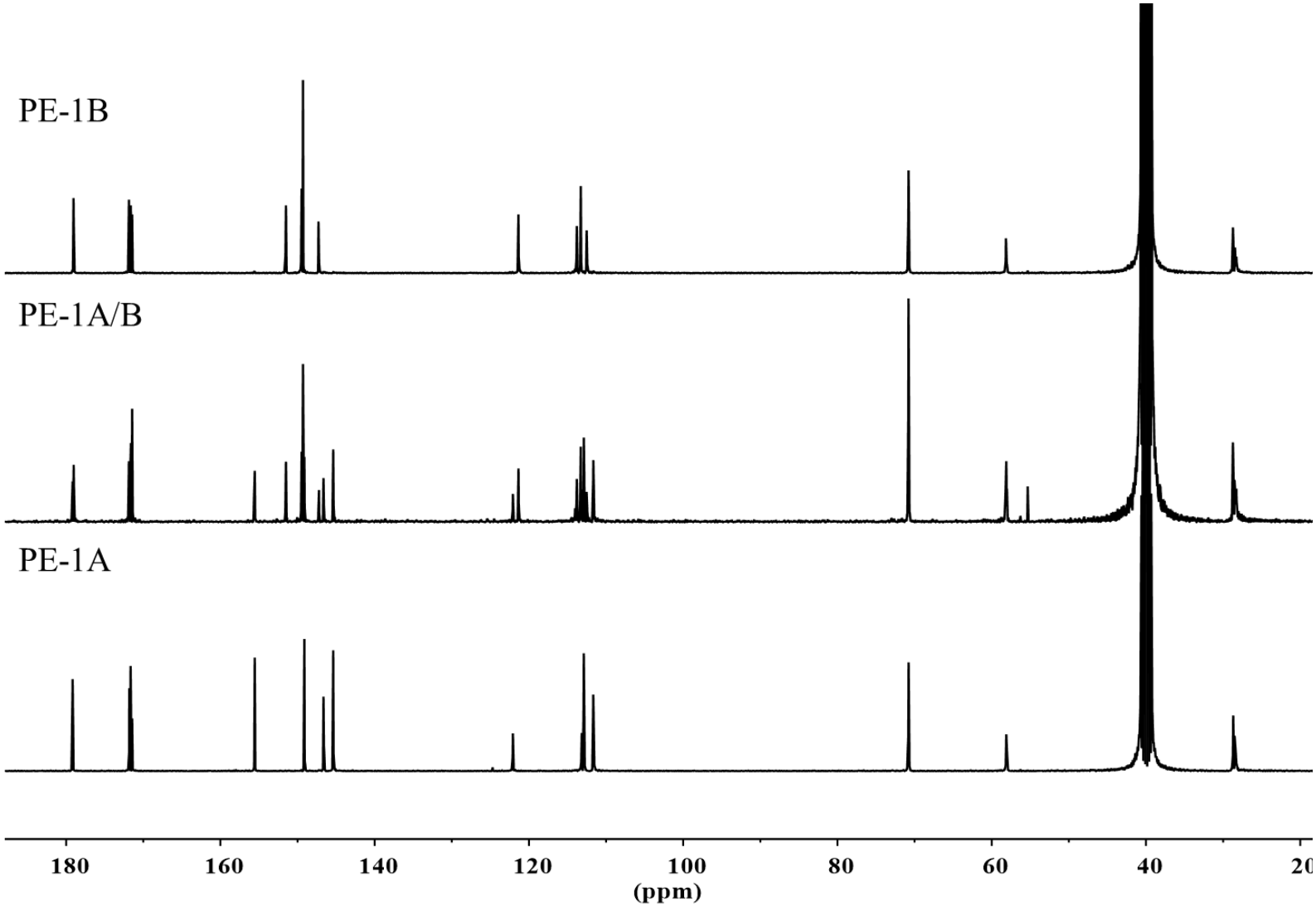

Figure S3.9. Stacked **PE-1** ^{13}C NMR series (DMSO-d_6) (Shows that the carbon signals for **PE-1A/B** match the polymer made from **A** and **B**)

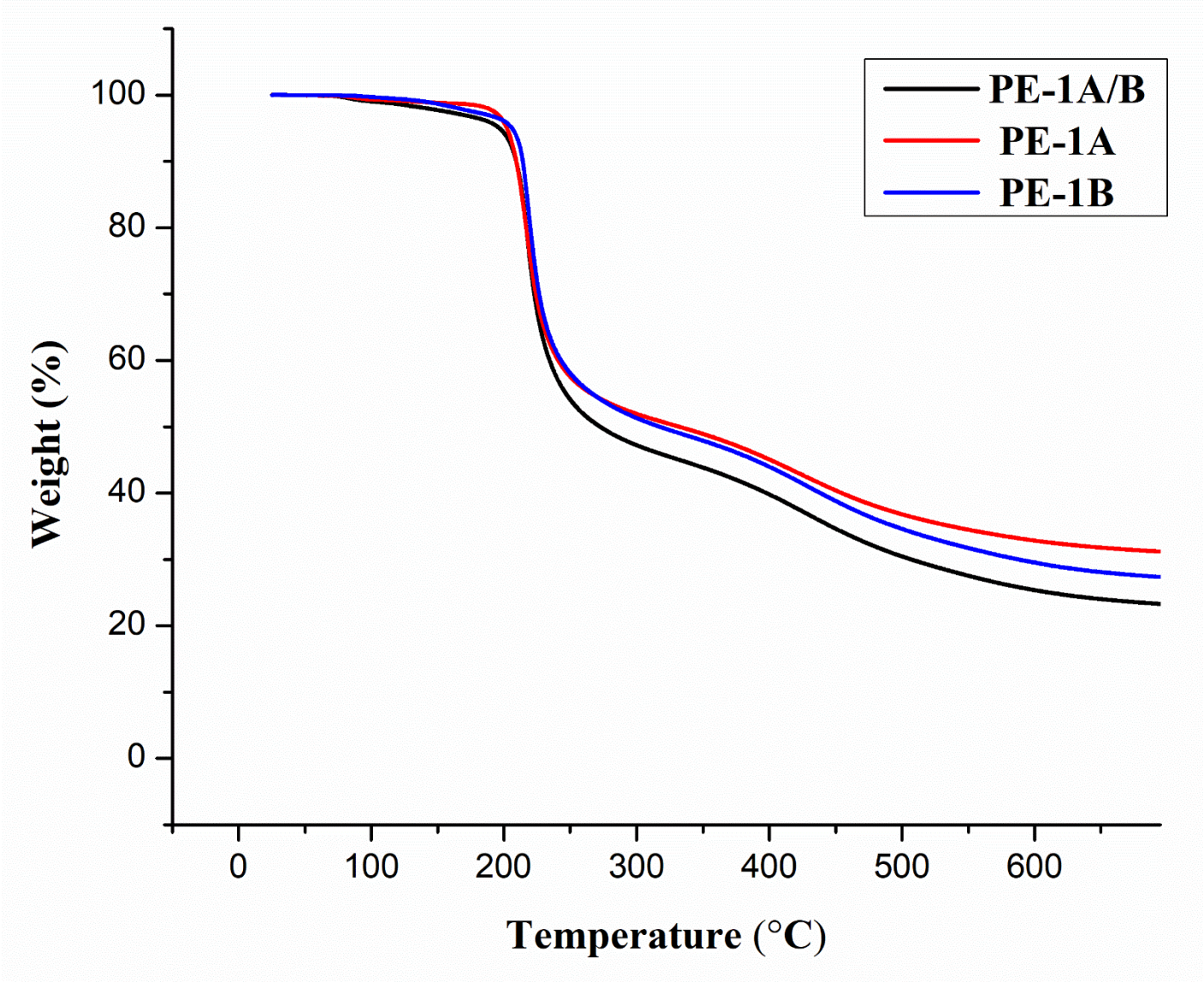

Figure S3.10. Overlay TGA **PE-1** series.

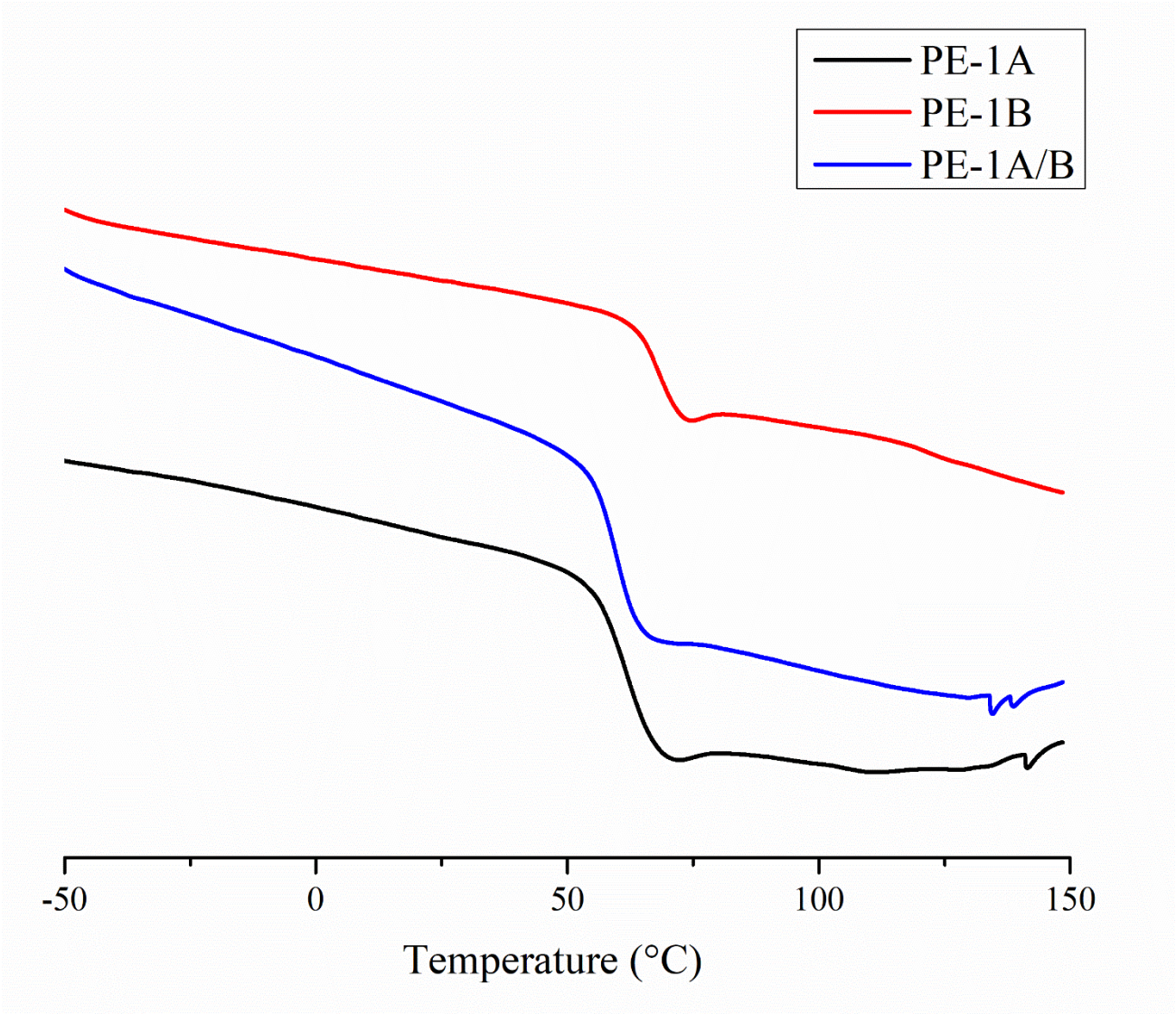

Figure S3.11. Overlay DSC **PE-1** series.

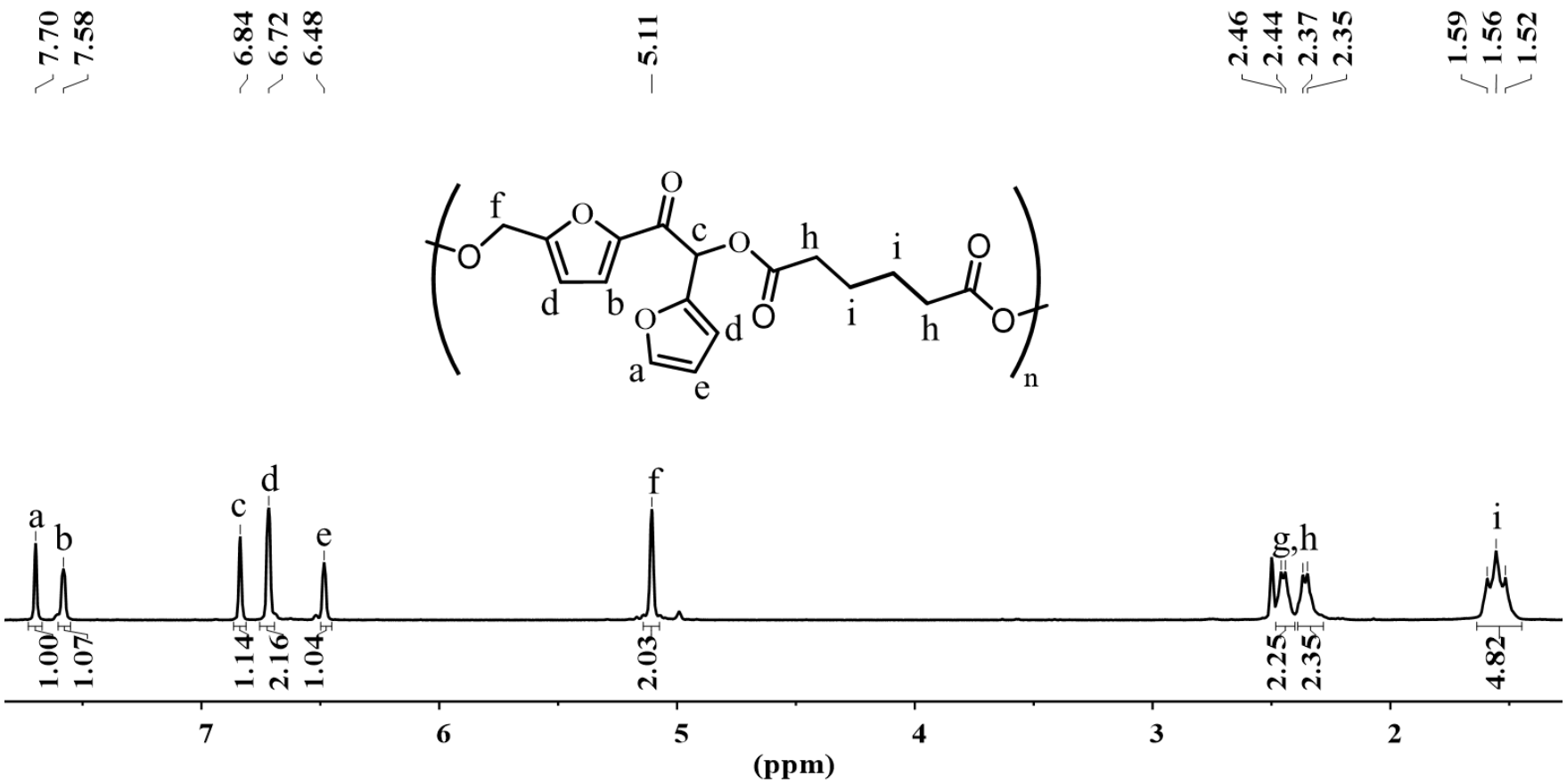

Figure S3.12. ^{1}H NMR (DMSO-d_6) of **PE-2A.**

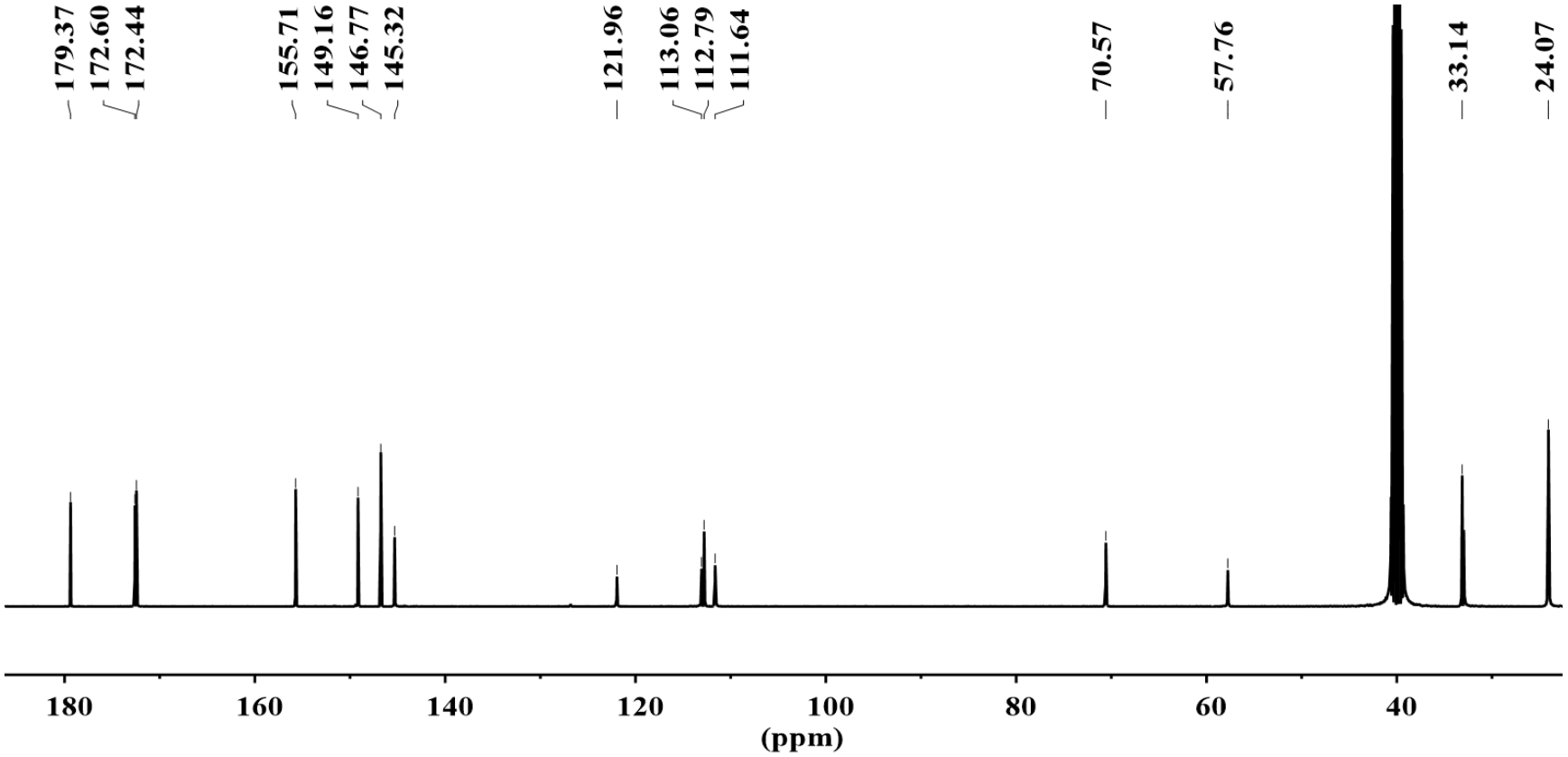

Figure S3.13. ^{13}C NMR (DMSO-d_6) of **PE-2A**.

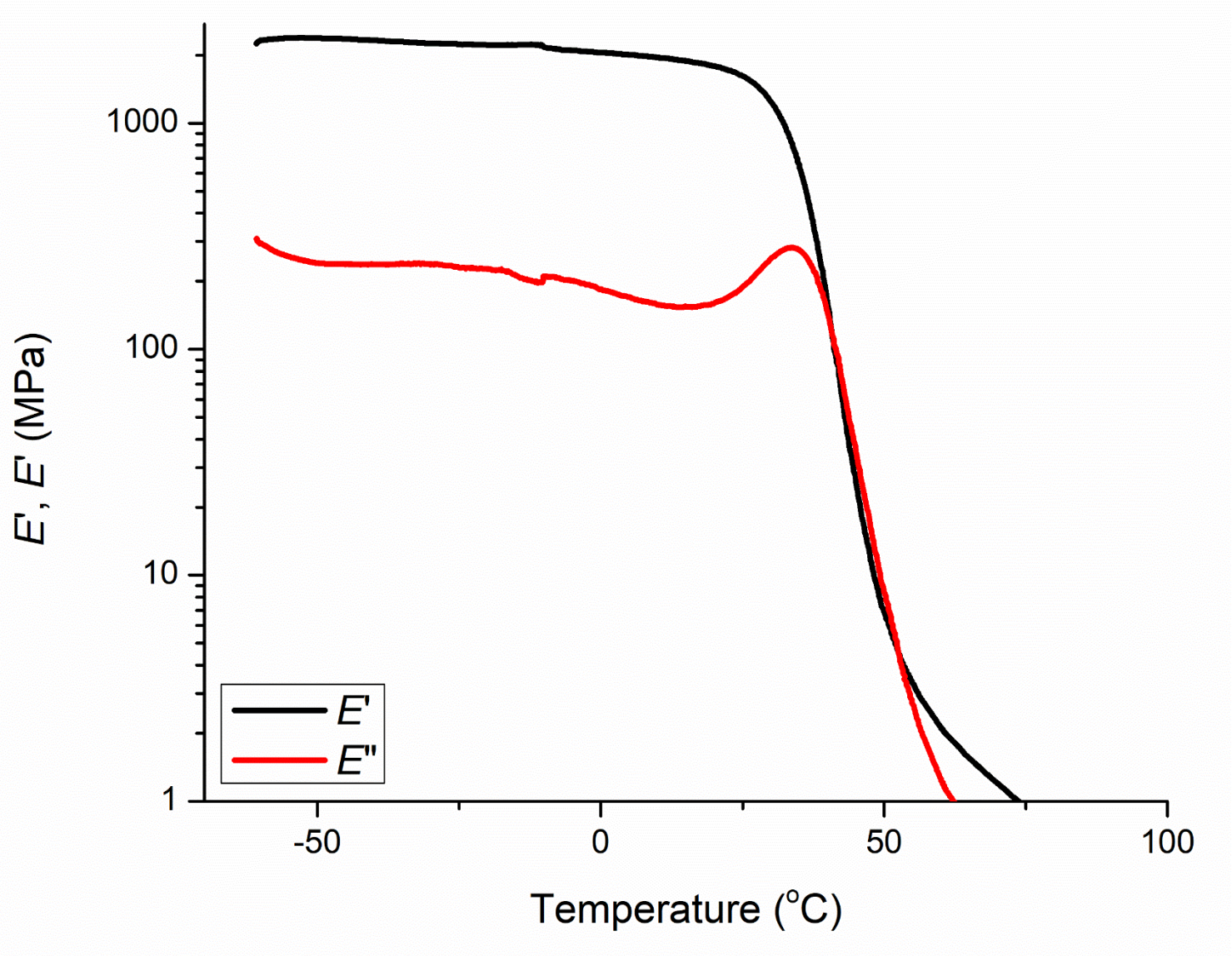

Figure S3.14. Overlay of storage modulus *E*' and loss modulus *E*" of **PE-2A**.

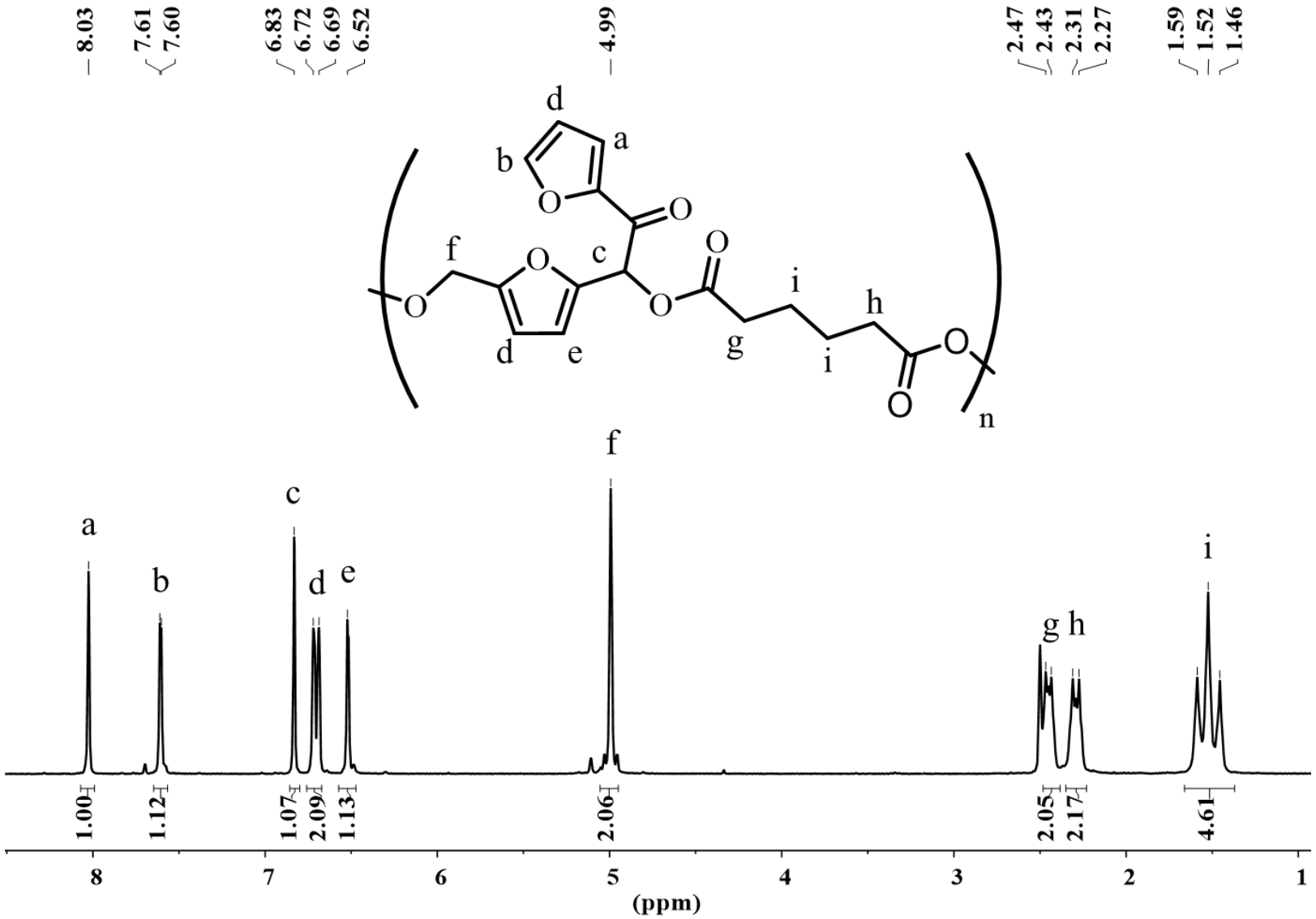

Figure S3.15. ^{1}H NMR (DMSO-d_6) of **PE-2B**.

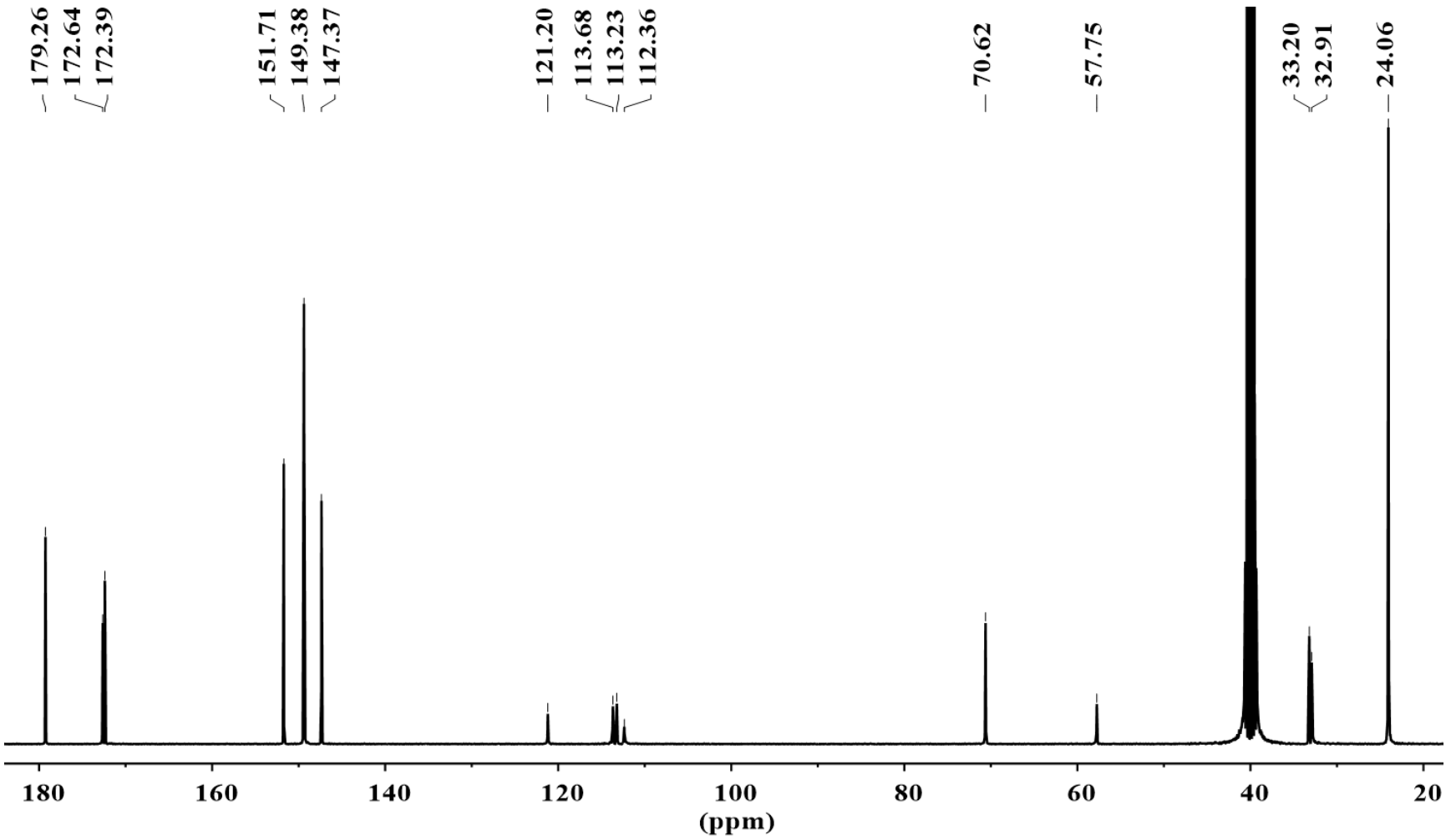

Figure S3.16. ^{13}C NMR (DMSO-d_6) of **PE-2B**.

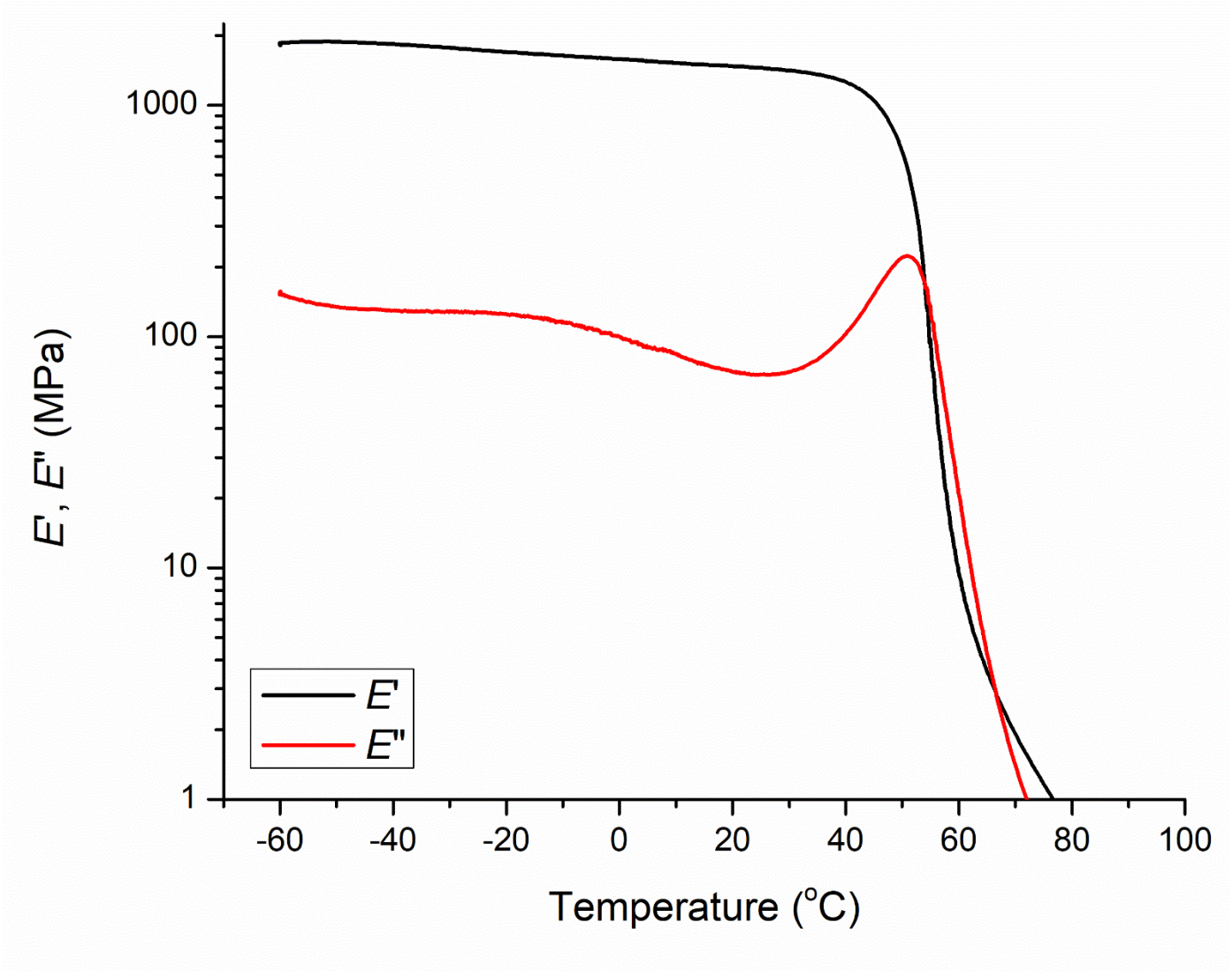

Figure S3.17. Overlay of storage modulus *E*’ and loss modulus *E*” of **PE-2B**.

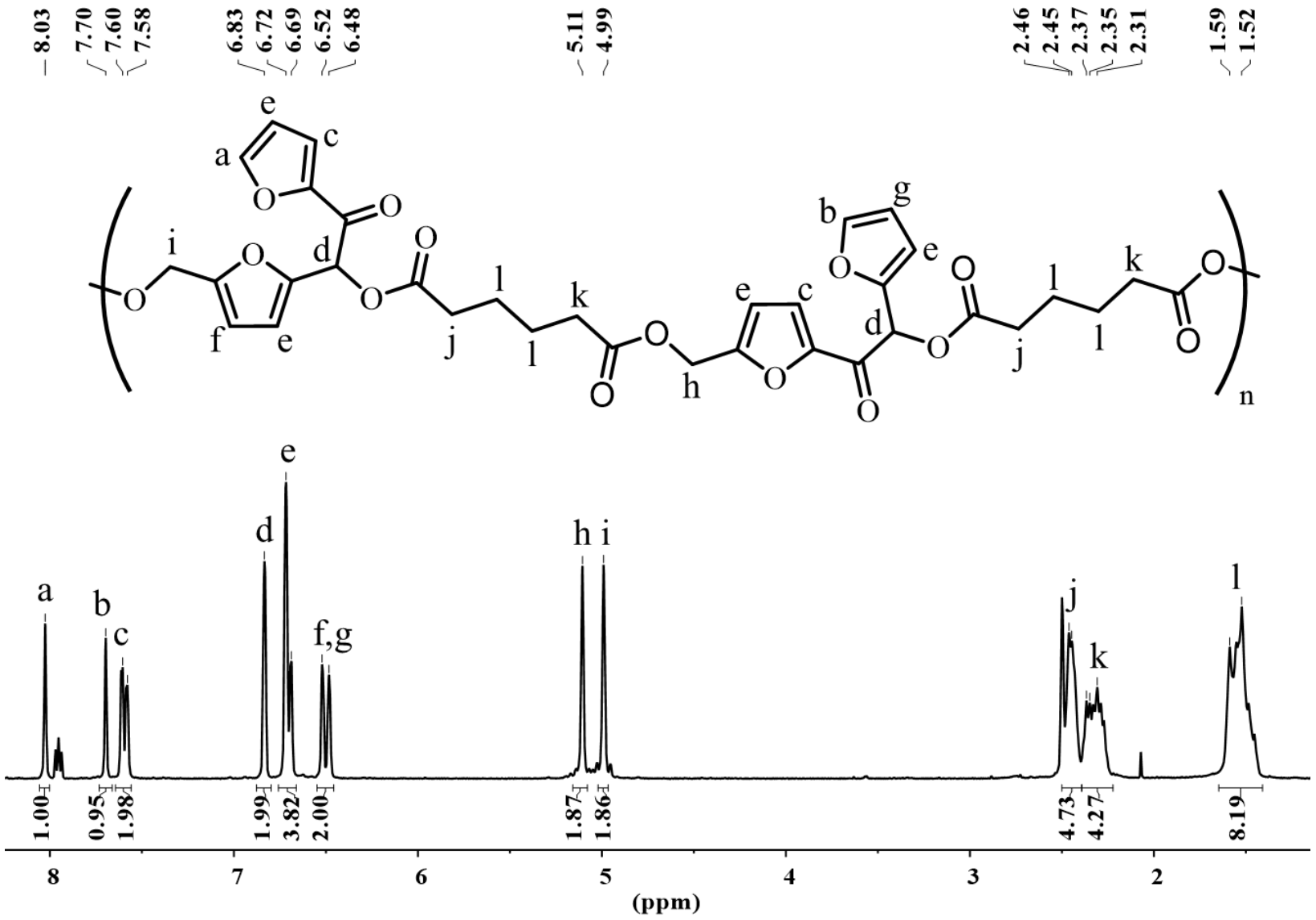

Figure S3.18. ^{1}H NMR (DMSO-d_6) of **PE-2A/B**.

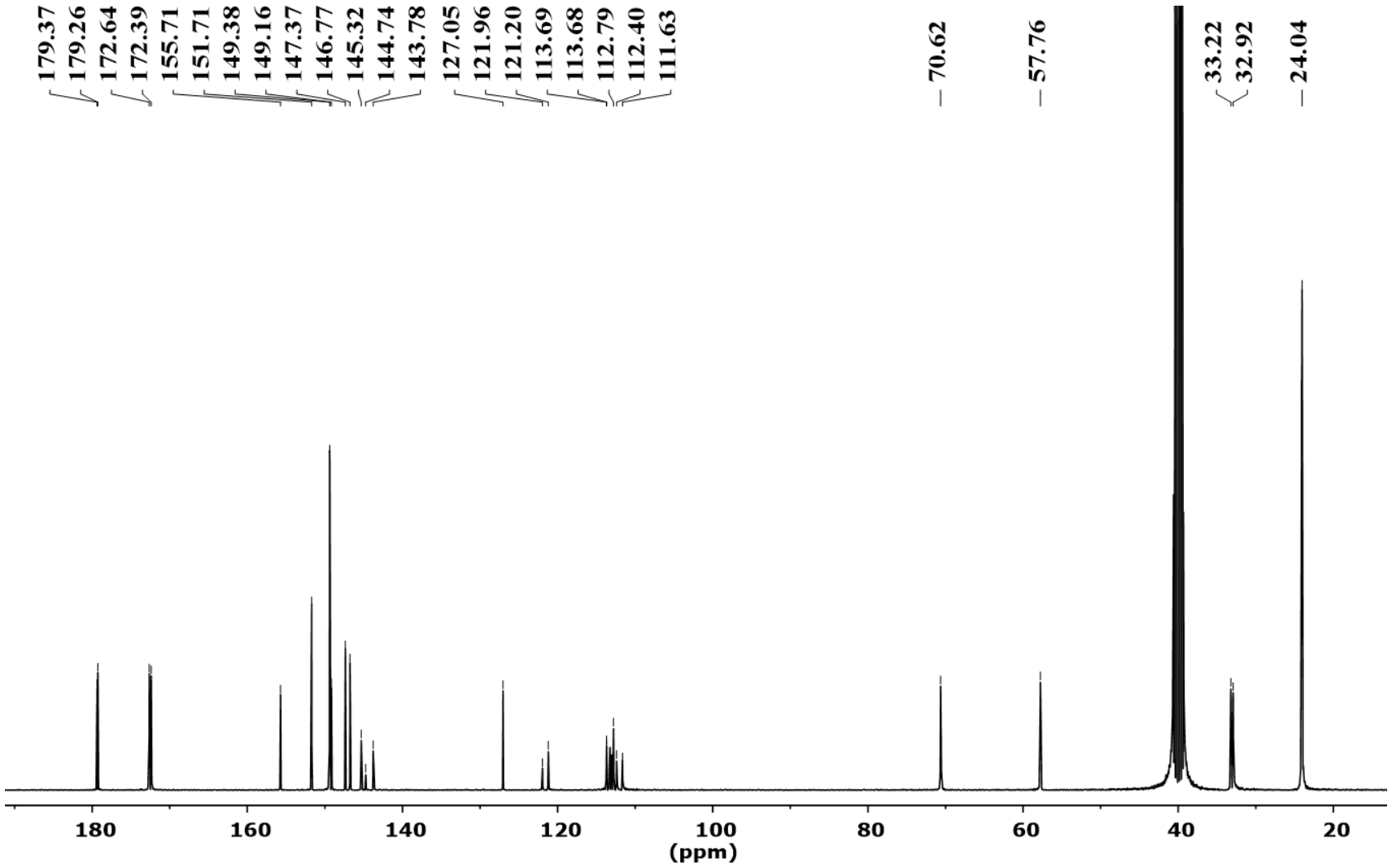

Figure S3.19. ^{13}C NMR (DMSO-d_6) of **PE-2A/B**.

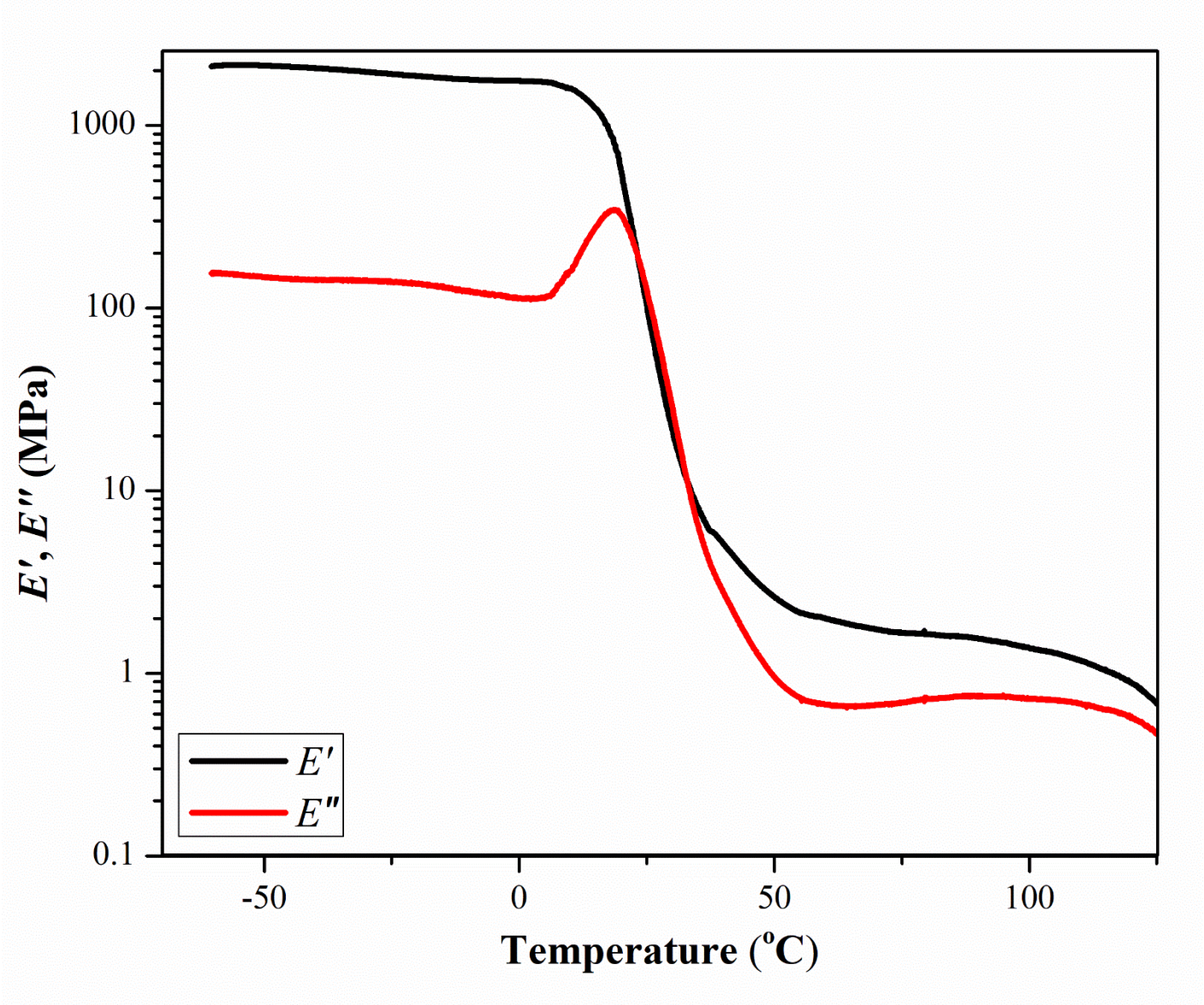

Figure S3.20. Overlay of storage modulus *E*' and loss modulus *E*" of **PE-3A/B**.

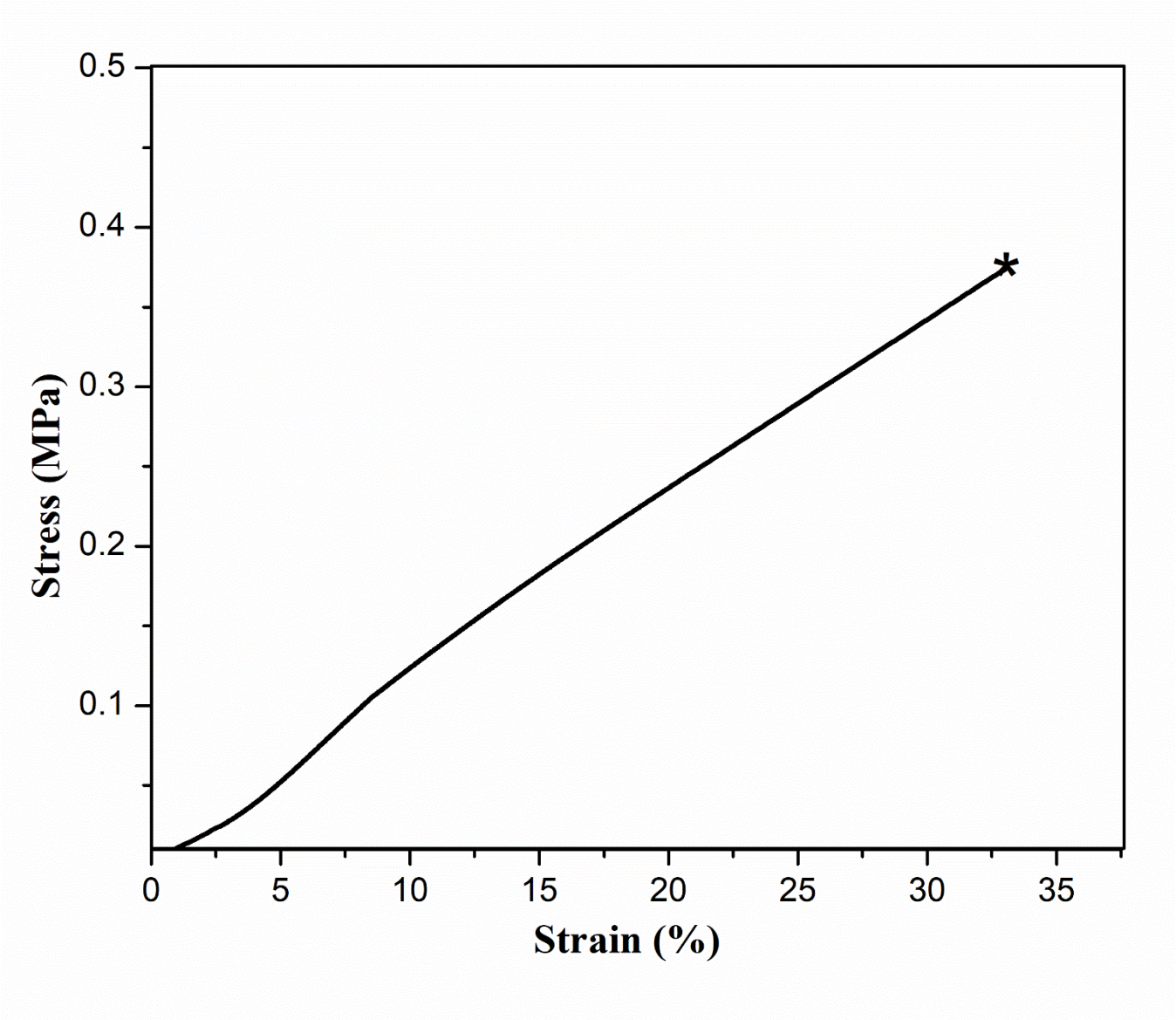

Figure S3.21. ^{1}H NMR (DMSO-d_6) of **PE-3A/B**.

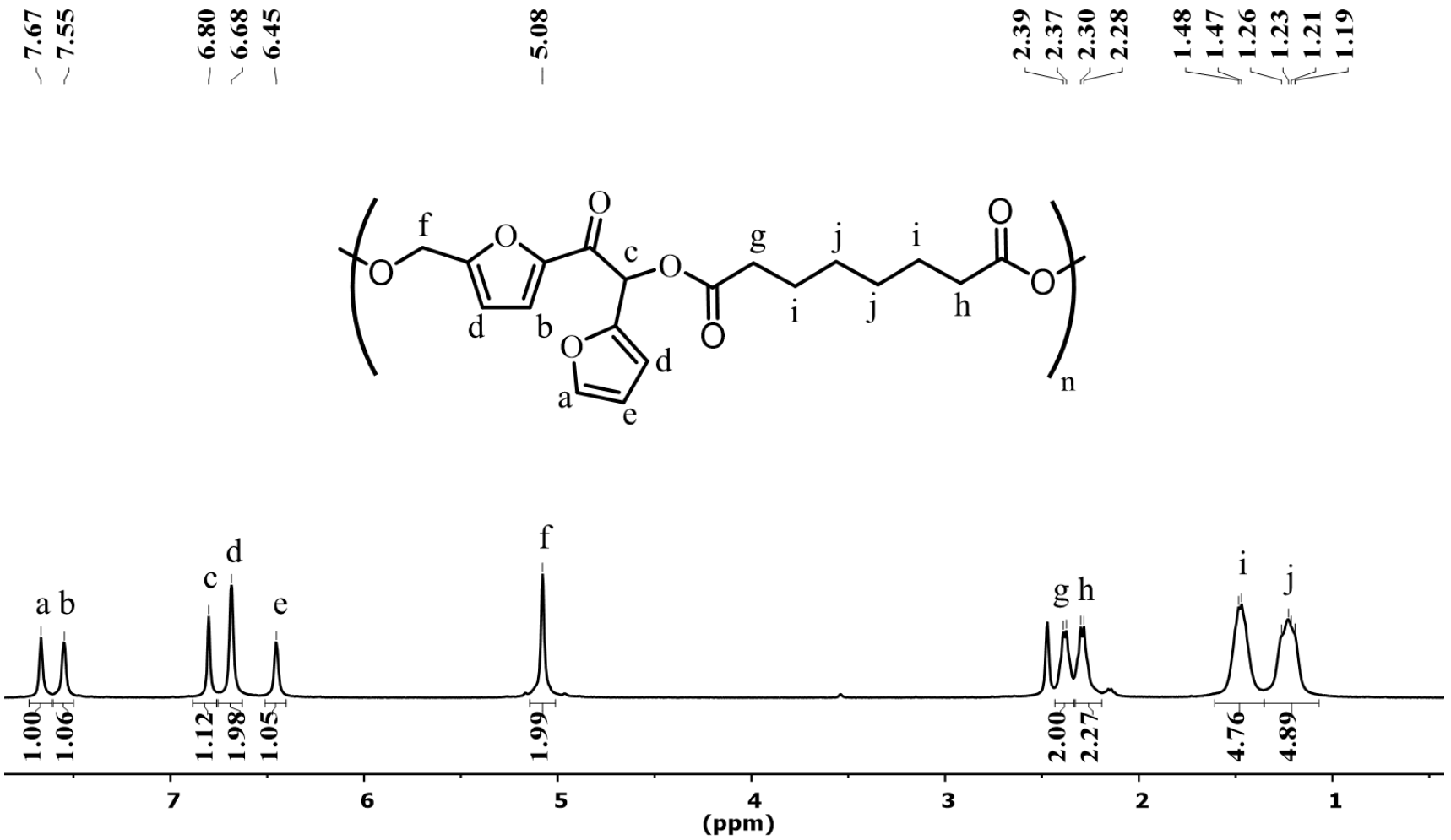

Figure S3.22. ^{1}H NMR (DMSO-d_6) of **PE-3A**.

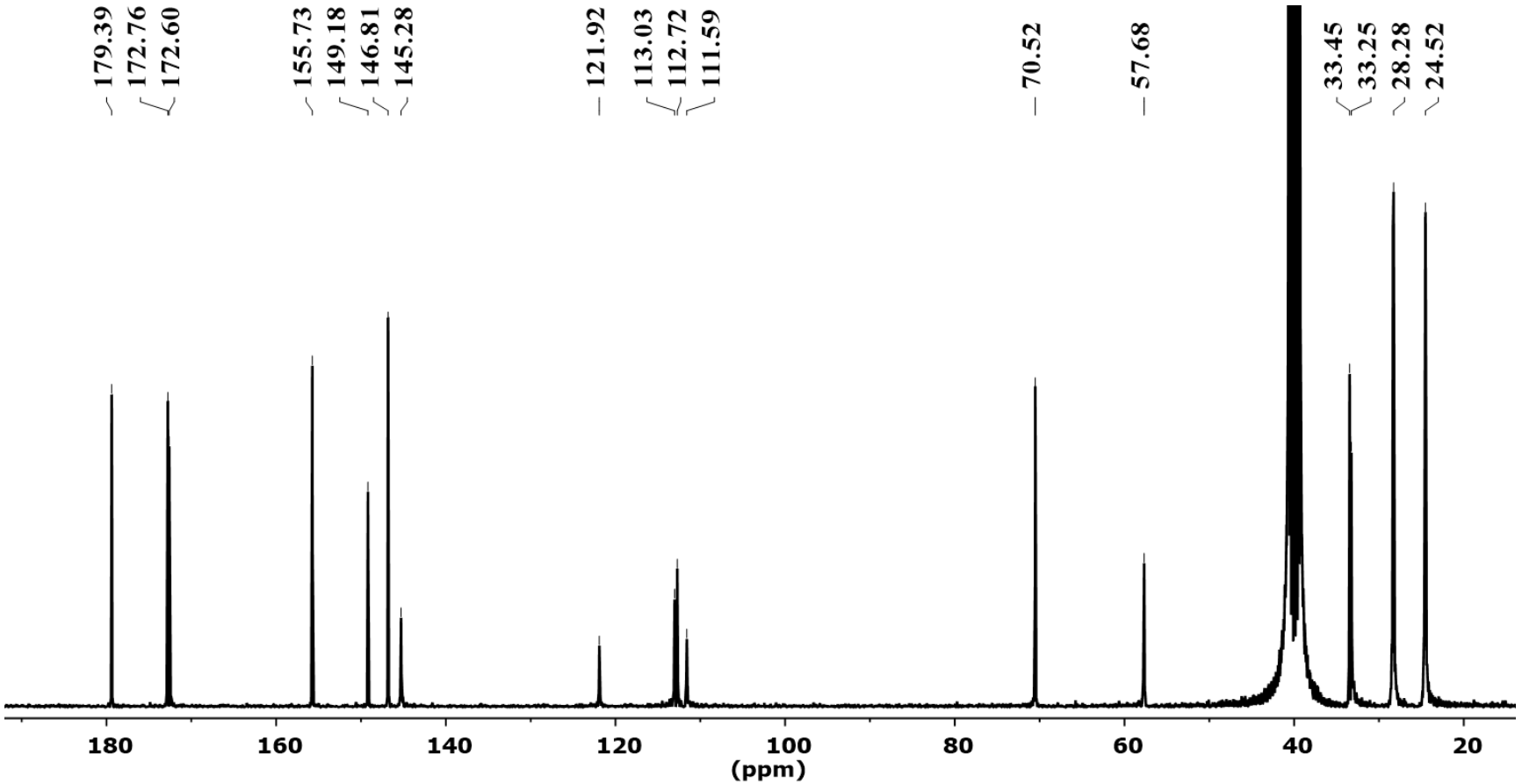

Figure S3.23. ^{13}C NMR (DMSO-d_6) of **PE-3A**.

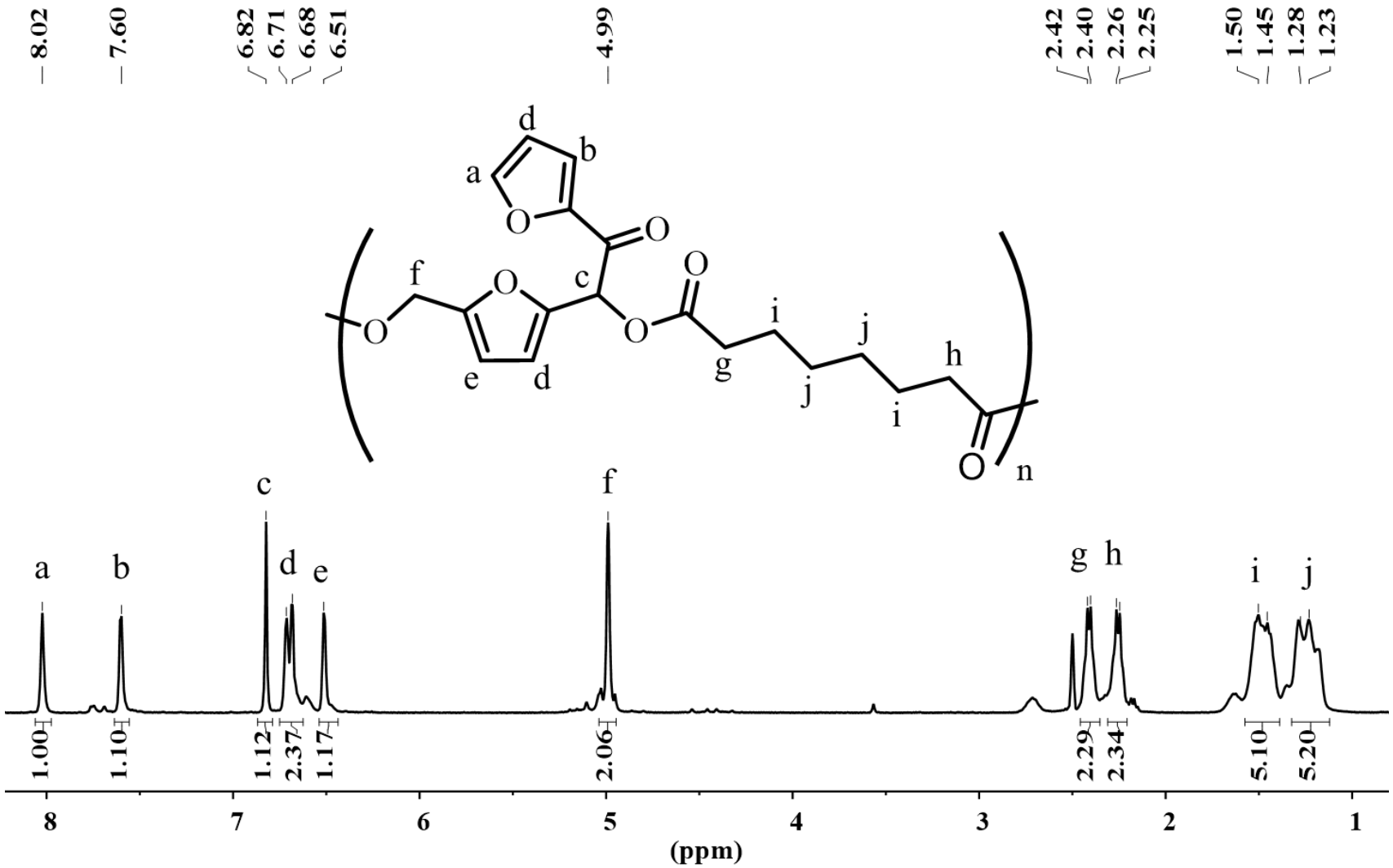

Figure S3.24. ^{1}H NMR (DMSO-d_6) of **PE-3B**.

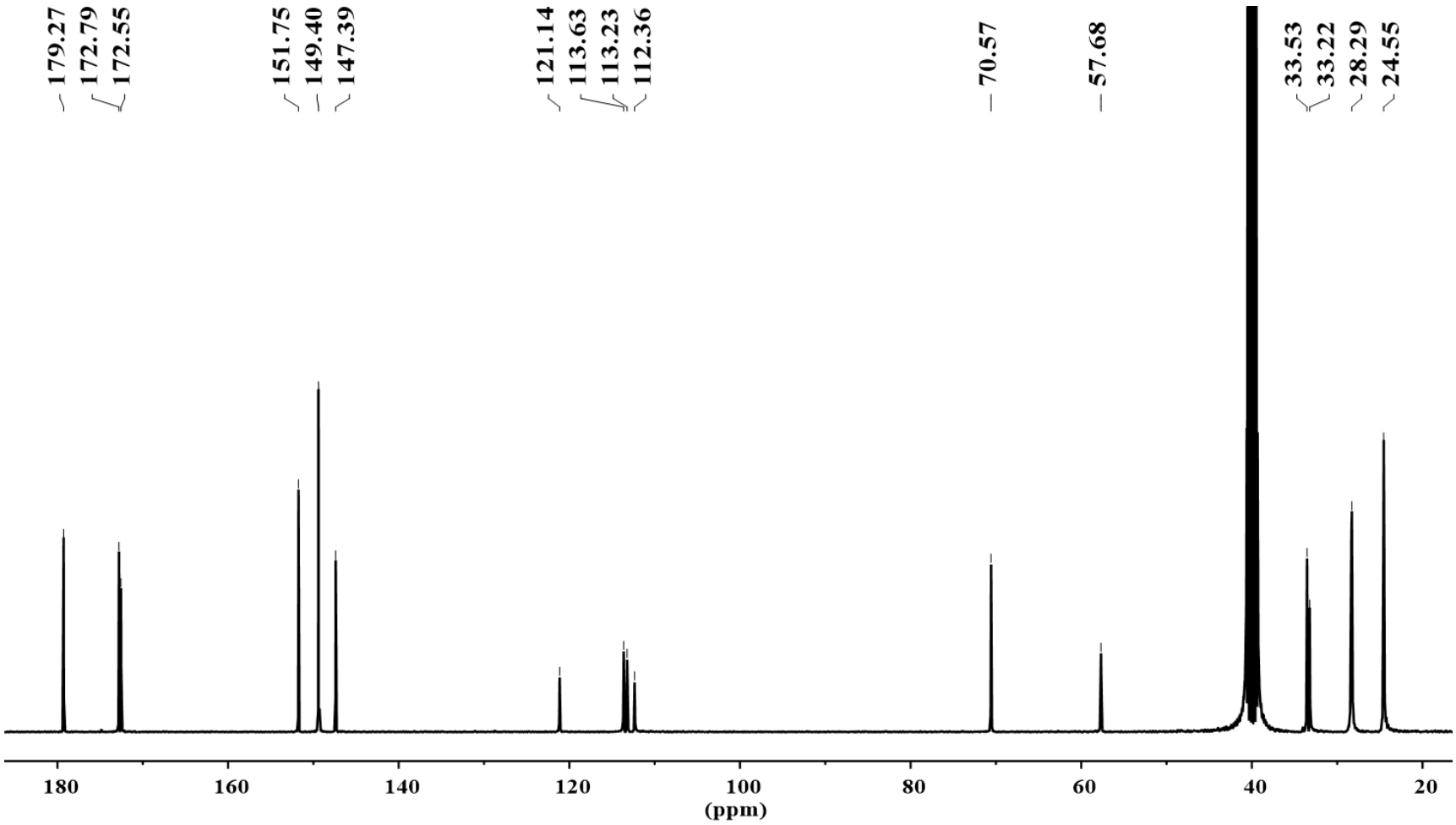

Figure S3.25. ^{13}C NMR (DMSO-d_6) of **PE-3A/B**.

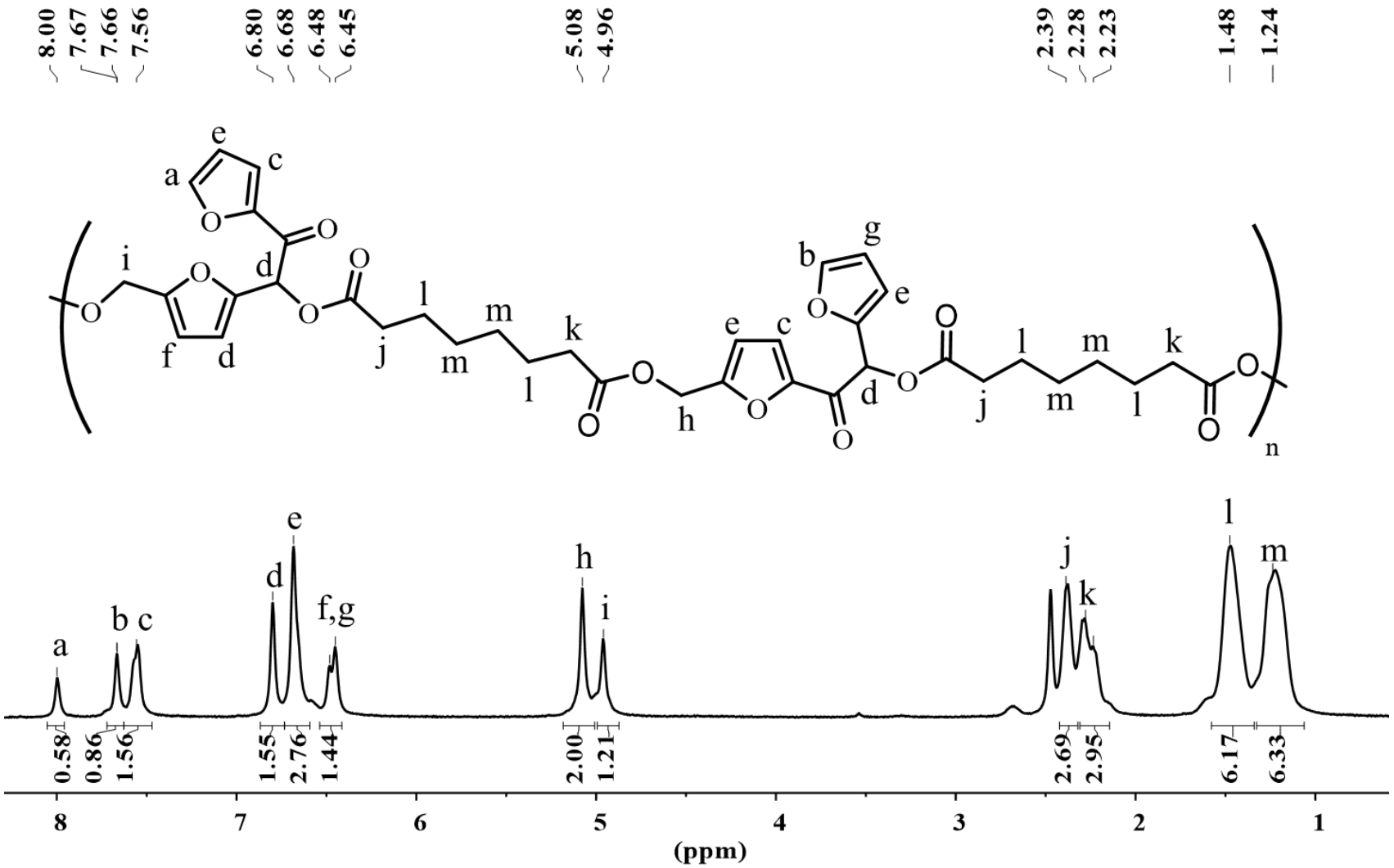

Figure S3.26. ^{1}H NMR (DMSO-d_6) of **PE-3A/B**.

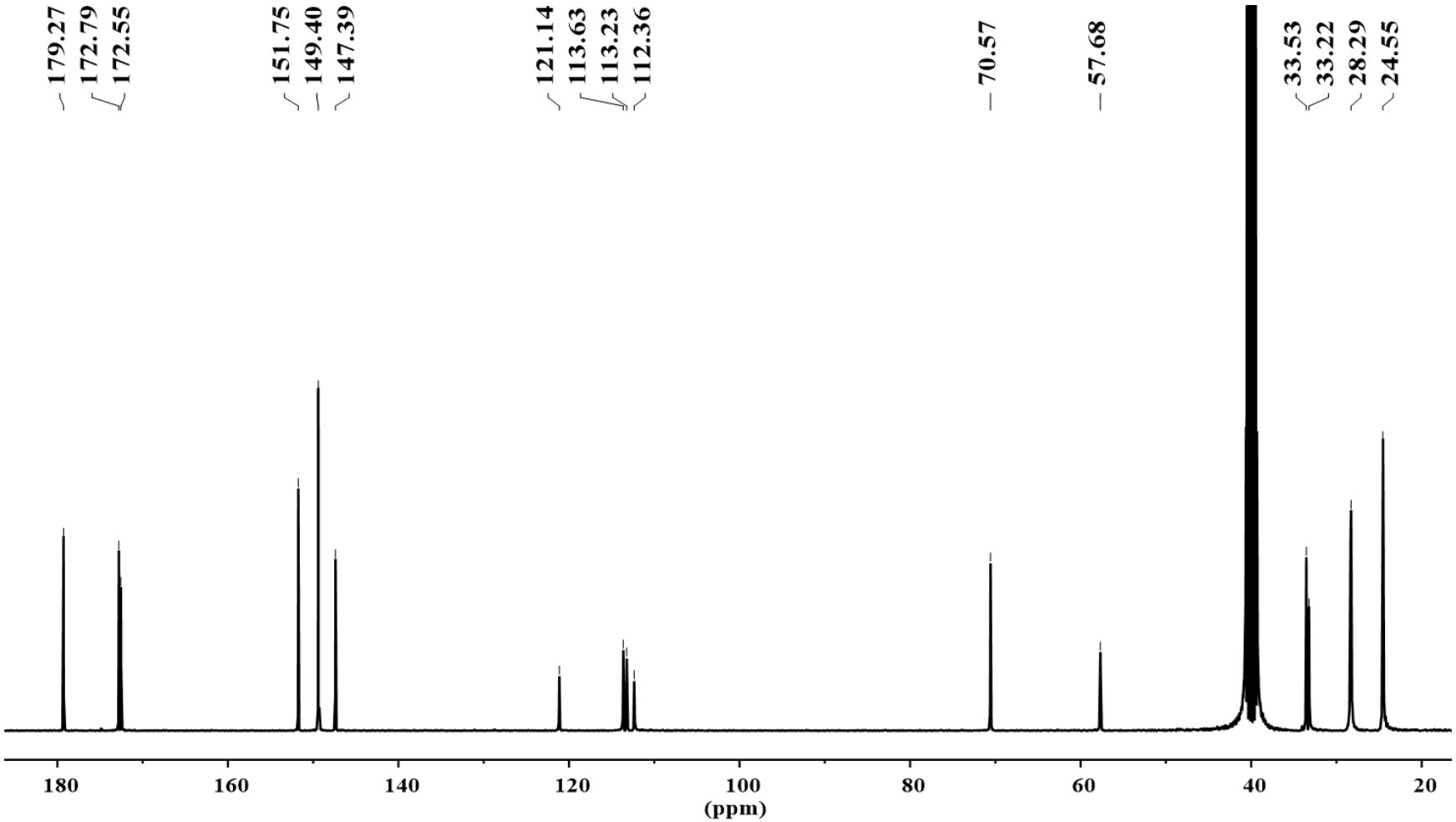

Figure S3.27. ^{13}C NMR (DMSO-d_6) of **PE-3A/B**.

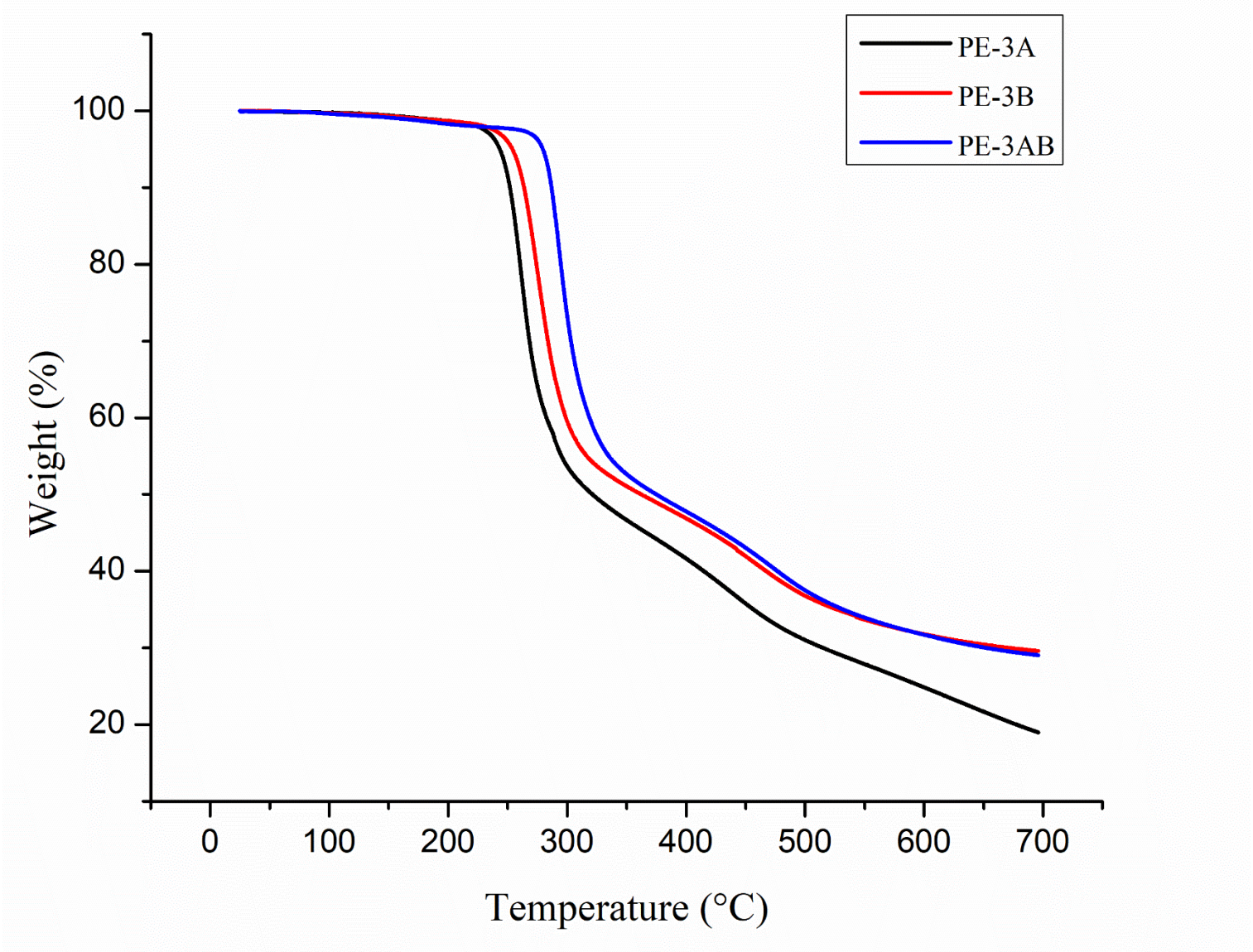

Figure S3.28. Overlay of **PE-3** TGA series.

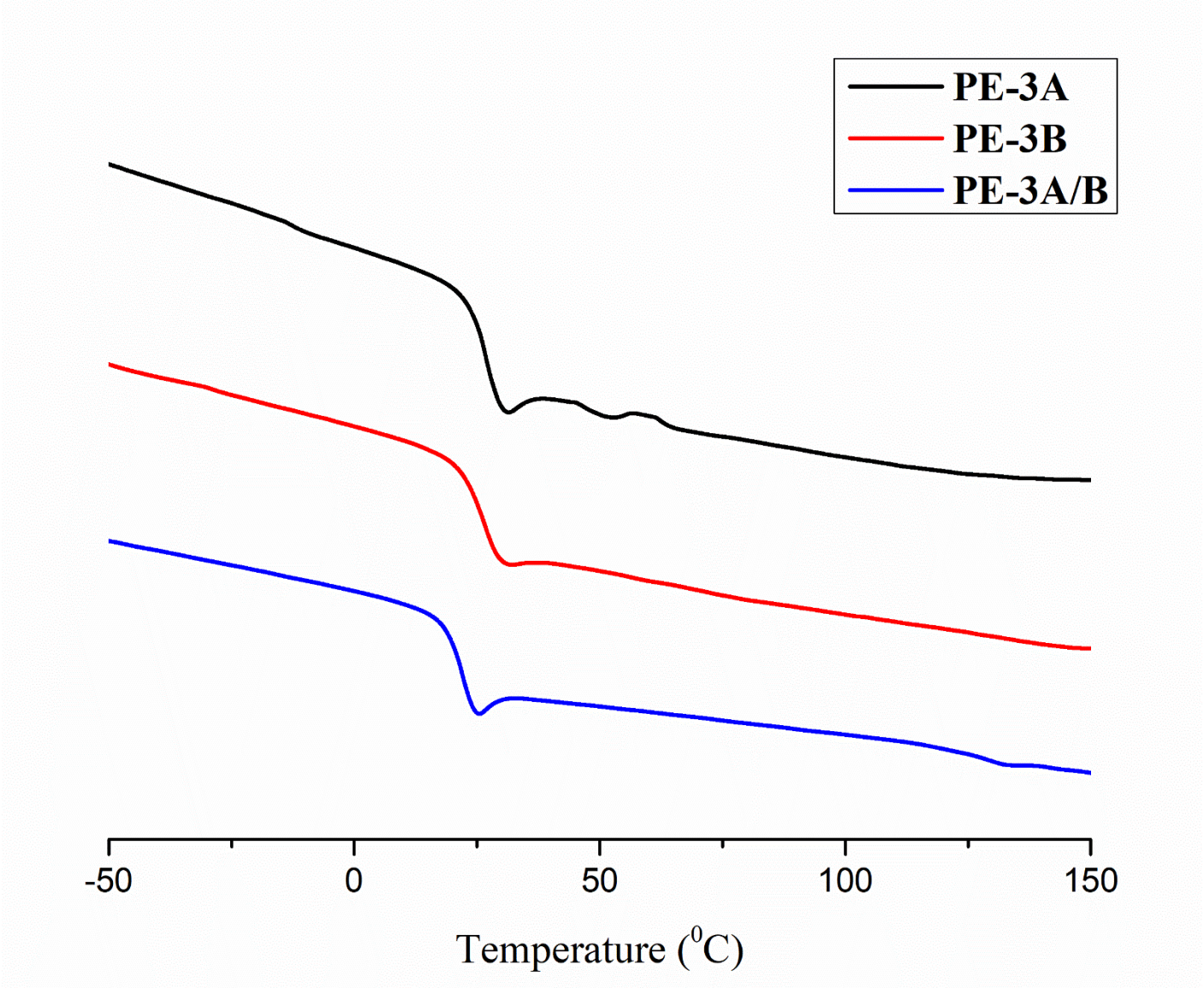

Figure S3.29. Overlay of **PE-3** DSC series.

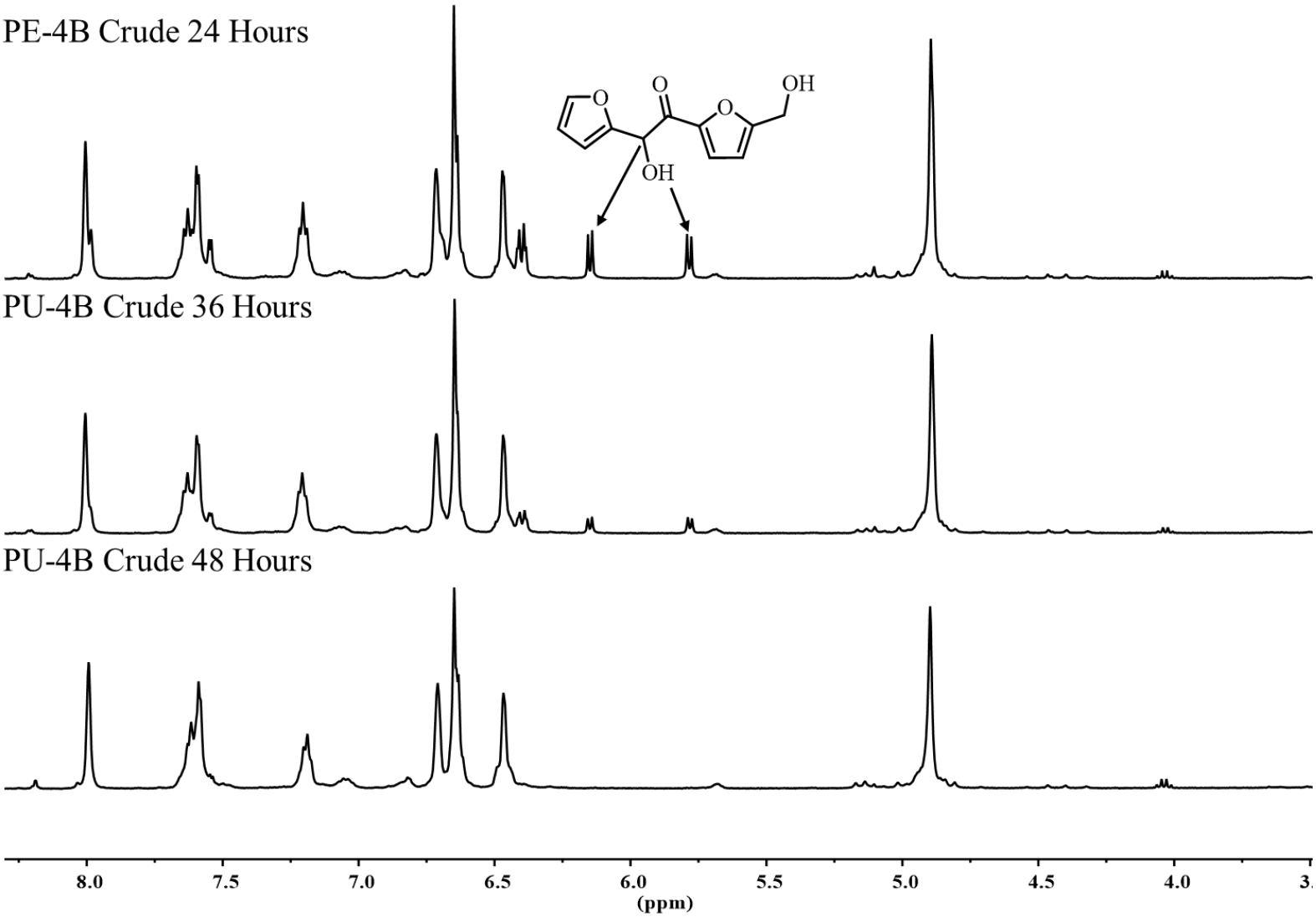

Figure S3.30. Stacked ^{1}H NMR (DMSO-d_6) of crude **PU-4B** reaction monitoring at 254 h, 36h, and 48 f showing conversion of alcohols.

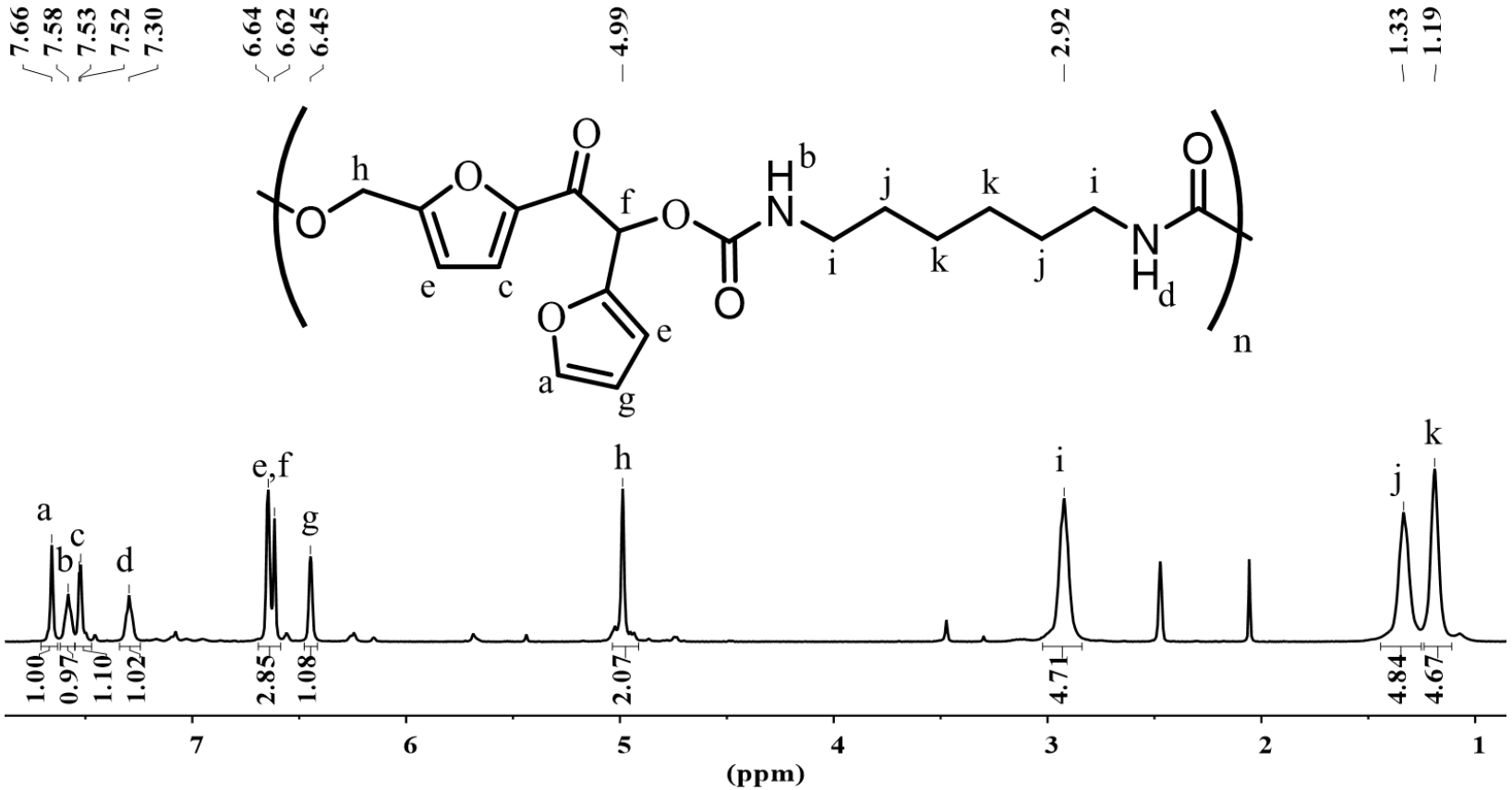

Figure S3.31. gCOSY (DMSO-d_6) of **PU-4A** (further supports proton assignment)

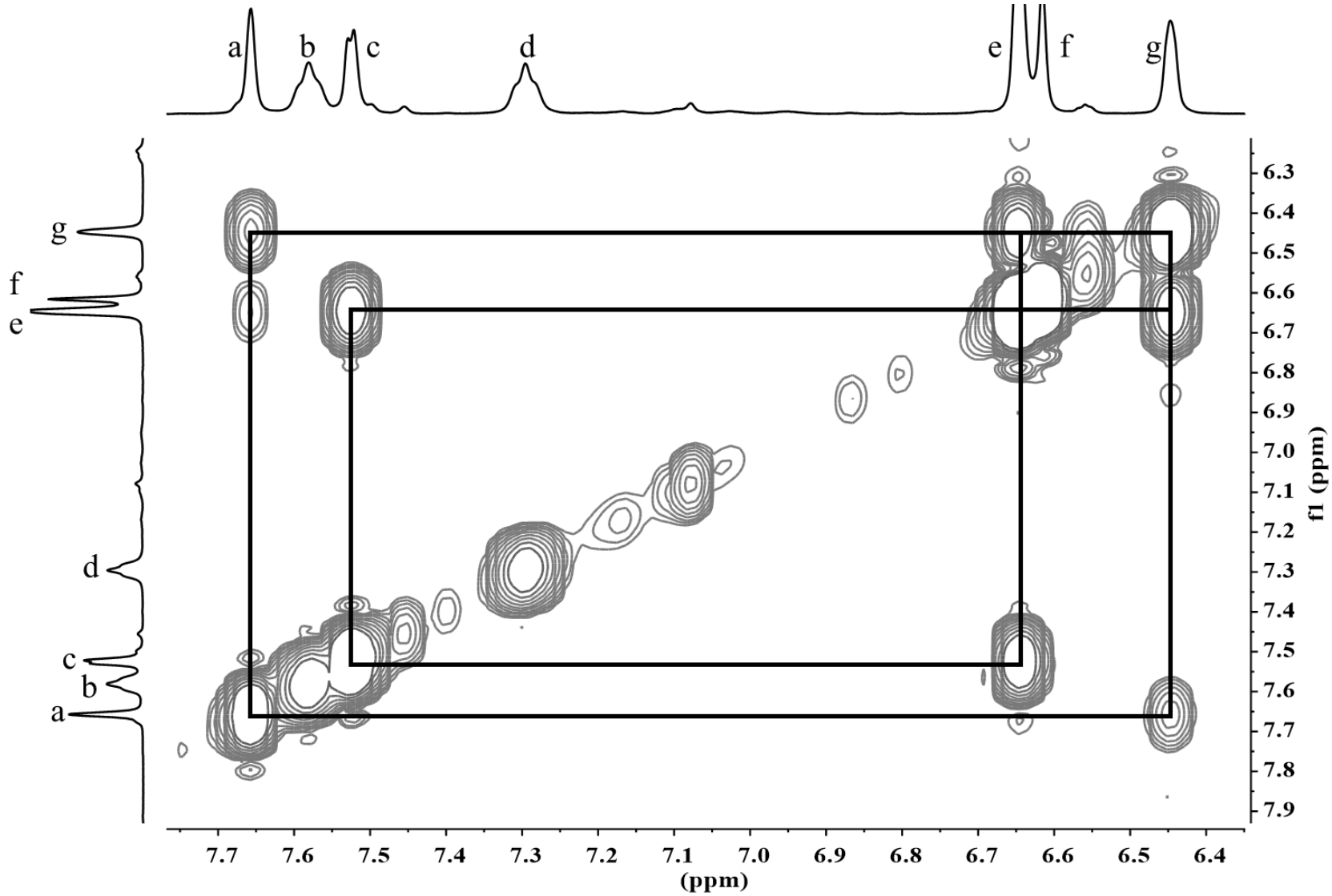

Figure S3.32. gCOSY (DMSO-d_6) of **PU-4A** (further supports proton assignment)

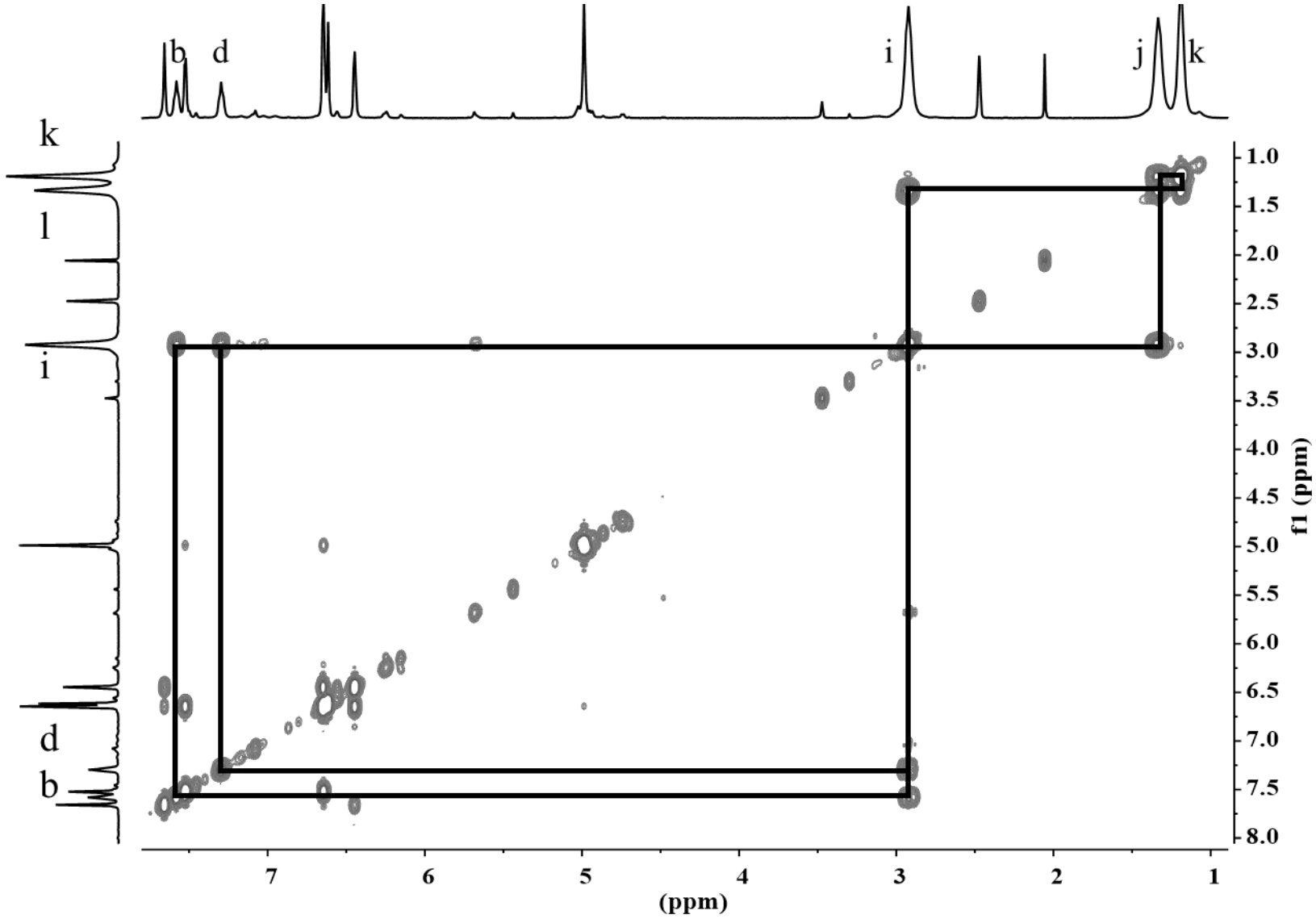

Figure S3.33. gCOSY (DMSO-d_6) of **PU-4A**.

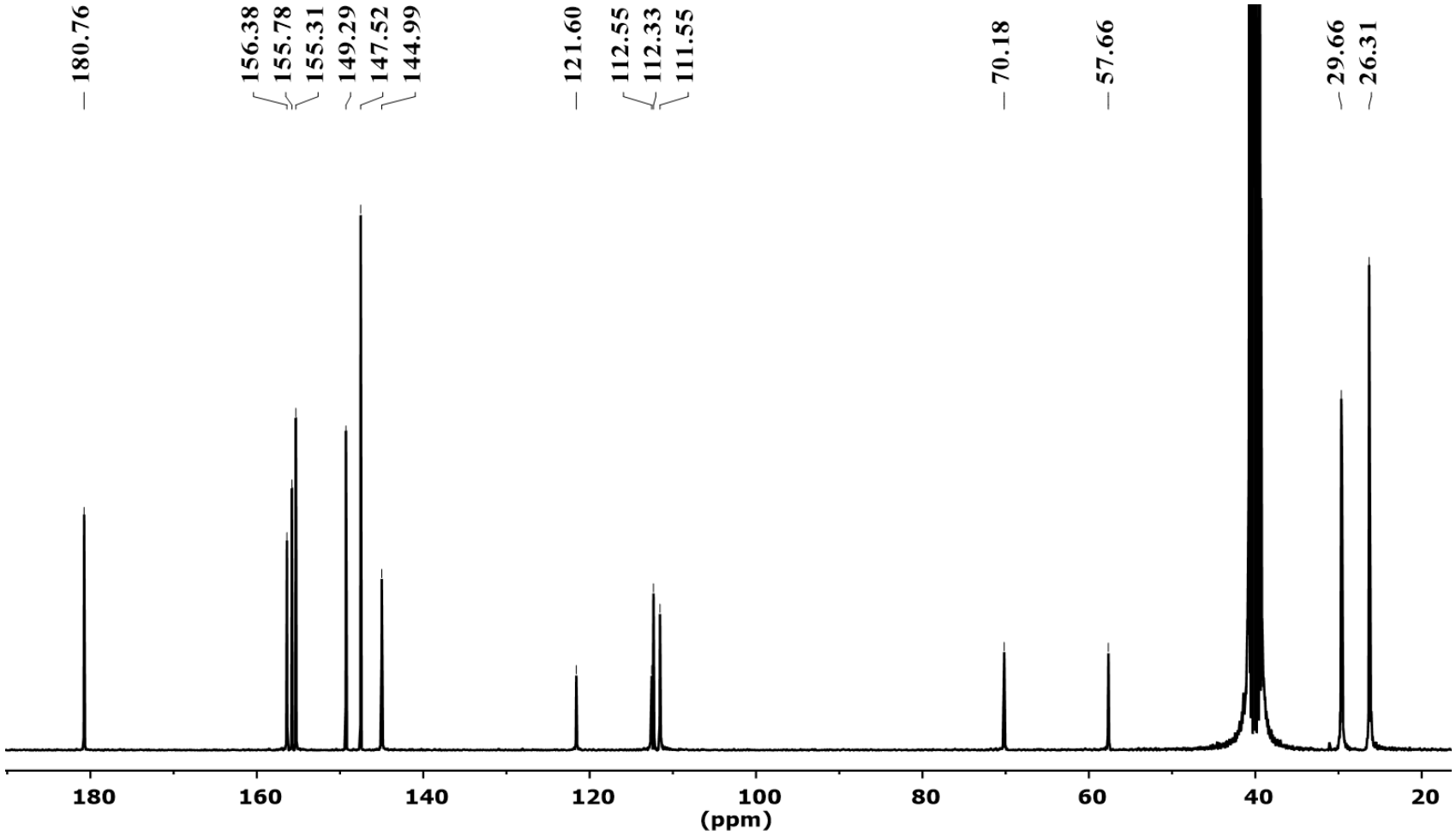

Figure S3.34. ^{13}C NMR (DMSO-d_6) of **PU-4A**.

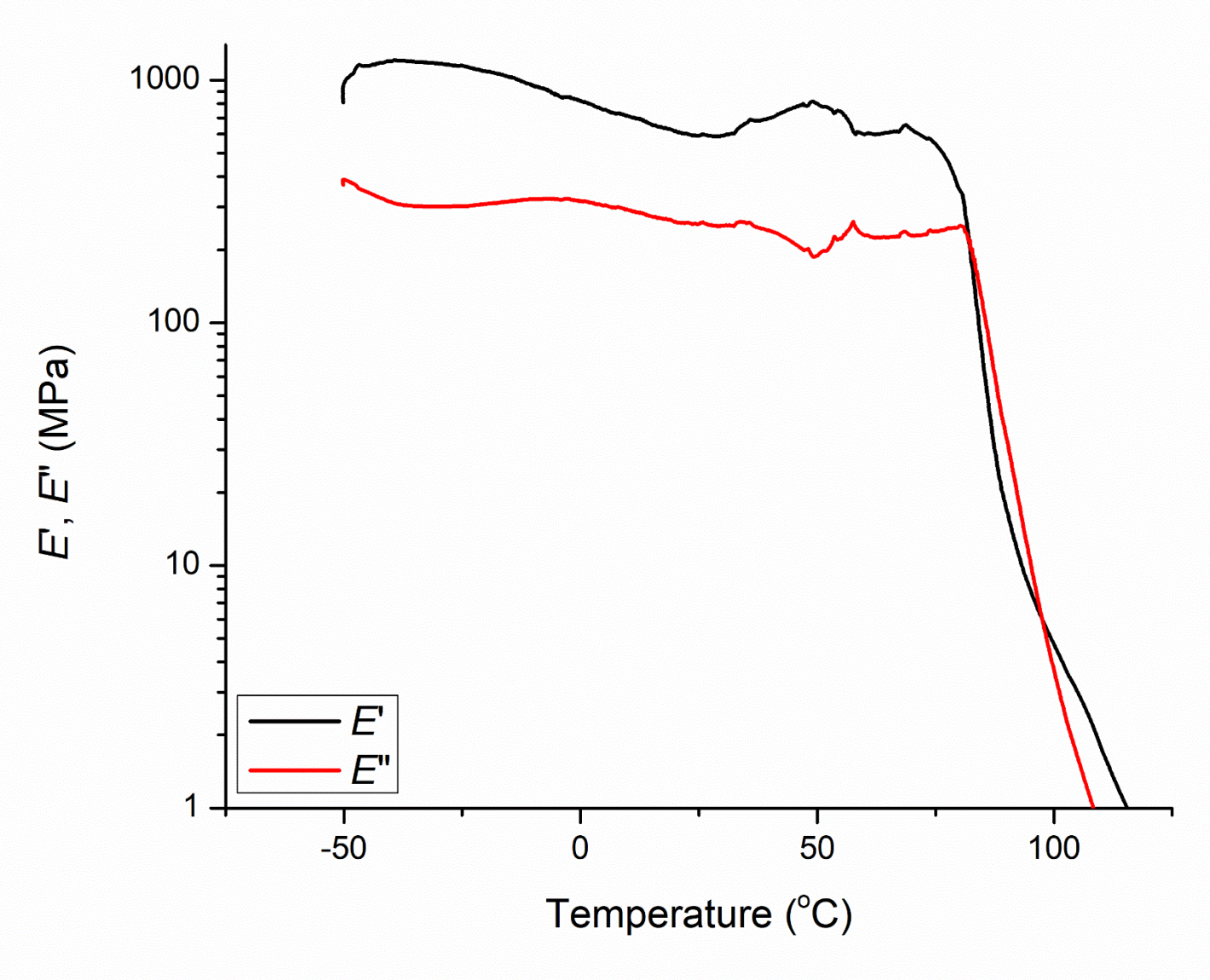

Figure S3.35. Overlay of storage modulus *E*’ and loss modulus *E*” for **PU-4A**.

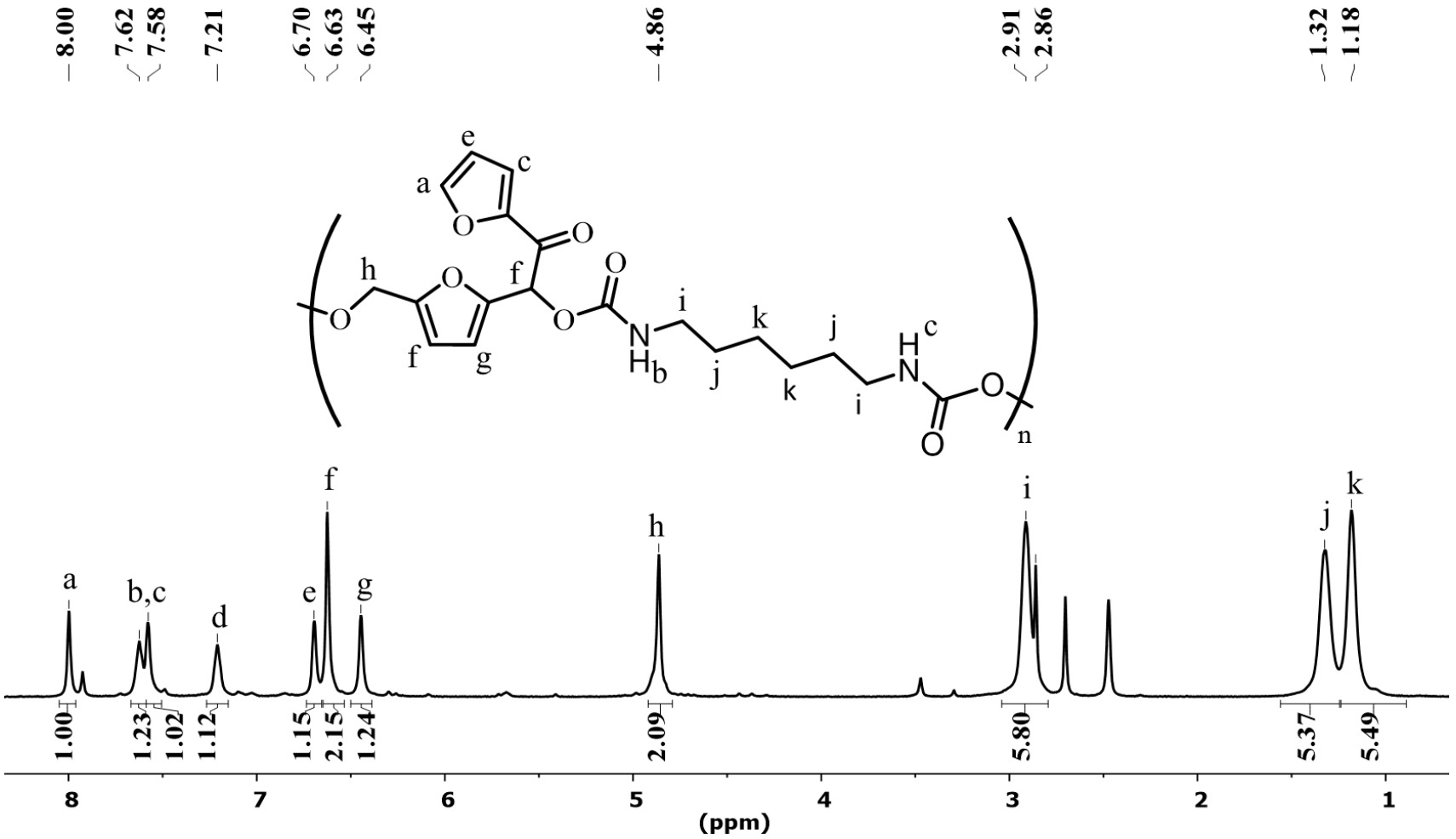

Figure S3.36. ^{1}H NMR (DMSO-d_6) of **PU-4B**.

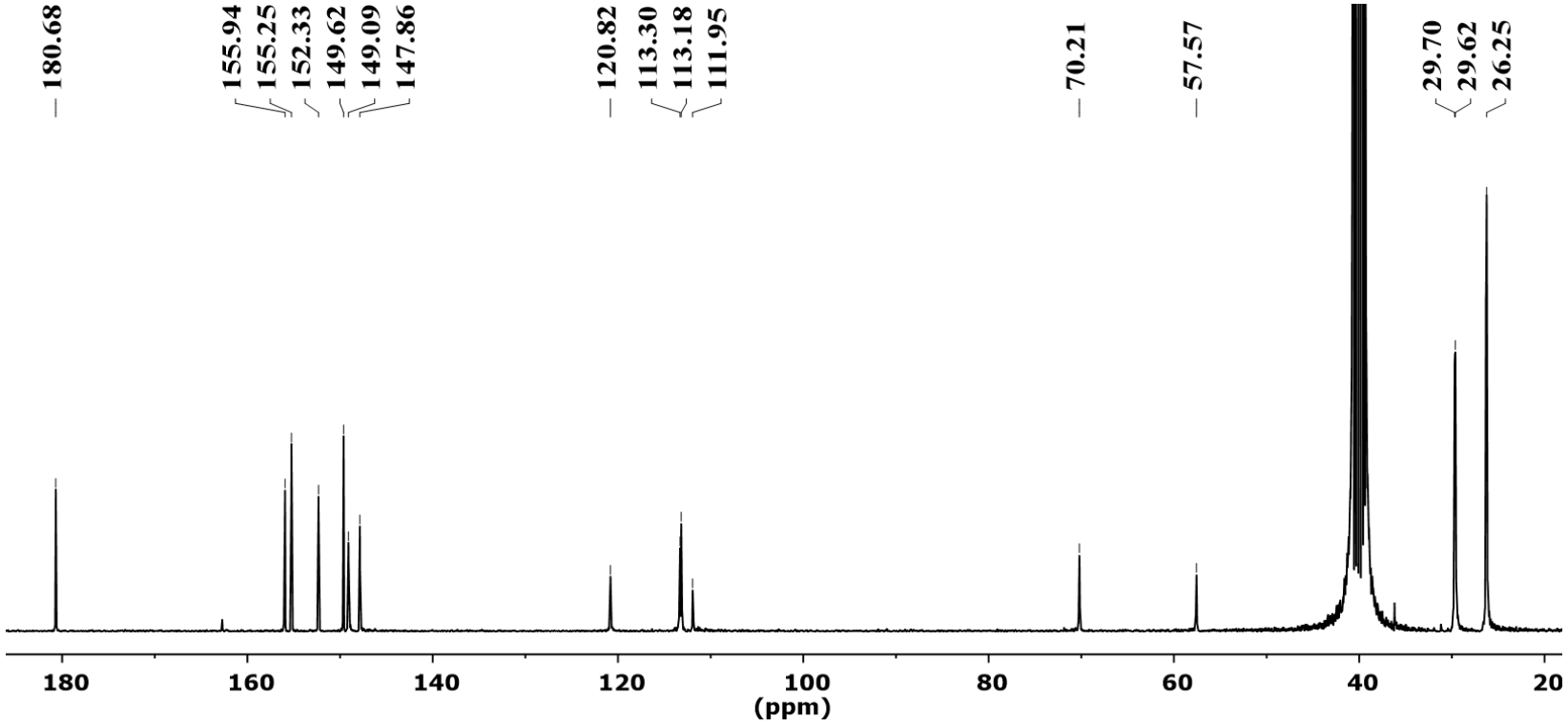

Figure S3.37. ^{13}C NMR (DMSO-d_6) of **PU-4B**.

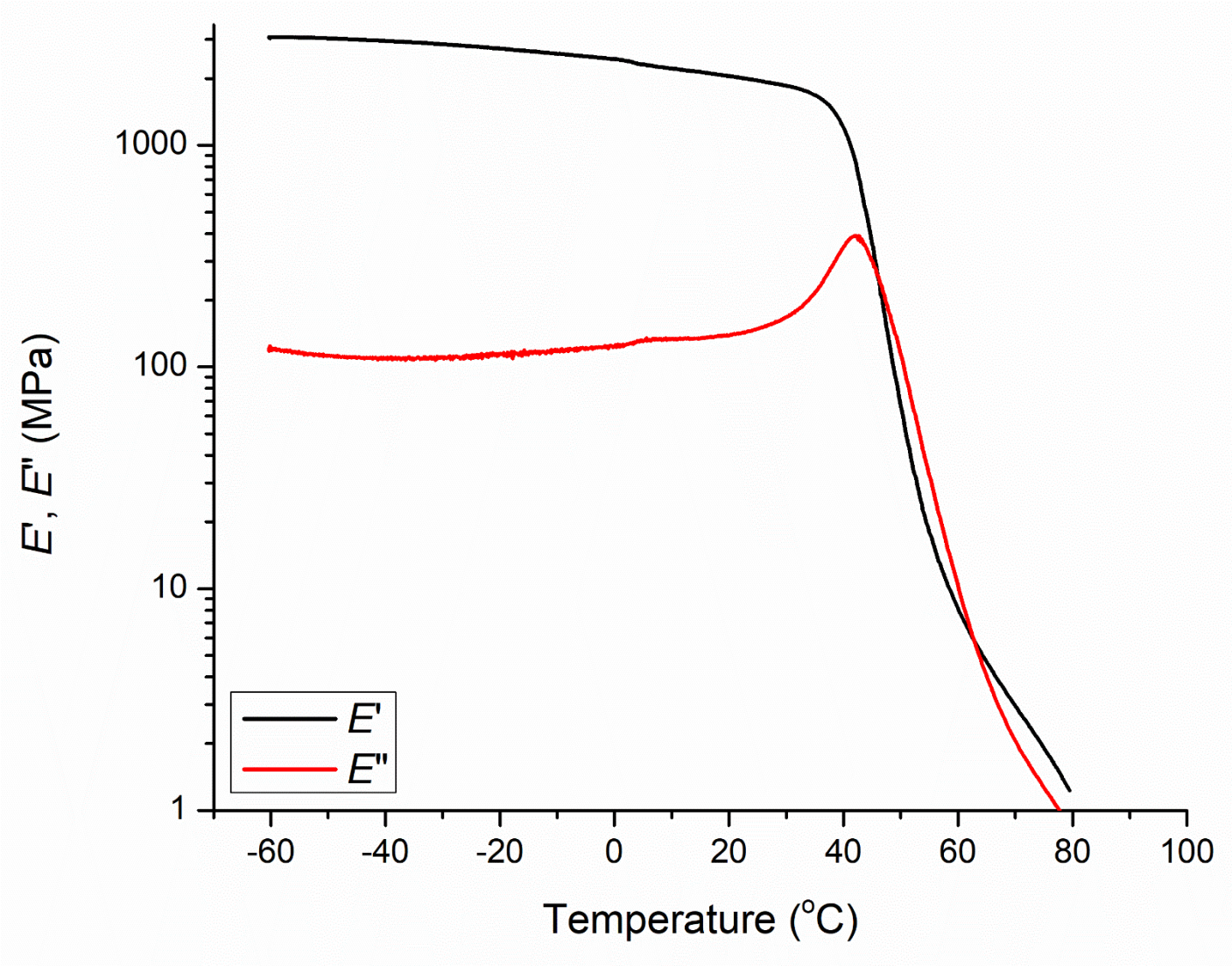

Figure S3.38. Overlay of storage modulus *E*' and loss modulus *E*" for **PU-4B**.

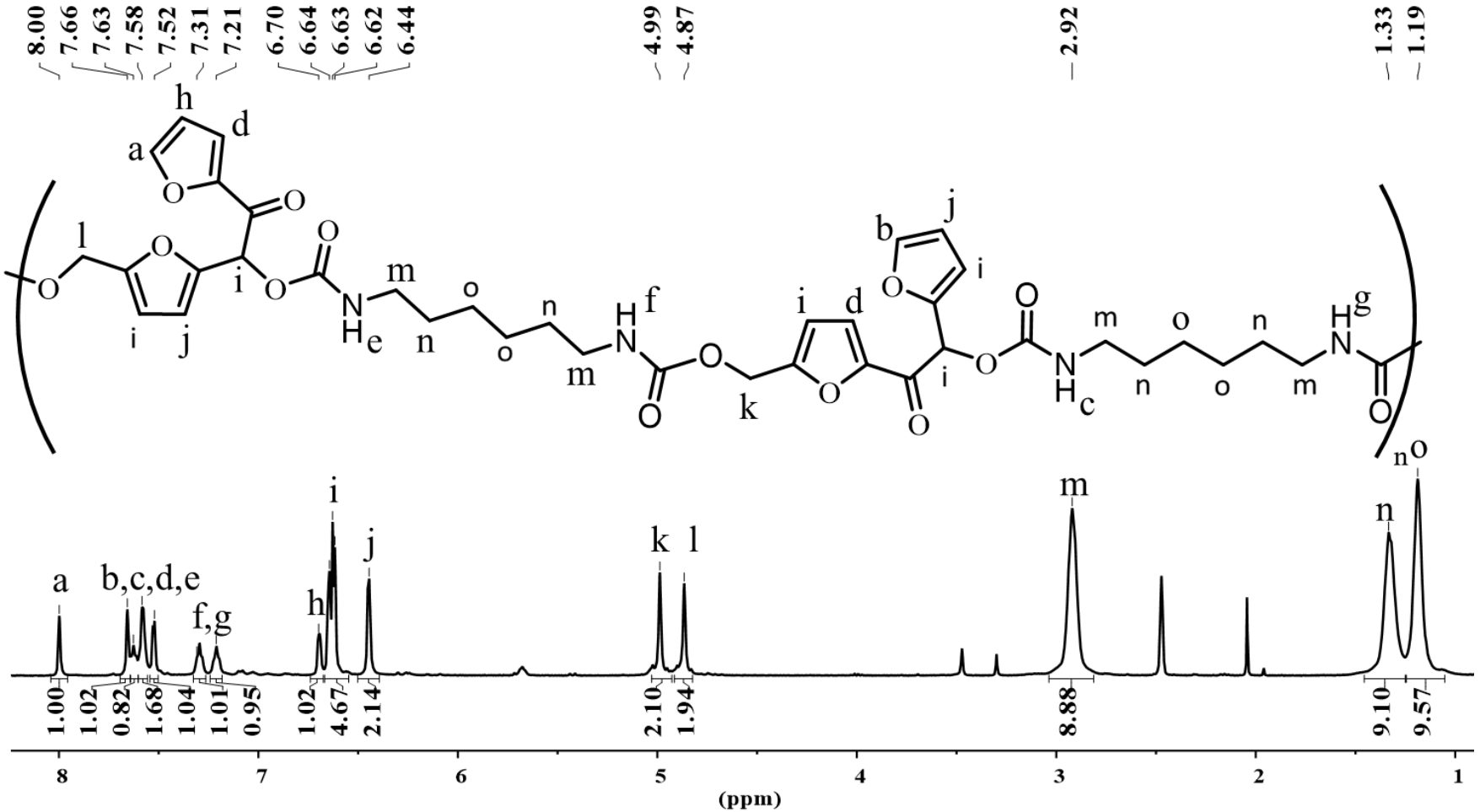

Figure S3.39. ^{1}H NMR (DMSO-d_6) spectra of **PU-4A/B**.

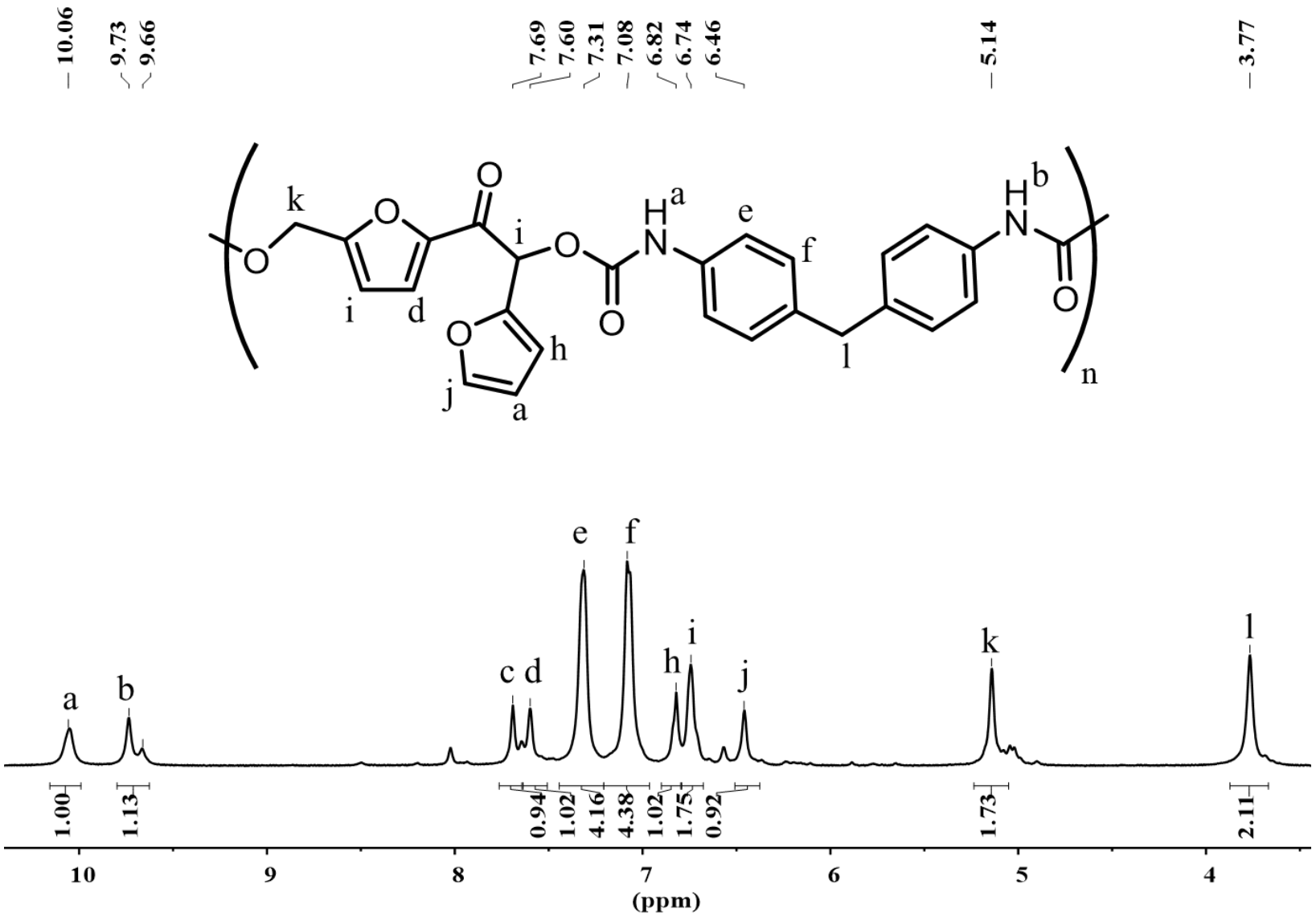

Figure S3.40. ^{1}H NMR (DMSO-d_6) of **PU-5A**.

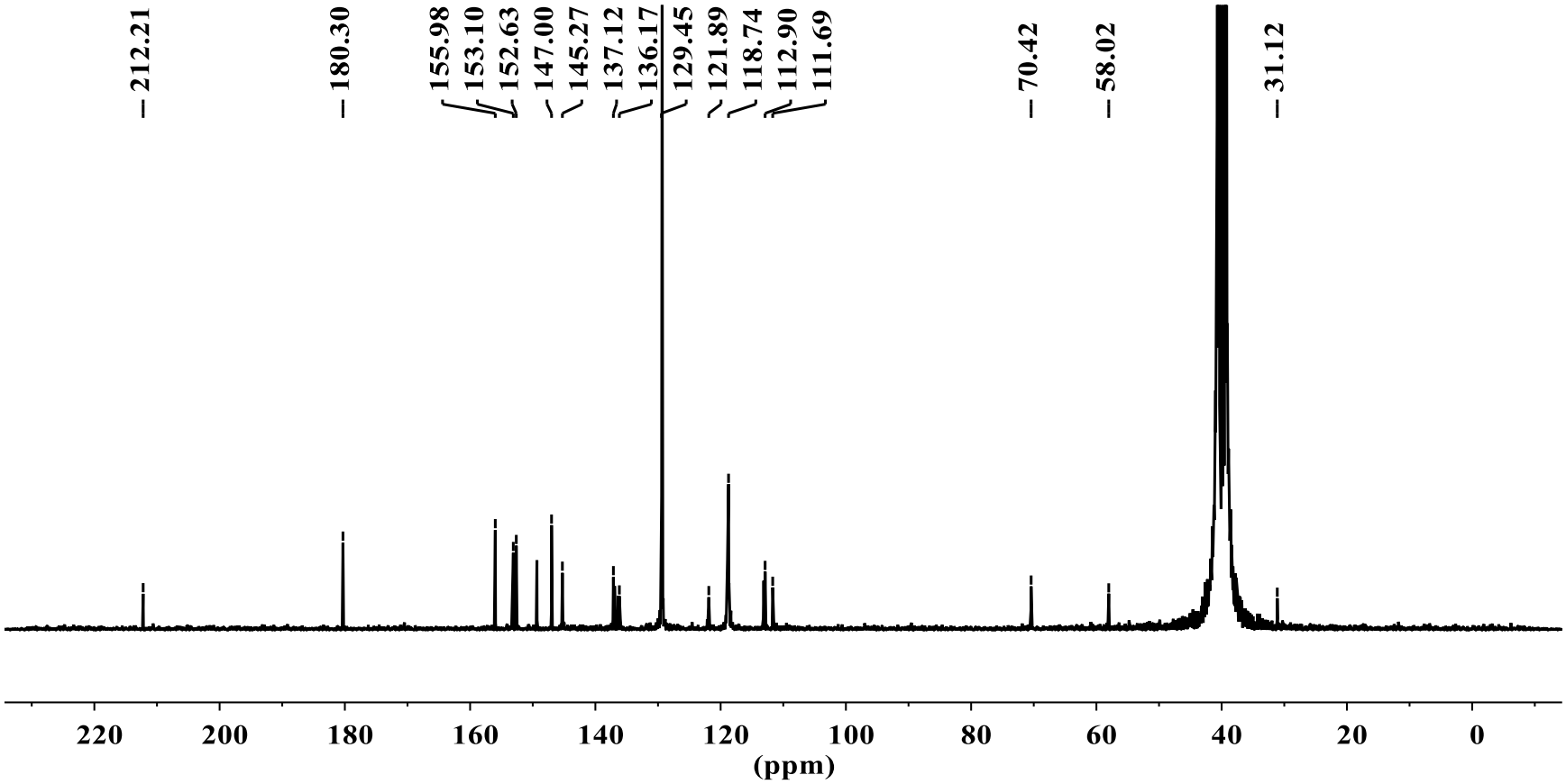

Figure S3.41. ^{13}C NMR (DMSO-d_6) of **PU-5A**.

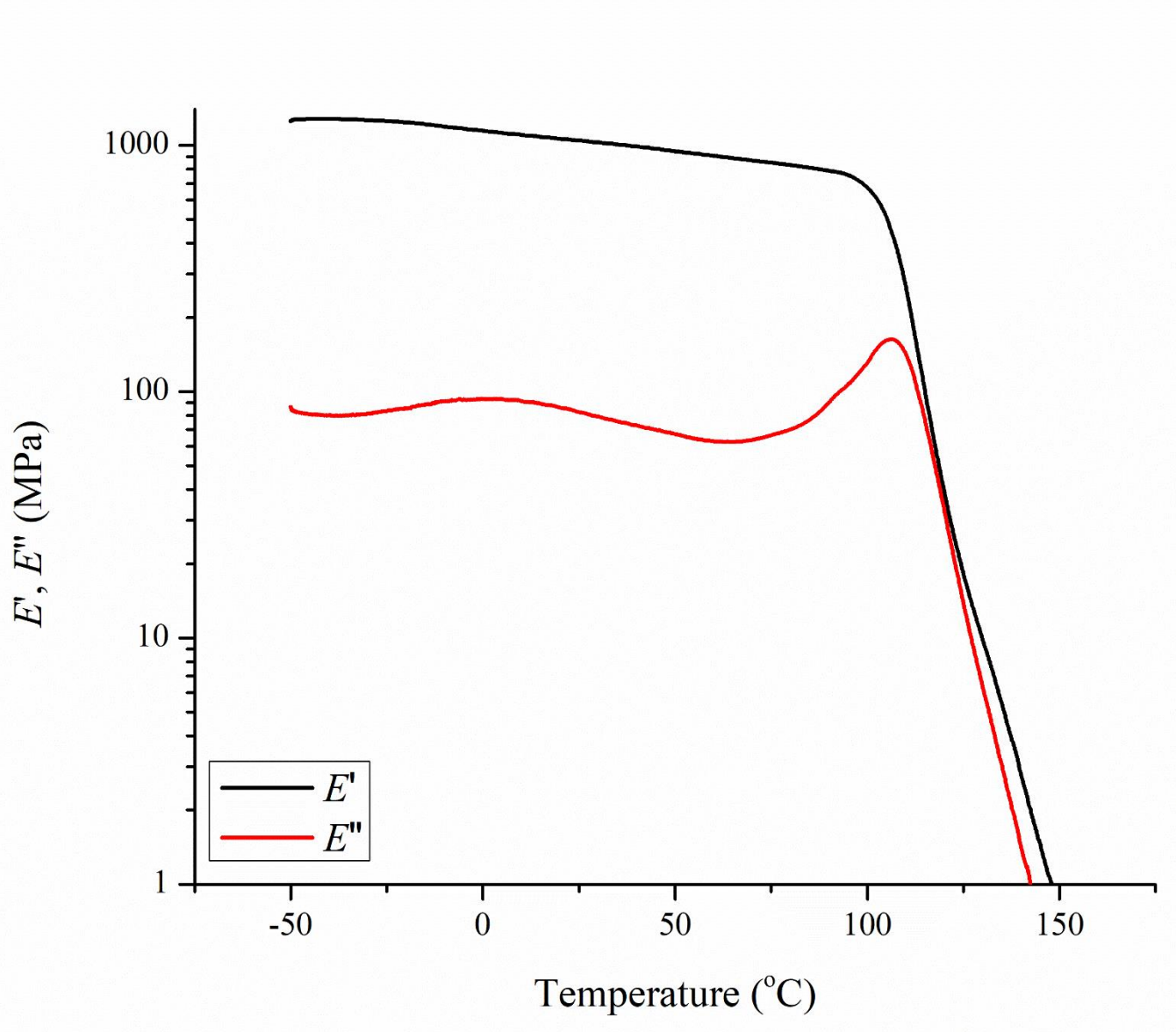

Figure S3.42. Overlay of storage modulus *E'* and loss *E"* for **PU-5A**.

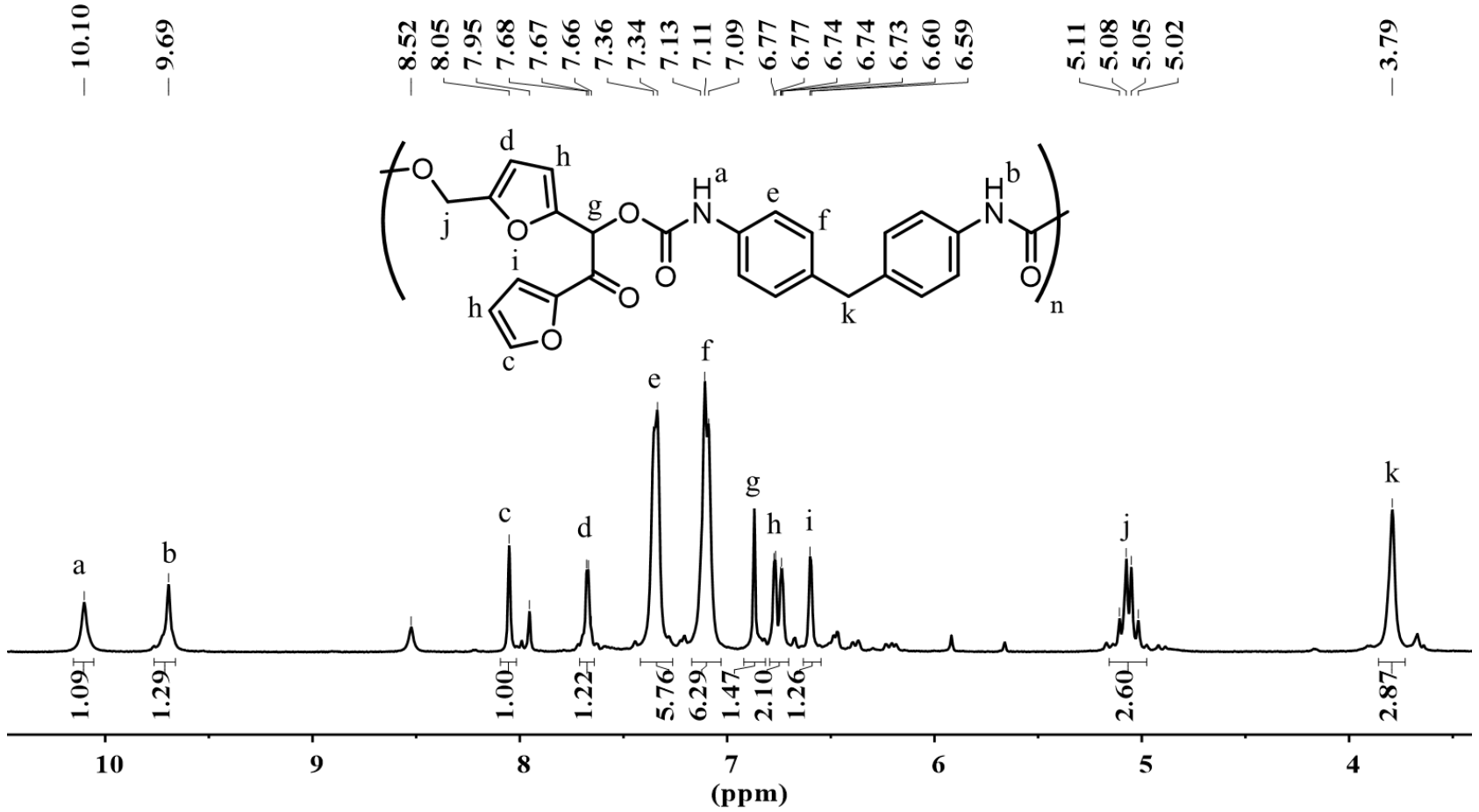

Figure S3.43. ^{1}H NMR (DMSO-d_6) at **PU-5B**.

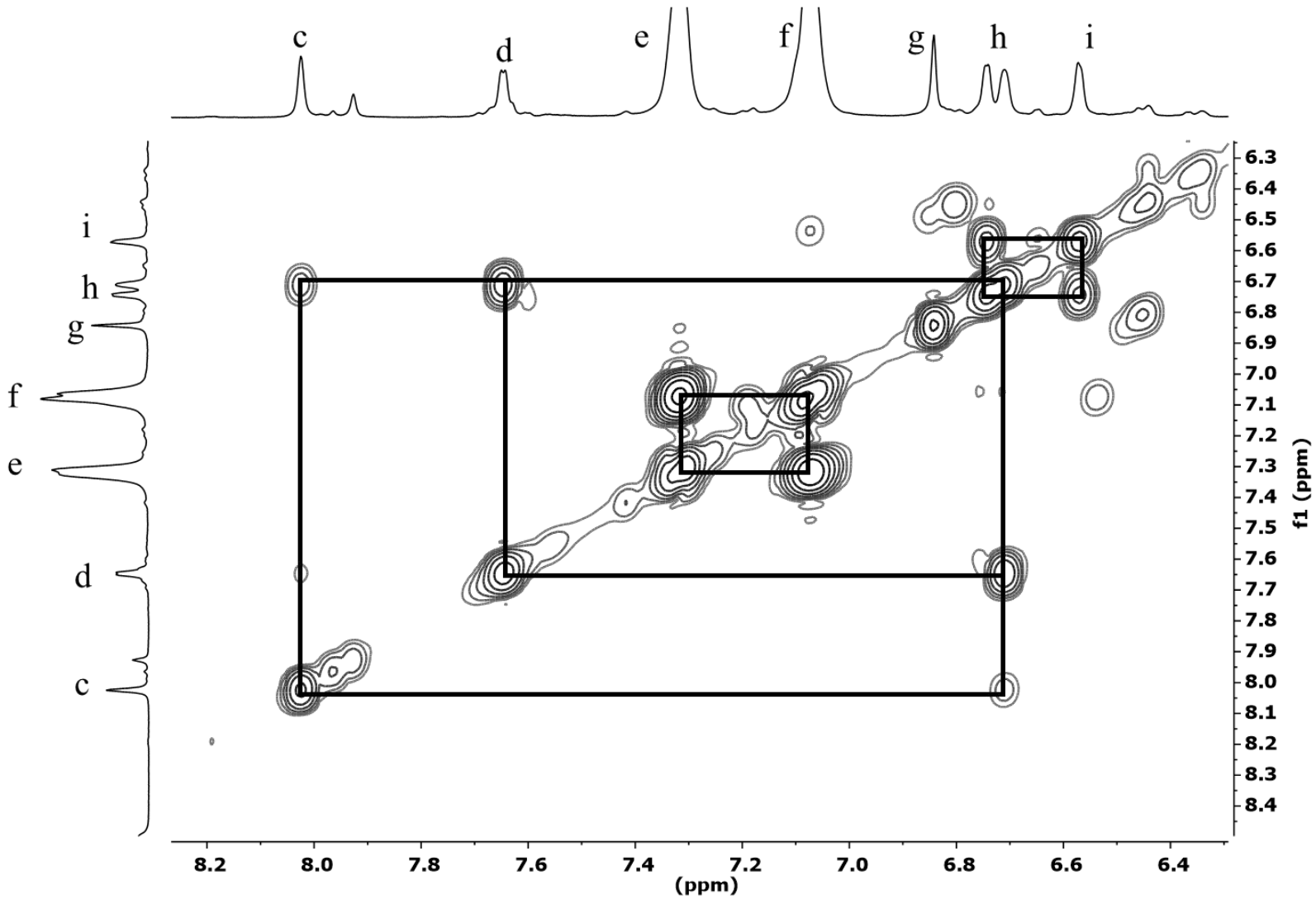

Figure S3.44. gCOSY (DMSO-d_6) of **PU-5B**.

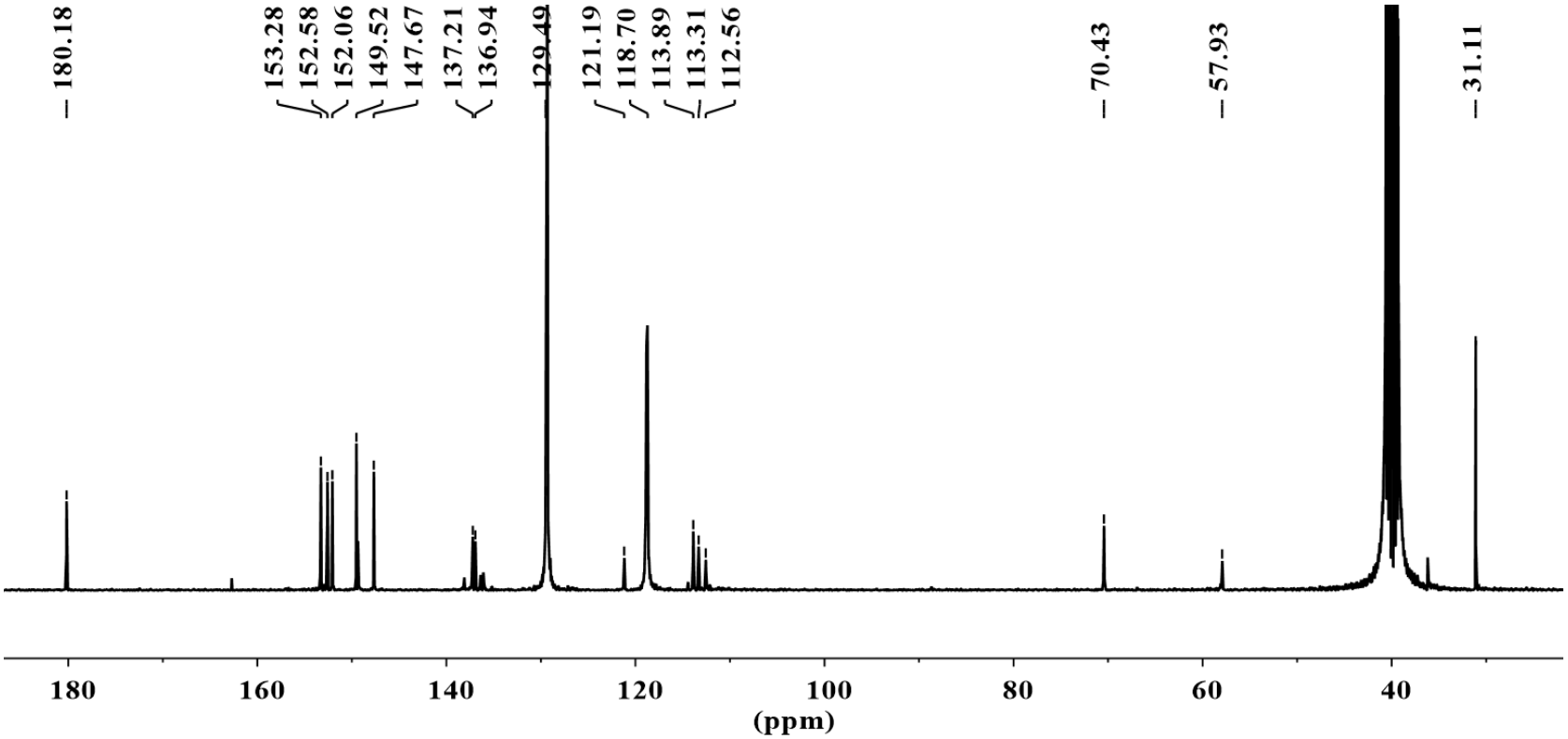

Figure S3.45. ^{13}C NMR (DMSO-d_6) of **PU-5B**.

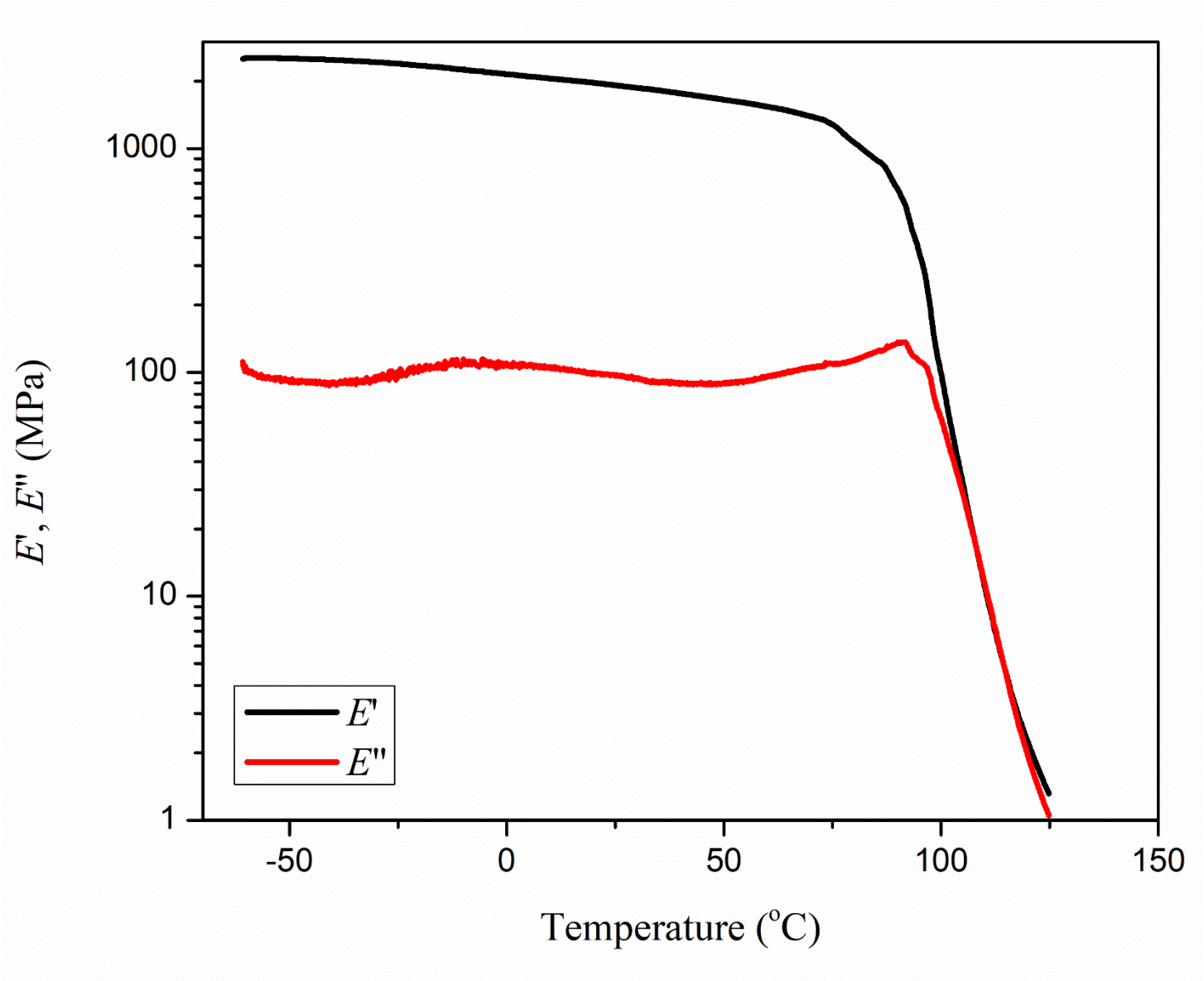

Figure S3.46. Overlay of storage modulus *E'* and loss modulus *E''* for **PU-5B**.

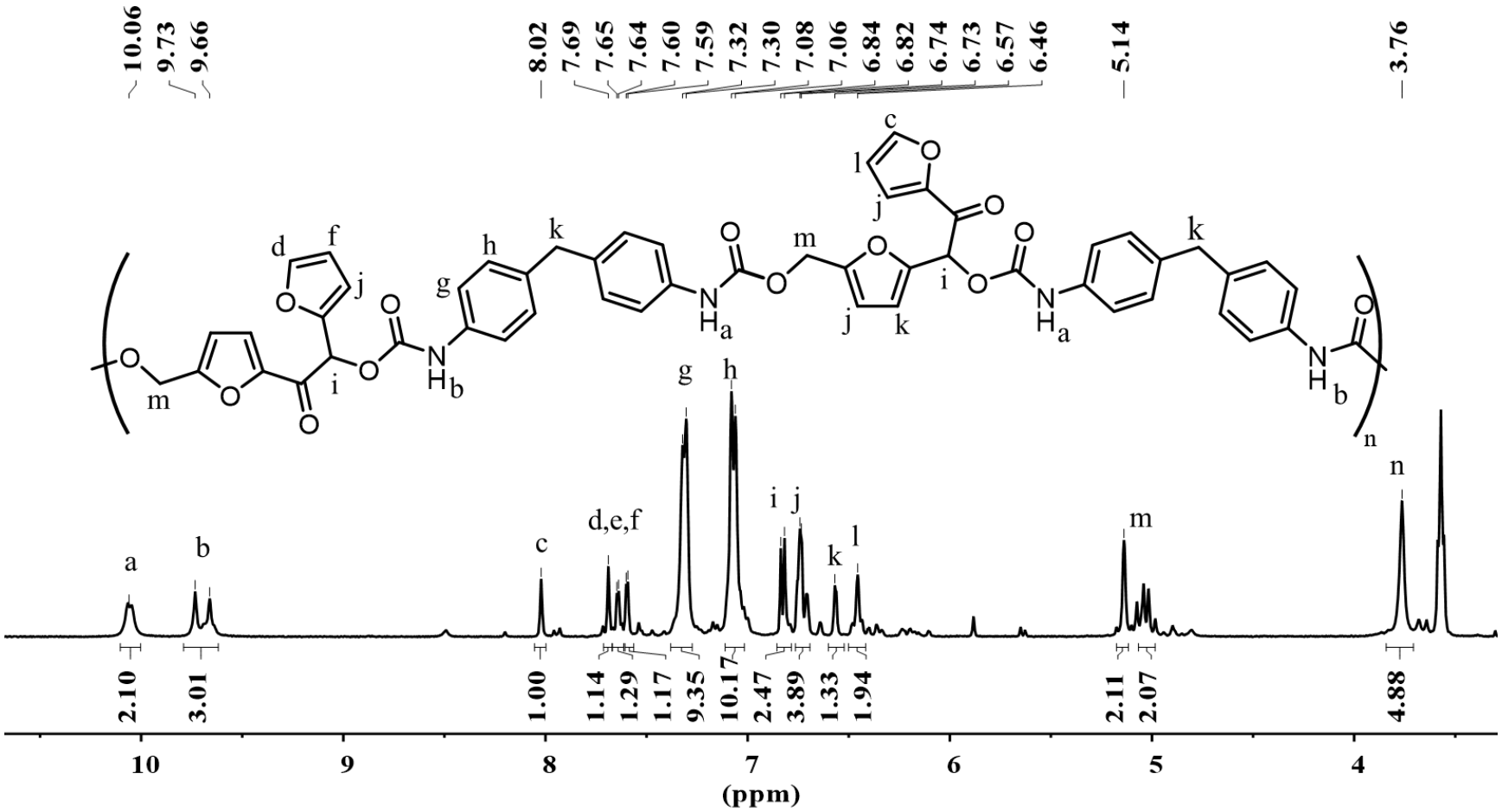

Figure S3.47. ^{1}H NMR (DMSO-d_6) of **PU-5A/B**.

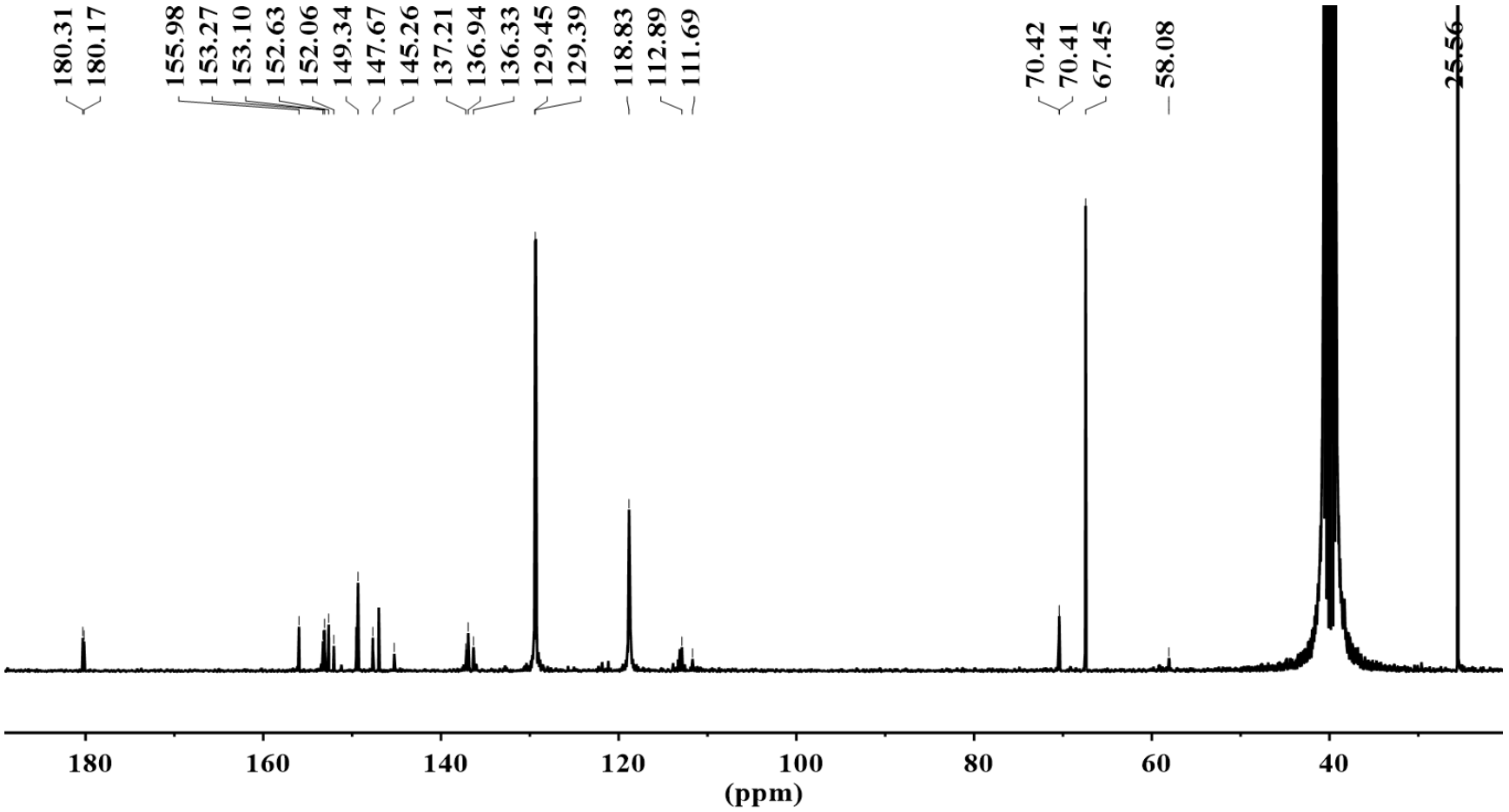

Figure S3.48. ^{13}C NMR (DMSO-d_6) of **PU-5A/B**.

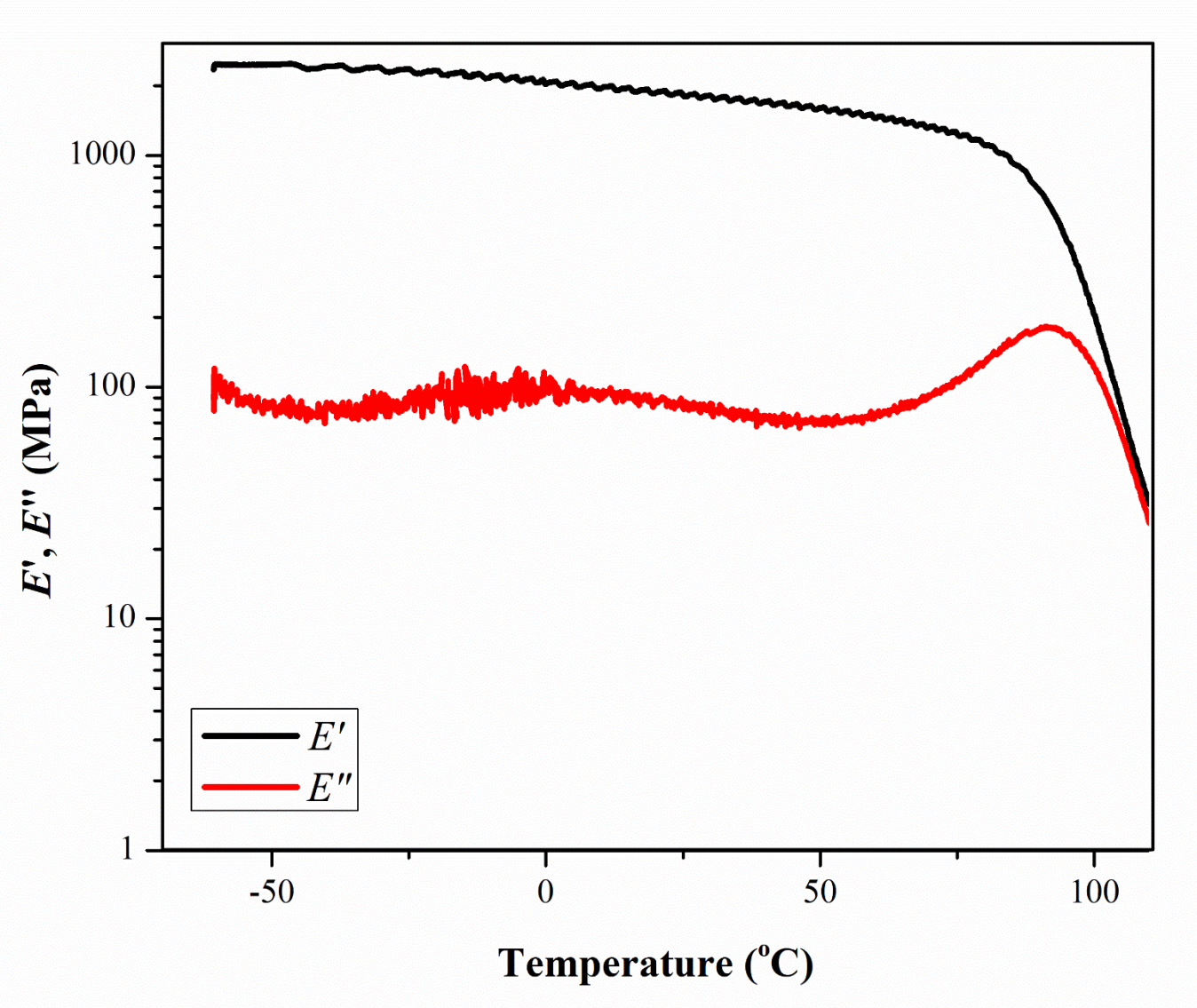

Figure S3.49. Overlay of storage modulus *E'* and loss *E"* for **PU-5A/B**.

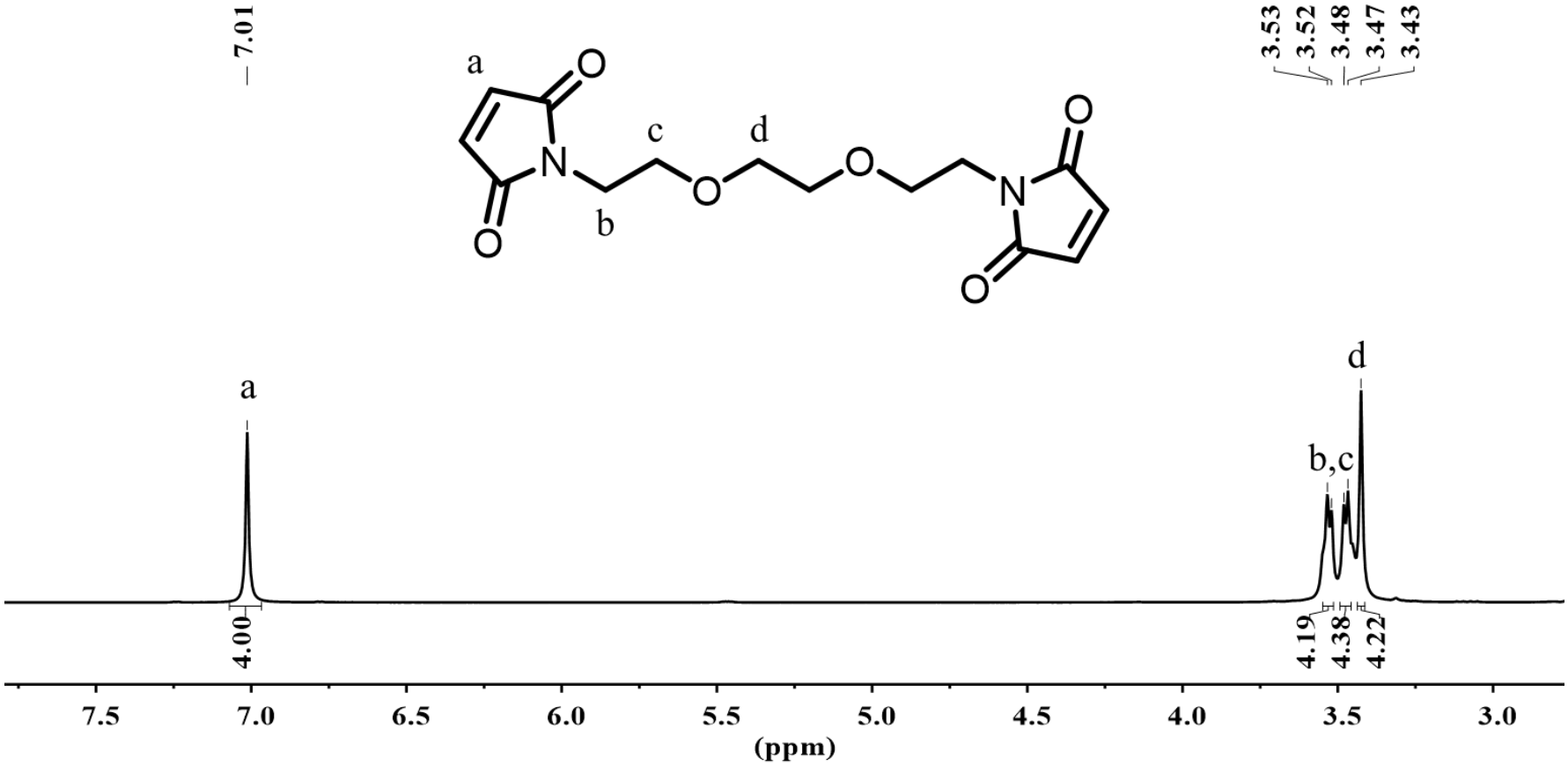

Figure S3.50. ^{1}H NMR (DMSO-d_6) of the bis-maleimide cross linker.

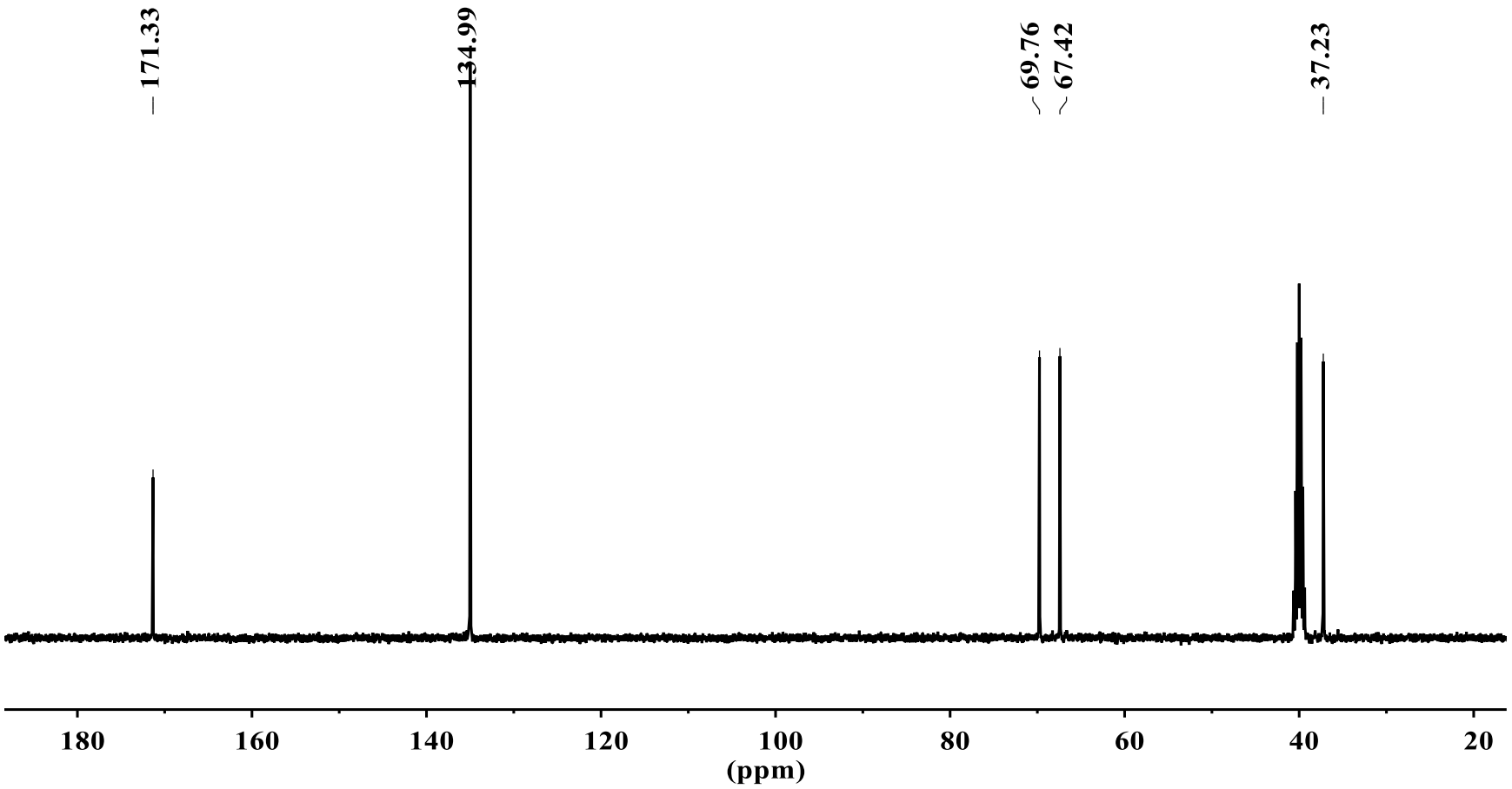

Figure S3.51. ^{13}C NMR (DMSO-d_6) of the bis-maleimide cross linker.

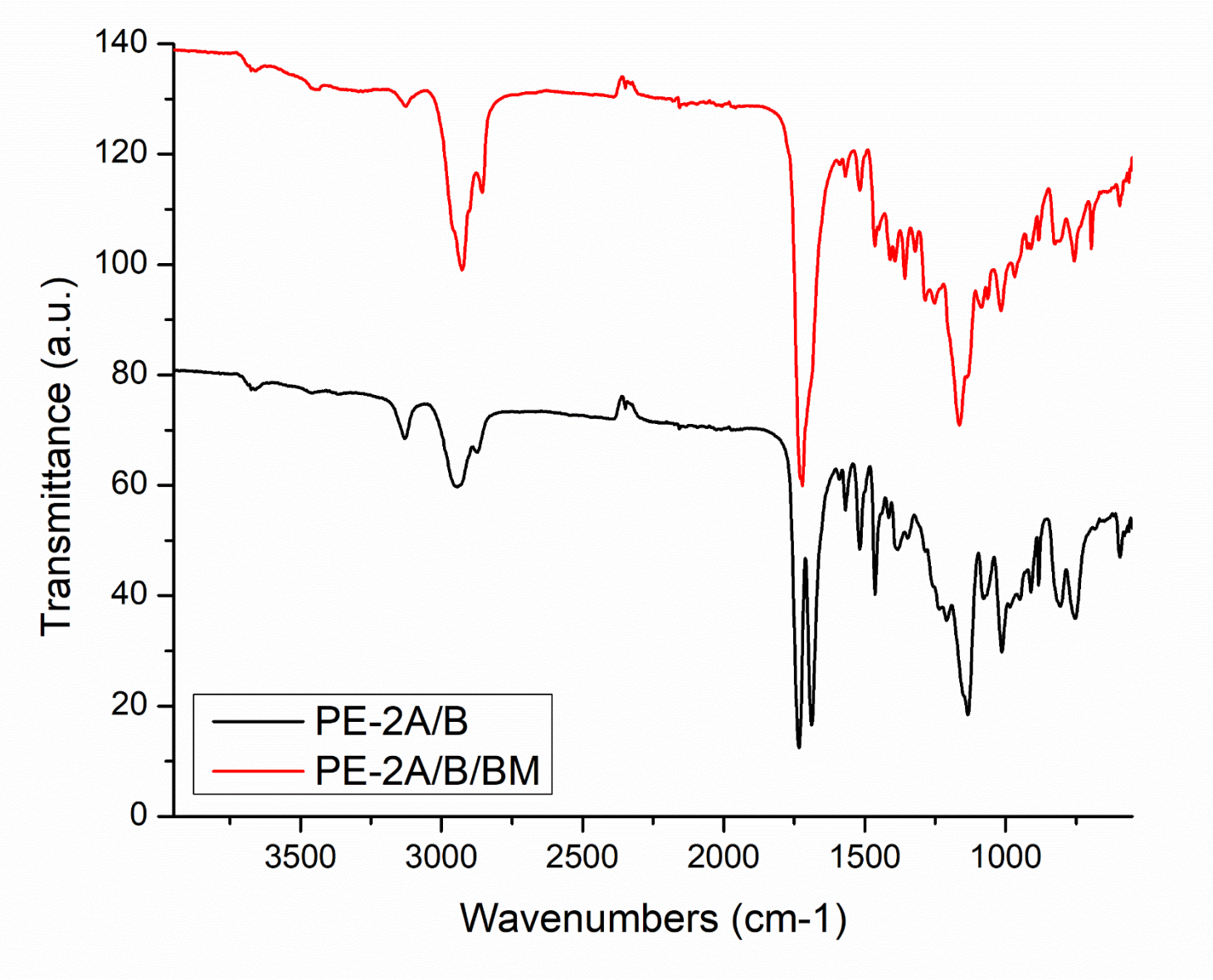

Figure S3.52. FTIR spectra of polymer **PE-2A/B** before and after BM addition.

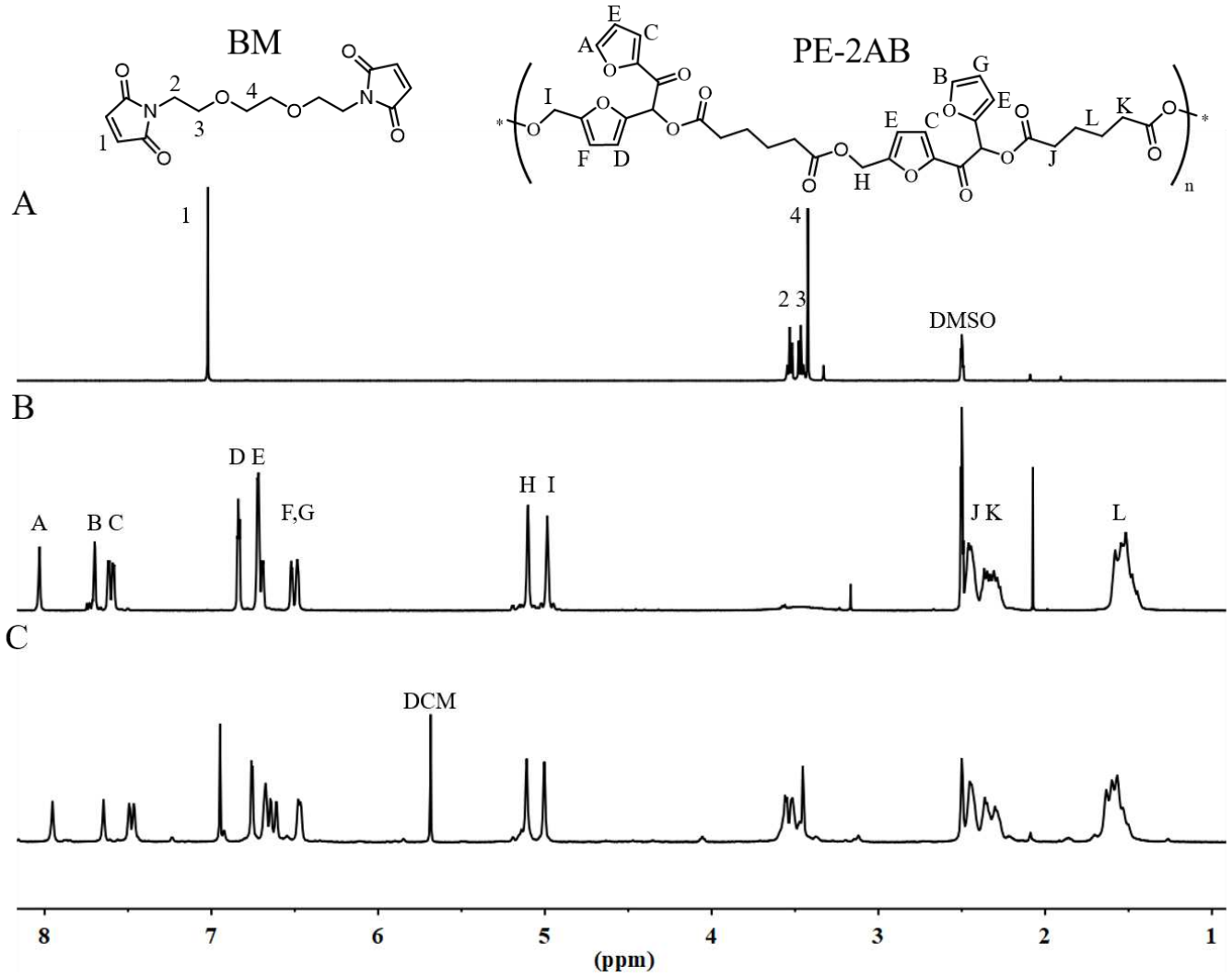

Figure S3.52. Stacked ^{1}H NMR series (DMSO-d_6). (A) bis-maleimide (BM), (B) **PE-2A/B**, **PE-2A/B** heated to 80° C (Shows the presence of **PE-2A/B** and **BM** at elevated temperatures)

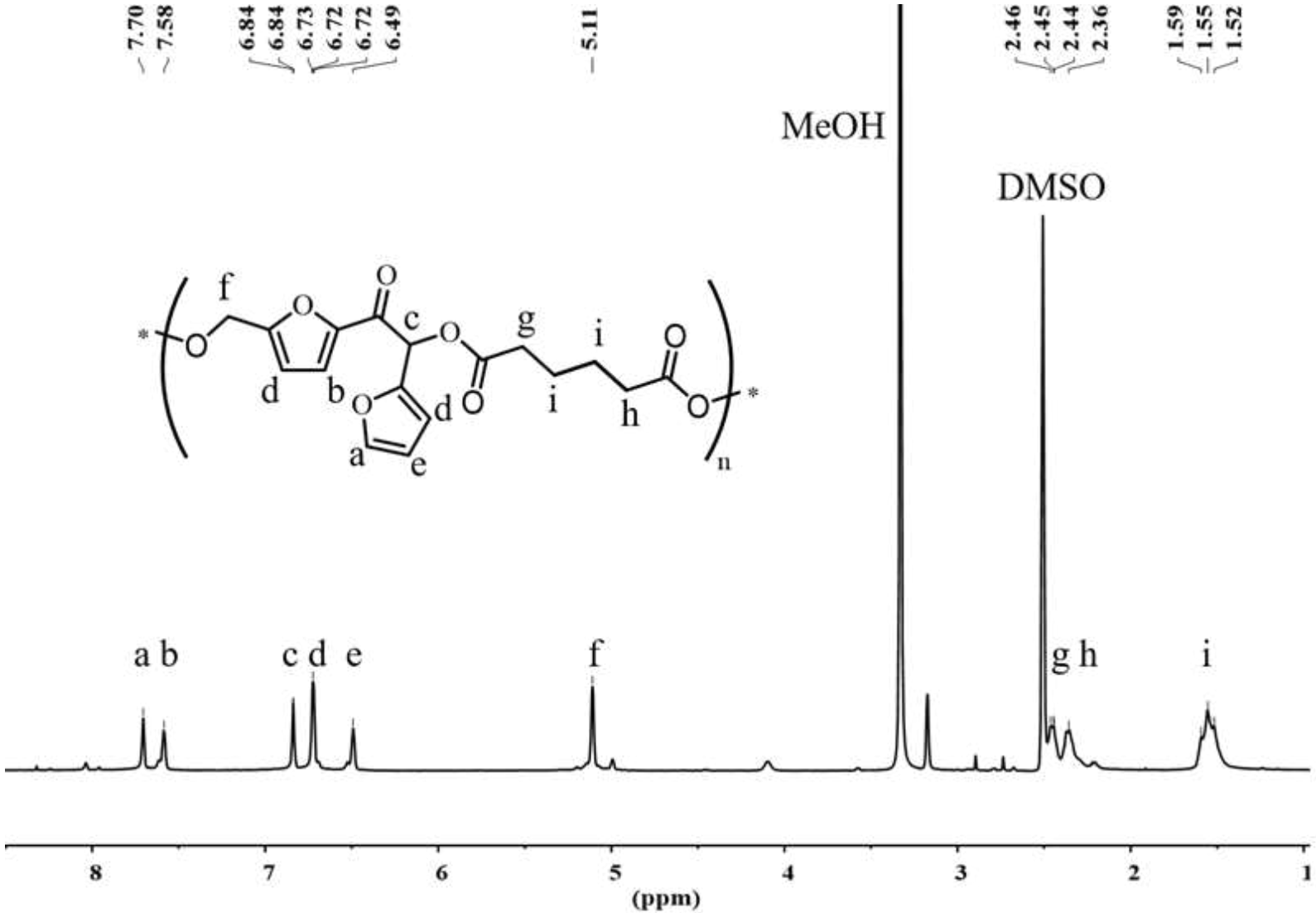

Figure S3.54. ^{1}H NMR (DMSO-d_6) of rDA product (after removing crosslinker) from **PE-2A BM**, showing the reformation of **PE-2A**.

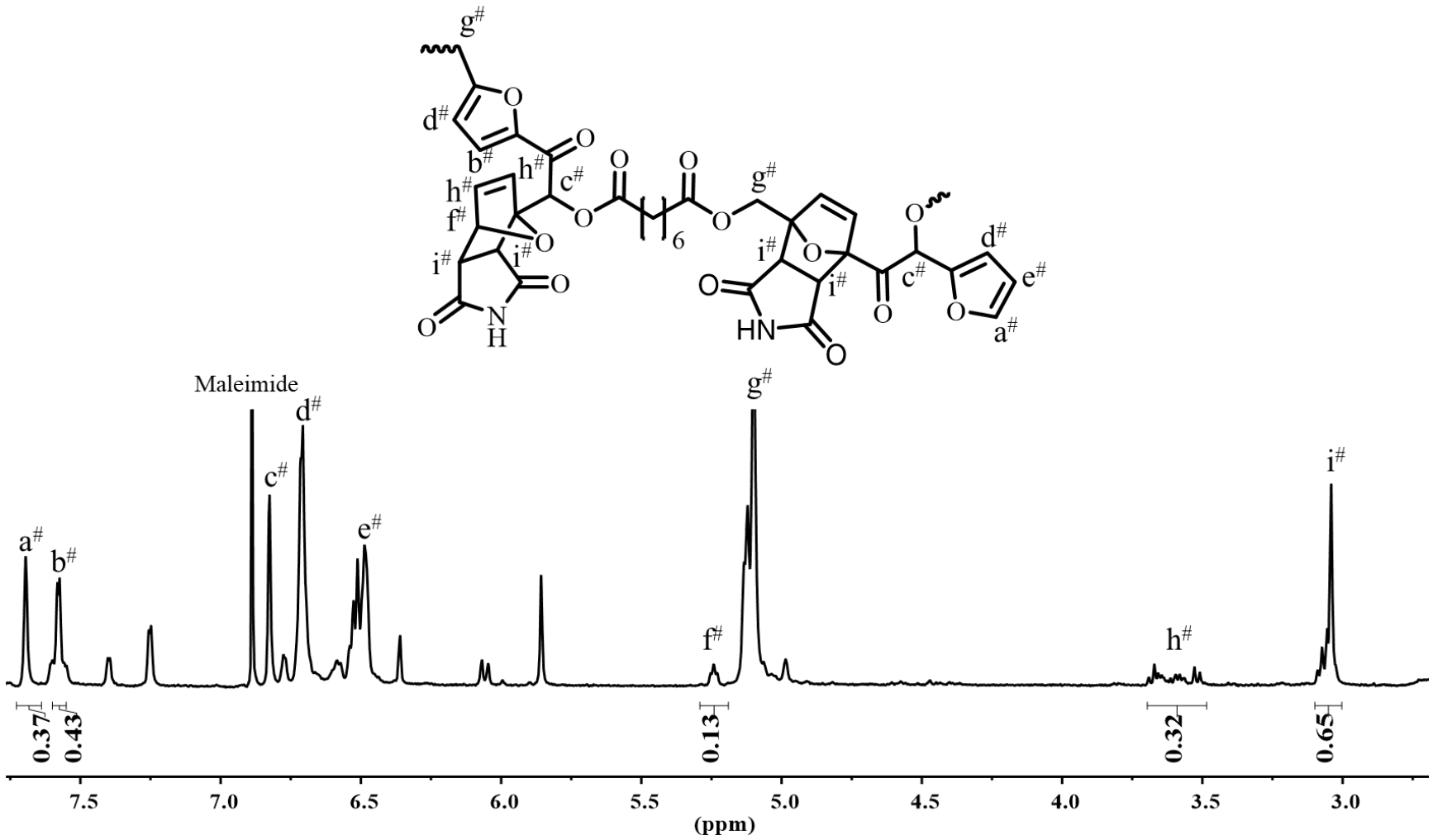

Figure S3.55. ^{1}H NMR (DMSO-d_6) of DA adduct of PE-3A and maleimid

References

(1) Kim, Y. H.; Stites, W. E., Effects of Excluded Volume upon Protein Stability in Covalently Cross-Linked Proteins with Variable Linker Lengths. *Biochemistry* **2008**, 8804-8814.

Appendix C

Experimental Details and Supporting Information for Chapter 4

C.1. Materials, Reagents, and Methods

All oxygen/moisture-sensitive manipulations were carried out in a nitrogen-filled glovebox or under nitrogen atmosphere using standard Schlenk techniques. HPLC-grade organic solvents were sparged extensively with nitrogen during filling of the solvent reservoir and then dried by passage through activated alumina for CH_2Cl_2 (DCM) followed by passage through Q-5-supported copper catalyst (for toluene) stainless steel columns. Tetrahydrofuran (THF) was refluxed over metallic sodium/potassium alloy with benzophenone and distilled under nitrogen atmosphere before use. Acetaldehyde (Acros Organics), Methyl acrylate (EDM Millipore), 1,3-dimesityl-1H-imidazol-3-ium-2-ide (IMes, TCI America), and 1,3-diisopropylthiourea (thiourea, Sigma-Aldrich) were used as received. Ethyl acetate (AcOEt, Fisher Scientific) was used as received. Hydroquinone and ethyl 3-(furan-2-yl) propionate were purchased from Sigma-Aldrich and used as received. Acetonitrile (Sigma-Aldrich) was distilled over calcium hydride. Furfural alcohol (TCI America) and 2-methylfuran (TCI America) were vacuum-distilled over calcium hydride prior to use. 5-Hydroxymethylfurfural (HMF, TCI America) was used as received. Boulder Scientific provided tris(pentafluorophenyl)borane which was sublimated twice at 40° C. Deuterated dimethyl sulfoxide (DMSO-d_6), deuterated chloroform ($CDCl_3$), and deuterated toluene (Toluene-d_8), and deuterated benzene (Benzene-d_6) were purchased from Cambridge Isotope Laboratories and degassed before being stored in a glovebox over activated Davison 4 Å molecular sieves. Methyl

2-((3aR,6R)-1-oxo-6,7-dihydro-3H-3a,6-epoxyisobenzofuran-7a(1H)-yl)acetate (**FIL**) was synthesized by literature procedures.[1]

^{1}H and ^{13}C NMR spectra were recorded on a Varian 400 MHz or a 500 Bruker (500 MHz, ^{1}H; 125 MHz), ^{13}C MHz spectrometer or a Bruker AVIII 400 MHz spectrometer (400 MHz, ^{1}H; 100 MHz, ^{13}C). Chemical shifts were referenced to internal solvent resonances corresponding to 7.26 ppm (chloroform), 7.16 ppm (benzene), 2.3 & 7.19 ppm (toluene), and 5.32 (DCM) reported as parts per million relatives to SiMe4. High-resolution mass spectrometry (HRMS) data were collected on an Agilent 6220 Accurate time-of-flight in electrospray mode. GC/MS data collected on Agilent 5973N Mass Selective Detector interfaced to a 6890 gas chromatograph which is equipped with a 7683 automatic liquid sampler. This instrument is a single quadrupole mass spectrometer utilizing an electron ionization source (EI).

Attempted Bronsted acid catalyzed Michael addition of methyl acrylate to furan alcohol and 2-methylfuran. Furan combined [furfural alcohol (1.47g, 1.50 mmole) or 2-methylfuan (1.23g, 1.50 mmol)] with 50 mL of 1:1 AcOH to H_2O in 130 mL sealed glass pressure reactor with stir bar, then methyl acrylate (1.4 mL, 0.15 moles) was added along with 500 ppm hydroquinone before reactor was sealed. Reaction heated for 14 H in a temperature regulated silicon oil bath at 130° C (75° C, 45° C), upon completion of heating reaction was allowed to cool to room temperature and then concentrated on rotary evaporator. The concentrated reaction mixture was slowly added to 150 ml saturated aqueous $NaCO_3$ and extracted 3 times with 20 mL AcOEt. The combined organic layers were rinsed with 20 mL DI H_2O 3 times. Then organic layer was dried with $MgSO_4$, filtered, and solvent removed with rotary evaporator. Products were then analyzed with proton ^{1}H NMR, only starting materials or transesterification product present.

Attempted Bronsted acid catalyzed Michael addition of methyl acrylate to furan alcohol and 2-methylfuran (microwave heating). 2-Methylfuan was combined with (2.05g, 25.0 mmole) 30 mL of 1:1 AcOH to H_2O in 100 mL PTFE microwave reactor, then added methyl acrylate (2.3 mL, 25.0 mmole) moles then 400 ppm hydroquinone was added before reactor was sealed. Reaction heated for 30 min in microwave reactor at 600W with a 20 min ramp followed by 10 min hold at 130° C, upon completion of heating reaction was allowed to cool to room temperature and then concentrated on rotary evaporator. Followed by slowly adding concentrated reaction mixture to 150 ml saturated aqueous $NaCO_3$. Aqueous solution was extracted 3 times with 20 mL AcOEt, combined organic layers were rinsed with 20 mL DI H_2O 3 times. Finally, organic layer was dried with $MgSO_4$, filtered, and solvent was removed with rotary evaporator. Analyzed the products with proton ^1H NMR, complete conversion to Diels-Alder adduct. ^1H NMR (400 MHz, Chloroform-*d*) δ 6.63 (s, 2H), 6.41 – 6.28 (m, 5H), 6.25 – 6.07 (m, 4H), 6.03 (d, *J* = 5.7 Hz, 2H), 5.09 – 4.96 (m, 4H), 4.87 (dd, *J* = 4.8, 1.8 Hz, 2H), 3.68 (s, 8H), 3.60 (d, *J* = 4.4 Hz, 9H), 3.23 (ddd, *J* = 8.9, 4.9, 3.9 Hz, 1H), 2.72 (dd, *J* = 9.2, 3.9 Hz, 2H), 2.50 (dd, *J* = 8.5, 4.0 Hz, 1H), 2.41 (dd, *J* = 8.1, 4.1 Hz, 1H), 2.31 – 2.23 (m, 1H), 2.24 (dd, *J* = 5.7, 3.3 Hz, 2H), 2.25 – 2.13 (m, 2H), 1.86 (dd, *J* = 11.5, 4.0 Hz, 1H), 1.78 (dd, *J* = 11.5, 9.1 Hz, 1H), 1.73 – 1.50 (m, 17H), 1.22 (d, *J* = 5.6 Hz, 1H).

Attempted Lewis acid catalyzed Michael addition of methyl acrylate to furfural alcohol (2-methylfuran). A 25 mL Schlenk flask that was dried for 24 H in oven at 150° C loaded with stir bar and cooled under flow of dry N_2 was sealed with septum and a small positive N_2 pressure was maintained throughout reaction. In N_2 filled glove box methyl acrylate (12.5 mmol), $B(C_6F_5)_3$ (0.180 g, 0.352 mmol), and 12 mL $CDCl_3$ were loaded into a 25 mL syringe which was removed and used to charge the 25 mL Schlenk flask. The boron complex and methyl acrylate were allowed

to stir for 15 min. before the first addition of furfural alcohol. The furfural alcohol (1.00 mL, 11.6 mmol) was combined with 1.5 mL $CDCl_3$ in N_2 filled glove box and removed. Four additions of 0.2 mL were made every 20 min and ^1H NMR was taken before each new addition. After 4^{th} addition the rest of the furfural alcohol was added and a ^1H NMR was taken at 14 h, 23 H, 72 H. No reaction was observed.

^1H NMR scale Lewis acid catalyzed Michael addition of methyl acrylate to 2-methylfuran. Stoichiometric equivalents of $B(C_6F_5)_3$ (0.06 mg, 0.113 μL) and methyl acrylate (11 μL, 0.113 μmol) were combined in J-Young tube with $CDCl_3$ in N_2 filled glove box. Tube was agitated by hand every 2 min over the course of 20 min. ^1H NMR was taken and then 1 stoichiometric equivalent of 2-methylfuran (10 μL, 0.113 μmol) was added, tube was agitated by hand every 20 min again then spectra was collected. This was followed by a second stoichiometric addition of both 2-methylfuran and methyl acrylate then manual agitation over 2 min over 20 min and collection of spectra.

Acid catalyzed addition of acetaldehyde to ethyl 3-(furan-2-yl) propionate. A 25 mL round bottom flask was charged with ethyl 3-(furan-2-yl) propionate (61 mmol), acetaldehyde (61 mmol), and 2 mL of solution of aqueous H_2SO_4 (1.8 ml H_2O, 0.2 mL conc. H_2SO_4). Mixture was stirred for 12 H and then quenched with 10 mL saturated aqueous $NaCO_3$ solution. Then the solution was extracted 3 times with 20 mL AcOEt. Followed by rinsing the combined organic layers with 20 mL DI H_2O 3 times. Dried organic layer with $MgSO_4$, filtered, and removed solvent with rotary evaporator. (Subsequent reactions were modified by increasing ratio of acetaldehyde to 1.25 and 1.5 to ethyl 3-(furan-2-yl) propanoate and adding 20 mL H_2O) Products analyzed with ESI-MS mass 380.20 g/mol ($C_{20}H_{26}O_6 + NH_4^+$), ^1H NMR, and COSY. ^1H NMR (400 MHz,

Chloroform-*d*) δ 5.81 (dd, *J* = 13.0, 3.1 Hz, 4H), 4.09 – 4.02 (m, 4H), 3.99 (s, 1H), 2.84 (t, *J* = 7.6 Hz, 4H), 2.60 – 2.44 (m, 4H), 1.93 (s, 1H), 1.45 (d, *J* = 7.2 Hz, 3H), 1.15 (t, *J* = 7.2 Hz, 7H).

Attempted ring opening polymerization of FIL with organic catalyst system. In a N_2 filled glovebox 20 mL scintillation vial with stir bar was charged with IMes, thiourea, benzyl alcohol, and FIL in a molar of ratio of 2.5/2.5/1/100. DCM was added until homogeneity was reached with a final concentration of 1.9M. Reaction was stirred for 24 H and analyzed with ^{1}H NMR. (an additional reaction was performed in toluene and reactant ratios of 2.5/2.5/1/50 with a concentration of 0.1M.

Attempted ring opening polymerization of FIL with organic catalyst system ^{1}H NMR scale. Stoichiometric amounts of IMes and thiourea were combined in a J-Young tube in a N_2 filled glove box with $CDCl_3$ and ^{1}H NMR was taken. Then a stoichiometric amount of benzyl alcohol was added in the glove box followed by a ^{1}H NMR. Finally, 2 separate stoichiometric equivalents FIL were added in the glove box followed by manual agitation. Spectra were collected immediately after FIL addition and every 20 minutes over 3 hours.

Attempted ring opening polymerization of FIL with metallic catalyst system. A 25 mL Schlenk flask that was dried for 24 H in oven at 150° C loaded with stir bar and cooled under flow of dry N_2 was sealed with septum and a small positive N_2 pressure was maintained throughout reaction. $La[N(TMS)_2]_3$ (62.0mg, 0.1 mmol), benzyl alcohol (31.1 μL, 0.3 mmol), and FIL (2.24g, 10 mmol) were dissolved in $CDCl_3$ at ratio of 1/3/100 obtaining a concentration of 1.7M, they were then loaded into a 25 mL syringe and removed from the glove box. Reactants were loaded into the vessel that was pre-cooled in acetonitrile and dry ice to -50° C. Spectra were collected by taking aliquots and immediately quenching with benzoic acid at 1 h, 6 h, 11h, 22 h, 27 h, and 48

h. (Modified reactions were performed in THF at a concentration of 0.7M and reactant ratios of 1/2/50, as well as in $CDCl_3$ with a concentration of 1.7M at ratios of 1/3/50)

Attempted ring opening polymerization of FIL with metallic catalyst system in melt. $La[N(TMS)_2]_3$ (92.0mg, 0.149 mmol) and FIL (1.21g, 4.99 mmol) were combined in a 20 mL scintillation vial in a N_2 filled glove box and removed to be heated to 135° C on an orbital shaker at 150 rpm for 48 h. Reaction was analyzed by GC/MS and ^1H NMR no polymer formed.

C.2.

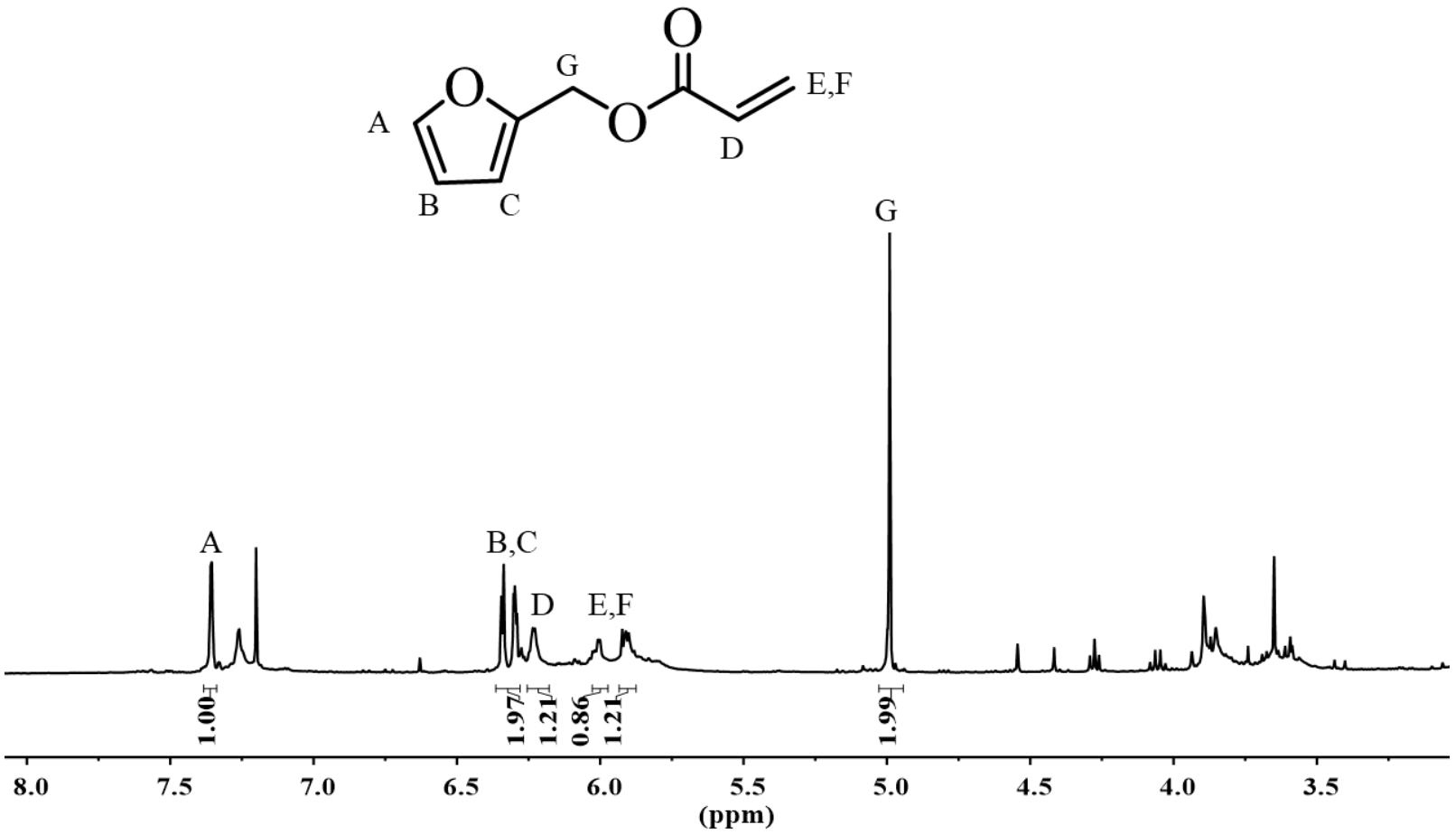

Figure S4.1 Transesterification product of furfural alcohol and methyl acrylate

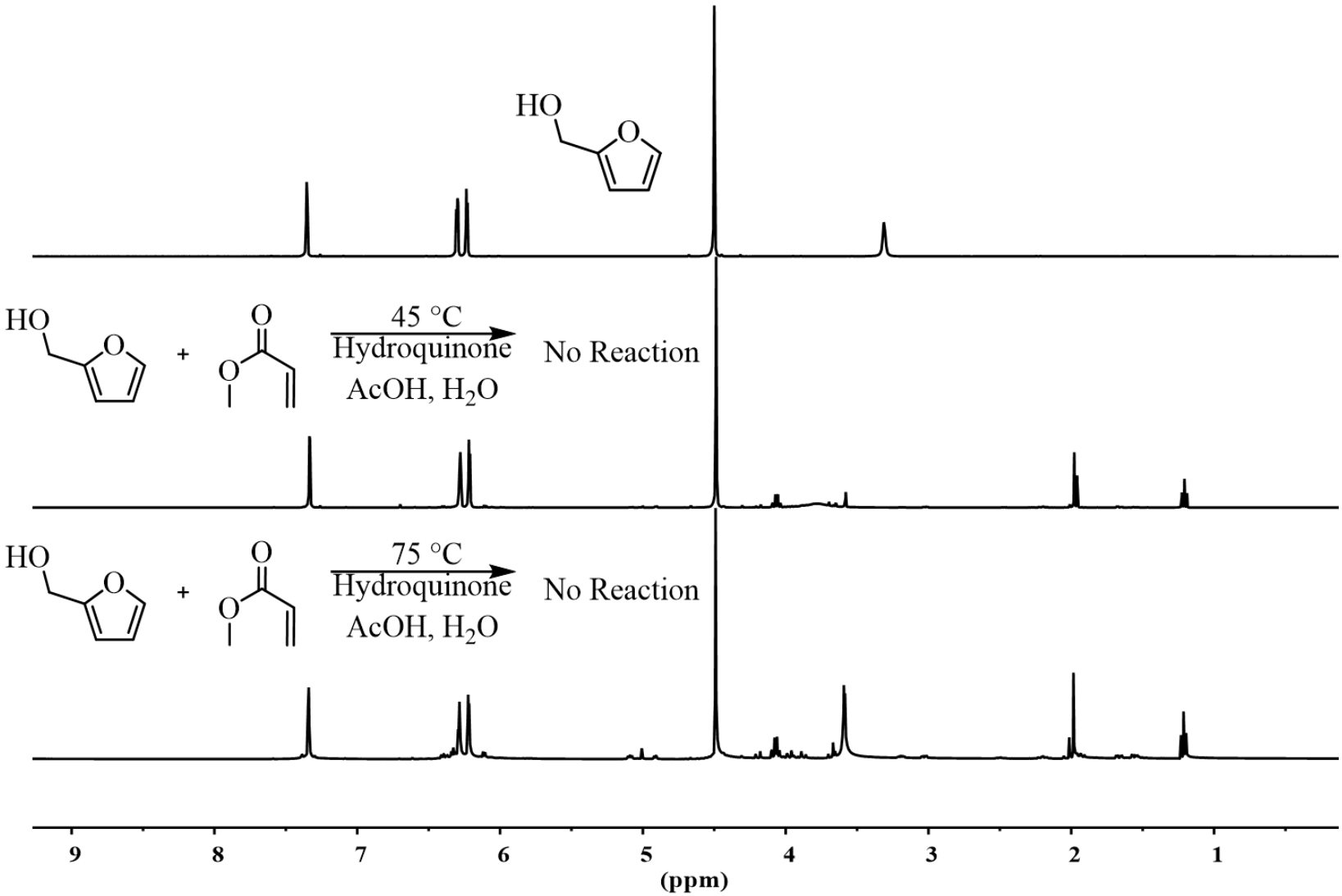

Figure S4.2 Lower reaction temperature prevented transesterification but did not produce the Michael addition Product

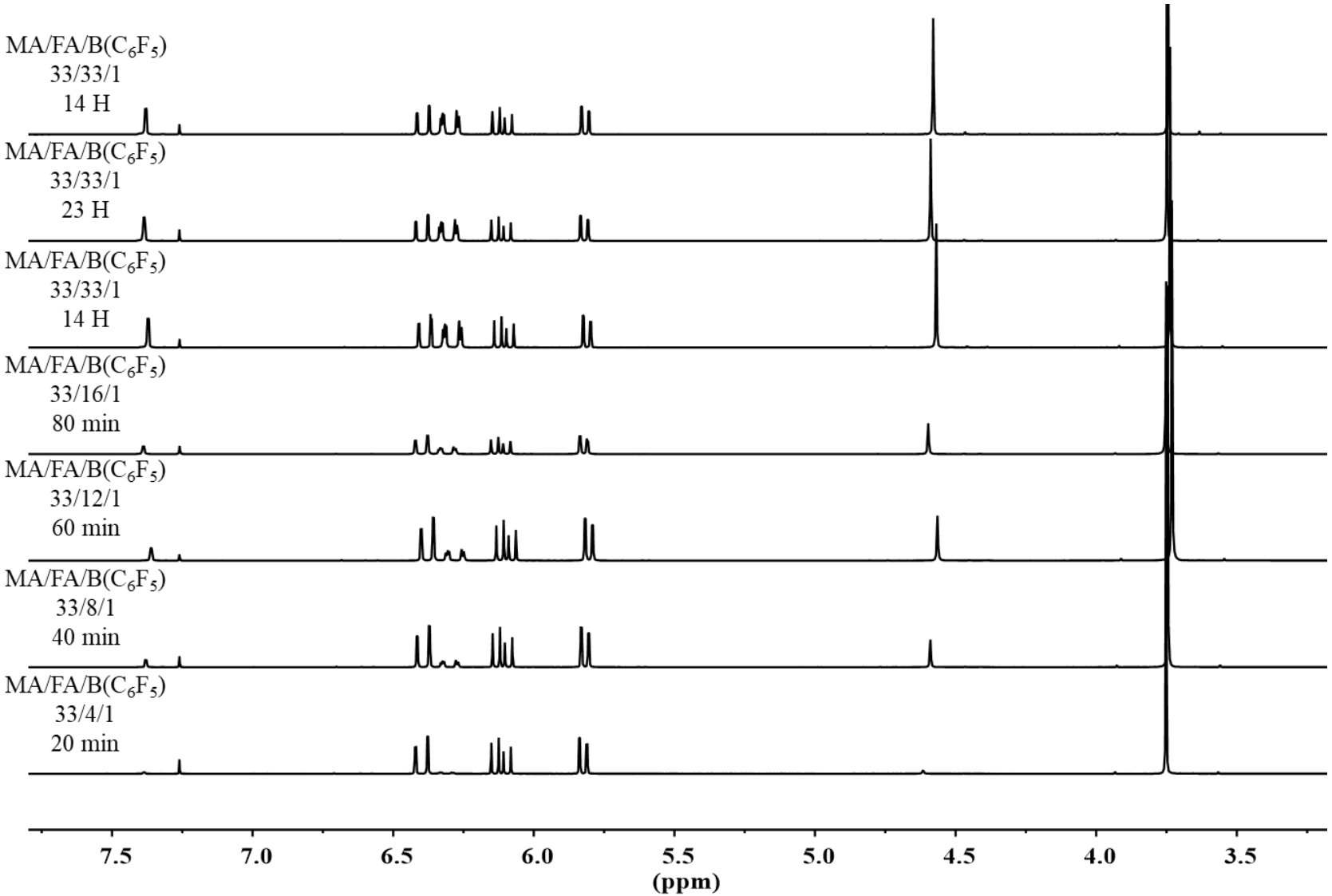

Figure S4.3. Attempted Lewis acid catalyzed Michael addition of methyl acrylate to furfural alcohol

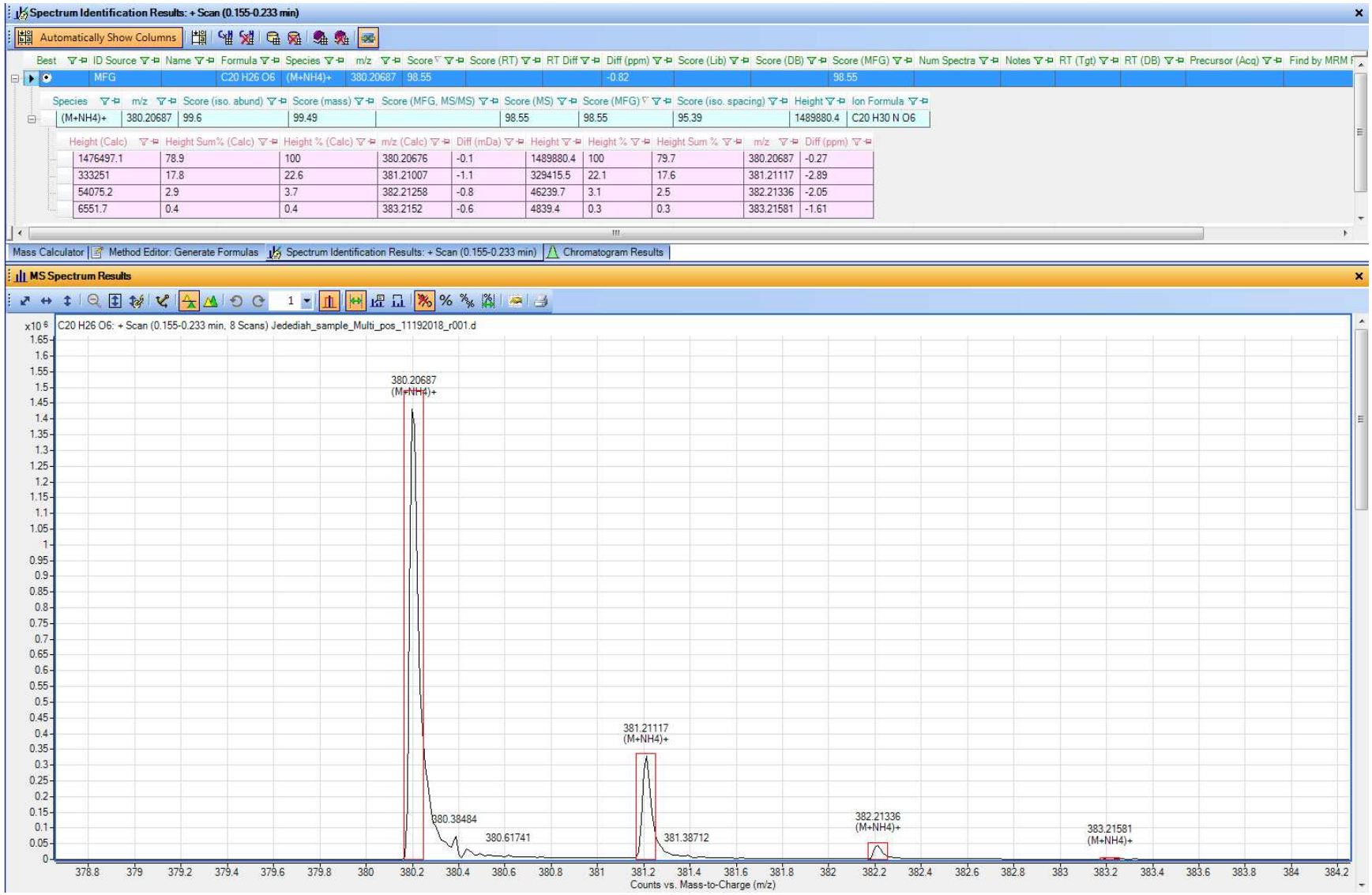

Figure S4.4 ESI-MS of ethyl 3-(furan-2-yl) propanoate acetaldehyde dimmer

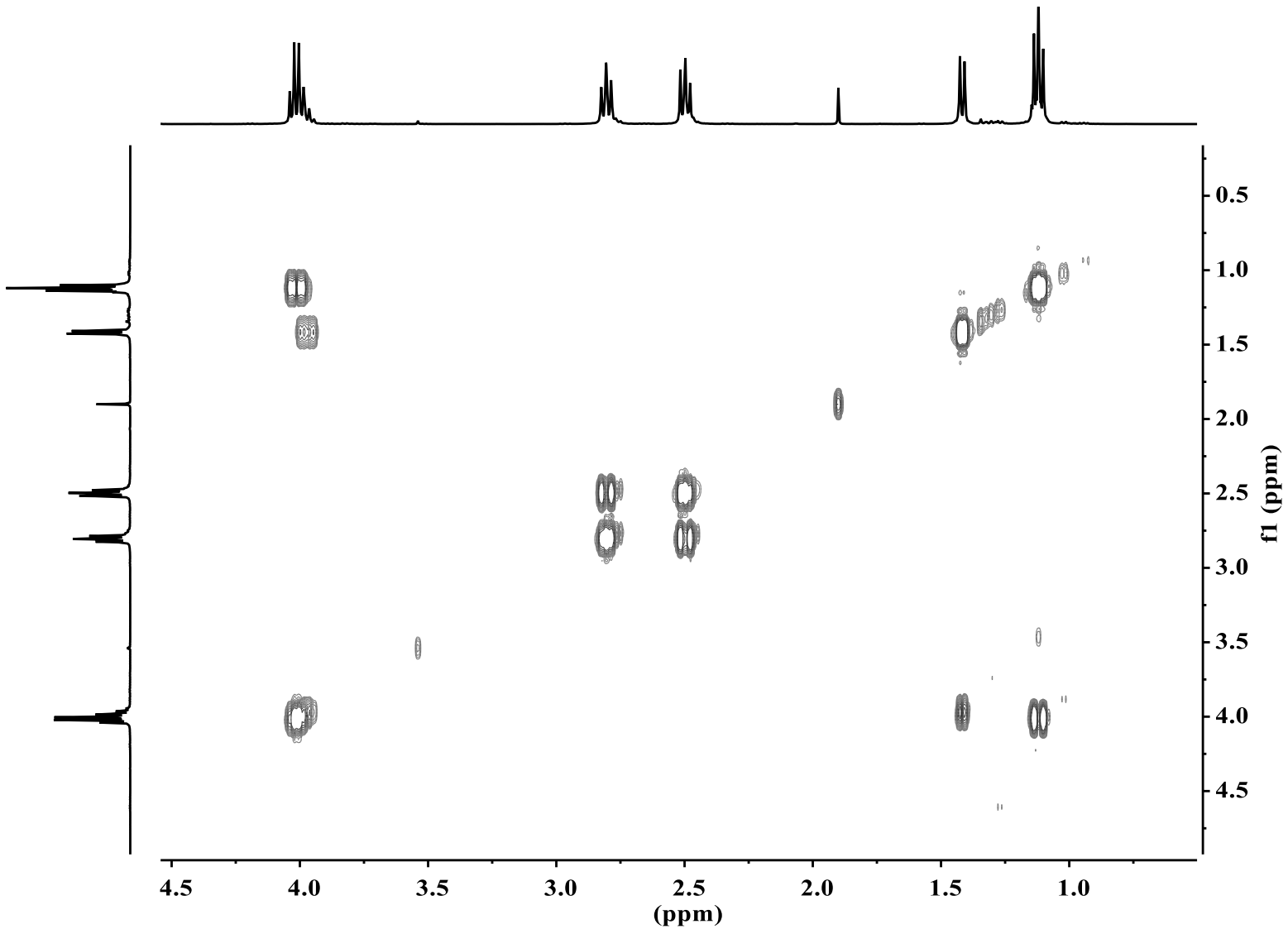

Figure S4.5 COSY of ethyl 3-(furan-2-yl) propanoate acetaldehyde dimmer

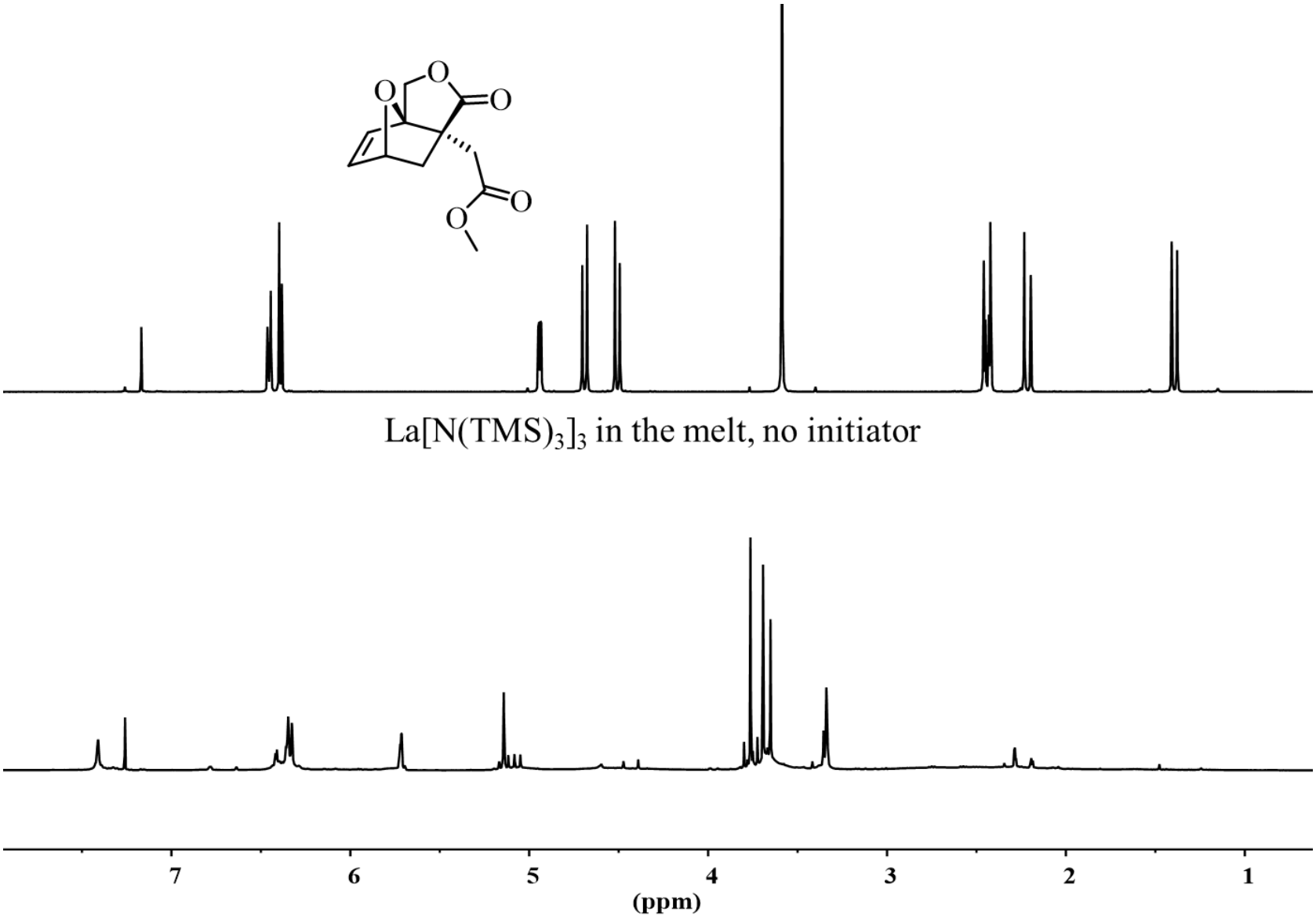

Figure S4.6 $La[N(TMS)_2]_3$ and FIL in melt

References

(1) Pehere, A. D.; Xu, S.; Thompson, S. K.; Hillmyer, M. A.; Hoye, T. R., Diels–Alder Reactions of Furans with Itaconic Anhydride: Overcoming Unfavorable Thermodynamics. *Organic Letters* **2016**, 2584-2587.

Appendix D

Experimental Details and Supporting Information for Chapter 5

D.1. Materials, Reagents, and Methods

All oxygen- and moisture-sensitive manipulations were carried out in a nitrogen-filled glovebox or under nitrogen atmosphere using standard Schlenk techniques. HPLC-grade organic solvents were sparged extensively with nitrogen during filling of the solvent reservoir and then dried by passage through activated alumina (for Et_2O and CH_2Cl_2) followed by passage through Q-5-supported copper catalyst (for toluene and hexanes) stainless steel columns. Tetrahydrofuran (THF) was refluxed over metallic sodium/potassium alloy with benzophenone and distilled under nitrogen atmosphere before use. Acetonitrile were distilled over calcium hydride while adipoyl chloride was purchased from Alfa Aesa and freshly distilled before use. 5-Hydroxymethylfurfural (HMF) was purchased from TCI America and used as received, while furfural (FF) was purchased also from TCI America but dried with CaH_2 for 24 h and then vacuum distilled. HPLC-grade dichloromethane (DCM) and *N,N*-dimethyl formamide (DMF) were sparged extensively with nitrogen during filling of the solvent reservoir and then dried by passage through activated alumina stainless steel columns. Tetrahydrofuran (THF) was dried by distillation over sodium with benzophenone as indicator under a nitrogen atmosphere. Anhydrous acetonitrile 99.8% was purchased from Sigma-Aldrich was used as received. Deuterated dimethyl sulfoxide (DMSO-d_6) was degassed and stored in a glovebox over activated Davison 4 Å molecular sieves. Pre-catalysts 5-methoxy-1,3,4-triphenyl-4,5-dihydro-1*H*-1,2,4-triazoline TPT-OMe were prepared according to literature procedures,[2-3] TPT-OMe was activated by heating to 80° C under vacuum for 48h.

^{1}H and ^{13}C NMR spectra were recorded on a Varian 400 MHz or a 500 Bruker (500 MHz, ^{1}H; 125 MHz), ^{13}C MHz spectrometer or a Bruker AVIII 400 MHz spectrometer (400 MHz, ^{1}H; 100 MHz, ^{13}C). Chemical shifts were referenced to internal solvent resonances corresponding to 7.26 ppm (chloroform), 7.16 ppm (benzene), 2.3 & 7.19 ppm (toluene), and 5.32 (DCM) reported as parts per million relatives to SiMe4. High-resolution mass spectrometry (HRMS) data were collected on an Agilent 6220 Accurate time-of-flight in electrospray mode. GC/MS data collected on Agilent 5973N Mass Selective Detector interfaced to a 6890 gas chromatograph which is equipped with a 7683 automatic liquid sampler. This instrument is a single quadrupole mass spectrometer utilizing an electron ionization source (EI).

Synthesis of Methacrylate Furan Aldehyde (MFA). A 250 mL round bottom flask was precooled to 0°C and charged with 120 mL acetonitrile, triethylamine (20.8 mL, 0.151 mol), and 5-hydroxyfuranaldehyde (12.07 g, 0.095 mol). Then the flask was sealed with a rubber septum and flushed for 10 min with dry N_2. Methacrylol chloride (10.9 mL, 0.100 mol) was loaded into a syringe with needle. The methacrylol chloride was added in 0.5 mL increments over the course of 30 min. The reaction was allowed to stir for 12 h while coming to room temperature. Solid triethylamine hydrochloride was filtered off and solvent was removed with rotary evaporation. Product was re-dissolved in 150 mL DCM and extracted with 3 times with 30 mL DI H_2O. Then DCM was dried with $MgSO_4$ and filtered. Final purification was performed by flash column chromatography with a 1:1 ethyl acetate, hexane solvent system followed by drying under vacuum at room temperature for 12 h (14.67 g, 79.6%). ^{1}H NMR (400 MHz, Chloroform-*d*) δ 9.56 (s, 1H), 7.15 (s, 1H), 6.55 (d, J = 3.5 Hz, 1H), 6.08 (q, J = 1.1 Hz, 1H), 5.55 (p, J = 1.5 Hz, 1H), 5.13 (s, 2H), 1.87 (t, J = 1.3 Hz, 3H).

Attempted TPT catalyzed auto-tandem polymerization of MFA Schenck line technique. A 25 mL Schlenk flask that was dried for 24 H in oven at 150° C loaded with stir bar and cooled under flow of dry N_2 was sealed with septum and a small positive N_2 pressure was maintained throughout reaction. MFA (0.511 g, 2.63 mmol), TPT (0.078 g, 0.263 mmol), *p*-methoxyphenol (0.003g, 0.026 mmol) and 12 mL toluene (THF, acetonitrile, DMF, benzene) were loaded into a 25 mL syringe which was removed and used to charge the 25 mL Schlenk flask. Reaction was heated to 80° C in temperature regulated oil bath with magnetic stirring for 24 h. After reaction had cooled sample was taken for ^{1}H NMR. Purification of FDMA was done with flash column chromatography with silica gel and 1:1 hexane, AcOEt solution.

Synthesis of furil dimethacrylate (FDMA). In a N_2 filled glove box a 125 mL glass pressure reactor was filled with 75 mL DCM, HMF (5.13g, 0.04 mole), and TPT-OMe (0.67 g, 2.0 mmol) sealed and removed from box. Reaction was allowed to stir at 60° C for 6 h. Product was removed from solvent with vacuum filtration. The DHMF was then dried under vacuum for 4 h and used directly in the next step (4.71 g, 92%). To a suspension of activated manganese dioxide (3.21 g, 37.0 mmol) in THF (200 mL) at room temperature was added DHMF (4.71 g, 18.6 mmol). The mixture was then magnetically stirred for 24 h, followed by filtering through Celite to remove the insoluble solid, while the filter cake was washed thoroughly with THF. The combined solution was dried over anhydrous $MgSO_4$ and concentrated with rotary evaporation to give the product used directly in the next reaction (4.42 g, 95%). A 250 mL round bottom flask was precooled to 0°C and charged with 100 mL acetonitrile, triethylamine (7.6 mL, 44.2 mmol), and 5,5'-bihydroxymethyl furil (BHMF) (4.42 g, 17.7 mmol). Then the flask was sealed with a rubber septum and flushed for 10 min with dry N_2. Methacrylol chloride (3.6 mL, 37.1 mmole) was loaded into a syringe with needle. The methacrylol chloride was added in 0.25 mL increments over the

course of 30 min. The reaction was allowed to stir for 12 h while coming to room temperature. Solids were filtered off and solvent was removed with rotary evaporation. Product was mixed with triethylamine HCl so the solids were re-dissolved in DCM and filtered to remove the majority of triethylamine HCl. To remove the remaining Et_3N HCl a 60 mL fine filter funnel was loaded with silica gel and DCM product solution was filtered through. Additional 500 mL of DCM were required to completely flush FDMA from silica gel. Solvent was concentrated with rotary evaporation and dried for 12 h under vacuum at room temperature (4.39 g, 64.3%). ^{1}H NMR (400 MHz, Chloroform-*d*) δ 7.54 (d, *J* = 3.6 Hz, 2H), 6.56 (d, *J* = 3.6 Hz, 2H), 6.10 (t, *J* = 1.2 Hz, 2H), 5.56 (p, *J* = 1.7 Hz, 2H), 5.28 – 5.11 (m, 1H), 5.17 (s, 4H), 1.89 (t, *J* = 1.2 Hz, 6H), 1.18 (s, 0H). ^{13}C NMR (101 MHz, Chloroform-*d*) δ 175.53, 165.56, 156.18, 148.17, 134.43, 125.84, 124.70, 111.95, 57.05, 44.86, 17.24, 7.67.

Analysis of Catalyst Substrate Intermediates. In a typical procedure, a Teflon-valve-sealed J. Young-type NMR tube was charged with TPT (0.0149 g, 0.05 mmol) in a glovebox. A solution of and *p*-methoxyphenol (0.6 mg, 0.005 mmol) and monomer (0.025 mmol) in 0.50 mL DMSO-d_6 (Benzene-d_6) was added to the above NMR tube *via* pipette at RT, and the resulting mixture was heated to 80° C in a temperature-controlled oil bath for pre-determined time. ^{1}H NMR spectra collected and additional equivalents of monomer were added followed by pre-determined periods of heating before next spectra collected.

D.2.

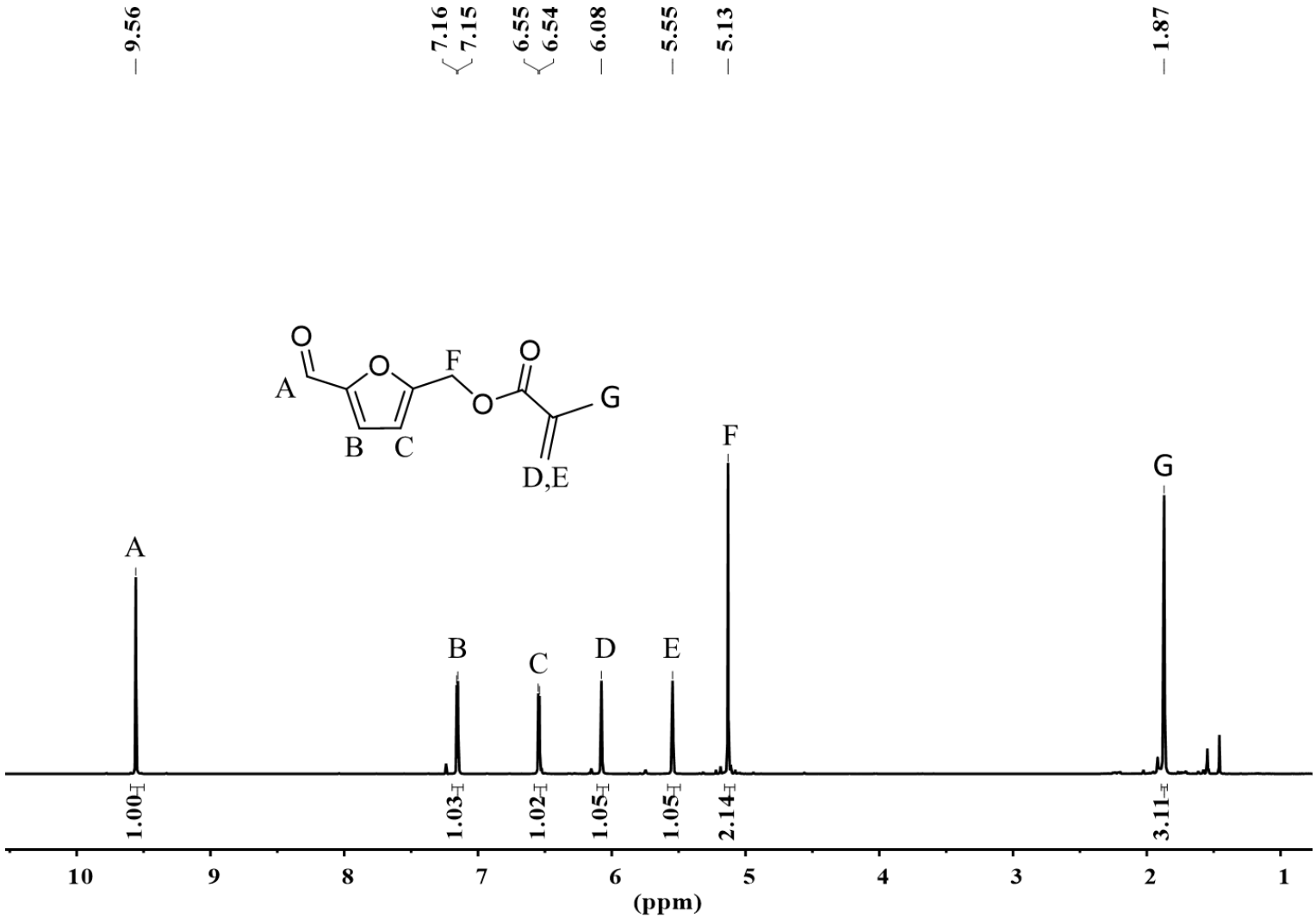

Figure S5.1. ^{1}H NMR in $CDCl_3$ of methacrylate furan aldehyde (MFA).

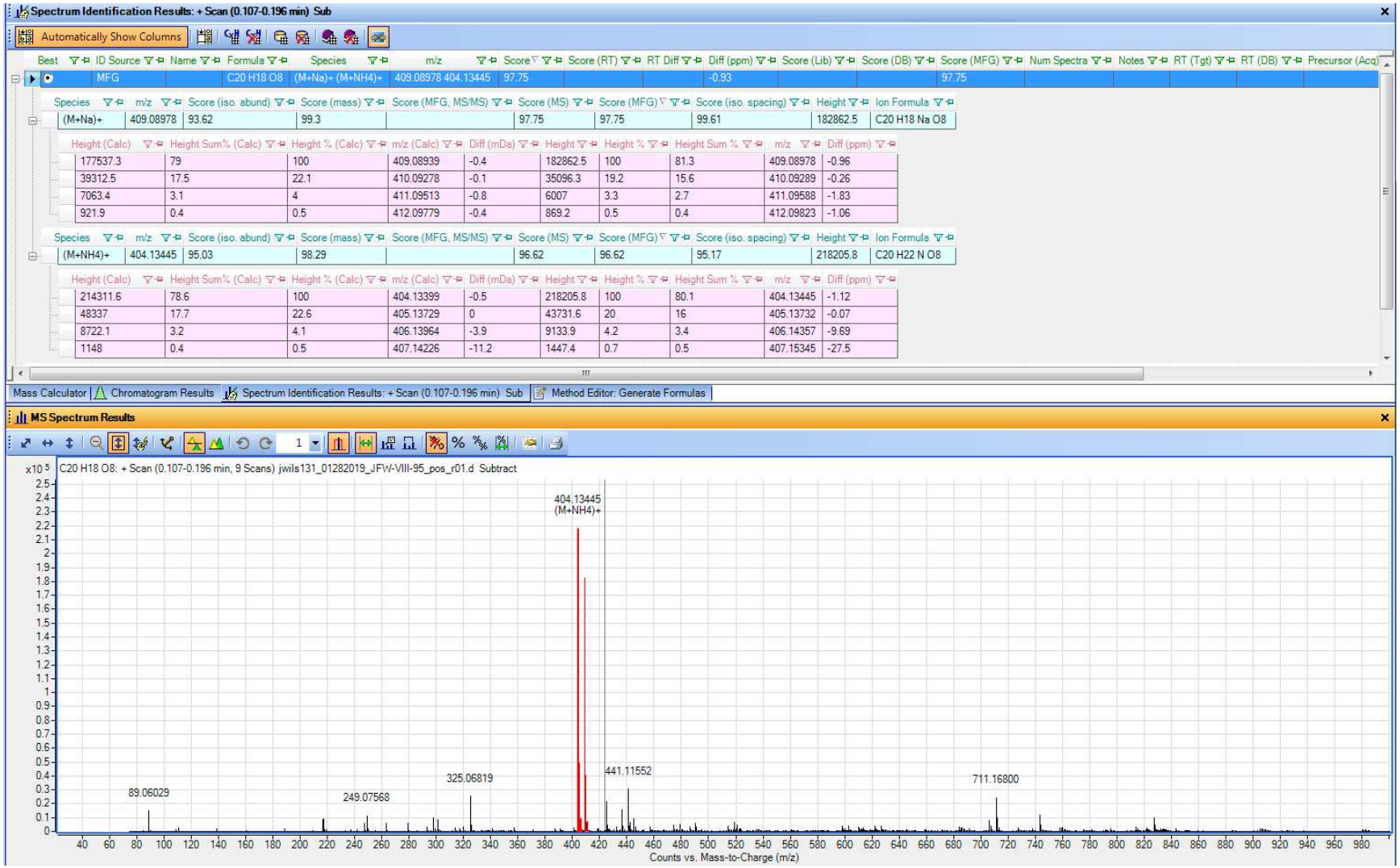

Figure S5.2. Mass spectrum of furil dimethacrylate (FDMA) produced from attempted cascading reaction.

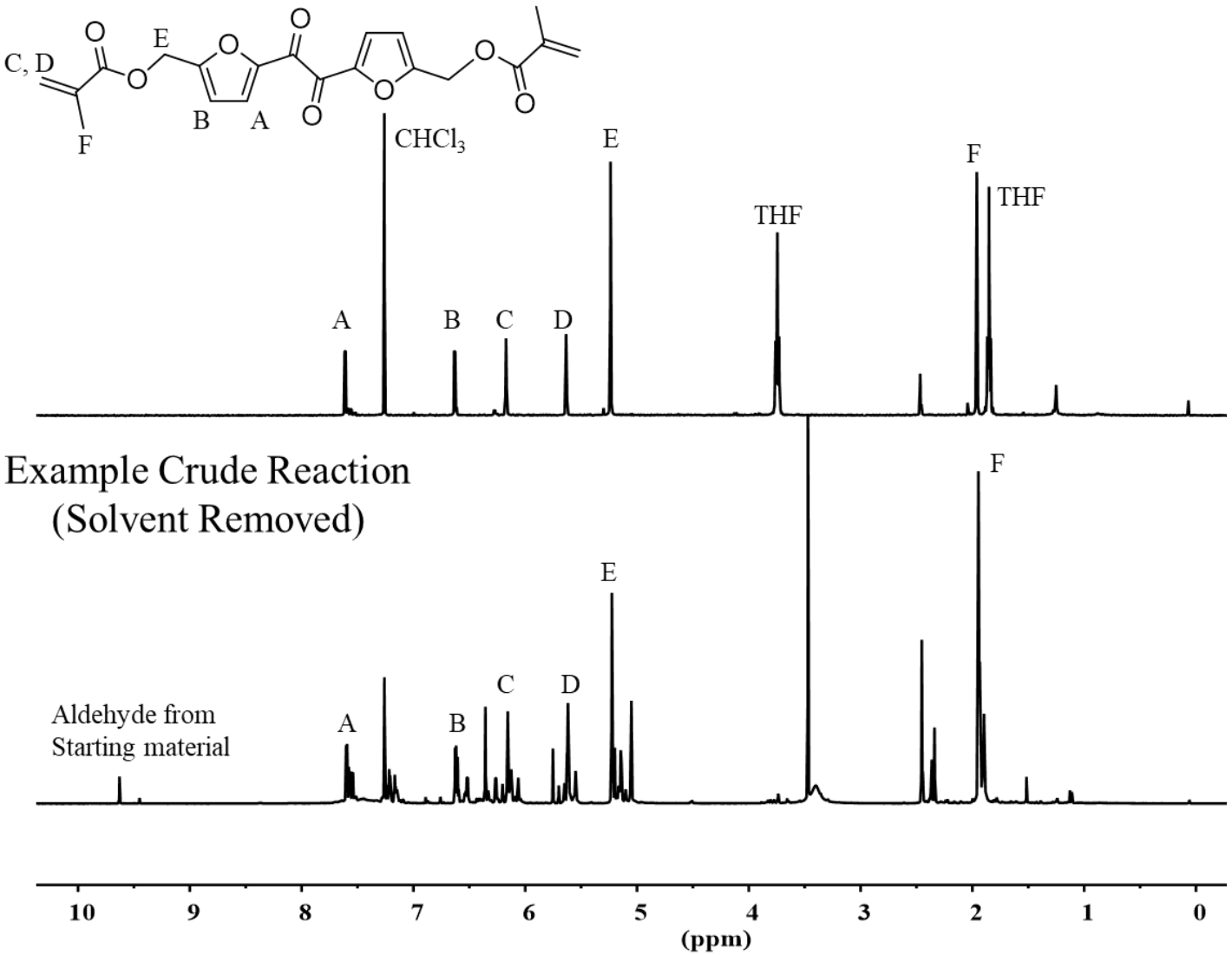

Figure S5.3. Comparison 1H NMR spectra of isolated FDMA and crude reaction between TPT and MFA.

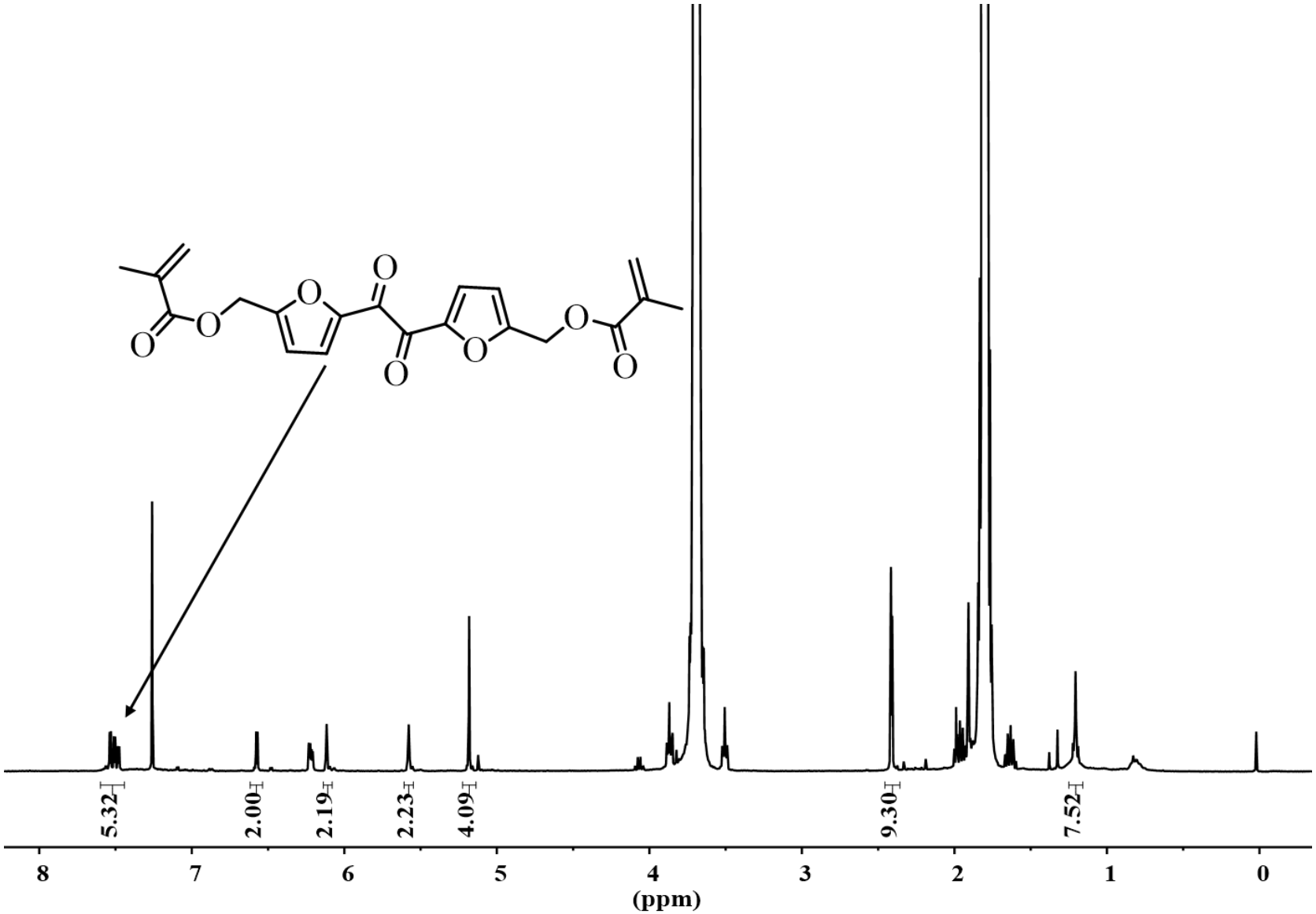

Figure S5.4. ^{1}H NMR of crude with TPT and FDMA.

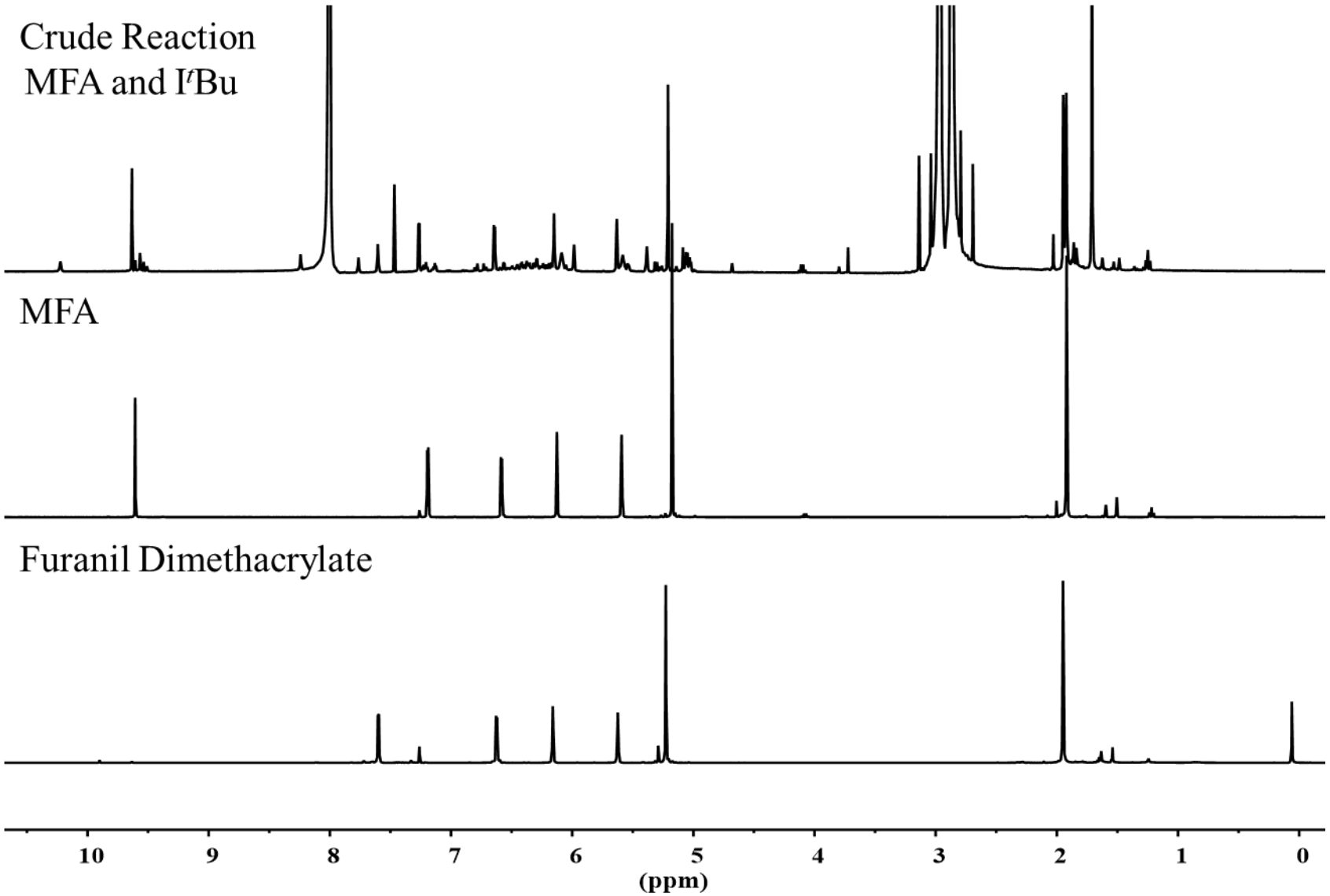

Figure S5.5. ^{1}H NMR in $CDCl_3$ of MFA and I^{t}Bu (NHC) compared to MFA and FDMA.

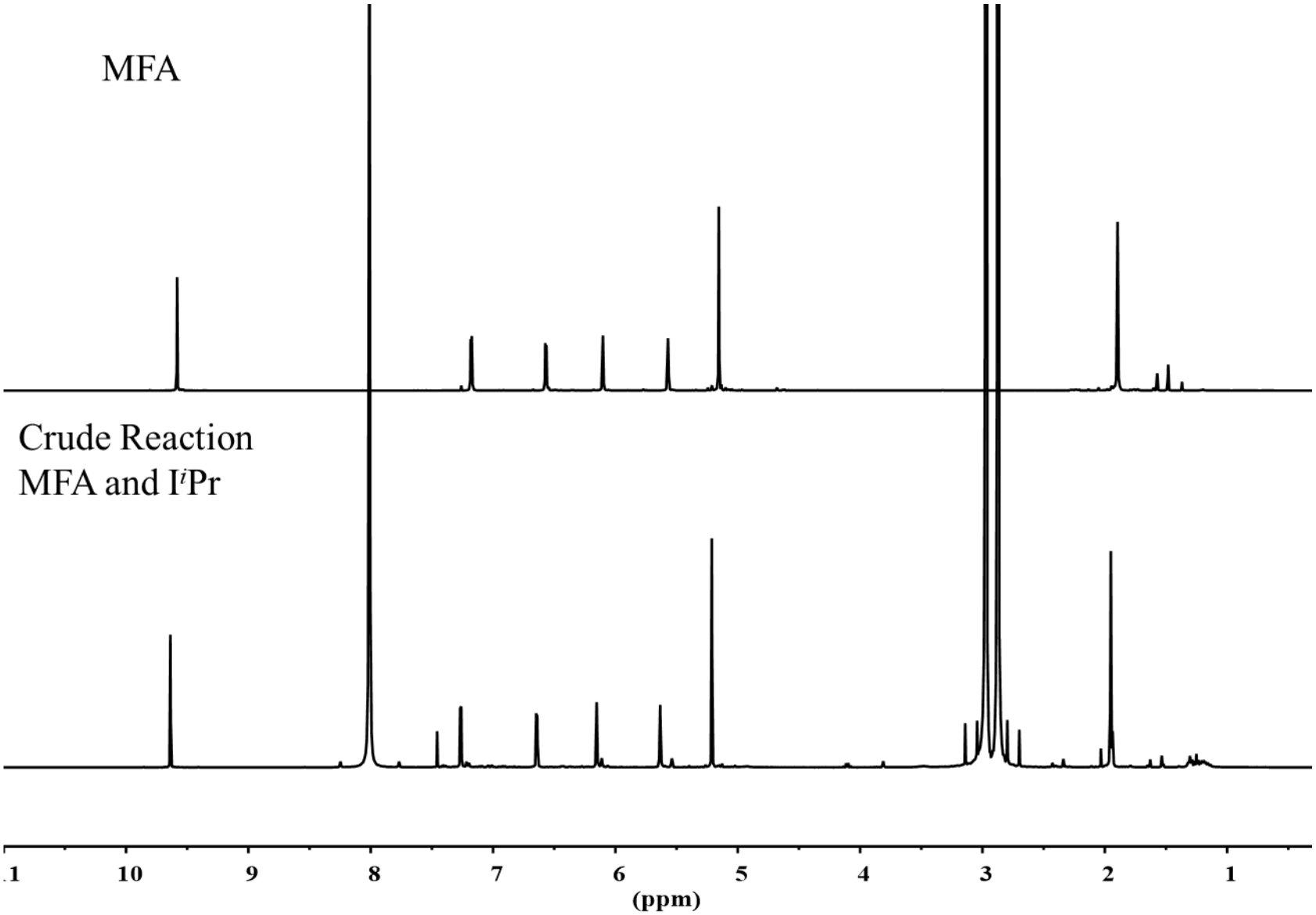

Figure S5.6. ^{1}H NMR of crude reaction in $CDCl_3$ with MFA and I^{i}Pr compered to FDMA starting material.

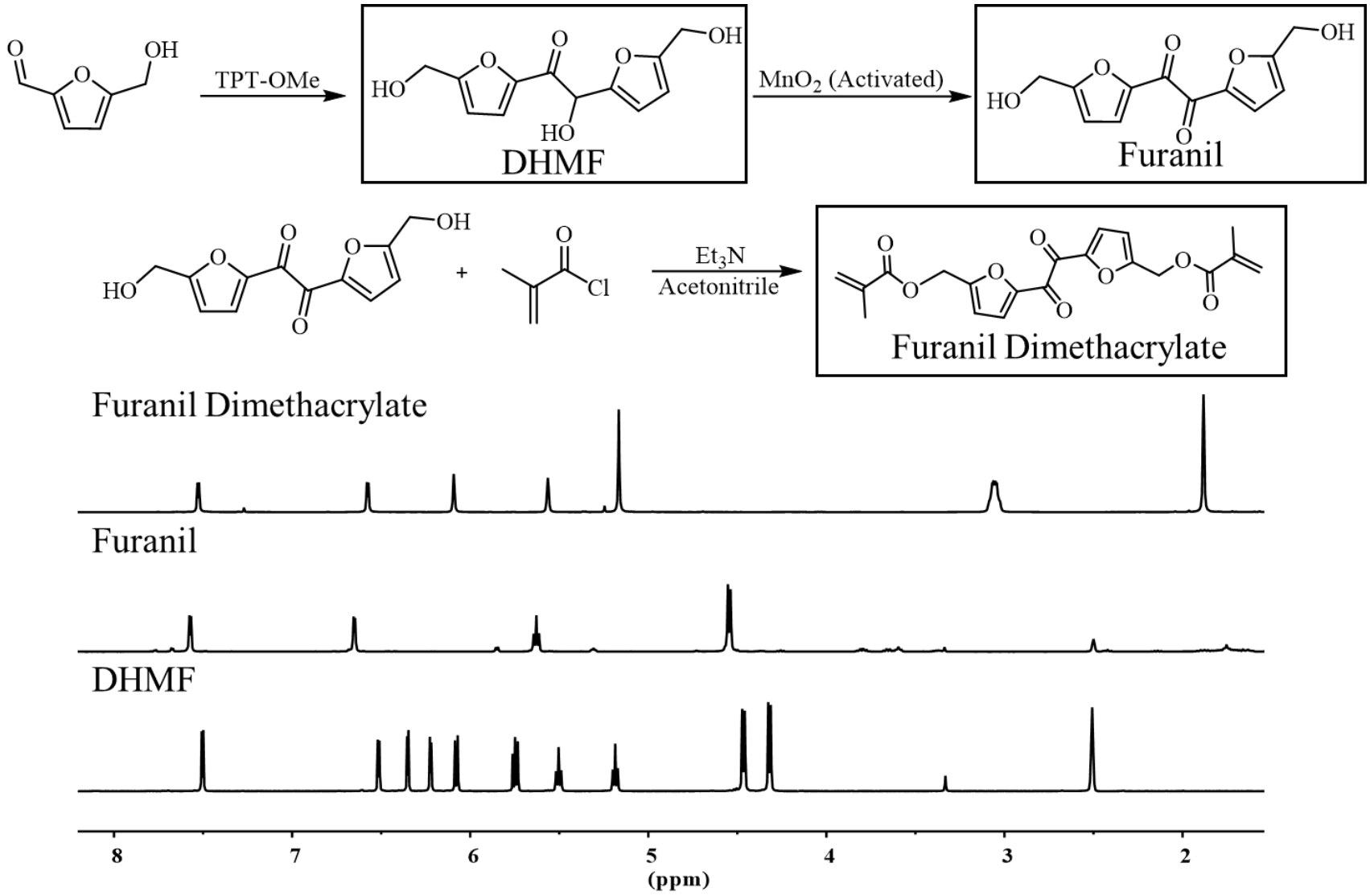

Figure S5.7. Synthesis of FDMA with ^{1}H NMR of each isolated step and final product.

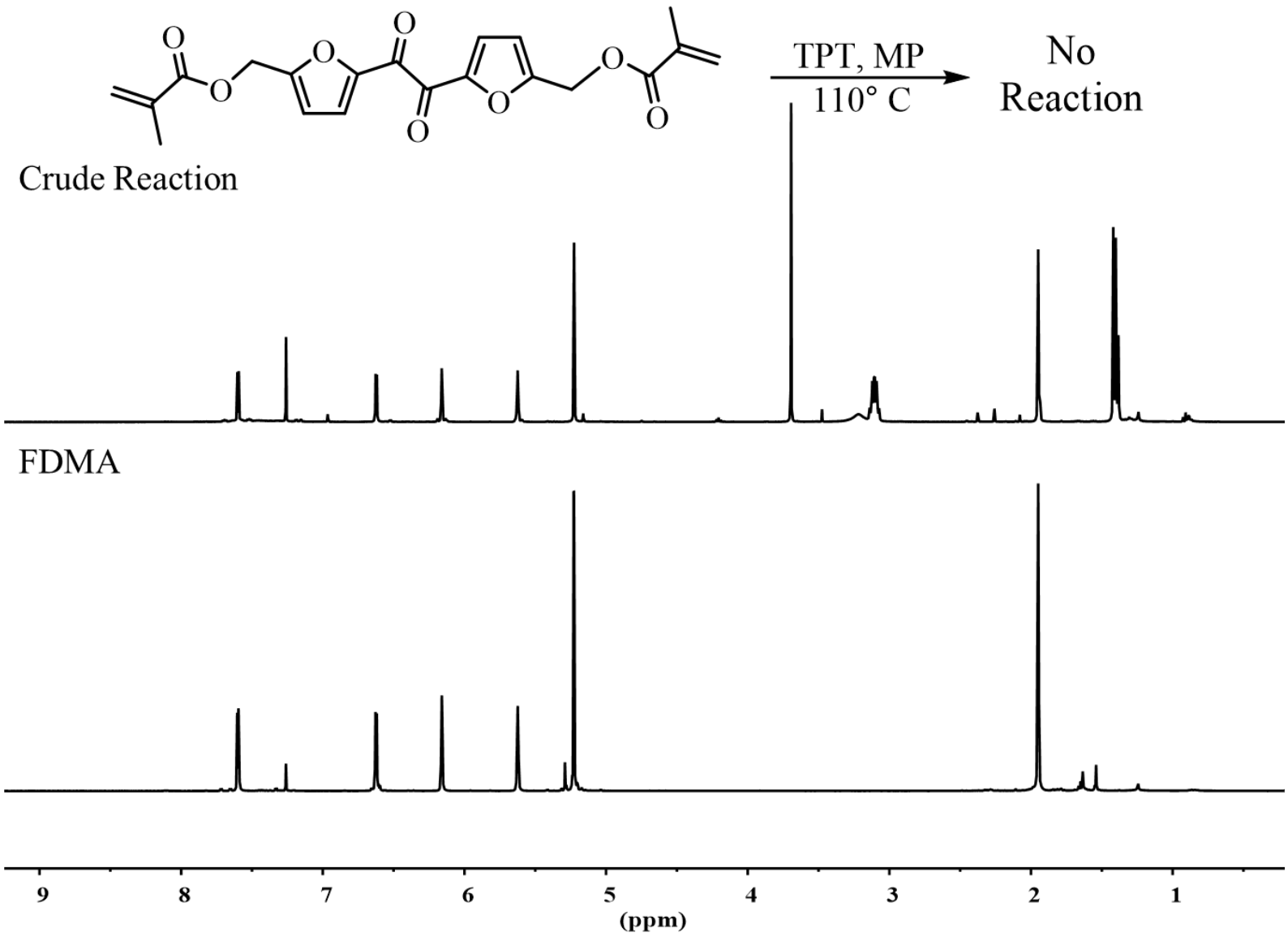

Figure S5.8. ^{1}H NMR in $CDCl_3$ of crude reaction between TPT and FDMA compared to FDMA starting material.

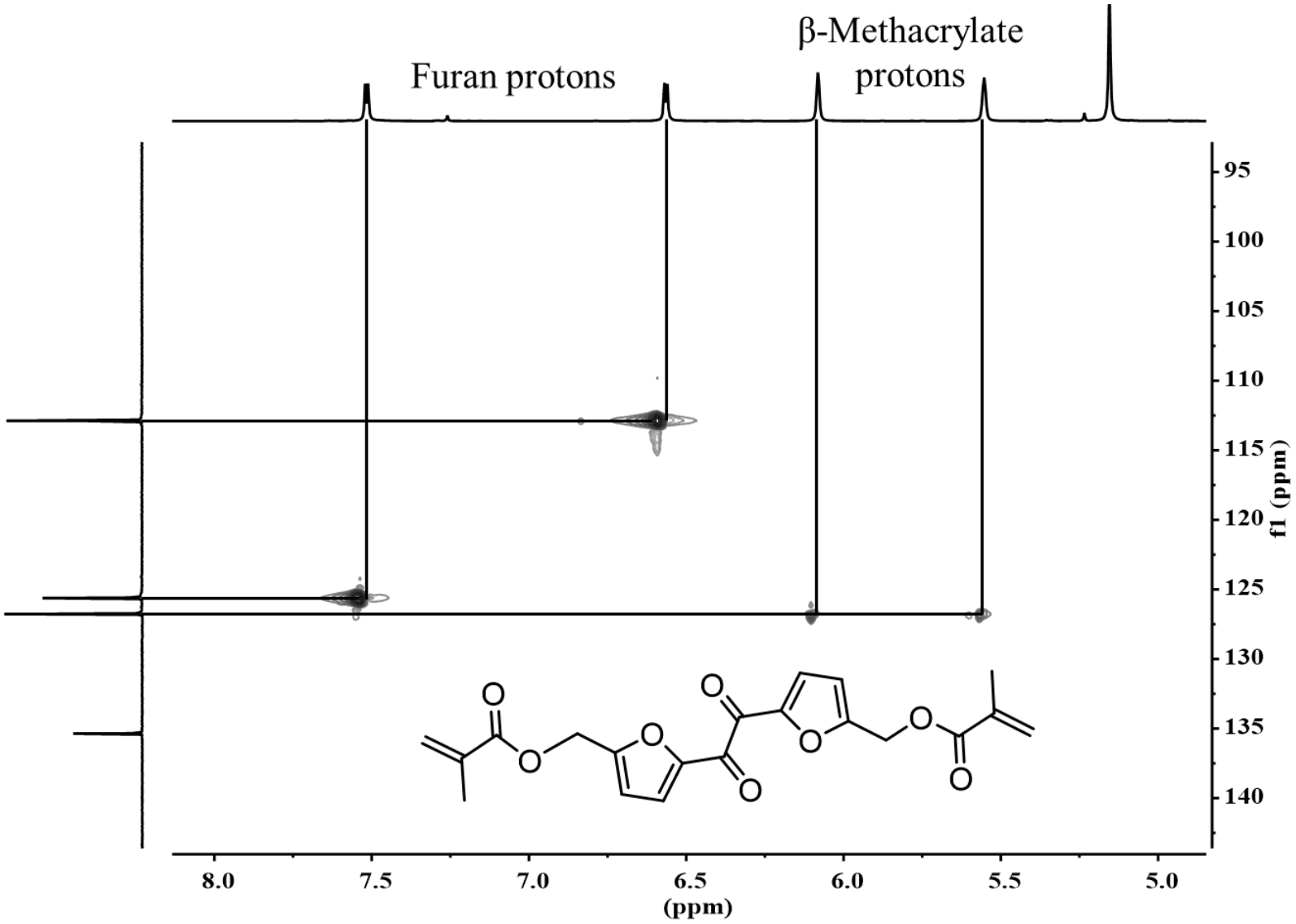

Figure S5.9. HMBC 2D NMR used to identify β-carbon signal.

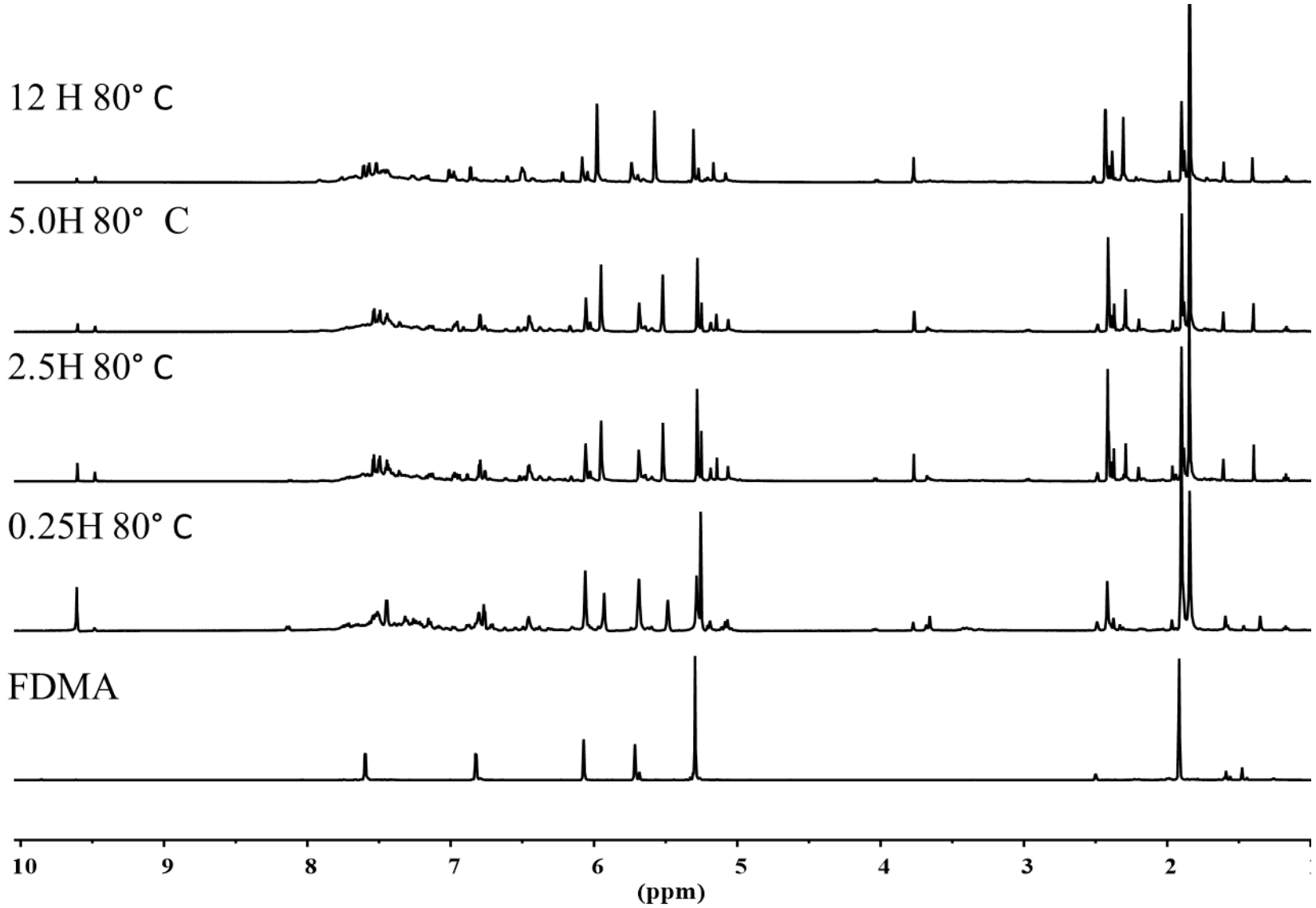

Figure S5.10. Variable temperature ^{1}H NMR run at 80° C TPT catalyzed reaction of MFA showing lack of enamine formation.

References

(1) Pehere, A. D.; Xu, S.; Thompson, S. K.; Hillmyer, M. A.; Hoye, T. R., Diels–Alder Reactions of Furans with Itaconic Anhydride: Overcoming Unfavorable Thermodynamics. *Organic Letters* **2016,** 18, 2584-2587.

(2) Enders, D.; Breuer, K.; Raabe, G.; Runsink, J.; Teles, J. H.; Melder, J.-P.; Ebel, K.; Brode, S., Preparation, Structure, and Reactivity of 1,3,4-Triphenyl-4,5-dihydro-1H-1,2,4-triazol-5-ylidene, a New Stable Carbene. *Angew. Chem. Int. Ed.* **1995,** 34, 1021-1023.

(3) Enders, D.; Kallfass, U., An Efficient Nucleophilic Carbene Catalyst for the Asymmetric Benzoin Condensation. *Angew. Chem. Int. Ed.* **2002,** 41, 1743-1745.